Carnegie Mellon University

CARNEGIE INSTITUTE OF TECHNOLOGY

THESIS

SUBMITTED IN PARTIAL FULFILLMENT OF THE REQUIREMENTS

FOR THE DEGREE OF Doctor of Philosophy

TITLE **Low Carbon Policy and Technology in the Power Sector: Evaluating Economic and Environmental Effects**

PRESENTED BY **David Luke Oates**

ACCEPTED BY THE DEPARTMENT OF

Engineering and Public Policy

Paulina Jaramillo — February 25, 2015
ADVISOR, MAJOR PROFESSOR — DATE

Douglas Sicker — February 27, 2015
DEPARTMENT HEAD — DATE

APPROVED BY THE COLLEGE COUNCIL

Vijayakumar Bhagavatula — March 11, 2015
DEAN — DATE

Low Carbon Policy and Technology in the Power Sector: Evaluating Economic and Environmental Effects

SUBMITTED IN PARTIAL FULFILLMENT OF THE REQUIREMENTS FOR

THE DEGREE OF

DOCTOR OF PHILOSOPHY

IN

ENGINEERING & PUBLIC POLICY

David Luke Oates

B.Sc. Eng. Engineering Physics, Queen's University, Canada

Carnegie Mellon University

Pittsburgh, PA

May 2015

ACKNOWLEDGEMENTS

This work was supported through the RenewElec project (www.renewelec.org) by the Doris Duke Charitable Foundation, the Richard King Mellon Foundation, the Electric Power Research Institute, and the Heinz Endowment. A portion of this work was also supported in collaboration with the National Energy Technology Laboratory through the Regional University Alliance (NETL-RUA), a collaborative initiative of the NETL, under the RES contract DE-FE0004000.

A great many people have contributed to this thesis through countless conversations. Roger Lueken and Allison Weis have been of great help in the development and testing phases of various models. Kathleen Spees was extremely helpful in identifying research questions and structuring the analysis in the portion of this work focused on the EPA's 111(d) rule. My collaboration with Peter Versteeg and Eric Hittinger on the flexible CCS portion of this work was one of the most rewarding phases of my PhD. Alan Jenn has critiqued my writing, presentations, and R code on numerous occasions. Todd Ryan has repeatedly focused my attention on the institutional details of electricity markets. I would particularly like to thank my committee Paulina Jaramillo (chair), Bri-Mathias Hodge, Ed Rubin, Cosma Shalizi, and Rebecca Nugent for their guidance and support over the years.

Finally, I owe a great deal to my parents, Anne Hill and Julian Oates. Their constant confidence and encouragement have helped enormously not only during my PhD, but during all 23 years of my education to date.

ABSTRACT

In this thesis, I present four research papers related by their focus on environmental and economic effects of low-carbon policies and technologies in electric power. The papers address a number of issues related to the operation and design of CCS-equipped plants with solvent storage and bypass, the effect of Renewable Portfolio Standards (RPS) on cycling of coal-fired power plants, and the EPA's proposed CO_2 emissions rule for existing power plants.

In Chapter 2, I present results from a study of the design and operation of power plants equipped with CCS with flue gas bypass and solvent storage. I considered whether flue gas bypass and solvent storage could be used to increase the profitability of plants with CCS. Using a price-taker profit maximization model, I evaluated the increase in NPV at a pulverized coal (PC) plant with an amine-based capture system, a PC plant with an ammonia-based capture system, and a natural gas combined-cycle plant with an amine-based capture system when these plants were equipped with an optimally sized solvent storage vessel and regenerator. I found that while flue gas bypass and solvent storage increased profitability at low CO_2 prices, they ceased to do so at CO_2 prices high enough for the overall plant to become NPV-positive.

In Chapter 3, I present results from a Unit Commitment and Economic Dispatch model of the PJM West power system. I quantify the increase in cycling of coal-fired power plants that results when complying with a 20% RPS using wind power, accounting for cycling costs not usually included in power plant bids. I find that while additional cycling does increase cycling-related production costs and emissions of CO_2, SO_2, and NO_X, these increases are small compared to the overall reductions in production costs and air emissions that occur with high levels of wind.

In proposing its existing power plant CO_2 emissions standard, the Environmental Protection Agency determined that significant energy efficiency would be available to aid in compliance. In Chapter 4, I use an expanded version of the model of Chapter 3 to evaluate compliance with the standard with and without this energy efficiency, as well as under several other scenarios. I find that emissions of CO_2, SO_2, and NO_X are relatively insensitive to the amount of energy efficiency available, but that production costs increase significantly when complying without efficiency.

In complying with the EPA's proposed existing power plant CO_2 emissions standard, states will have the choice of whether to comply individually or in cooperation with other states, as well as the choice of whether to comply with a rate-based standard or a mass-based standard. In Chapter 5, I present results from a linear dispatch model of the power system in the continental U.S. I find that cooperative compliance reduces total costs, but that certain states will prefer not to cooperate. I also find that compliance with a mass-based standard increases electricity prices by a larger margin than does compliance with a rate-based standard, with implications for the distribution of surplus changes between producers and consumers.

TABLE OF CONTENTS

List of Tables

List of Figures

Chapter 1: INTRODUCTION

The electric power system is changing. New institutional arrangements, new technologies, and pressures to reduce environmental impact are challenging some of the ideas that have guided the industry since its infancy. Utilities are no longer the tightly regulated, vertically integrated entities that dominated the industry for much of the 20th century, having been replaced with a mixture of generation owners, transmission operators, and load serving entities. All of these entities must navigate increasingly complex market structures and respond to market signals in an effort to earn a profit.

Large segments of the public are no longer content that our electricity system delivers cheap, reliable power. Now it must also be clean. The nation's regulatory apparatus has been extremely successful in dramatically reducing air emissions of certain pollutants. Problems remain, however, notably in the area of greenhouse gas emissions that drive climate change. The advent of (relatively) inexpensive renewable energy in the form of wind power holds great promise to aid in the de-carbonization of the power system, but this technology exacerbates the old problem of balancing supply and demand with its variable and unpredictable output. Carbon Capture and Sequestration (CCS) technology promises to allow the continued exploitation of fossil fuel resources while still meeting environmental goals, but the technology has not been widely adopted and is expensive. In an attempt to spur the de-carbonization of the power system, the Environmental Protection Agency (EPA) has issued new rules to control CO_2 emissions from electric power plants, but the rules are dauntingly complex and may have a number of unforeseen consequences.

In the coming years we may well see continued growth of renewable energy sources, further proliferation of environmental regulations, and maybe even the deployment of Carbon Capture and Storage (CCS) at scale. Yet we should not expect the existing system to disappear overnight. Today's electric power system is made up of large numbers of expensive, long-lived assets. If only because of

the immense pressure to recover investment costs, change in the electric power system is likely to be incremental. The effectiveness of many low-carbon technologies depends on their interactions with the fossil fleet. Renewable energy resources such as wind and solar require dispatchable backup generators to smooth their output and most dispatchable generators are fossil-based. Furthermore, renewables do not directly remove CO_2 from the atmosphere. It is only by displacing energy from fossil fueled power plants that renewables can have any environmental benefit. Given the operating constraints of power systems and the growth in demand for electricity, renewable resources will likely be unable to completely displace all fossil-based generation. We may therefore need strategies, such as the use of CCS, to reduce the carbon intensity of the fossil fleet. In short, in heralding the arrival of the electricity system of the future, we should not loose sight of the electricity system of the present.

In this thesis, I present four research projects conducted during my time at Carnegie Mellon University. Each of these projects in some way models a low carbon policy or technology embedded in the larger system. The projects are related in their focus on the environmental and economic effects of policies and technologies designed to reduce greenhouse gas emissions from the electric power sector. They are also related in their use of mixed integer optimization methods to model the operation of power plants. The research focuses on flexible Carbon Capture and Storage (CCS) technology, wind power in the context of Renewable Portfolio Standards (RPS), and the EPA's CO_2 emissions rule for existing power plants.

In Chapter 2, I examine the possibility of operating plants equipped with Carbon Capture and Storage (CCS) in a flexible manner. Flue gas bypass and solvent storage would allow CCS-equipped plants to temporarily overcome the energy penalty of CCS, allowing increased output during periods when electricity prices are high. In this chapter, I evaluate whether increased flexibility could increase the profitability of CCS-equipped plants, thereby leading to more rapid deployment of the

technology. Using a price-taker profit-maximizing operation and design model, I find that flexibility increases the Net Present Value (NPV) of CCS-equipped plants, but only for low CO_2 prices. For CO_2 prices high enough that the CCS-equipped plant breaks even on an NPV basis, the private value of flexibility drops to zero.

In Chapter 3, I evaluate the effects of compliance with a 20% Renewable Portfolio Standard (RPS) in the western portion of the PJM Interconnection using wind power. Since the electricity system lacks substantial storage, dispatchable generators must balance the variable output of wind to ensure that supply and demand for electricity are equal. Due to the fact that much of wind's variability occurs at inter-hour timescales[1], much of this balancing might be done using coal fired power plants. However, such balancing would increase the operating costs of these plants and result in additional emissions of CO_2 and other air pollutants. Using a Unit Commitment and Economic Dispatch (UCED) model, I evaluate the increase in cold, warm, and hot startups of coal units that occurs in a 20% wind scenario. I use estimates of the cost of cycling coal-fired units that include incremental wear and tear on the plant and account for the additional air emissions that occur during startup and shutdown cycling. While startups of coal-fired power plants do increase in the 20% wind scenario, the resulting increase in cycling emissions is small compared to the emissions reductions associated with reduced overall use fossil plants. Furthermore, I find that while the additional cycling does increase production costs of coal units, the more significant effect of wind on coal profitability is the reduction in capacity factors and electricity prices that accompanies high wind penetrations.

In Chapter 4, I expand on the model developed in chapter 3 to evaluate some of the effects of the EPA's proposed rule (the "111(d) rule") on CO_2 emissions for existing Electricity Generating Units (EGUs). Using a multi-stage UCED that incorporates wind forecast error in ERCOT, ISO NE, and PJM West, I evaluate the production cost and air emissions impacts of complying with the

[1] Apt, J. (2007). The spectrum of power from wind turbines. *Journal of Power Sources*.

existing plant rule under a number of scenarios. I report emissions due to normal operations and startup/shutdown cycling in the same way as chapter 3, but I also report "idling" emissions that occur when plants operate inefficiently at less than their design capacity. I find that while production costs decline under compliance with the 111(d) rule using the EPA's assumptions about energy efficiency, they increase substantially if that energy efficiency does not materialize. Furthermore, I find that compliance without energy efficiency dramatically increases generation from natural gas fired EGUs. I also find that while compliance leads to increased startup and idling emissions from fossil generators, this increase is not enough to have a meaningful impact on the emissions reductions achieved by the existing plant rule. Finally, I find that compliance with the rule using the current fleet of EGUs is either impossible or an extremely costly proposition.

In Chapter 5, I consider the effects of the 111(d) rule on a national level. In proposing the rule, the EPA indicated that states had the choice of whether to comply individually or in cooperation with other states. States also have the option to comply using a rate-based standard or a mass-based standard. Using a 64-region model of the electricity system in the continental U.S., I evaluate some economic effects of these decisions. I find that while cooperation between states reduces the total costs of compliance at a national level, some states lose out. Furthermore, I find that compliance with the rule significantly increases electricity pries, increasing producer surplus at the expense of consumer surplus, and that this effect is greatest under a mass-based standard. Finally, I find that while producers generally fare better under mass-based standards, in certain states, NGCC units fare better under rate-based standards.

Reducing the environmental impact of electricity generation is a major challenge in our times. Like any major challenge, there are large numbers of little problems that must be solved in order to move forward. The work in this thesis attempts to solve a few of these small problems that arise when integrating renewable and low-carbon electricity sources into electric power systems and in

implementing low-carbon regulations. I hope that this work can contribute in some way to the cost effective transition to a low carbon future.

Chapter 2: PROFITABILITY OF CCS WITH FLUE GAS BYPASS AND SOLVENT STORAGE

Abstract

We performed a study to determine whether flue gas bypass and solvent storage can increase the profitability of a power plant equipped with post-combustion carbon capture technology. By increasing flexibility, these technologies allow increased output when electric energy prices are high. We used the Integrated Environmental Control Model to characterize cost and operational parameters of a pulverized coal (PC) plant with both amine and ammonia carbon-capture systems, as well as a natural gas combined cycle plant with amine capture. We constructed profit-maximization operating models with both perfect and imperfect information about electric energy prices in a large electricity market in the Eastern United States. We optimized the size of the regenerator and solvent storage vessels to maximize profitability. Results indicate that the profitability benefits of flexible CCS range from 0 to 35%. Most of the potential benefit is capital savings from allowing the regenerator to be undersized. The benefits of flexible CCS were found to decline with increasing CO_2 prices, with steady-state units preferable above a CO_2 emissions price of $40/tonne. Flexible CCS was never optimal when the overall plant was profitable. While flexible CCS can boost profitability under policies that force plants with CCS to be built even where they are not profitable, it is less relevant under market-based policies that incentivize CCS through CO_2 prices.

This paper was published as Oates, D. L., Versteeg, P., Hittinger, E., & Jaramillo, P. (2014). Profitability of CCS with Flue Gas Bypass and Solvent Storage. *International Journal of Greenhouse Gas Control*, *27*(0), 279–288. doi:10.1016/j.ijggc.2014.06.003

2.1 Introduction

Please note that this chapter of the thesis is based on work performed in conjunction with Peter Versteeg and Eric Hittinger. I constructed the main operating model, fit the energy penalty model to data from the IECM, produced the results plots, and wrote all the text. Peter Versteeg conducted the IECM modeling to provide input parameters for the operating model. Eric Hittinger constructed the imperfect information model. I have included all work on this paper below, as removing parts of it would have made the work less understandable. However, I have inserted bolded notes attributing work to Peter and Eric where appropriate.

Carbon capture and storage (CCS) has been proposed as a means of enabling continued use of fossil fuels for power generation while simultaneously reducing greenhouse gas emissions from this sector. A variety of technologies have been proposed as viable options for capturing carbon dioxide from fossil-based power plants. In post-combustion systems, CO_2 is extracted from the flue gases, yielding a highly pure stream of CO_2. In pre-combustion systems, the environment of combustion is modified such that a highly pure CO_2 stream is essentially the only product of combustion. In this work, we examined two post-combustion systems. One uses a monoethanolamine solvent, and the other uses a chilled ammonia solvent. In these systems, flue gases pass through one or more capture trains where the capture fluid absorbs the CO_2. The rich solvent is then regenerated, yielding a highly pure CO_2 stream that can be fed into a pipeline, as well as lean solvent that can be used to absorb more CO_2.

Though enabling technologies have long been available, no full-scale CCS projects have been deployed to date. The lack of such projects has often been attributed to the high costs associated with a new plant with CCS as compared to a plant without a capture system. Equipping a new plant with CCS increases both capital and operating costs. Capital costs are driven primarily by expensive

regenerator and absorber systems, as well as by the need to oversize the plant to overcome the energy penalty associated with regenerating solvent. Operating costs are driven by the energy penalty associated with regenerating solvent, which requires increased fuel use per MWh of electricity generated.

Many techno-economic analyses of CCS assume steady-state operations of the plant. Such studies often begin with engineering assessments of plant efficiency, component costs, and input costs. After assuming a capacity factor, capital and operating costs are converted into a Levelized Cost of Electricity (LCoE) metric. While steady-state analyses capture many effects relevant for comparing technologies, they ignore the effect of variability in electric energy prices. In 2010, hourly day-ahead electric energy prices in PJM[2] varied from $5/MWh to $195/MWh, with a load-weighted average of $48/MWh [1]. All else being equal, a plant with sufficient flexibility to maximize output when electric energy prices are high and minimize output when prices are low will be more profitable than an inflexible unit.

Several authors have discussed the technical potential for more flexible operation of plants with CCS. Haines and Davidson [2], Lucquiaud et al. [3], and Chalmers et al. [4] concluded that both flue gas bypass and solvent storage could increase flexibility in plants equipped with post-combustion CCS. Flue gas bypass enables increased power output and reduction in marginal costs by selling the electricity otherwise used for CCS, thereby temporarily increasing emissions of CO_2. Solvent storage enables decoupling of the absorption and regeneration processes. Since regeneration is responsible for most of the energy penalty of CCS [4], a plant with CCS and solvent storage can increase its

[2] The PJM Interconnection is a large Regional Transmission Organization in the Eastern U.S. PJM operates several electricity markets, including electric energy, capacity, and ancillary service markets. To avoid ambiguity, we will avoid the term "electricity prices" and will instead refer to "electric energy prices".

output for a limited time by storing rich solvent and avoiding the regeneration energy penalty. Such flexibility has the potential to increase profitability.

As pointed out by Chalmers et al. [4], quantifying the profitability increase associated with this flexibility requires a model of a plant's operation in an electricity energy market. Cohen [5], [6] approached this problem by building a profit-maximizing optimization model to determine the value of solvent storage for a PC unit with amine capture facing increasing CO_2 emissions prices over time. The authors used a heuristic to determine the required size of the regenerator and solvent storage tank. The study concluded that solvent storage increased the operating profits of such a plant, but that benefits were highest at moderate CO_2 emissions prices.

Brasington [7] constructed a similar model of a PC plant with amine capture, but included a more detailed assessment of capital costs and a dynamic model of the capture system. The study used a heuristic to determine regenerator oversize and concluded that solvent storage does not increase profitability under current electric energy price spreads in the South-Eastern U.S.

Patiño-Echeverri and Hoppock [8] assessed the impact of electric energy price volatility on the profitability benefits of solvent storage. The authors found a threshold value of energy price volatility that would make solvent storage profitable and identified regions of the U.S. where 2008 price volatility exceeded the threshold.

Versteeg et al. [9] considered the profitability of flexible CCS with solvent storage with optimally sized storage and regenerator, but without considering flue gas bypass, sale of CO_2 for Enhanced Oil Recovery, the effect of a policy limiting annual emissions rates, or the effect of flexibility on breakeven CO_2 emissions prices. The authors concluded that flexible CCS increased profitability at low CO_2 emissions prices.

The profitability benefits of flexibility are not limited to post-combustion CCS. Newcomer and Apt [10] considered the similar problem of whether syngas storage could reduce the breakeven

carbon price for an Integrated Gasification Combined Cycle (IGCC) power plant. The authors found that syngas storage can reduce the break-even carbon price for IGCC plants in the U.S. by approximately 25%.

In this work, we considered the profitability effects of flue gas bypass and solvent storage on the operation of power plants with post-combustion capture when these plants were operated as profit-maximizing price takers in the PJM electric energy market. We considered the case where flue gas bypass was constrained by an annual average emissions rate cap. Our work extended that of previous authors by allowing solvent storage capacity and regenerator size to be chosen so as to maximize profits; considering the effects of imperfect information on operational and design decisions; examining three different post-combustion capture configurations; studying the effect of revenues from CO_2 sales for enhanced oil recovery (EOR); and imposing an emissions rate limit representative of the proposed U.S. New Source Performance Standards for greenhouse gases (GHGs).

2.2 Methods

Our analytical framework employed technical and cost parameters for plants equipped with CCS and electric energy prices at a range of CO_2 emissions prices as inputs. It also employed a model of the performance of each plant when bypassing flue gases and storing solvent, operating models based on perfect and imperfect information, and a solvent storage design optimization model.

2.2.1 System Design

Note that the work described in section 2.2.1 was largely performed by Peter Versteeg. I retain it here for clarity in understanding the overall work.

Our plant designs for amine- and ammonia-based capture were based on Case 12 and Case 14, respectively, of the 2010 NETL baseline report [11]. Other authors have described these systems in

some detail [12]-[14]. Performing flue gas bypass and solvent storage required modifications to the base plant design. We sized the low-pressure turbine, condenser, and generator to handle steam flows during minimum solvent regeneration or maximum bypass. We sized the CO_2 capture system heat exchangers, pumps, CO_2 compressors, transport pipeline and associated equipment for maximum solvent regeneration or no bypass. We assumed that saline aquifer injectivity was not affected by variable CO_2 output. We note that design of pipelines and injection wells for variable CO_2 flow is not a well-studied problem and it is not one we address here. However, it is likely quite surmountable [4].

Figure 2.1 shows a simplified process flow diagram for a plant equipped for CCS, flue gas bypass, and solvent storage. To perform bypass, flue gases are re-directed up-stream of the gas pre-processing unit and vented. With partial bypass, the flue gas fraction flowing through the absorber is treated for 90% capture. This treated stream is then mixed with the untreated bypass stream, resulting in less than 90% capture overall. To enable solvent storage, the design also incorporates lean and rich storage tanks[3]. These tanks are connected between the absorber and regenerator. The capacity of the solvent storage tanks and the regenerator were chosen as part of the design optimization described in section 2.2.7. Note that flue gas bypass results in reduced effective CO_2 capture efficiency, while solvent storage maintains capture efficiency.

[3] The rich and lean storage vessels are coupled. Throughout the paper we refer only to the rich vessel, with the understanding that when the rich vessel is charging, the lean vessel is discharging and vice versa.

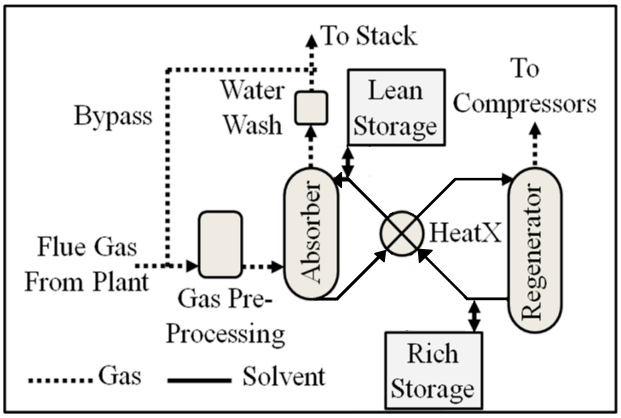

Figure 2.1: Simplified process flow diagram for plant equipped with CCS and solvent storage.

2.2.2 Plant Parameters

We used the Integrated Environmental Control Model (IECM) [15] to determine technical and cost parameters for all three base plants. We assumed that solvent storage tanks had flat bottoms, were fabricated on-site, above ground, with 304 stainless steel. The amine and ammonia tanks were assumed to have domed and internal floating roofs, respectively. We assumed the tanks had working capacities of 80% of their maximum capacities [16]. We further estimated solvent storage tank costs using Perry's Handbook [17] and scaled these costs to 2010 dollars using the Marshall and Swift Cost Index [18]. Parameters for each plant configuration are reported in Table 2.1. Further parameters are reported in the Supplementary Information.

Table 2.1: Plant parameters for each of the three technologies. PC = Pulverized Coal, NG = Natural Gas. Performance parameters based on IECM plant designs. Fuel prices based on 2010 utility-delivered prices in the U.S. [19]

	PC Amine	*PC Ammonia*	*NG Amine*
Max. Fuel Flow Rate [GJ/h]	6,790	6,790	3,790
Net Capacity [MW]	523	518	452
Reduction in Max Power from CCS	20.3%	14.1%	10.2%
CO_2 Concentration Into Absorber [%]	12.0%	12.0%	4.0%
Solvent Concentration [wt%]	30.0%	14.4%	30.0%
Max. CO_2 Capture Efficiency	90%	90%	90%
Steady State CCS Plant Capital [$M]	1,320	1,460	485
Cost for 100 min Storage Capacity [$M]	3.9	2.4	2.0
Fuel Price [$/GJ]	2.37	2.37	6.66

2.2.3 CO_2 Emissions and Sales Prices

A number of proposed climate mitigation policies, including carbon taxes and cap and trade, would create a price on CO_2 emissions. A sufficiently high price would be an important incentive for CCS, as it would directly penalize CO_2 emissions. It would also exert upward pressure on electric energy prices. We present results for CO_2 emissions prices, ranging from $0/tonne to $100/tonne, that are constant over the life of the plant. We recognize CO_2 emissions price regimes would likely feature increasing, rather than constant prices. We adopted a constant price model both to improve transparency and to avoid confounding the effect of the *level* of CO_2 emissions prices with the *trajectory* of these prices.

We acknowledge that CO_2 emission price trajectories, such as those studied by the EIA in their assessment of the American Power Act of 2010 [20], may be more representative of actual carbon pricing schemes than constant prices. However, annualizing the carbon prices under such a trajectory provides an approximate map from the trajectories to the constant CO_2 emissions prices considered here. We discuss this matter further in the Supplementary Information.

Use of captured CO_2 for enhanced oil recovery (EOR) offers a potential new revenue stream for operators of CCS-equipped power plants. Though the GHG reduction merits of using captured CO_2 for EOR have been challenged [21], our primary interest here is its effect on profitability. To the

best of our knowledge, there is not a well-established price paid to providers of CO2 for the purposes of EOR. Rubin et al. [22] uses a price of $10/tonne, while Austell et al. [23] uses a price of $48/tonne. In this work, we considered CO_2 sales prices ranging from $0/tonne to $50/tonne.

In our results, we refer to the price paid *by* a plant to emit a tonne of CO_2 into the atmosphere as the *CO_2 emissions price*. We refer to the price paid *to* the plant by an EOR operator, in exchange for a tonne of the plant's captured CO_2, as the *CO_2 sales price*. We refer to both prices jointly as *CO_2 prices*.

2.2.4 CCS Energy Penalty

The largest portion of the CCS energy penalty is incurred in operating the regenerator (see Figure 2.1). Both types of flexibility considered in this paper allow the regenerator flow rate, and therefore the energy penalty, to be temporarily reduced. During flue gas bypass, the regenerator flow rate is reduced and capture efficiency decreases, while during solvent storage, the regenerator flow rate is reduced and capture efficiency is maintained.

Equation (2.1) shows the model used to assess the energy penalty for both bypass and solvent storage. The model shows a relationship between heat input to the boiler $x^H(t)$ (GJ/h), the heat rate of the unit at steady-state regeneration *HR* (GJ/MWh), net power output $x^P(t)$ (MWh), and the regenerator flow rate $x^R(t)$ (tonne/h). The model incorporates proportionality constants k (GJ/tonne) and N (tonne/GJ), which are related to plant and carbon capture technologies and were estimated based on IECM parameters, as detailed in the Supplementary Information.

$$x^P(t) = \frac{x^H(t)}{HR}\left[1 + k\left(N - \frac{x^R(t)}{x^H(t)}\right)\right] \tag{2.1}$$

We note that this model represents a simplification of the actual dynamics of a CCS-equipped plant. The model assumes both that the capture system operates with a constant rich solvent to lean solvent CO_2 loading and that the energy required to regenerate a unit of rich solvent is constant regardless of regenerator flow rate. Furthermore, equation (2.1) assumes that steam diverted from the regenerator to the turbine has a constant effect on plant output whereas in reality turbines are

optimized for a particular steam flow rate. Real systems may deviate from these assumptions, but these deviations likely represent second-order effects.

2.2.5 Electric Energy Price Modeling

We employed a method similar to that of Cohen et al. [6] to determine the effect of a CO2 emissions price on electric energy prices. In the presence of a CO2 emissions price, marginal costs would increase for CO2-emitting generators. This increase in marginal costs would lead to an increase in electric energy prices. Using PJM marginal fuel postings [24], we determined marginal CO_2 emissions factors as a function of load. We used these emissions factors to construct a carbon price adder, which we added to the weighted-average 2010 PJM Day-Ahead Locational Marginal Price (LMP)[4] time series. Details of this method are available in the Supplementary Information.

Our method of adjusting LMPs implicitly assumes that system dispatch and emissions factors do not change with a CO_2 emissions price. In reality, we would expect to see increased dispatch of less CO_2-intensive generators and the eventual deployment of CCS across the power system. This might occur if the marginal unit had a higher emissions factor than the first out of merit unit and the CO_2 emissions price were high enough to swap the position of these two units in the dispatch curve. However, at low CO_2 prices, we would not expect changes in the dispatch order or large-scale deployment of CCS. Nonetheless, our method may result in exaggerated LMP increases at CO_2 prices above which CCS becomes profitable. Since our results indicate that flexibility is not profitable in this region, this limitation is unlikely to affect our qualitative results and conclusions.

[4] Locational Marginal Prices specify the electric energy price at each node in the PJM network for each hour of the year. The weighted average LMP used in this work is a time series constructed by PJM by weighting each node by its load and averaging.

2.2.6 Operating Model

In order to determine the value of flexible CCS, we constructed an optimization model that makes operating decisions for the plant in such a way as to maximize profits. The full formulation of the model is available in the Supplementary Information, but the objective function is described here.

The operating objective function shown in equation (2.2) includes the marginal revenues and costs associated with operating the plant. Revenues are the product of hourly electric energy prices $P^{E}(t)$ ($/MWh) and net electric power output $x^{P}(t)$ (MW) plus the product of hourly CO_2 sales price P^{CO2} ($/tonne) and hourly CO_2 sales $x^{G}(t)$ (tonne/h). Variable operations and maintenance costs have a component C_H^{VOM} ($/GJ) depending on heat input $x^{H}(t)$ (GJ/h), and a component C_R^{VOM} ($/tonne/h/h) depending on regenerator flow rate $x^{R}(t)$ (tonne/h). Carbon emissions costs are calculated as the product of the CO_2 emissions price C^{CO2} ($/tonne) and the hourly CO_2 emissions $x^{CO2}(t)$ (tonne/h). Note that the CO_2 emitted depends on the amount of CO_2 bypassed, as well as the heat input to the plant. Startup costs $C^{SU}(t)$ ($/start) are also included. The parameter δ corresponds to the model time step of 1 hour. More formulation details are available in the Supplementary Information.

$$\pi^{A} = \delta \sum_{t \in T} \left[\begin{array}{l} x^{P}(t)P^{E}(t) + x^{G}(t)P^{CO2} - x^{H}(t)C_H^{VOM} - x^{R}(t)C_R^{VOM} \\ -C^{CO2}x^{CO2}(t) - C^{SU}(t) \end{array} \right] \tag{2.2}$$

The operation of the plant was subject to constraints capturing the energy penalty of CCS (as in equation (2.1)), the dynamics of the solvent storage system, plant ramp rate limits, minimum regenerator flow rates, coupling between regenerator and absorber with solvent storage, and the relationship between heat input and CO_2 produced.

2.2.7 Optimal Sizing Model

A plant with CCS and solvent storage could be designed with a range of storage vessel capacities and regenerator sizes. A larger storage vessel size allows the unit to sustain elevated power output levels for longer times while maintaining capture efficiency. An oversized regenerator allows the plant to be operated at maximum fuel input rate while drawing down the level of the rich solvent storage tank. Rather than use a heuristic to determine the sizes of these components, our approach was to optimally size the storage vessel and regenerator so as to maximize the net present value of the plant over its operating life. For this analysis, we assumed that the plant would face the same real prices and costs every year of its operating lifetime.

In order to determine the solvent storage capacity and regenerator size, the operating model was nested inside a discounting model that selects these design parameters in order to maximize the net present value of the plant. Equation (2.3) shows the model used for this purpose. The net present value z ($) includes a discounted annual cost component that is the product of a discount factor P/A (dimensionless) and the difference between the annual operating profits π^A (from equation (2.2)) and annual fixed O&M costs C^{FOM} ($). It also includes capital costs C^K ($). Note that fixed O&M costs are dependent on the regenerator size, and capital costs are dependent on the solvent storage capacity and regenerator size. For all technologies, a real weighted average cost of capital of 7% and plant lifetime of 30 years were used [15].

$$z = P/A\left(\pi^A - C^{FOM}\right) - C^K \tag{2.3}$$

2.2.7.1 Regenerator Undersizing Constraint

Allowing the regenerator to be undersized can lead to a condition in which plant components are reduced in size to the point where the plant can no longer operate. We therefore constrained plant designs to be able to operate at full heat input rate for a minimum of 8 hours without

bypassing. This constraint implies that solvent storage capacity must be increased as regenerator size decreases. Operation of a unit with an undersized regenerator is described in more detail in section 1.1.1. Details of the undersizing constraint can be found in the Supplementary Information.

2.2.8 Imperfect Information

Note that the work described in section 2.2.8 was largely performed by Eric Hittinger. I retain it here for clarity in understanding the overall work.

The operating model described in section 2.2.6 has perfect foreknowledge of all electric energy prices over the life of the plant. While results from that model provide a useful upper bound on the value of flexibility, real operators do not possess such knowledge. In order to obtain a lower bound, we constructed an operating model based on imperfect information.

Conceptually, the perfect and imperfect information models are similar in that they both determine how a plant should be operated in order to maximize profits. However, whereas the perfect information model sees all current and future electric energy prices and can choose any operating schedule within the operating constraints of the plant, the imperfect information model is much more limited. It looks only at current and a limited set of past electric energy prices in deciding how to operate the plant in the current period.

Specifically, when the electric energy price exceeds the plant's marginal cost of production, the imperfect information model increases the plant's output, subject to ramp rate limitations, minimum and maximum generation levels, and other operating constraints. When the price is below marginal costs, the plant reduces its output subject to the same constraints.

To determine whether to startup or shutdown, the imperfect information model performs a highly simplistic forecast of the next twenty-four hours, making the assumption that the next twenty-four hours will experience the same price changes as the last twenty-four hours, relative to the current electricity price. For example, if the current price is $10/MWh higher than the same

hour yesterday, the model assumes that the prices for the next twenty-four hours will all be $10/MWh higher than the same hour the day before. Using this forecast of electricity prices, if the plant is offline and it forecasts positive profits over the next twenty-four hours (accounting for startup costs), it will start up (otherwise it will stay offline). If the plant is online and forecasts a loss over the next twenty-four hours, it will shut down (otherwise it will stay online). Note that the decision to start up or shut down is made every hour based on that hour's electric energy prices and the prices over the previous twenty-four hours.

The imperfect information model makes decisions about solvent storage and bypass by comparing the current period's electric energy price to a set of *threshold prices*: $P_{process} < P_{store} < P_{bypass}$. If the current period's electric energy price is below $P_{process}$, the plant regenerates additional rich solvent. If the current period's electric energy price is above $P_{process}$ and below P_{store}, the plant regenerates at steady state. If the current period's electric energy price is above P_{store} and below P_{bypass}, the plant reduces the regenerator flow rate and stores rich solvent. If the current period's electric energy price exceeds, P_{bypass}, the plant performs flue gas bypass.

The threshold prices were determined independently for each technology and set of CO_2 prices by using an optimization procedure to determine the threshold prices that maximize plant NPV. The selected threshold prices are constant throughout the year.

2.2.9 New Source Standard for GHGs

Following its finding of endangerment for greenhouse gases [25], the EPA proposed a new source standard for GHG emissions that would limit the (gross) CO_2 emissions rate of new electric generating units to 1,000 lb/MWh [26]. Though the agency has not finalized the rule, a June 2013 Presidential Memorandum directed the agency to propose a new rule by September 2013 [27]. The proposed rule imposes an emissions rate limit of 1,000 lb/MWh for some unit types and 1,100 lb/MWh for others [28].

In order to simulate the effect of an eventual new source standard, we imposed an annual-average emissions rate limit of 1,000 lb/MWh on the plants considered in this study. Note that since the final rule is still pending, this constraint is only intended to approximate the effect of the eventual rule. The annual average emissions rate constraint limits the total amount of flue gas bypass at a plant, but retains the operator's flexibility to bypass larger amounts during peak periods.

2.2.9.1 Technology Parameters

In our results, we report the capacity of the solvent storage system in electric energy units (MWh) rather than physical units (tonne). This choice of units makes more apparent the difference in useful energy storage available between the three technologies and provides a metric more directly related to the potential for the storage to increase revenue in the electric energy market. The relationship between the physical and energy storage capacities follow from equation (2.1) and are reported explicitly in equation (2.4). The solvent storage capacity expressed in MWh, $\overline{x^E}$, is proportional to the solvent storage capacity expressed in tonne, $\overline{x^S}$, with parameters k and HR as in equation (2.1).

$$\overline{x^E} = \frac{k}{HR}\overline{x^S} \tag{2.4}$$

2.3 Results and Discussion

Note that the results for the imperfect information model described in section 2.3 are largely the work of Eric Hittinger. I retain them here because they lend additional insight.

Across a number of scenarios, flexibility was found to increase the NPV of all three technologies for low CO_2 emissions and sales prices. Under some scenarios, a portion of this "flexibility benefit" could be attributed to undersizing the regenerator. We found that the flexibility benefit declined with increasing CO_2 emissions and sales prices. Furthermore, we found that this decline was such that the flexibility benefit declined to zero by the time CO_2 prices reached a level where the overall plant was

NPV positive. In other words, flexibility had no effect on break-even CO_2 prices. These results were robust to the use of the imperfect information model.

We discuss results in the absence of CO_2 prices in section 2.3.1. In section 1.1.1, we discuss how a plant can be operated with an undersized regenerator and how this can improve profitability. In section 2.3.3 we show the effect of increasing CO_2 emissions prices on optimal plant design and the flexibility benefit. In section 2.3.4 we show that the flexibility benefit declines to zero before the plant's NPV becomes positive and therefore does not affect breakeven CO_2 emissions or sales prices. In section 2.3.5 we show cost and revenue break downs for the PC+Amine technology under a variety of scenarios and CO_2 prices.

2.3.1 Effects of Flexibility on NPV and Optimal Design Without CO_2 Prices

Table 2.2 shows the increases in NPV with flexibility (the "flexibility benefit"), as well as optimal solvent storage capacities and regenerator sizes, in the absence of both CO_2 emissions and CO_2 sales prices. The flexibility benefit was positive for all technologies and scenarios, but not large enough to overcome the large negative NPV of the *Base* scenario.

Table 2.2 shows results for a non-flexible base scenario and three flexibility scenarios. In the *Base* scenario, the unit is equipped with CCS at 90% capture, but flue gas bypass and solvent storage are not allowed. The *Full Flex* scenario allows flue gas bypass, solvent storage, and regenerator undersizing[5]. The *No Undersize* scenario allows bypass and solvent storage, but the regenerator is constrained to be at least as large as would be required for steady state operations. The *No Bypass* scenario allows solvent storage and regenerator undersizing, but the unit is constrained to route all

[5] Regenerator undersizing involves selecting a regenerator smaller than what would be required to achieve 90% capture in the absence of solvent storage. We discuss undersizing in detail in section **Error! Reference source not found.**.

flue gases through the capture train. Note that all bypass scenarios are constrained by the annual average emissions rate cap.

In the *Full Flex* scenario, flexibility results in an NPV increase of just over half a billion dollars for the PC+Amine technology, an increase of 27% compared to the *Base* scenario NPV. The PC+Ammonia and NG+Amine technologies show NPV increases of 22% and 18%, respectively. The optimal design for all three technologies is to use the maximum allowable solvent storage capacity and the minimum allowable regenerator size.

In the *No Undersize* scenario, flexibility results in an NPV increase of $300 million for the PC+Amine technology, an increase of 13% compared to the *Base* NPV. The PC+Ammonia and NG+Amine technologies show NPV increases of 8% and 6%, respectively. In the *No Undersize* scenario, the optimal regenerator size is still the smallest allowable (now 100% of the steady state size). However, while some storage capacity is optimal here, storage is not deployed to the maximum extent as it is in the scenario of full flexibility.

In the *No Bypass* scenario, flexibility results in an NPV increase of $150 M for the PC+Amine technology, an increase of 7% compared to the *Base* NPV. The PC+Ammonia and NG+Amine technologies show NPV increases of 8% and 6%, respectively. In the *No* Bypass scenario, the optimal regenerator is undersized, but not to the maximum extent possible. For the PC+Amine and NG+Amine technologies, some, but not maximum, storage capacity is optimal. Storage is maximized for the PC+Ammonia technology.

The fact that the flexibility benefit is higher for the PC+Amine technology under the *Full Flex* and *No Undersize* scenarios can be attributed to the fact that this technology has a higher CCS energy penalty compared to the PC+Ammonia and NG+Amine technologies. This translates into a larger increase in output with flexibility. However, the flexibility benefit is about equal for all technologies

under the *No Bypass* scenario, suggesting that the additional flexibility benefit of the PC+Amine plant is mostly attributable to flue gas bypass.

Table 2.2: Increase in NPV ("ΔNPV") compared to the Base scenario, annual-average gross emissions rate (Ave. E.R.), optimal solvent storage capacity and regenerator size, at zero CO_2 emissions and sales prices. Results are presented for the Full Flex, No Undersize, and No Bypass scenarios.

Tech	*Base*		*Full Flex*				*No Undersize*				*No Bypass*			
	NPV [$B]	Ave. E.R. [lb/MWh]	ΔNPV [$B]	Ave. E.R. [lb/MWh	Solvent Storage [MWh]	Regen [%]	ΔNPV [$B]	Ave. E.R. [lb/MWh	Solvent Storage [MWh]	Regen [%]	ΔNPV [$B]	Ave. E.R. [lb/MWh	Solvent Storage [MWh]	Regen [%]
PC + Amine	-2.2	1,000	0.59	1,000	450	58%	0.29	1,000	67	100%	0.15	210	320	70%
PC + Ammonia	-2.4	1,000	0.52	1,000	290	58%	0.19	1,000	220	100%	0.20	225	290	67%
NG + Amine	-.83	710	0.15	710	170	59%	0.05	685	13	100%	0.05	80	140	65%

2.3.2 Regenerator Undersizing

Table 2.2 shows that the *No Undersize* scenario (where the regenerator size is at least as large as for steady-state operations) has a lower NPV than the *Full Flex* scenario (where the regenerator size can be smaller than for steady-state operations). This result was somewhat surprising. Much of the previous literature on CCS with solvent storage assumed that the regenerator would have to be larger than what would be required for steady state capture [5]-[8]. An oversized regenerator is necessary to maintain full heat input while regenerating additional solvent.

However, our results indicated that NPV strongly decreased with increasing regenerator size. Figure 2.2A) illustrates this result, showing the NPV of the PC+Amine plant as a function of regenerator size for several solvent storage capacities. This result derives from the fact that the regenerator is a large component of the plant capital costs.

Furthermore, as shown in Figure 2.2B), a plant with an undersized regenerator can be operated in such a way as to maintain steady state capture[6]. Though all plants in this work are able to perform flue gas bypass and solvent storage, for simplicity Figure 2.2B) shows a plant *without* flue gas bypass.

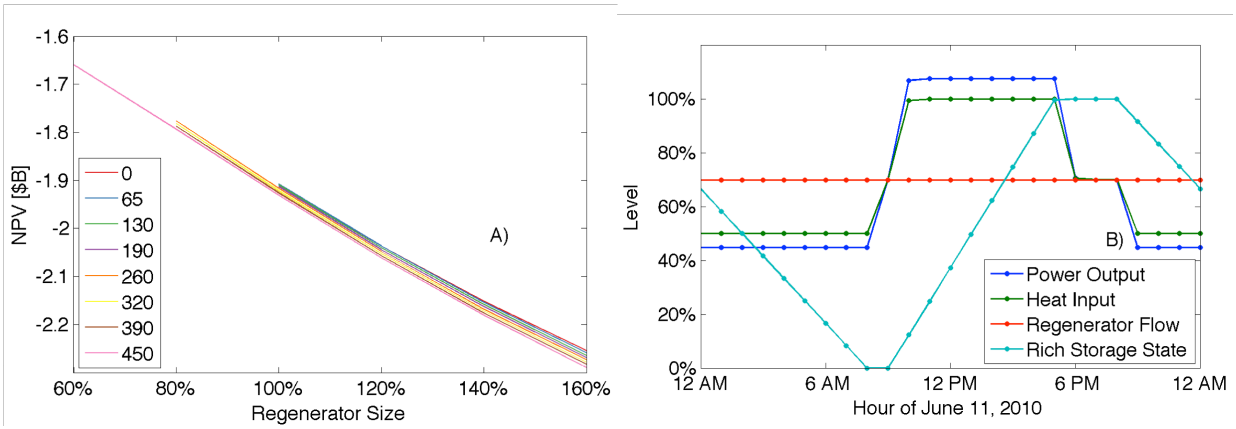

Figure 2.2: A) NPV of the PC+Amine plant vs. regenerator size in the *Full Flex* scenario, in the absence of CO2 prices. Colors indicate solvent storage vessel sizes in MWh. Results only shown for allowable region under the constraint that the plant must be able to operate at full heat input without bypassing for at least eight hours. B) Single day of operation of a

[6] Provided the absorber is scaled for steady state capture, something we assume throughout our results.

PC+Amine plant in the *No Bypass* scenario with $0/ton CO2 prices. Baseline levels: Power Output - maximum output of plant at steady state regeneration (523 MW); Heat Input - maximum heat input for the plant (6790 tonne/h); Regenerator Flow – flow rate through a regenerator sized for steady state capture at maximum heat input (8840 tonne/h); Rich Storage State – maximum solvent storage capacity (450 MWh).

The operations shown in Figure 2.2B) can be explained as follows. During the day, when electric energy prices are high, the plant produces maximum output. This is accomplished by applying full heat input and regenerating at less than the steady state rate. Operating in this manner entails producing more rich solvent than can be regenerated, so the level of the rich solvent storage vessel increases. Overnight, electricity prices fall, and the operator reduces heat input and electric energy output. Regenerating solvent at the same rate as it was being regenerated during the day now causes the rich solvent storage level to be reduced. This operation is timed in such a way as to empty the rich solvent vessel in time for high electric energy prices the next day. We note that though undersizing the regenerator leads to increased NPV through reduced capital cost, it also tends to reduce operating profits and that the overall NPV remains negative in the absence of CO_2 prices. This is discussed in more detail in section 2.3.5.

2.3.3 Effects of Increasing CO_2 Prices on Optimal Design

While we showed in Table 2.2 that bypass and solvent storage increase NPV in the absence of CO_2 prices (the "flexibility benefit"), we found that the benefit declines as CO_2 prices increase. Figure 2.3 shows this result. The figure shows optimal solvent storage capacity, regenerator size, and the flexibility benefit as functions of CO_2 emissions price, with CO_2 sales price set to zero. We note that the effect of CO_2 sales and emissions prices are quite similar, as will be shown in Figure 2.4, and we hold CO_2 sales price constant here only for simplicity of presentation.

Figure 2.3 shows results both for the *Full Flex* and *No Undersizing* scenarios. In the *Full Flex* scenario, solvent storage and regenerator undersizing are optimal below a CO_2 emissions price of $30/tonne for the PC+Amine technology, $40/tonne for the PC+Ammonia technology, and $50/tonne for the NG+Amine technology. However, above these prices, the flexibility benefit

disappears. In the *No Undersizing* scenario, none of the technologies show flexibility benefits above a CO_2 emissions price of $30/tonne.

Figure 2.3 also shows that results for the perfect and imperfect information models are broadly similar in terms of optimal storage capacity, regenerator size, and NPV. The maximum NPV difference between perfect and imperfect information models is about $100 million, or about 10% of the overall NPV. The perfect and imperfect information results become identical above the CO_2 emissions price where the flexibility benefit goes to zero.

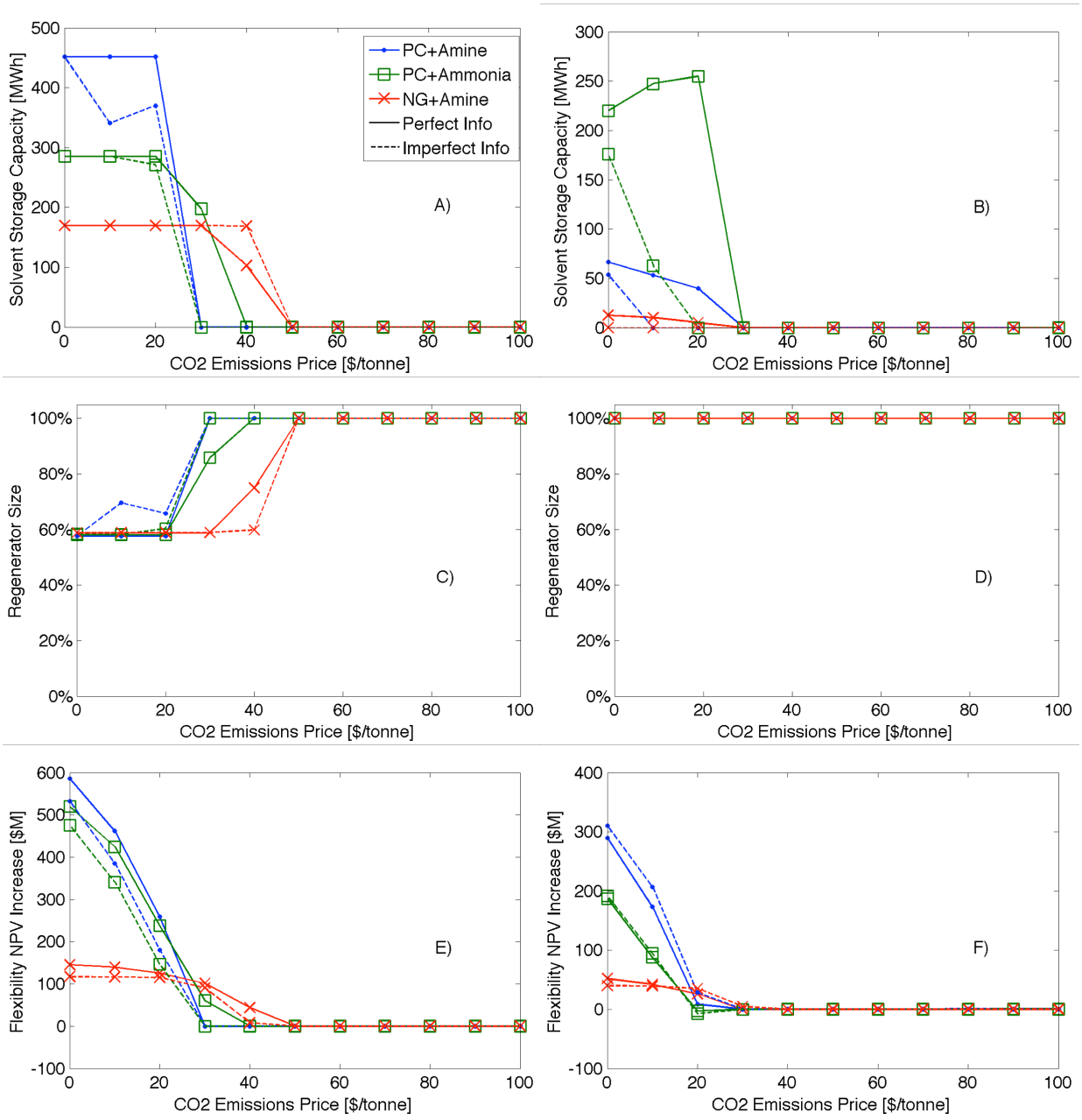

Figure 2.3: Optimal solvent storage capacity, in the absence of a CO2 sales price, in A) the *Full Flex* scenario, B) the *No Undersizing*. Regenerator size, in the absence of a CO2 sales price, in C) the *Full Flex* scenario, D) the *No Undersizing* scenario. NPV increase associated with flexibility (the "flexibility benefit") in E) the *Full Flex* scenario, F) the *No Undersizing* scenario.

Figure 2.3 shows that the flexibility benefit decreases with CO_2 emissions price for all technologies. Both bypass and solvent storage contribute to the flexibility benefit. The bypass component decreases with CO_2 prices because increased CO_2 prices lead to either increased direct costs or opportunity costs in the form of lost revenues from CO_2 sales. The solvent storage

component decreases with CO_2 prices because, in the absence of an oversized regenerator (and the capital costs of regenerator oversizing make it prohibitively expensive), using solvent storage requires that the plant eventually reduce its output for a time so that rich solvent can be regenerated (as in Figure 2.2B). This reduction in capacity factor is essentially an opportunity cost of using solvent storage and this opportunity cost increases with CO_2 emissions and sales prices.

2.3.4 Effects of Flexibility on Breakeven CO_2 Prices

Figure 2.4 shows NPV at optimal storage configuration, in the *Full Flex* scenario, for all three technologies, as a function of CO_2 emissions price and CO_2 sales price. It also shows the region for which flexibility increases NPV and the region where the overall plant is NPV-positive. As can be seen from the figure, these two regions do not overlap. Flexibility does not increase NPV for CO_2 prices where the overall plant has positive NPV for any of the three technologies.

The above observation implies that flexibility does not affect breakeven CO_2 emissions or sales prices. As we observed in Figure 2.3 and discussed in section 2.3.3, the flexibility benefit declines with CO_2 emissions prices due to the increasing opportunity cost of reduced plant output during regeneration. Figure 2.4 shows that the flexibility benefit falls to zero at CO_2 prices below those at which the overall plant becomes NPV positive.

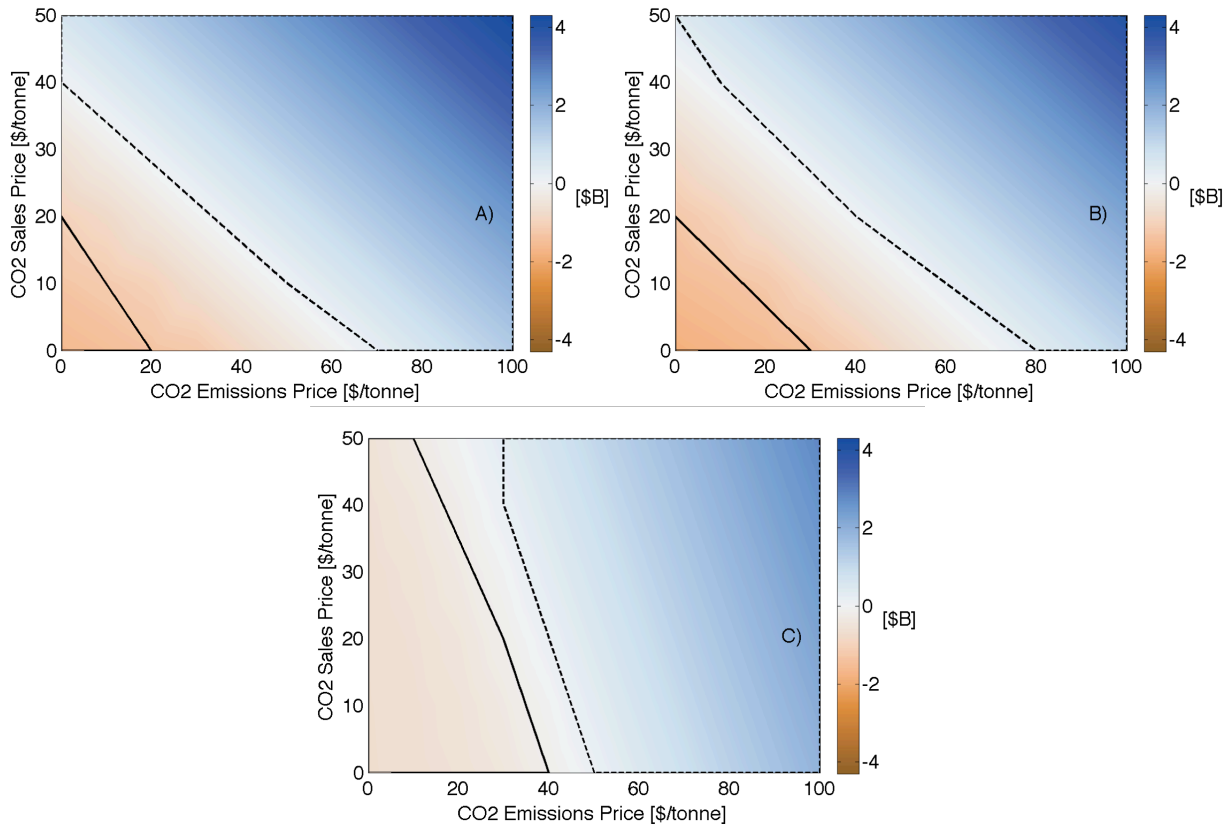

Figure 2.4: NPV as a function of CO2 emissions and sales prices, in the *Full Flex* scenario, for A) the PC+Amine plant, B) the PC+Ammonia plant, and C) the NG+Amine plant. Regions where flexibility increases NPV are enclosed in a solid black line. Regions where the overall plant is NPV positive are enclosed in a dashed black line.

Figure 2.4 also emphasizes that the flexibility benefits reported in Table 2.2 accrue to a plant with negative NPV. Though unlikely, we believe there are a couple of reasons that such a plant could conceivably be built. First, the plant might be the recipient of direct government subsidies. Such a subsidy could flip the sign on the after-subsidy NPV, but would not affect the unsubsidized NPV calculated in this paper. Second, a negative NPV plant might be built because it creates some value not measured in the NPV framework. Perhaps the generation owner believes that resource diversity is valuable and does not want to find themselves exclusively building gas plants. In section 2.4, we discuss future work that attempts to quantify some of the value that goes unmeasured in the framework of this work.

2.3.5 Cost and Revenue Breakdown

Figure 2.5 shows cost and revenue breakdowns for the PC+Amine technology for several scenarios and CO_2 prices. Figure 2.5A) shows the breakdown in the absence of any CO_2 prices, under four scenarios. Note that for all scenarios in Figure 2.5A), flexibility increases NPV compared to the *Base* scenario, but not enough to result in positive NPV.

In the *Base* scenario, no flexibility is allowed, whereas some flexibility is allowed in the *Full Flex*, *No Undersize*, and *No Bypass* scenarios. We observe that the "Turbine Capital" cost component is zero in the *Base* scenario and non-zero everywhere else, as an oversized turbine is required to handle the additional steam load incurred during bypass or solvent storage. We also note that the "Regenerator Capital" cost component is largest for the *Base* and *No Undersize* scenarios, as regenerator undersizing is not possible in these scenarios. The *Base* and *No Undersize* scenarios also have higher fixed O&M, as a portion of this cost component is attributable to the regenerator.

The *Base* scenario also features a lower "Energy Sales" revenue component than the other scenarios. Most of the additional energy sales are due to bypass. This is evident from the fact that sales are lower in the *No Bypass* scenario compared to the other two flexibility scenarios. Energy sales are, however, slightly higher in the *No Bypass* scenario than in the *Base* scenario.

Figure 2.5B) shows cost and revenue breakdowns for three CO_2 emissions / sales price combinations. For all of these CO_2 price combinations, flexibility does *not* increase NPV and the optimal plant is not flexible. Therefore, there is no difference between the *Base*, *Full Flex*, *No Undersize*, and *No Bypass* results and we only show one for each CO_2 price combination. Under \$40/\$0 CO_2 emissions/sales prices, the plant still has negative NPV. Under \$70/\$0 CO_2 emissions/sales prices, the plant has positive NPV. CO_2 costs increase, but energy sales increase even more, due to the fact that electricity prices increase with CO_2 prices. The \$40/\$0 CO_2 emission/sales price results show how the plant can break even due revenues from CO_2 sales.

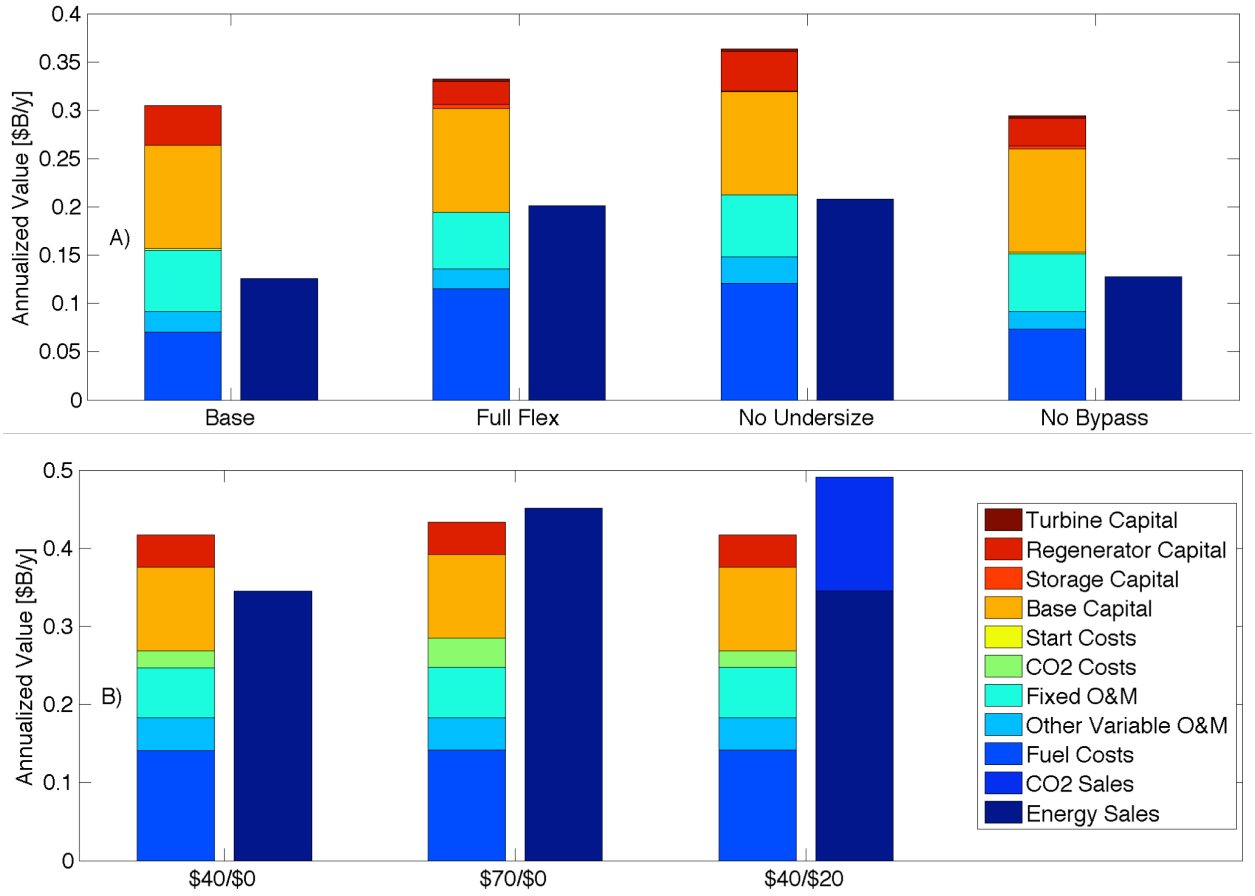

Figure 2.5: Annualized cost and revenue breakdown for the optimal design for the PC+Amine technology. A) shows results for four scenarios in the absence of CO_2 emissions and sales prices. Flexibility increases NPV compared to the *Base*, no-flexibility scenario in this part of the figure. B) shows results at three CO_2 emissions / CO_2 sales price combinations. Flexibility *does not* increase NPV in this part of the figure, so only a single scenario is shown for each combination of CO_2 prices.

2.4 Conclusions

We performed a study to examine the effects of flue gas bypass and solvent storage on the profitability of power plants equipped with CCS. Our framework incorporated both a design optimization model to determine how to size the solvent storage vessel and regenerator, and an operating model to determine how a flexible CCS plant would be optimally operated. At low CO_2 emissions and sales prices, flexibility led to large increases in NPV (the "flexibility benefit") for the PC+Amine plant, the PC+Ammonia plant, and the NG+Amine plant, relative to the no-flexibility scenario. Some of the flexibility benefit derived from allowing the regenerator to be undersized. We

found that the flexibility benefit decreased with CO_2 emissions and sales prices, reaching zero below CO_2 prices where the overall plant was NPV-positive. Flexibility therefore had no impact on breakeven CO_2 emissions or sales prices. We conclude that flexibility can provide a profitability boost for plants built under policies that force 90% capture-efficient CCS without pricing CO_2. However, flexibility is not justified on profitability grounds under policies that create high CO_2 emissions or sales prices.

Our results also have implications for the design of flexible CCS systems. Where flexible CCS was optimal, it was often built with maximum solvent storage capacity. Additionally, the optimal regenerator size was always the steady state size or *less*. In contrast to the assumptions made in much of the work on the topic of flexible CCS, we conclude that oversizing the regenerator for the purposes of flexibility is unlikely to be economic.

Our results have a number of limitations that are worth highlighting. Our model of electric energy prices in the presence of CO_2 emissions prices, though building on a model found in the literature [6], is a significant driver of uncertainty due to the wide range of effects CO_2 prices might have on the electric energy market. Further, cost and performance parameters for plants with CCS, though modeled in great detail in the IECM, are inherently uncertain due to the absence of data from full-scale plants. Changes in these parameters could result in units being NPV-positive at lower CO_2 prices. However, they are unlikely to alter our conclusion that the value of storage declines with CO_2 prices.

We intentionally adopted a simplified accounting framework in order to facilitate comparisons between different storage configurations. A framework that tracked accounting details (e.g. taxation and depreciation) in greater detail might affect our quantitative results, though we would not expect it to affect our qualitative conclusions. We also note that our deterministic NPV framework ignores option values. We expect that a full options framework would increase the apparent value of

flexibility. Finally, we have elected to model only the market for electric energy. It might be possible for flexible CCS to earn revenues by providing ancillary services. However, due to the fact that the markets for these services are very small compared to the energy market [29], we consider this to be a minor effect.

We have concluded that flexible CCS is not privately profitable when the overall plant is NPV positive. However, the avoided cost to the grid of flexibility may still exceed the private costs. Through the (imperfect) analogy between solvent storage and grid-scale electric energy storage, flexible CCS provides a number of grid benefits. In future work, we will consider some of these benefits in order to value flexible CCS not just in terms of energy arbitrage, but also in terms of its potential to reduce electricity prices and generation capacity requirements, and to support the deployment of renewable generators.

2.5 References

[1] PJM, *Hourly Day-Ahead Bid Data 2010*. Valley Forge, PA: PJM Interconnection, 2011.

[2] M. R. Haines and J. E. Davison, "Designing carbon capture power plants to assist in meeting peak power demand," *Energy Procedia*, vol. 1, no. 1, pp. 1457–1464, Feb. 2009.

[3] M. Lucquiaud, H. Chalmers, and J. Gibbins, "Potential for flexible operation of pulverised coal power plants with CO2 capture," *Energy Materials: Materials Science and Engineering for Energy Systems*, vol. 2, no. 3, pp. 175–180, Sep. 2007.

[4] H. Chalmers, M. Lucquiaud, J. Gibbins, and M. Leach, "Flexible operation of coal fired power plants with postcombustion capture of carbon dioxide," *Journal of Environmental Engineering*, vol. 135, no. 6, pp. 449–458, 2009.

[5] S. M. Cohen, G. T. Rochelle, and M. E. Webber, "Optimal operation of flexible post-combustion CO2 capture in response to volatile electricity prices," *Energy Procedia*, vol. 4, no. C, pp. 2604–2611, 2011.

[6] S. M. Cohen, G. T. Rochelle, and M. E. Webber, "Optimizing post-combustion CO2 capture in response to volatile electricity prices," *International Journal of Greenhouse Gas Control*, vol. 8, pp. 180–195, May 2012.

[7] R. D. Brasington, "Integration and operation of post-combustion capture system on coal-fired power generation: load following and peak power," Massachusetts Institute of Technology, 2012.

[8] D. Patino-Echeverri and D. C. Hoppock, "Reducing the Energy Penalty Costs of Postcombustion CCS Systems with Amine-Storage," *Environ. Sci. Technol.*, vol. 46, no. 2, pp. 1243–1252, Jan. 2012.

[9] P. Versteeg, D. L. Oates, E. Hittinger, and E. S. Rubin, "Cycling Coal and Natural Gas-fired Power Plants with CCS," *Energy Procedia*, vol. 37, pp. 2676–2683, 2013.

[10] A. Newcomer and J. Apt, "Storing Syngas Lowers the Carbon Price for Profitable Coal Gasification," *Environ. Sci. Technol.*, vol. 41, no. 23, pp. 7974–7979, Dec. 2007.

[11] M. C. Woods, P. J. Capicotto, J. L. Haslbeck, N. J. Kuehn, M. Matuszewski, L. L. Pinkerton, M. D. Rutkowski, R. L. Schoff, and V. Vaysman, "Cost and performance baseline for fossil energy plants. Volume 1: Bituminous coal and natural gas to electricity final report," *National Energy Technology Laboratory*, 2010.

[12] A. B. Rao and E. S. Rubin, "A technical, economic, and environmental assessment of amine-based CO2 capture technology for power plant greenhouse gas control," *Environ. Sci. Technol.*, vol. 36, no. 20, pp. 4467–4475, 2002.

[13] P. Versteeg and E. S. Rubin, "A technical and economic assessment of ammonia-based post-combustion CO2 capture at coal-fired power plants," *International Journal of Greenhouse Gas Control*, vol. 5, no. 6, pp. 1596–1605, Nov. 2011.

[14] E. S. Rubin and H. Zhai, "The Cost of Carbon Capture and Storage for Natural Gas Combined Cycle Power Plants," *Environ. Sci. Technol.*, p. 120302160545000, Mar. 2012.

[15] CMU, "Integrated Environmental Control Model." Carnegie Mellon University, Pittsburgh, 2012.

[16] M. Baker, "The Basics of API 650," presented at the 2009 Aboveground Storage Tank Management Conference and Trade Show, Houston, 2009.

[17] R. H. Perry, D. W. Green, and J. O. Maloney, *Perry"s chemical engineers" handbook*, vol. 7. McGraw-Hill New York, 2008.

[18] CEJ, *Marshall & Swift Equipment Cost Index*, vol. 116, no. 64. Chemical Engineering, 2012, p. 2012.

[19] EIA, "Annual Energy Outlook 2012," *US Energy Information Administration*, pp. 1–252, Jul. 2012.

[20] M. Daymude, "Energy Market and Economic Impacts of the American Power Act of 2010," pp. 1–24, Jul. 2010.

[21] P. Jaramillo, W. M. Griffin, and S. T. McCoy, "Life Cycle Inventory of CO 2in an Enhanced Oil Recovery System," *Environ. Sci. Technol.*, vol. 43, no. 21, pp. 8027–8032, Nov. 2009.

[22] E. S. Rubin, A. B. Rao, and C. Chen, "Comparative assessments of fossil fuel power plants with CO2 capture and storage," 2004.

[23] J. M. Austell, M. E. Moore, and C.-W. Hustad, "CO2 for enhanced oil recovery needs enhanced incentives," presented at the Fourth annual conference on carbon capture and sequestration, Alexandria, Virginia, 2005, p. 8.

[24] PJM, *PJM Marginal Fuel Posting, 2010*. Monitoring Analytics, LLC, 2011.

[25] EPA, *Endangerment and Cause or Contribute Findings for Greenhouse Gases Under Section 202 (a) of the Clean Air Act*. 74 FR 66496, 2009.

[26] EPA, *Standards of Performance for Greenhouse Gas Emissions for New Stationary Sources: Electric Utility Generating Units*. 77 FR 22391, 2012.

[27] B. Obama, "Presidential Memorandum -- Power Sector Carbon Pollution Standards," *White House*, 25-Jun-2013.

[28] EPA, *Standards of Performance for Greenhouse Gas Emissions from New Stationary Sources: Electric Utility Generating Units*. 2013, pp. 1–463.

[29] MMU, "State of the Market Report for PJM - 2011," Monitoring Analytics, LLC, Mar. 2012.

[30] PJM, *PJM Day-Ahead LMP Data 2010*. PJM Interconnection, 2011.

A Appendix

A.1 Imperfect Information Model

Note that section A.1 describes the imperfect information model constructed largely by Eric Hittinger.

The imperfect information model uses the same set of operating constraints, the same energy penalty model, the same costs, and the same discounting framework as the perfect information model. It also uses the same set of input parameters (see below). It differs in that it considers only current and a limited set of past electric energy prices in making current period operating decisions. This is in contrast to the perfect information model, which considers all electric energy prices when making operating decisions. The decision-making in the imperfect information model is very simplistic and can be described in its entirety in several sentences. The explanatory text in the manuscript provides the reader a better understanding of the imperfect information model.

A.2 Model Parameters

Table A-1: Fixed model parameters. The same set of parameters were used for the perfect and imperfect information models.

Parameter	PC+Amine	PC+Ammonia	NG+Amine	Unit
$\overline{A}$	8840	3875	3035	tonne/h
$\overline{B}$	0.7	0.7	0.7	Dimensionless
C_B^K	1315000000	1464000000	485000000	$
C_{STO}^K	1.8767e+03	711.0900	2.1413e+03	$/tonne
C_{REG}^K	5.7100e+04	1.2931e+05	5.7957e+04	$/tonne/h
C_B^{FOM}	51500000	51500000	16200000	$/year
C_{REG}^{FOM}	1436.7	3277.4	2142	$/year/tonne/h
C^F	2.3739	2.3739	6.6649	$/GJ
C_B^{VOM}	0.26396	0.26387	0.060215	$/GJ
C_{REG}^{VOM}	3.8230e-05	2.3195e-04	1.4159e-04	$/GJ/tonne/h
C^{HS}	30008	30008	30008	$
C^{WS}	37969	37969	37969	$
C^{CS}	49604	49604	49604	$
C_T^K	30800000	19600000	11349000	$
$\overline{E}$	0.4536	0.4536	0.4536	tonne CO2/MWh
$\overline{H}$	6791	6791	3791	GJ/h
$\underline{G}$	0	0	0	tonne
$\overline{G}$	Unbounded	Unbounded	Unbounded	tonne
HR	12.996	13.117	8.3838	GJ/MWh
$\overline{H}'$	2000	2000	3791	GJ/h/h
$\underline{H}$	3395.5	3395.5	1895.5	GJ/h
k	0.19563	0.28775	0.14225	GJ/tonne
N	1.3017	0.57061	0.80058	tonne/GJ
$\overline{R}$	17680	7750	6070	tonne/h
$\underline{R}$	1768	775	607	tonne/h
$\overline{S}$	30000	13000	10000	tonne
$\underline{S}$	0	0	0	tonne
δ	1	1	1	hours
ε	0.090535	0.090535	0.050294	tonne/GJ
η	0.9	0.9	0.9	Dimensionless
ρ	0.070905	0.070905	0.070905	Dimensionless
τ^L	30	30	30	Years
τ^{WS}	12	12	12	hours
τ^{CS}	48	48	48	hours
$\tau^{\overline{H}}$	8	8	8	Hours
ϕ	0.2	0.2	0.2	Dimensionless

A.3 Electric Energy Price Model

In order to determine adjusted LMPs for futures in which generators were paying a CO2 price, we used a method similar to [6]. We used PJM marginal fuel data [24] along with emissions rates by fuel type to generate hourly marginal emissions rates. We then performed a spline regression to calculate the expected value of the marginal emissions rates as a function of load, using a different fit for summer and winter months. Marginal carbon costs as a function of load were generated by multiplying the carbon price by the smoothed marginal emissions curve. Each hourly LMP [1] was then translated up by the marginal emissions cost corresponding to its load. Figure A-1 shows a schematic of this process. For this analysis, we assumed that the plant would face the same prices and costs every year of its operating lifetime.

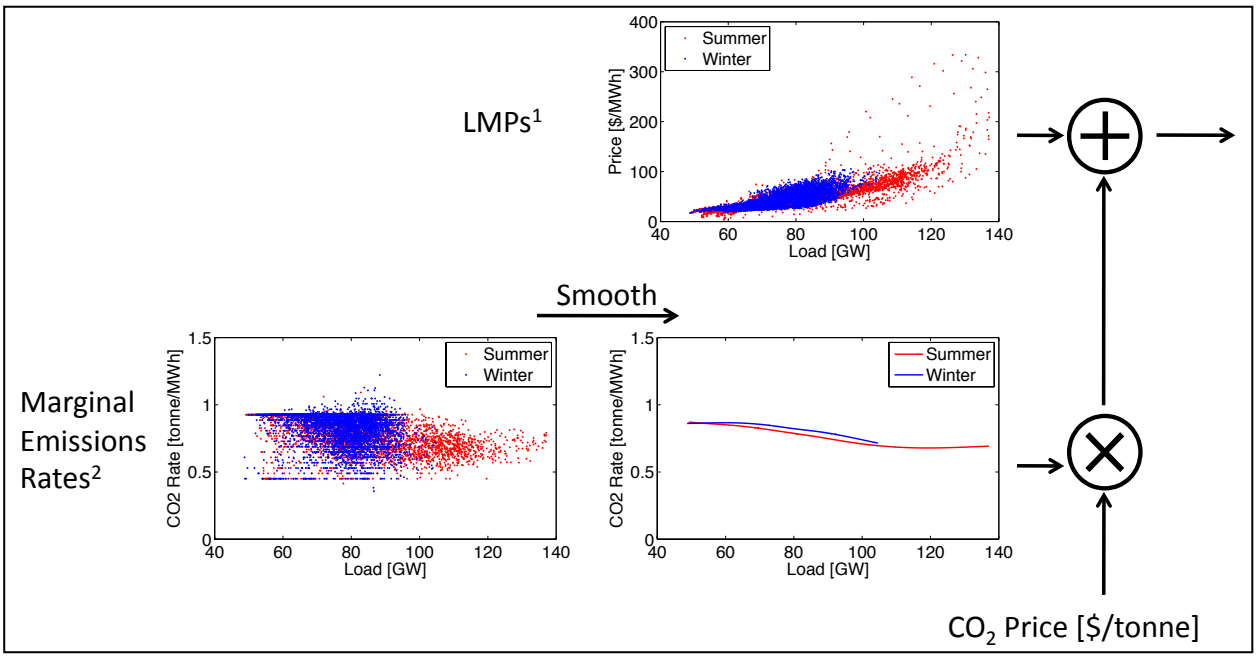

Figure A-1: Diagram showing the process of adjusting LMPs for a carbon dioxide price. Data sources: 1) [30] 2) [24]

Figure A-2 shows the modeled electric energy prices at CO_2 prices between \$0/tonne and \$100/tonne. Note that although the increase in electric energy prices with CO_2 prices is not quite linear, it is pretty close (see Figure A-5).

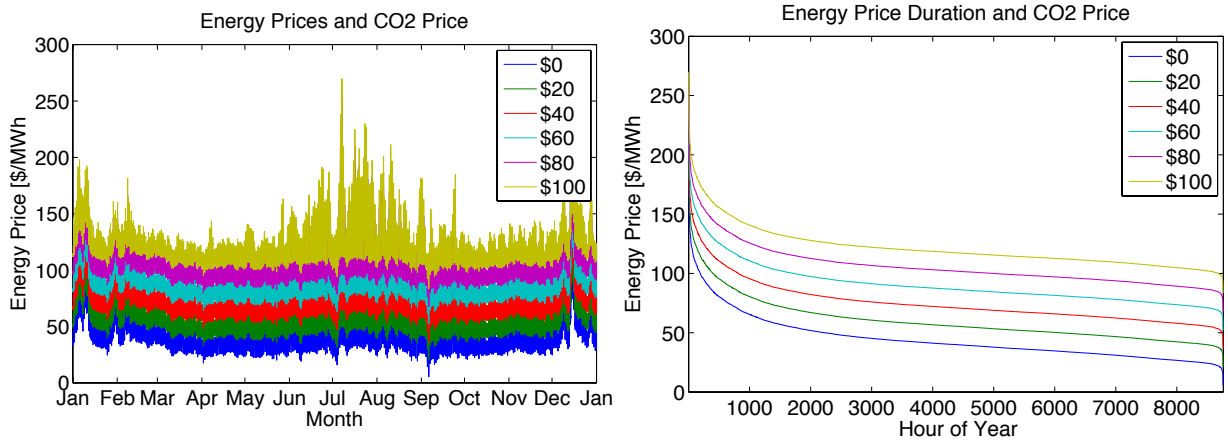

Figure A-2: Modeled electric energy prices in the different CO_2 price scenarios.

A.4 Energy Penalty Model

A key equation in the model formulation shows the relationship between heat input $x^H(t)$ [GJ/h], regenerator flow rate $x^R(t)$ [tonne/h], and net power output $x^P(t)$ [MW] for a unit equipped with flexible CCS. N [tonne/GJ] is the solvent required to capture 90% of the CO_2 produced during the combustion of a single GJ of fuel. It can be obtained directly from the IECM by dividing the steady state capture solvent flow rate by the maximum heat input of the plant. The parameter HR [GJ/MWh] is the heat rate of the unit at steady state. The parameter k [GJ/tonne] is the energy penalty of regeneration and N [tonne/GJ] is the solvent required to maintain 90% capture. These last two parameters were estimated for each technology by rearranging equation (2.5) as described below.

The energy penalty equation in the formulation can be rearranged to give equation (2.5), where $HR^N(t) = x^H(t)/x^P(t)$ is the net heat rate of the plant. As can be seen from examining equation(2.5), we expect a plot of $HR^N(t)$ vs. $x^R(t)/x^P(t)$ to be a straight line. The slope of the line should be k/(1+kN) and the intercept should be $HR^S/(1+kN)$.

$$HR^N(t) = \frac{1}{(1+k\cdot N)} HR^S + \frac{k}{(1+k\cdot N)} \frac{x^R(t)}{x^P(t)} \qquad (2.5)$$

Figure A-3 shows net heat rate vs. regenerator flow rate to net power output ratios for the three technologies from the IECM, as well as least squares fits of the data. R^2 values for the linear fits are all above 0.998. The slope and intercept of the fits can be compared to equation (2.5) to determine values for HR^S and k (using the known value of N).

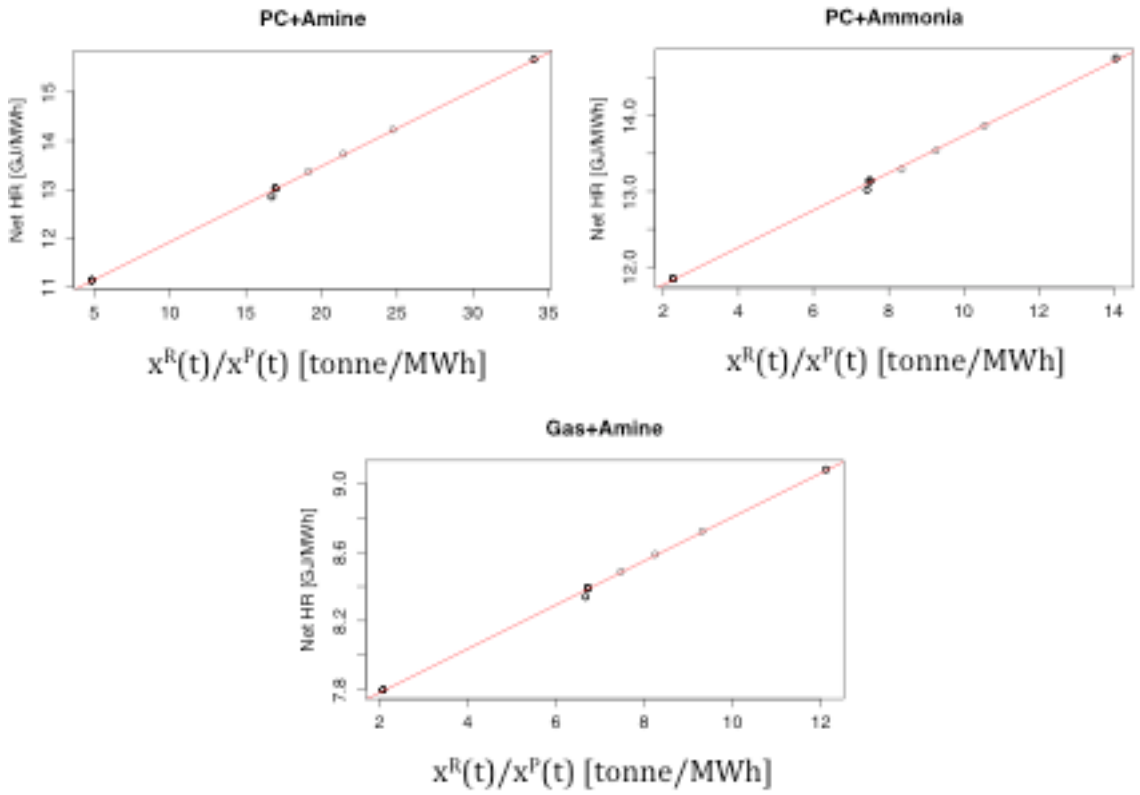

Figure A-3: Net heat rate vs. regenerator flow rate to net power output ratio for the three unit types. The intercepts on these plots are 10.4 GJ/MWh, 11.2 GJ/MWh, and 7.5 GJ/MWh for the PC+Amine, PC+Ammonia, and Gas+Amine plots, respectively.

Table A-1 shows parameters estimated from the fits in Figure A-3. Note that the values for N differ between the PC plants because the energy required to regenerate a tonne of amine solvent differs from that required regenerate a tonne of ammonia solvent. The values differ between the PC and Gas plants with amine solvent due to the lower concentration of CO_2 in the rich solvent in the gas plant.

Table A-2: Energy – heat – regenerator flow rate relationship parameters estimated from data in Figure A-3. Note that energy penalty of regeneration was calculated directly from the IECM and not estimated from the linear model.

	HR^S [GJ/MWh]	k [GJ/tonne]	N [tonne/GJ]
PC+Amine	13.0	0.196	1.3
PC+Ammonia	13.1	0.288	0.571
Gas+Amine	8.38	0.142	0.801

A.5 CO_2 Price Trajectories

This section discusses the implications of assuming a flat CO_2 price when it is more likely that such prices would follow an increasing trajectory over time. Figure A-4 shows CO_2 allowance price trajectories for several cases constructed by the EIA in analyzing the American Power Act of 2010. The allowance prices represent the market's response to the cap and trade system with declining emissions cap proposed by the Act. By 2035, the end of the modeling horizon, they expected allowance prices to range from $50/tonne in their lowest cost scenario to $185/tonne in the highest cost scenario.

A brief description of the CO_2 price trajectory scenarios follows. The Basic scenario involves large deployment of low-carbon technologies. The zero bank scenario assumes no allowances will be banked at the end of the 2035 time horizon. The High NG scenario is based on high availability of shale gas resources. The High Cost case is similar to the base case but involves higher capital costs for some baseload units. The No Intl. case does not allow use of international offsets. The Limited/No Intl. case combines the No Intl. case with low availability of low-carbon technologies. For more information on these scenarios, see [20].

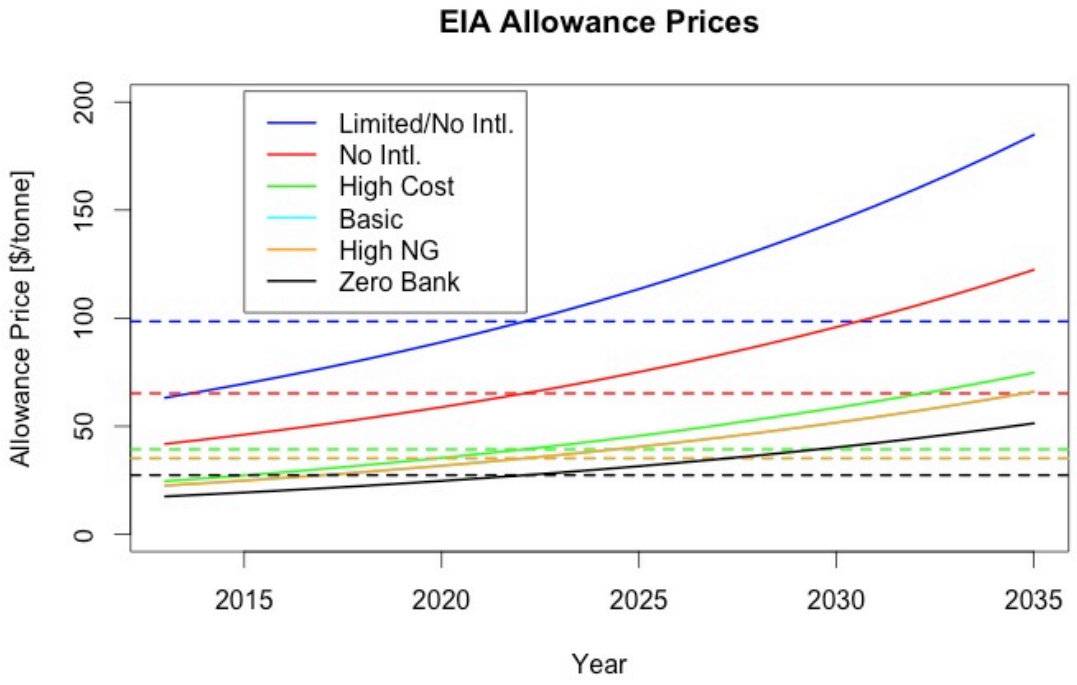

Figure A-4: CO_2 allowance price evolution over time from EIA modeling scenarios (solid lines), taken from [20]. Also shows annualized allowance prices (dashed lines) over the 23 year period at a 7% discount rate.

Figure A-4 also shows annualized allowance prices as dashed lines. The annualized prices are calculated by using an annualization factor (with an interest rate of 7% and period of 30 y [15]) to convert annual prices into a constant value. These annualized prices capture, in a single parameter, most of the effect of carbon prices on NPV. The annualization procedure can be thought of as a weighted average of the carbon prices, where early years receive higher weights compared to later years. Table A-3 shows the same annualized values that are shown in the figure.

Table A-3: Annualized CO_2 allowance prices.

Scenario	Annualized Price [$/tonne]
Zero Bank	27
High Natural Gas Resource	35
Basic	35
High Cost	39
No International	65
Limited / No International	99

The rational for performing this annualization is to allow interpretation of our results as roughly corresponding to one of the trajectories outlined by the EIA. For example, our results at \$100/tonne CO_2 correspond roughly to the Limited / No International scenario envisioned by the EIA. Our results at \$27/tonne correspond roughly to the Zero Bank scenario.

It should be noted that this correspondence is approximate. To understand this, note that the annualized allowance price metric defines an equivalence class for allowance price trajectories: trajectories resulting in the same annualized price belong to the same class. If the NPV of plants facing all allowance price trajectories in an equivalence class were equal, we could interpret our results for a given CO_2 price as corresponding *exactly* to an EIA trajectory with the same annualized price (rather than *roughly* as described in the preceding paragraph). This is not necessarily the case.

The fact that the approximation is useful reflects the fact, illustrated in Figure A-5, that electric energy prices are proportional to CO_2 emissions prices. This means that if a plant's operating schedule were the same for any CO_2 emissions price, the NPVs of plants facing allowance price trajectories in the same class would be equal (and the solvent storage capacity and regenerator size at optimality would also be equal).

However, plants are not operated the same way for any CO_2 emissions price. The value of flexibility in our results is essentially a step function. At low CO_2 emissions prices, the plant uses flexibility to obtain higher NPV, and at high CO_2 emissions prices, it does not. We therefore expect that allowance price trajectories (with equal annualized prices) that have years with CO_2 prices low enough for storage to be valuable prices would have higher NPV than those without.

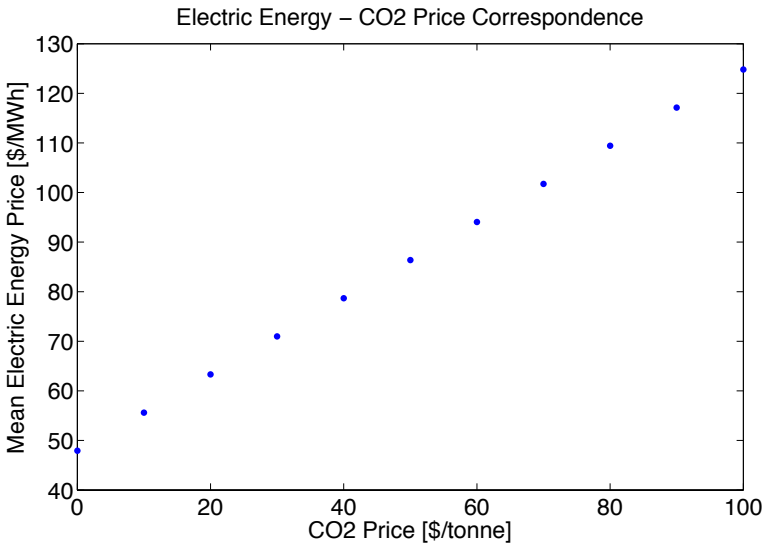

Figure A-5: The relationship between electricity price and CO_2 price, as captured by our CO_2 price-electric energy price model - is linear.

A.6 Model Formulation

Sets

$t \in T$	Time, in hours, from 1 to 8760
$t' \in T$	Alias for time, from 1 to 8760

Parameters

$P^E(t)$	Electric energy sale price in each period [$/MWh]
$\overline{S}$	Maximum capacity of solvent storage tanks [tonne]
$\underline{S}$	Minimum capacity of solvent storage tanks [tonne]
$\overline{R}$	Maximum regenerator size [tonne/h]
$\underline{R}$	Minimum regenerator size [tonne/h]
ϕ	Minimum regenerator flow rate as fraction of maximum
ρ	Weighted average cost of capital
τ^L	Lifetime of the plant [years]
C_B^K	Base plant capital cost [$]
C_{STO}^K	Capital cost scaling with size of storage vessel [$/tonne]
C_{REG}^K	Capital cost scaling with size of regenerator [$/tonne/h]
C_B^{FOM}	Base plant fixed O&M cost [$/year]
C_{REG}^{FOM}	Fixed O&M scaling with size of regenerator [$/year/tonne/h]
$\tilde{R}$	Estimated optimal regenerator size (for iterative solving) [tonne/h]
$\overline{H}$	Maximum heat input of plant [GJ/h]
$\overline{A}$	Absorber capacity [tonne/h]
C^F	Fuel cost [$/GJ]
C_B^{VOM}	Base plant variable O&M cost [$/GJ]
C_{REG}^{VOM}	Variable O&M scaling with size of regenerator [$/GJ/tonne/h]
L^H	Heat input in period before start of optimization [tonne/h]
L^{ON}	On/off status of plant in period before start of optimization
N	Solvent required at absorber to achieve 90% capture efficiency [tonne/GJ]
HR	Plant heat rate at steady state regeneration [GJ/MWh]
k	Heat required to regenerate solvent [GJ/tonne]
$\overline{H}'$	Maximum rate of change of heat input (ramp rate limit) [GJ/h/h]
$\underline{H}$	Minimum heat input of plant [GJ/h]
τ^{WS}	Offline time above which a start is considered warm [h]
τ^{CS}	Offline time above which a start is considered cold [h]
C^{HS}	Hot start cost [$]
C^{WS}	Warm start cost [$]
C^{CS}	Cold start cost [$]
ε	Base CO_2 emissions rate [tonne/GJ]
C^{CO2}	CO_2 emissions cost [$/tonne]
η	Maximum capture efficiency
$\overline{B}$	Maximum bypass possible, as fraction of total CO_2 emissions

$\overline{E}$	Maximum annual-average net emissions rate [tonne CO2/MWh]
$\tau^{\overline{H}}$	Minimum number of periods unit must be able to operate at max heat input [h]
C_T^K	Capital cost to oversize turbine if solvent storage or bypass are used [$]
$\underline{G}$	Minimum annual CO2 sales to satisfy contract [tonne]
$\overline{G}$	Maximum annual CO2 sales to satisfy contract [tonne]
P^{CO2}	CO2 sales price [$/tonne]
δ	Period length [hours]

Calculated Parameters

H^{SU}	Maximum heat that can be reached during first period of operation [GJ/h]
H^{SD}	Maximum heat that can be reached during final period before shutdown [GJ/h]
P/A	Present value factor

$$H^{SU} = \begin{cases} \underline{H}, \overline{H}' \le \underline{H} \\ \overline{H}', \overline{H}' > \underline{H} \end{cases} \quad [1]$$

$$H^{SD} = H^{SU} \quad [2]$$

$$P/A = \frac{(1+\rho)^{\tau^L} - 1}{\rho(1+\rho)^{\tau^L}} \quad [3]$$

Variables

z	Objective function value [$]	$(-\infty,\infty)$
π^A	Annual operating profits including fixed O&M [$/y]	$(-\infty,\infty)$
$y^{ON}(t)$	Binary on/off status of the plant in period t	{0,1}
$y^{SU}(t)$	Binary indicating that unit is starting up in period t	{0,1}
$y^{SD}(t)$	Binary indicating that unit is shutting down in period t	{0,1}
$y^{SUWARM}(t)$	Binary indicating that unit is performing a warm (or hot) start	{0,1}
$y^{SUCOLD}(t)$	Binary indicating that unit is performing a cold start	{0,1}
$x^P(t)$	Electric power produced by plant in period t [MW]	$[0,\infty)$
$x^H(t)$	Heat input to plant in period t [GJ/h]	$[0,\overline{H})$
$x^{RS}(t)$	Rich solvent storage vessel state in period t [tonne]	$[0,\infty)$
$x^{LS}(t)$	Lean solvent storage vessel state in period t [tonne]	$[0,\infty)$
$x^A(t)$	Solvent flow rate through absorber in period t [tonne]	$[0,\infty)$
$x^R(t)$	Solvent flow rate through the regenerator in period t [tonne]	$[0,\infty)$
$C^{SU}(t)$	Total start up cost incurred in period t [$]	$[0,\infty)$
$\overline{x^S}$	Solvent storage capacity [tonne]	$[\underline{S},\overline{S}]$
$\overline{x^R}$	Regenerator size [tonne/h]	$[\underline{R},\overline{R}]$
L^{RS}	State of rich solvent storage in period before start (depends on capacity)	$[0,\infty)$

	[tonne]	
L^{LS}	State of lean solvent storage in period before start [tonne]	$[0,\infty)$
$x^{B}(t)$	CO2 bypassing the absorber in period t [tonne/h]	$[0,\infty)$
y^{STORE}	Binary indicating whether unit is able to store solvent	{0,1}
y^{BYPASS}	Binary indicating whether unit is allowed to bypass absorber	{0,1}
$y^{OVERSIZE}$	Binary indicating whether unit must have oversized turbine	{0,1}
$x^{G}(t)$	CO2 sold at sale price [tonne/h]	$[0,\infty)$
$f(t)$	McCormick envelope variable for minimum regenerator flow rate constraint	$(-\infty,\infty)$

Objective

The objective is to maximize z, the net present value of plant operations over its lifetime. Equation 4 calculates the NPV by discounting the annual operating profits, after subtracting fixed O&M, and then subtracting capital costs. The capital costs depend on storage vessel and regenerator sizes.

Equation 5 calculates the annual operating profit. Profits include revenues from sale of electricity and CO_2, as well as fuel and other variable O&M costs (related to regenerator size) and CO_2 emissions costs. A portion of CO2 emitted is due to bypass, and a portion is due to imperfect capture efficiency.

$$z = P/A\left(\pi^{A} - C_{B}^{FOM} - C_{REG}^{FOM}\cdot\overline{x^{R}}\right) - C_{B}^{K} - C_{STO}^{K}\cdot\overline{x^{S}} - C_{REG}^{K}\cdot\overline{x^{R}} - C_{T}^{K}\cdot y^{OVERSIZE} \quad [4]$$

$$\pi^{A} = \delta\sum_{t\in T}\begin{bmatrix} x^{P}(t)\cdot P^{E}(t) + x^{G}(t)\cdot P^{CO2} - x^{H}(t)\cdot\left(C^{F} + C_{B}^{VOM}\right) - x^{R}(t)\cdot\left(C_{REG}^{VOM}\cdot\tilde{R}\right) \\ -C^{CO2}\cdot\left(x^{B}(t) + \varepsilon\cdot x^{H}(t)\cdot(1-\eta)\right) - C^{SU}(t) \end{bmatrix} \quad [5]$$

Storage Constraints

Equations 6-9 show the constraints that capture the dynamics of the rich and lean solvent storage vessels. Because these are difference equations, different constraints are required in the first period.

$$x^{RS}(t) = x^{RS}(t-1) + x^{A}(t) - x^{R}(t), \forall t > 1 \quad [6]$$

$$x^{RS}(t) = L^{RS} + x^{A}(t) - x^{R}(t), \forall t = 1 \quad [7]$$

$$x^{LS}(t) = x^{LS}(t-1) + x^{R}(t) - x^{A}(t), \forall t > 1 \quad [8]$$

$$x^{LS}(t) = L^{LS} + x^{R}(t) - x^{A}(t), \forall t = 1 \quad [9]$$

Energy Penalty Constraint

Equation 10 shows the energy penalty associated with regeneration. As shown by the equation, the more regeneration is performed, the less of the heat input can be converted into net electric power output.

$$x^{P}(t) \cdot HR = (1 + k \cdot N) \cdot x^{H}(t) - k \cdot x^{R}(t) \quad [10]$$

Ramping Constraints

Equations 11-14 are constraints on the change in heat input to the plant that can occur over time. They prevent changing heat input beyond a maximum heat input ramp rate. As these are difference equations, the first period constraints are different.

$$x^{H}(t) \le x^{H}(t-1) + \overline{H}' y^{ON}(t-1) + H^{SU} \cdot y^{SU}(t), \forall t > 1 \quad [11]$$

$$x^{H}(t) \le L^{H} + \overline{H}' L^{ON} + H^{SU} \cdot y^{SU}(t), \forall t = 1 \quad [12]$$

$$x^{H}(t) \ge x^{H}(t-1) - \overline{H}' y^{ON}(t) - H^{SD} \cdot y^{SD}(t), \forall t > 1 \quad [13]$$

$$x^{H}(t) \ge L^{H} - \overline{H}' y^{ON}(t) - H^{SD} \cdot y^{SD}(t), \forall t = 1 \quad [14]$$

Startup Binary Constraints

Equations 15-17 ensure that the startup binary is one when the unit has just started up and zero otherwise, and that the shutdown binary is one when the unit has just shutdown and zero otherwise.

$$y^{SU}(t) - y^{SD}(t) = y^{ON}(t) - y^{ON}(t-1), \forall t > 1 \quad [15]$$

$$y^{SU}(t) - y^{SD}(t) = y^{ON}(t) - L^{ON}, \forall t = 1 \quad [16]$$

$$y^{SU}(t) + y^{SD}(t) \le 1 \quad [17]$$

Heat Input Constraints

Equations 18-19 constrain the heat input to the plant to lie between the minimum and maximum levels, if the plant is on, and to be zero if the plant is off.

$$x^{H}(t) \geq y^{ON}(t) \cdot \underline{H} \quad [18]$$

$$x^{H}(t) \leq y^{ON}(t) \cdot \overline{H} \quad [19]$$

Startup Costs

Equations 20-22 ensure that warm and cold starts are penalized appropriately, and calculate total startup costs incurred in each period.

$$y^{SUWARM}(t) \geq y^{SU}(t) - \sum_{t'=t-\tau^{W}}^{t'=t-1} y^{ON}(t'), \forall t > \tau^{W} \quad [20]$$

$$y^{SUCOLD}(t) \geq y^{SU}(t) - \sum_{t'=t-\tau^{C}}^{t'=t-1} y^{ON}(t'), \forall t > \tau^{C} \quad [21]$$

$$C^{SU}(t) \geq y^{SU}(t) \cdot C^{HS} + y^{SUWARM}(t) \cdot \left(C^{WS} - C^{HS}\right) + y^{SUCOLD}(t) \cdot \left(C^{CS} - C^{WS}\right) \quad [22]$$

Solvent Storage and Regenerator Limits

Equations 23-26 constrain the operation of the regenerator and solvent storage vessel, ensuring that these do not exceed their capacities.

$$x^{RS}(t) \leq \overline{x^{S}} \quad [23]$$

$$x^{LS}(t) \leq \overline{x^{S}} \quad [24]$$

$$x^{R}(t) \leq \overline{x^{R}} \quad [25]$$

$$\overline{x^{S}} \leq y^{STORE} \cdot \overline{S} \quad [26]$$

Minimum Regenerator McCormick Envelope

Equations 27-31 show the McCormick envelope that constrains the minimum regenerator flow rate to a fraction of the maximum value. The McCormick envelope is necessary to avoid a quadratic term.

$$f(t) \le x^R(t) \quad [27]$$

$$f(t) \le y^{ON}(t) \cdot \phi \cdot \overline{R} \quad [28]$$

$$f(t) \le \phi \cdot \overline{x^R} + y^{ON}(t) \cdot \phi \cdot \underline{R} - \phi \cdot \underline{R} \quad [29]$$

$$f(t) \ge \phi \cdot \overline{x^R} + y^{ON}(t) \cdot \phi \cdot \overline{R} - \phi \cdot \overline{R} \quad [30]$$

$$f(t) \ge y^{ON}(t) \cdot \phi \cdot \underline{R} \quad [31]$$

Set Solvent Storage States in Previous Period

Equations 32-33 initialize the state of the rich and lean solvent storage vessels to half of their capacity.

$$L^{RS} = 0.5 \cdot x^S \quad [32]$$

$$L^{LS} = 0.5 \cdot x^S \quad [33]$$

Absorber Flow

Equation 34 shows the absorber flow rate that must be maintained in order to process the emissions produced by the heat input.

$$x^A(t) = N\left(x^H(t) - \frac{x^B(t)}{\varepsilon}\right) \quad [34]$$

Emissions Rate

Equation 35 shows the constraint on the gross emissions rate of the plant.

$$\overline{E}\sum_{t\in T}\left[x^P(t) + \frac{k}{HR}x^R(t)\right] \ge \sum_{t\in T}\left[x^B(t) + \varepsilon \cdot x^H(t) \cdot (1-\eta)\right] \quad [35]$$

Minimum Periods at Maximum Heat

In our preliminary results, we observed that the optimization was occasionally returning solutions where the plant was unable to operate at maximum heat input for very long. This arose

when CO_2 prices (and therefore electric energy prices) were low enough that reducing capital costs as far as possible and not operating were the most profitable strategy. Since we were interested only in comparing the profitability of *operating* plants with CCS with and without flexibility, it made sense to require the plant to operate. We therefore added a constraint requiring plants to be able to operate at maximum heat input for at least 8 hours without bypassing. Equation 36 shows this constraint.

$$\overline{H} \le \frac{1}{N}\left(x^R + \frac{x^S}{\tau^{\overline{H}}}\right) \quad [36]$$

CO_2 Sales and Bypass Constraints

Equations 37-40 constrain the amount of CO_2 that can be sold by the unit, as well as the bypass.

$$x^G(t) \le \eta \cdot \varepsilon \cdot x^H(t) - x^B(t) \quad [37]$$

$$x^B(t) \le \varepsilon \cdot \overline{H} \cdot \overline{B} \cdot y^{BYPASS} \quad [38]$$

$$\sum_{t \in T} x^G(t) \ge \underline{G} \quad [39]$$

$$\sum_{t \in T} x^G(t) \le \overline{G} \quad [40]$$

Turbine Oversizing Constraints

Equations 41-42 ensure that the turbine is oversized if the unit uses either bypass or storage.

$$y^{OVERSIZE} \ge y^{BYPASS} \quad [41]$$

$$y^{OVERSIZE} \ge y^{STORE} \quad [42]$$

Chapter 3: Production Cost and Air Emissions Impacts of Coal-Cycling in Power Systems with Large-Scale Wind Penetration

Abstract

Wind power introduces variability into electric power systems. Due to physical characteristics of wind, most of this variability occurs at inter-hour time scales and coal units are therefore technically capable of balancing wind. Operators of coal-fired units have raised concerns that additional cycling will be prohibitively costly. Using PJM bid-data, we observe that coal operators are likely systematically under-bidding their startup costs. We then consider the effects of a 20% wind penetration scenario in the coal-heavy PJM West area, both when coal units bid business as usual startup costs, and when they bid costs accounting for the elevated wear and tear that occurs during cycling. We conclude that while 20% wind leads to increased coal cycling and reduced coal capacity factors under business as usual startup costs, including full startup costs shifts the burden of balancing wind onto more flexible units. This shift has benefits for CO_2, NO_X, and SO_2 emissions as well as for the profitability of coal plants, as calculated by our dispatch model.

This paper was published as Oates, D. L., & Jaramillo, P. (2013). Production cost and air emissions impacts of coal cycling in power systems with large-scale wind penetration. *Environmental Research Letters*, *8*(2), 024022. doi:10.1088/1748-9326/8/2/024022

3.1 Introduction

Operation of an electric grid depends on dispatchable generating capacity, such as coal and natural gas power plants, which can be cycled in response to variability. Traditionally, variability was largely limited to the demand side. However, an ever-increasing penetration of variable renewable energy technologies, such as wind, promises to increase the amount of cycling performed by dispatchable generators.

APTECH [1] defined cycling as "The process of bringing plants on and offline or increasing and decreasing unit output to meet load demand." Denny [2] and Valentino [3] used similar definitions. Here we adopted the definition suggested by APTECH and considered cycling operations to include both shutdown-startup cycles, where we differentiated between hot, warm, and cold cycles by the time spent offline; and load cycling, in which output is increased or decreased without shutting down. For reasons discussed later, we focused on shutdown-startup cycles.

As described by Katzenstein et al. [4] and Fertig et al. [5], the spectrum of variation introduced by wind generators is not flat across all frequencies. Wind power varies much more at multi-hour than it does at sub-hourly time-scales. Units with small ramp rate limits, such as coal, might therefore be expected to balance much of wind's variability. However, coal plants were by and large designed to provide baseload power Denny [2], and increased cycling of these plants in response to high wind penetrations could have unforeseen consequences.

Previous work has suggested that using thermal plants to balance wind may result in emissions penalties. Katzenstein & Apt [4] considered the implications of using a gas + wind + solar combination to produce baseload power. Their findings indicated that ramping a simple or combined-cycle gas turbine over its full operating range to balance wind and solar variability resulted in significant emissions penalties for NO_X and SO_2. The emissions model used by the authors allowed emissions rates to vary with both power output and ramp rate.

Valentino [3] examined the relative contribution of startups to fleet-wide emissions at a range of wind penetration levels. Focusing on the state of Indiana, their results suggested that while cycling increased the emissions rates of individual units, the effect was small compared to the overall emissions reductions that resulted from the displacement of fossil-fueled power by wind power.

Increased cycling of thermal power plants is also likely to result in increased operating costs. Intertek APTECH assessed the cost implications of cycling coal-fired thermal units [1], [6], while Lefton [7] and Shibli [6] studied steam units generally. The large and time-varying thermal loads imposed by cycling were found to increase the risk of creep and fatigue damage, with implications for operations and maintenance (O&M) costs, capital maintenance costs, and several other cost categories. Using data from two coal-fired power plants, APTECH [1] reported that these costs were highest for shutdown-startup cycles and could be on the order of $100,000/cycle. Bentek [8] suggested that most modeling efforts do not account for the full costs of cycling coal power plants, an omission that might underestimate the costs of integrating wind.

We examined the distribution of startup costs bid into PJM and found that these are far lower than the costs calculated by APTECH, suggesting that actual markets may not fully account for the costs of cycling. The comparison is shown in Figure 3.1. There are several possible reasons for this cycling cost gap. First, it is possible that operators are unable to attribute individual component failures and forced outages to cycling operations. Second, it is possible that while operators are aware of the costs incurred during cycling, market rules do not allow them to include these costs in their bids. While PJM's market rules appear to provide a mechanism to account for startup-related wear and tear in the form of a Start Maintenance Adder [9], it is unclear whether costs of the magnitude suggested by APTECH would gain approval by PJM. Finally, it is possible that operators have concluded that bidding actual startup costs would result in a reduction in their capacity factors and energy market revenues, and are bidding strategically in order to avoid this outcome.

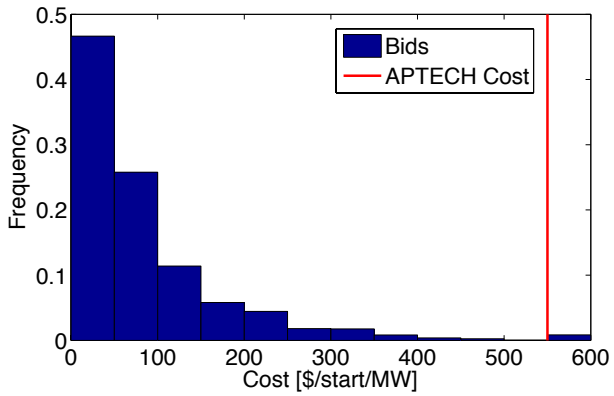

Figure 3.1: Distribution of cold start costs bid in PJM in 2007 [10] and average APTECH startup cost figures [1], [11], normalized by capacity. The vertical line attributed to APTECH here is the capacity-weighted average of figures for the Harrington and Pawnee plants. The vast majority of startup cost bids far fall below the APTECH figure.

This under-bidding may lead to problems as wind penetration increases. Under current market conditions coal operators may be able to generate sufficient revenues in the energy market to offset the cycling cost gap. However, as wind penetration increases and coal plants are required to cycle more often, profit margins may narrow to the point where cycling costs cannot be recovered. As pointed out by [12], the operation of an energy market is often sensitive to unit startup costs. Here we determined the increase in coal cycling that could be expected in a high wind penetration scenario in the PJM-West area under business as usual startup cost bidding, along with associated emissions and system cost penalties. We then considered low- and high-wind scenarios where operators of coal plants bid startup costs at the elevated levels suggested by APTECH.

We constructed a Unit Commitment and Economic Dispatch (UCED) model with an hourly time step for the PJM West area, as it existed in 2006. This included the PJM sub-regions of AEP, AP, Dayton, Dominion, and Duquesne. Using simulated wind data generated by the National Renewable Energy Lab [13], we considered a scenario with 20% wind energy penetration that approximated compliance with renewable portfolio standards in the region [14]. To account for the effects of cycling on emissions of CO_2, NO_x, and SO_2, we employed energy penalty curves derived from the EPA's Clean Air Markets data [15] and input emissions rates from the National Electric Energy Data System [16].

We found that a high level of wind penetration led to a large increase in the cycling of coal units and to an increase in cycling-induced cost and emissions penalties, but that these penalties were small compared to the system wide savings associated with wind. This finding is consistent with the results of Valentino [3]. Furthermore, we found that coal cycling, along with its emissions penalties, was reduced if the full costs of cycling such units were taken into account in operator bids. The high wind with elevated coal start cost scenario was associated with higher normal operations costs, compared to the high-wind scenario with low coal start costs, due to fuel switching from coal to gas. Total costs were still lower, however, than in the no-wind case. While incorporating elevated coal startup costs reduced coal unit capacity factors, the combination of reduced startup costs and increased energy prices led to increased aggregate coal unit profitability under the elevated coal start cost scenarios.

3.2 Methods

3.2.1 Unit Commitment and Economic Dispatch Model

We used a Unit Commitment and Economic Dispatch (UCED) model to determine the operating schedule for the PJM West area. The UCED schedules generators so as to meet demand at the lowest possible production cost, subject to unit operating constraints and system security constraints. The operation of the generators in PJM West was modeled day by day over the course of a year. The solution for each day was generated by optimizing over a 48-hour period, then stepping forward 24 hours. The state of all generators at the end of each day was fed into the next day's optimization in order to enforce ramp rate and minimum up- and down-time constraints across days. The model was formulated as a mixed-integer programming problem and solved using CPLEX.

The UCED model uses generating unit and load data from the PJM West area in 2006. The model attempts to meet net load (load minus available wind plus curtailment) at least cost. Similar to several other authors, the model does not include transmission constraints [2], [3], [17]. We argue that the effect of omitting transmission constraints on cycling is likely small, due to the fact that the average transmission line in PJM was constrained during only 4% of hours in 2014 [18]. Furthermore, we argue that it is not clear whether the omission would lead to an increase or a decrease in cycling. Transmission constraints lead to variation in LMPs across nodes. If a generating unit is located at a node with a higher LMP under a transmission constrained model than under our model, we might expect the unit to start up under the transmission-constrained model where it wouldn't under our model. Conversely, if a unit is located at a node with a lower LMP, we might expect it not to start up under the transmission-constrained model where it would have under our model.

Note that the model was built with the assumption of perfect load and wind forecasts over each 48-hour period of model execution. In real power systems, forecast errors lead to the occurrence of short time-scale corrections, mostly performed by fast-ramping units procured through the ancillary service markets, which we did not model. Since this work focused on slow-ramping coal units, we expect this limitation had a minor impact on results as they relate to the operations of coal power plants. A detailed description of the model formulation is included in the Supporting Information.

Production costs used in the model include fuel, variable O&M, and startup costs. Fuel costs were calculated at the unit level as the product of power output, heat rate, and utility-delivered fuel price. Fuel prices used in this study varied state by state, and month by month (see Supplementary Information), as reported by EIA's Electric Power Monthly [19]. Nuclear fuel was assumed to have a fuel price of $0.25/MMBTU, placing it lower on the dispatch stack than all fossil fuel plants.

Startup costs in the base case were estimated based on observed hot-, inter-, and cold-start bids in PJM in 2007 [10].

For the scenario in which bids included the elevated costs of coal cycling, we used an average of the per MW start-up values determined by APTECH for the Harrington and Pawnee coal plants [1], [11]. Note that steam units are expected to incur the most damage during cycling and the cycling damage studies performed by many authors focus on these units [1], [6], [7], [11]. Due to this fact and the availability of cost data, we have focused on coal steam units in this work. Note that we expect units other than coal to incur damage during cycling as well. For a sensitivity analysis using a different set of cost data, see the Supplementary Information.

Capacity-weighted average fuel prices and startup costs used in the model are reported in Table 1. Variable O&M costs were based on estimates in the Ventyx Velocity Suite [20]. While natural gas prices are currently at record low levels, the values used for this analysis are consistent with the forecasted delivery price to the power generation sector reported by the Energy Information Administration up to 2025 [21].

Table 3.1: Average fuel prices and start costs used in the model. Fuel prices are based on 2010 prices [19], with the exception of nuclear. Coal unit start costs are based on PJM data [10] in the low case, and APTECH figures [1], [11] in the elevated case.

	Fuel Price [$/MMBTU]	Cold Start Cost [$1,000/start]		Warm Start Cost [$1,000/start]		Hot Start Cost [$1,000/start]	
		Low	Elevated	Low	Elevated	Low	Elevated
Nuclear	0.25	74	74	56	56	44	44
Coal	2.6	52	350	40	210	31	170
NG CC	4.8	25	25	19	19	15	15
NG CT	4.8	10	10	7.6	7.6	6	6
NG Steam	5.02	14	14	11	11	8.8	8.8
Oil CT	20.4	2.2	2.2	1.7	1.7	1.3	1.3
Oil Steam	19.2	62	62	48	48	38	38
Other	20.9	3.9	3.9	3	3	2.4	2.4

Generator operating constraints included minimum and maximum generation levels, up and down ramp rate limits, minimum run times, and minimum down times. Following NERC guidelines

[22], the UCED imposed a spinning reserve requirement of 3% of the maximum daily load, and a 3% non-spinning reserve requirement. The spinning reserve requirement increased with wind penetration, following a heuristic proposed by NREL [23], requiring additional 10-minute responsive spinning reserves equal to 5% of the wind energy generated in each period.

3.2.2 Outages

Planned and un-planned unit outages reduce available generating capacity in the PJM West area. In order to incorporate this effect in the model, equivalent forced outage rate data from PJM were used to simulate outages at the unit level (details in Supplementary Information). The number of outages in a year for each unit was taken to be a Poisson process with a mean equal to the value from NERC, and the start times of the outages were distributed across the year by sampling from a uniform distribution. Outage durations were also taken to be Poisson distributed with mean equal to the NERC values.

3.2.3 Wind Power

In order to simulate high penetrations of wind energy, sites were selected from the Eastern Wind Interconnection and Transmission Study's database. The National Renewable Energy Laboratory (NREL) generated spatially and temporally correlated wind speed time series for these sites for the years 2004-2006. Data from 2006 were used in this work. Sites were selected in order of decreasing capacity factor and then aggregated to produce a wind power time series for 20% wind. This method was designed to properly account for geographic smoothing and the correlation between wind and load.

3.2.4 Emissions

Having obtained an operating schedule from our UCED[7], we used it and an emissions model to calculate emissions. Our emissions model consists of two parts. During normal operation of the unit, we used unit-level input emissions factors and heat rates from the National Electric Energy Data System and the EIA to calculate emissions of CO_2, NO_X, and SO_2 as a function of power output. Emissions factors are summarized in Table 3.2. Note that with an hourly time step, observable ramp rates are too small to have an impact on emissions and are therefore not accounted for in the emissions model (see Supplementary Information for a detailed discussion on this issue).

Table 3.2: Average steady-state emissions factors by unit type in PJM West from (CO_2 from [24], others from [16]). Uncontrolled NO_X rates were used during startup and shutdown.

	CO_2 Rate (ton/MMBTU)	SO_2 Permit Rate (lb/MMBTU)	Uncontrolled NO_X Rate (lb/MMBTU)	Controlled NO_X Rate (lb/MMBTU)
Coal	0.10	2.2	0.50	0.19
NG CC	0.058	0.062	0.10	0.077
NG Steam	0.058	1.3	0.097	0.097
NG CT	0.058	2.0	0.093	0.09
Oil Steam	0.087	1.7	0.26	0.26
Oil CT	0.081	1.6	0.82	0.82
Other	0.069	0.68	1.7	1.6

To capture emissions during startup, we constructed heat rate penalty curves as a function of load for each unit type. As suggested by Klein [25], the heat-input vs. power-output curve of a unit can be modeled as a cubic function. Average heat rate curves can then be developed in the form of equation (3.1), where x represents power output in MW and HR represents the average heat rate in MMBTU/MWh. We extended this notion and calculated heat rate penalties P as the percent difference between the heat rate and the steady state heat rate HR_0, as in equation (3.2). We then generated heat rate penalty curves in the form of equation (3.3), where X represents the percent

[7] In keeping with current operations of electric power systems, emissions are not included in the objective function constrained in the UCED.

load. Heat rate curves were averaged across all units of a particular type. The resulting heat rate penalty curves, shown in Figure 2, were used to capture emissions penalties associated with startup and shutdown. The heat rate penalty curves were generated using a selection of units from CAMD [15] in 2006 that were located in PJM and whose data was usable. Startup emissions calculated using heat rate penalties found in Valentino [3] differed from those reported here by a maximum of 10%.

$$HR = ax^2 + bx + c + \frac{d}{x} \tag{3.1}$$

$$P = \frac{HR - HR_0}{HR_0} \tag{3.2}$$

$$P = AX^2 + BX + C + \frac{D}{X} \tag{3.3}$$

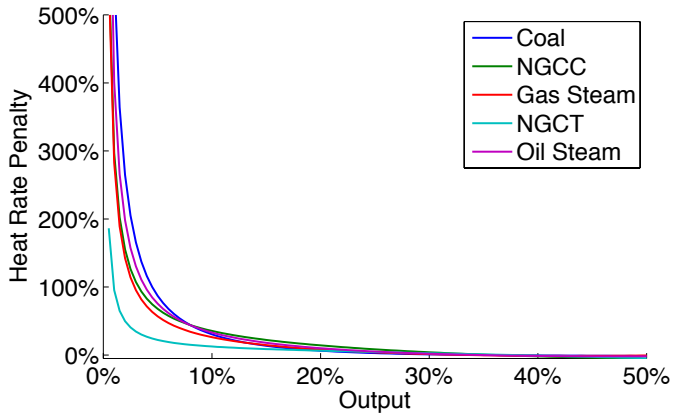

Figure 3.2: Heat rate penalty curves as a function of power output by unit type based on data from the EPA's Clean Air Markets Database [15].

NO_X emissions result from oxidation of atmospheric nitrogen and emissions rates are a complex function of control technology and the thermodynamic state of the boiler [26]. It is unlikely that NOX emissions control technologies would operate properly during startup or shut down. To calculate startup emissions, we therefore used uncontrolled emissions factors from NEEDS, as listed in Table 3.2.

3.3 Results

The low coal start cost / 20% wind scenario was associated with increased startups of all types of units, increased startup-related costs, and increased startup-related emissions compared to the no-wind case. Figure 3.3 A) and B) show annual startups across the three scenarios for coal units and flexible units (simple- and combined-cycle gas units), respectively. Coal startups of all types increased by 14% - 640% in the high-wind scenarios compared to the no-wind scenarios at each startup cost. The percentage increase was greater with elevated coal startup costs, though the absolute values were greater with low start costs. Flexible unit startups increased by 40%-90% in the high wind scenarios. Despite the increase in startups, system-wide costs and emissions were lower in the high wind scenarios due to displacement of fossil fuels by wind.

The scenarios in which elevated coal startup costs were incorporated showed dramatic reductions in coal startups over the low coal start cost scenarios. As expected, flexible units appear to have compensated and startups for these units increased dramatically over the low coal startup cost scenarios. As shown in Figure 3.3 C), coal capacity factors were reduced under the high-wind and elevated coal startup cost scenarios. Capacity factors for natural gas simple and combined cycle units increased slightly with wind penetration and more substantially with elevated coal startup costs. Figure 3.3 D) shows that incorporating elevated coal startup costs had the effect of increasing curtailment of wind up to nearly 2% of available wind energy, most of it occurring in the early morning hours. Wind curtailment is most likely to occur during periods when wind output is high and load is low. In PJM West, these conditions arise most frequently at night.

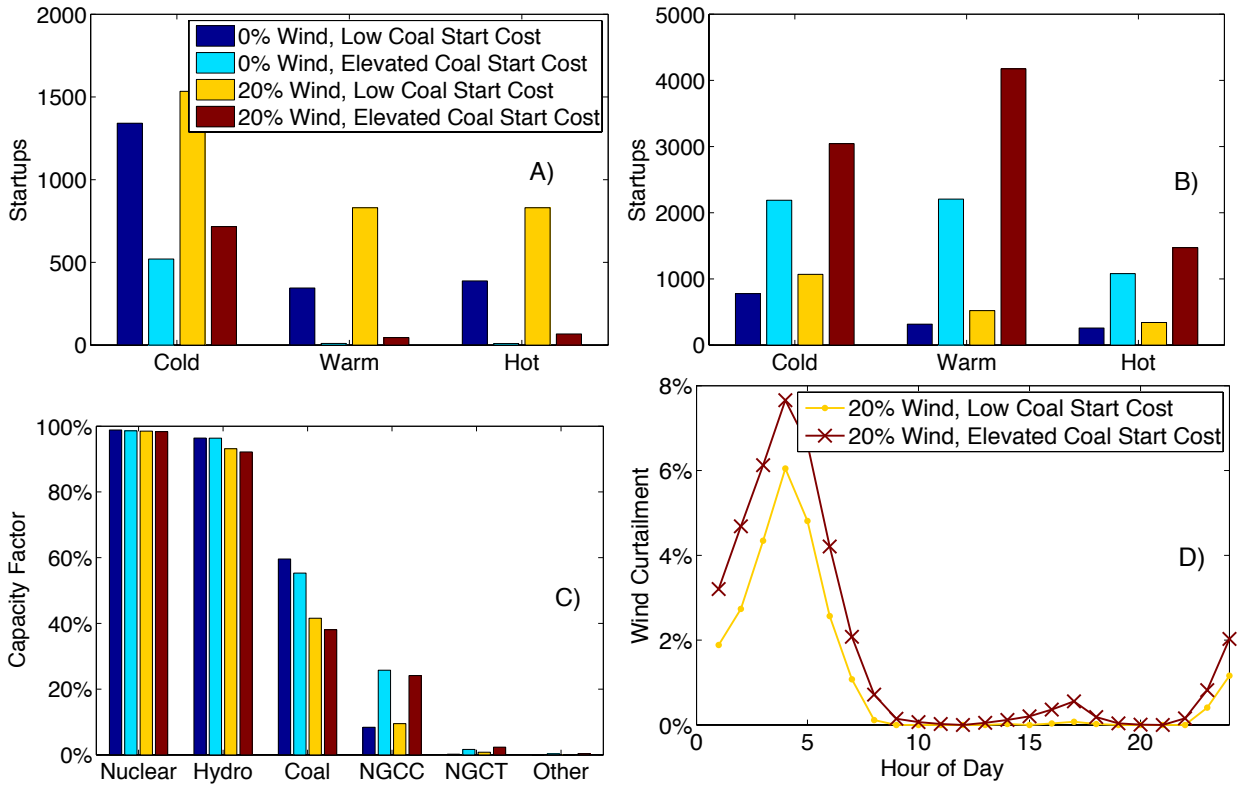

Figure 3.3: A) Annual coal startups across the four scenarios. B) Annual flexible-unit startups. C) Average capacity factor by unit type. NGCC and NGCT indicate natural gas combined and simple cycle units, respectively. D) Hourly average wind curtailment vs. hour of day, as a percentage of average available wind in that hour, for 20% wind scenario with low and elevated coal start costs. Total wind curtailment in the low start cost and elevated start cost scenarios were 1.1% and 1.8%, respectively.

Table 3.3 shows emissions from normal operations, as well as startup-related emissions of CO_2, SO_2, and NO_X, which increased by approximately a factor of 2 under the 20% wind scenario. However, startups represented a small portion of overall emissions: a maximum of 2% across all scenarios. Incorporating elevated coal startup costs had the effect of substantially reducing startup-induced emissions, but, more significantly, also reduced emissions during normal operations. This is due to increased utilization of gas units as opposed to coal units.

Table 3.3: Annual emissions of CO_2, NO_X, and SO_2 across the three scenarios.

		0% Wind, Low Coal Start Cost	0% Wind, Elevated Coal Start Cost	20% Wind, Low Coal Start Cost	20% Wind, Elevated Coal Start Cost
Normal Operations	CO_2 [M ton]	210	200	150	140
	NO_X [M lb]	740	690	470	420
	SO_2 [M lb]	4,500	4,200	3,100	2,800
Startups	CO_2 [M ton]	1.0	0.63	2.0	0.99
	NO_X [M lb]	4.3	2.1	9.5	3.5
	SO_2 [M lb]	18	9.1	42	15

Resource use varied substantially across the three scenarios considered and is shown in Figure 3.4. Comparing the first and third columns shows that the addition of 20% wind largely had the effect of displacing energy production by coal units, leaving nuclear and hydro production virtually unchanged. The scenario incorporating elevated startup costs for coal units had the effect of further displacing coal and replacing it by combined cycle gas.

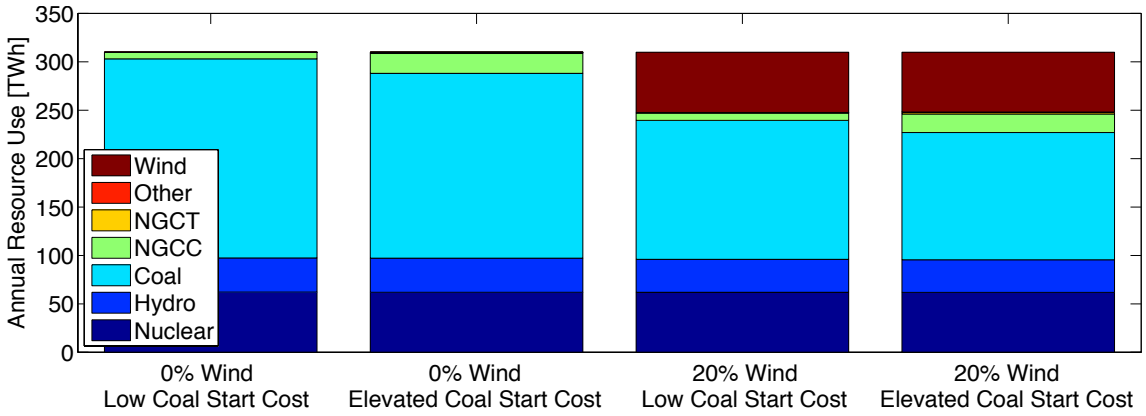

Figure 3.4: Annual resource use in PJM West across the three scenarios. NGCT and NGCC indicate simple and combined-cycle natural gas, respectively.

Table 3.4 shows a range of economic indicators across the four scenarios, for suppliers as a whole, and for coal units in particular. Producer surpluses, and changes in consumer surplus over the 0% Wind / Low Coal Start Cost scenario, were calculated. Producer surplus here includes the difference between annual revenues and total production costs, and consumer surplus is the area between the demand curve and the market-clearing price in each period, summed over the year.

Note that since we have modeled demand as inelastic, we set a price cap and report only differences in consumer surplus. Revenue and surplus figures were calculated using prices generated endogenously in the UCED model. These prices do not account for congestion or transmission costs and we include them simply to illustrate that startup costs can make an important contribution to energy prices.

Under business as usual coal startup costs, the wind-induced increase in startups was associated with an 80% increase in total startup costs. The majority of this increase was borne by coal units. Incorporating elevated coal start up costs reduced coal cycling costs dramatically and though it is clear from Figure 3.3 C) that coal capacity factors were reduced in this scenario, the impact on coal unit surpluses was less clear. Table 3.4 shows that, on the aggregate, producer surpluses were -$300M for coal plants in the high wind/low start cost scenario. However, when elevated coal startup costs were incorporated, aggregate coal unit producer surpluses increased to $610M due partially to a reduction in cycling and partially to a 12% increase in average energy prices over the high wind/low start cost scenario. We again emphasize the limited ability of our modeling framework to forecast prices.

Table 3.4: Normal operations and start costs, revenues and profits for all unit types (including coal) and coal in three scenarios. Normal operations costs include fuel and variable O&M. Total production costs are the sum of normal operations and startup costs.

	0% Wind, Low Coal Start Cost		0% Wind, Elevated Coal Start Cost		20% Wind, Low Coal Start Cost		20% Wind, Elevated Coal Start Cost	
	All	Coal	All	Coal	All	Coal	All	Coal
Normal Operations Cost ($B)	5.7	5.2	5.9	4.8	4.2	3.6	4.3	3.2
Total Start-Up costs ($B)	0.29	0.27	0.18	0.12	0.53	0.50	0.27	0.19
PJM Start Cost ($B)	0.060	0.042	0.071	0.018	0.11	0.082	0.11	0.029
Start-up costs not included PJM bids ($B)	0.23	0.23	0.11	0.10	0.42	0.42	0.16	0.16
Total Production Costs ($B)	5.99	5.47	6.08	4.92	4.73	4.1	4.57	3.39
Producer Revenues ($B)	8.8	5.9	9.8	6.1	6.4	3.8	7.3	4.0
Producer Surplus ($B)	2.8	0.43	3.7	1.2	1.7	-0.30	2.7	0.61
Consumer Surplus Change over 0% Wind, Low Coal Start Cost Scenario ($B)	-	-	-1.0	-1.0	1.1	1.1	0.12	0.12

3.4 Conclusions

A study was conducted for the PJM West area to determine the effect of wind on the cycling of coal-fired power plants, emissions of CO_2, NO_X, and SO_2, and production costs. High wind penetration scenarios were examined both under business as usual coal startup cost bidding, and under elevated coal startup cost bidding. When only the business as usual coal startup costs were used in the optimization, results indicated that wind penetration increased cycling of slow-ramping coal units and that this cycling led to emissions and cost penalties for these plants. On a system level, the magnitude of the penalties was found to be small compared to the overall savings associated with wind. By incorporating the full costs of coal cycling in the dispatch model, emissions and cost penalties associated with cycling were reduced. This scenario is representative of the decision of coal operators to change their bidding strategies to reflect full start up costs. Including

full start up costs reduced coal capacity factors due to switching from coal to gas. However, the increase in energy prices associated with this switching led to increased surplus for coal plants compared to the high-wind/business as usual startup cost scenario.

Our result that coal producer surpluses increased when elevated coal startup costs were incorporated deserves further discussion. Predictions of energy prices are inherently uncertain. This means that the result should be viewed with some caution. Also, while we have argued that bidding elevated startup costs would increase producer surpluses for coal operators in the high wind scenario, it is not certain that such bidding would occur. Since operators are trying to maximize overall profits, it may be more optimal to under-bid startup costs so as to earn higher revenues in the energy market. Under the increased startup requirements of a high wind scenario, we consider it likely, but not certain, that such a strategy would be less viable. Our high wind, high coal startup cost scenario should therefore be considered as a bounding case, and interpreted with the uncertainty in bidding strategies in mind.

Our modeling framework made a number of assumptions and approximations. While we do not expect the lack of transmission constraints to affect the implications of the aggregate results, it could affect the individual generators called on to perform cycling. Though we have focused on shutdown-startup cycles because of their larger per unit costs, it remains unclear whether changes in load cycling, in which output is increased or decreased without shutting down, could be a major cost driver. Also, while we have focused here on the current fleet of plants, several policy and economic factors may lead to a change in the composition of the fleet in the coming years. Finally, our analysis was based on the PJM West region. While we expect many of our qualitative results to hold for systems with different fuel mixes, care must be taken in generalizing our results to these other systems. In future work, we expect to examine some of these issues in more detail.

Despite the aforementioned limitations, we expect our qualitative conclusions regarding coal cycling are robust. Incorporating full cycling costs in bids transfers the burden of balancing wind to units that can perform this service at lower cost, has environmental benefits and could improve the profitability of coal plants in a high-wind scenario. Incorporating full startup costs into unit commitment may be a good strategy for reducing the burden of coal cycling in a high wind future.

3.5 References

[1] APTECH, "Integrating Wind," Xcel Energy, Sunnyvale, CA, Mar. 2009.

[2] Denny, "Quantifying the Total Net Benefits of Grid Integrated Wind," *IEEE Trans. Power Syst.*, vol. 22, no. 2, pp. 605–615, May 2007.

[3] L. Valentino, V. Valenzuela, A. Botterud, Z. Zhou, and G. Conzelmann, "System-Wide Emissions Implications of Increased Wind Power Penetration," *Environmental Science & Technology*, vol. 46, no. 7, pp. 4200–4206, Apr. 2012.

[4] W. Katzenstein and J. Apt, "Air Emissions Due To Wind And Solar Power," *Environmental Science & Technology*, vol. 43, no. 2, pp. 253–258, Jan. 2009.

[5] E. Fertig, J. Apt, P. Jaramillo, and W. Katzenstein, "The effect of long-distance interconnection on wind power variability," *Environ. Res. Lett.*, vol. 7, no. 3, p. 034017, Aug. 2012.

[6] A. Shibli, J. Gostling, and F. Starr, "Damage to Power Plants Due to Cycling," EPRI, Jul. 2001.

[7] S. Lefton, "Effects of Flexible Operation on Turbines and Generators," EPRI, Dec. 2004.

[8] Bentek, *How Less Became More: Wind, Power, and Unintended Consequences in the Colorado Energy Market*. 2010.

[9] PJM, *PJM Manual 15: Cost Development Guidelines*. PJM Interconnection, 2012, pp. 1–113.

[10] PJM, *PJM Daily Energy Market Bid Data*. PJM Interconnection, 2012.

[11] D. D. Agan, P. M. Besuner, G. P. Grimsrud, and S. A. Lefton, "Cost of Cycling Analysis for Pawnee Station Unit 1 Phase 1: Top-Down Analysis," APTECH, Oct. 2008.

[12] J. A. Cullen and O. Shcherbakov, "Dynamic Response to Environmental Regulation in the Electricity Industry," *Harvard University*, 2010.

[13] EnerNex Corporation, "Eastern Wind Integration and Transmission Study," NREL, Feb. 2011.

[14] PJM, *Comparison of Renewable Portfolio Standards (RPS) Programs in PJM States*. PJM Environmental Information Services, 2011, pp. 1–8.

[15] EPA, *EPA Clean Air Markets Data*. 2006.

[16] EPA, *National Electric Energy Data System (NEEDS)*, 4 ed. EPA, 2010.

[17] B. Nyamdash, E. Denny, and M. O'Malley, "The viability of balancing wind generation with large scale energy storage," *Energy Policy*, vol. 38, no. 11, pp. 7200–7208, Nov. 2010.

[18] PJM, *Day-Ahead Transmission Constraints 2014*. PJM Interconnection, 2015.

[19] EIA, *EIA Electric Power Monthly 2010*. Energy Information Administration, 2012.

[20] Ventyx, *Ventyx Velocity Suite*. 2011.

[21] EIA, "Annual Energy Outlook 2012," *US Energy Information Administration*, pp. 1–252, Jul. 2012.

[22] NERC, *Reliability Standards for the Bulk Electricity Systems of North America*. 2011, pp. 1–951.

[23] R. Piwko, K. Clark, L. Freeman, and G. Jordan, *Western wind and solar integration study*. National Renewable Energy Laboratory, 2010, p. 260.

[24] EIA, "Voluntary Reporting of Greenhouse Gases Program Fuel Emission Coefficients," *US Energy Information Administration*, 31-Jan-2011. [Online]. Available: http://www.eia.gov/oiaf/1605/coefficients.html. [Accessed: 27-Aug-2012].

[25] J. Klein, "The use of heat rates in production cost modeling and market modeling," 1998.

[26] C. E. Mulkey, "Evaluation of Nitrogen Oxide Emissions during Startup of Simple Cycle Combustion Turbines," 2003.

[27] "2006 State of the Market Report," PJM Market Monitoring Unit, Mar. 2007.

[28] J. Apt, "The spectrum of power from wind turbines," *Journal of Power Sources*, 2007.
[29] N. Kumar, P. Besuner, S. Lefton, D. D. Agan, and D. D. Hillerman, "Power Plant Cycling Costs," National Renewable Energy Laboratory, AES 12047831-2-1, Apr. 2012.

B Appendix

B.1 Wind Power

The EWITS wind dataset, which provides simulated power output from individual wind farms, was used to generate the wind power time series for this study. We selected EWITS sites in order of decreasing capacity factor (based on 2006 output) and then summed the power output time series for each site. We selected 72 sites within or near the PJM West footprint, enough to create an (approximately) 20% wind scenario. The locations of the sites selected are shown in Figure B-1 and the capacity-weighted average capacity factor of the selected sites was 31%.

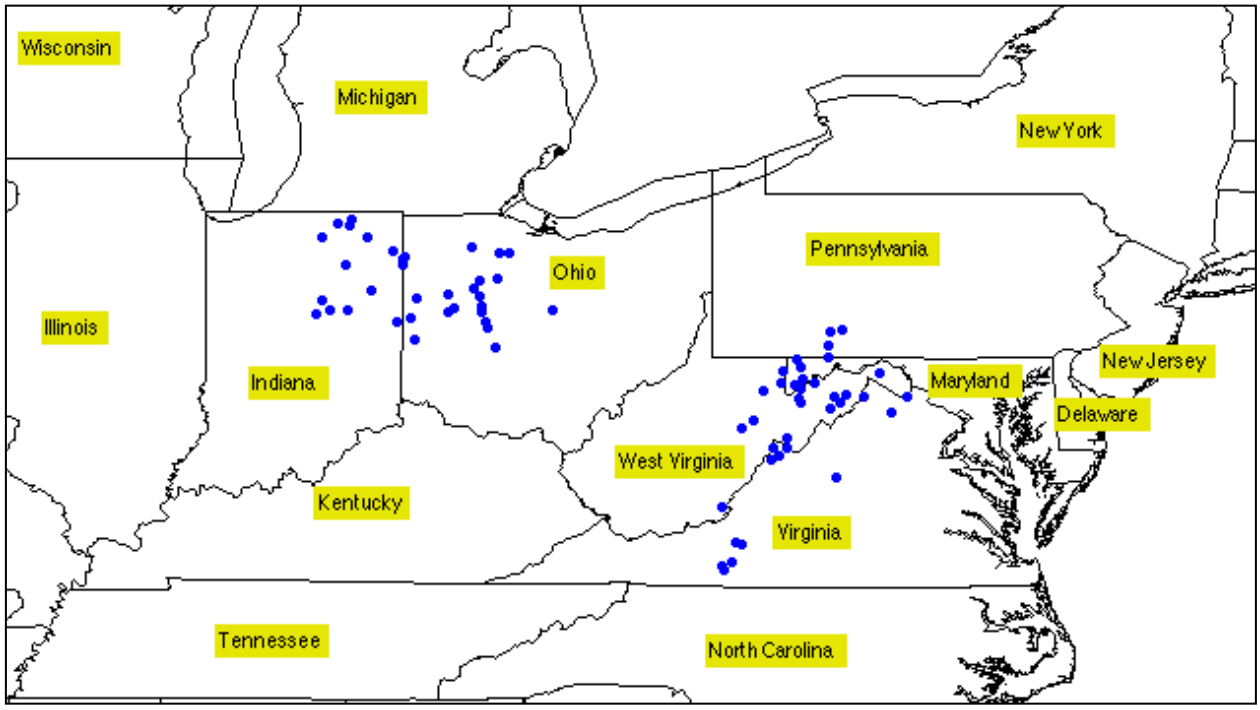

Figure B-1: Location of the EWITS sites (blue dotes) used in the 20% wind scenario in this work.

B.2 Emissions Rates

The process of constructing heat rate penalty curves from CAMD data is illustrated in Figure B-2. Heat input and power output data from CAMD were used to regress heat input as a cubic function of power output for each unit in the database. This generated the coefficients a, b, c, and d

in the first equation of Figure B-2. The same coefficients can be interpreted as the coefficients of an average heat rate vs. power output function in the form of the second equation in Figure B-2. The coefficients were then transformed according to equation (3.4) into heat rate penalty curves, using the maximum capacity and reference heat rates of each unit. Heat rate penalty curves were then averaged across all units of a particular type to generate type-level heat rate penalty curves. Note that it was not possible to simply use unit-level heat input/power output curves because the CAMD database does not include all units in the actual PJM-West system.

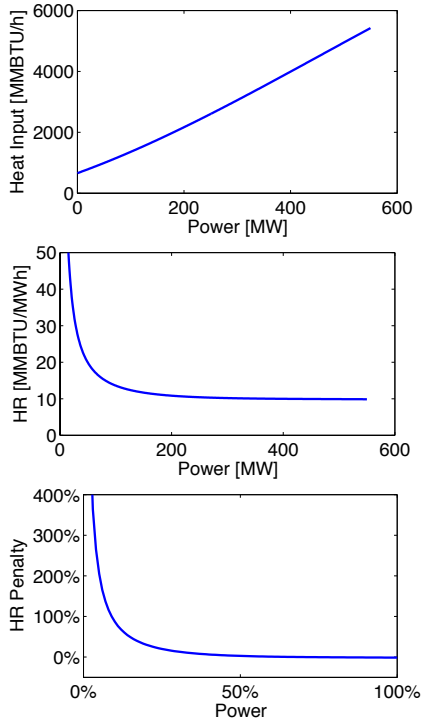

Heat Input / Power Output

$$H = ax^3 + bx^2 + cx + d$$

Average Heat Rate

$$HR = ax^2 + bx + c + \frac{d}{x}$$

Heat Rate Penalty

$$P = AX^2 + BX + C + \frac{D}{X}$$

Figure B-2: Process for generating type-level heat rate penalty curves.

$$x = X \cdot \bar{x} \qquad P = \frac{HR - HR_0}{HR_0}$$

$$A = \frac{\bar{x}^2}{HR_0} a \quad B = \frac{\bar{x}}{HR_0} b \quad C = \frac{c}{HR_0} - 1 \quad D = \frac{d}{\bar{x} \cdot HR_0} \tag{3.4}$$

Figure B-3 shows the procedure for using type-level heat rate penalty curves and unit-level parameters from NEEDS (Heat Rate Reference, Capacity) to obtain startup emissions. First, unit-level heat input/power output curves were constructed by scaling the type-level heat rate penalty curves. Using unit-level ramp rate limits and minimum generation levels, these curves were then integrated over a startup/shutdown cycle to determine the heat input required during such a cycle. The heat input was then multiplied by an appropriate unit-level input emissions factor to obtain startup emissions which were applied each time the Unit Commitment and Economic Dispatch model indicated a startup.

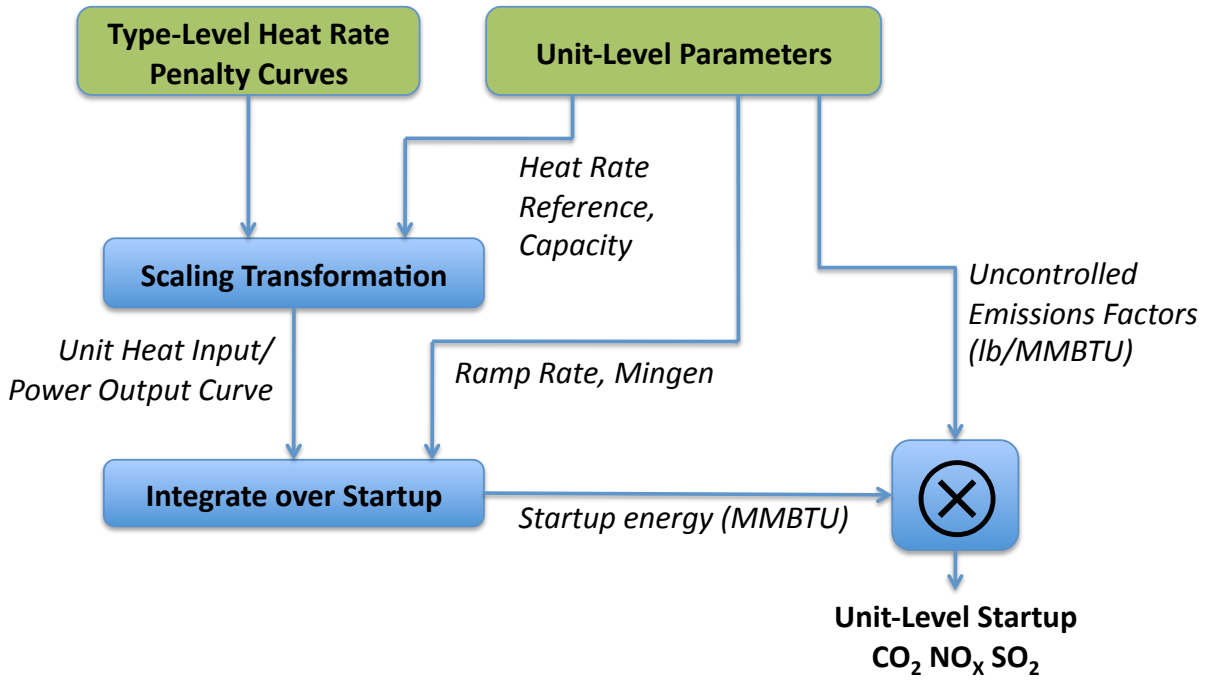

Figure B-3: Schematic diagram illustrating the calculation of startup CO_2, NO_X, and SO_2 emissions.

The process for determining emissions during normal operations was considerably simpler and is outlined in Figure B-4. Unit-level power output time series from the UCED were multiplied by the unit heat rate and input emissions factor from NEEDS. The resulting emissions time series was summed over the period of interest. During NO_X season (May through September in PJM),

controlled NO_X emissions factors were used to calculate emissions during normal operations, while uncontrolled factors were used during the rest of the year.

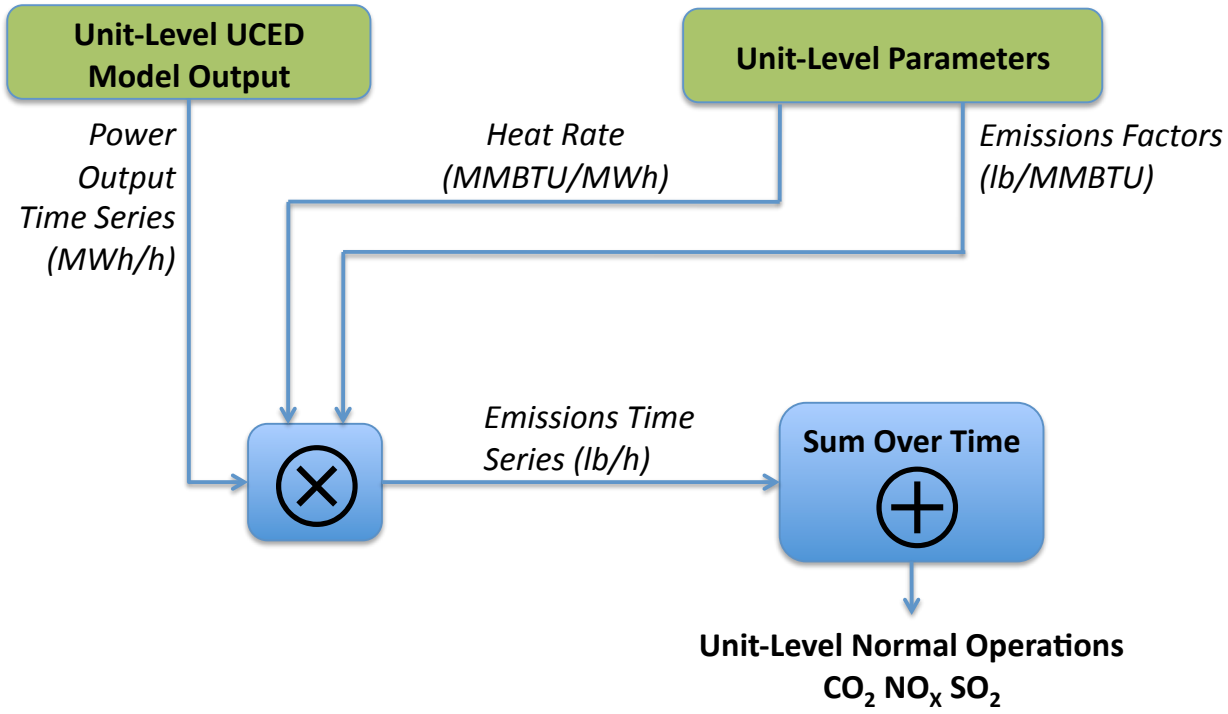

Figure B-4: Process for calculating emissions during normal operations.

B.3 PJM West Sub-Region

The PJM West region considered includes the PJM sub-regions of AEP, AP, Dayton, Dominion, and Duquesne as they existed in 2006. See p. 5 of volume 1 of [27] for a map of these regions. Table B-1 shows number, capacity, and average heat rate by unit type in the PJM West region, based on data from NEEDS [16]. This is a coal heavy region with a substantial presence of simple and combined cycle gas turbines, and nuclear.

Table B-1: Number, capacity, and average heat rate by unit type in PJM West.

Type	Number	Total Capacity (MW)	Average Heat Rate (BTU/kWh)
Nuclear	8	7,180	10,684
Hydro	48	4,185	N/A
Coal	119	39,497	9,993
NG CC	34	9,145	8,819
NG CT	99	9,118	12,147
NG Steam	2	309	10,521
Oil CT	18	330	16,704
Oil Steam	3	1,686	11,073
Other	17	478	13,449

B.4 Fuel Price Variation

Utility-delivered fuel prices vary substantially with location and to a certain degree with time. To capture this, we used utility-delivered fuel price data from the EIA [19] at the state and monthly levels as input to the UCED model. Figure B-5 shows an example of the variation in coal price among PJM member states in January 2006.

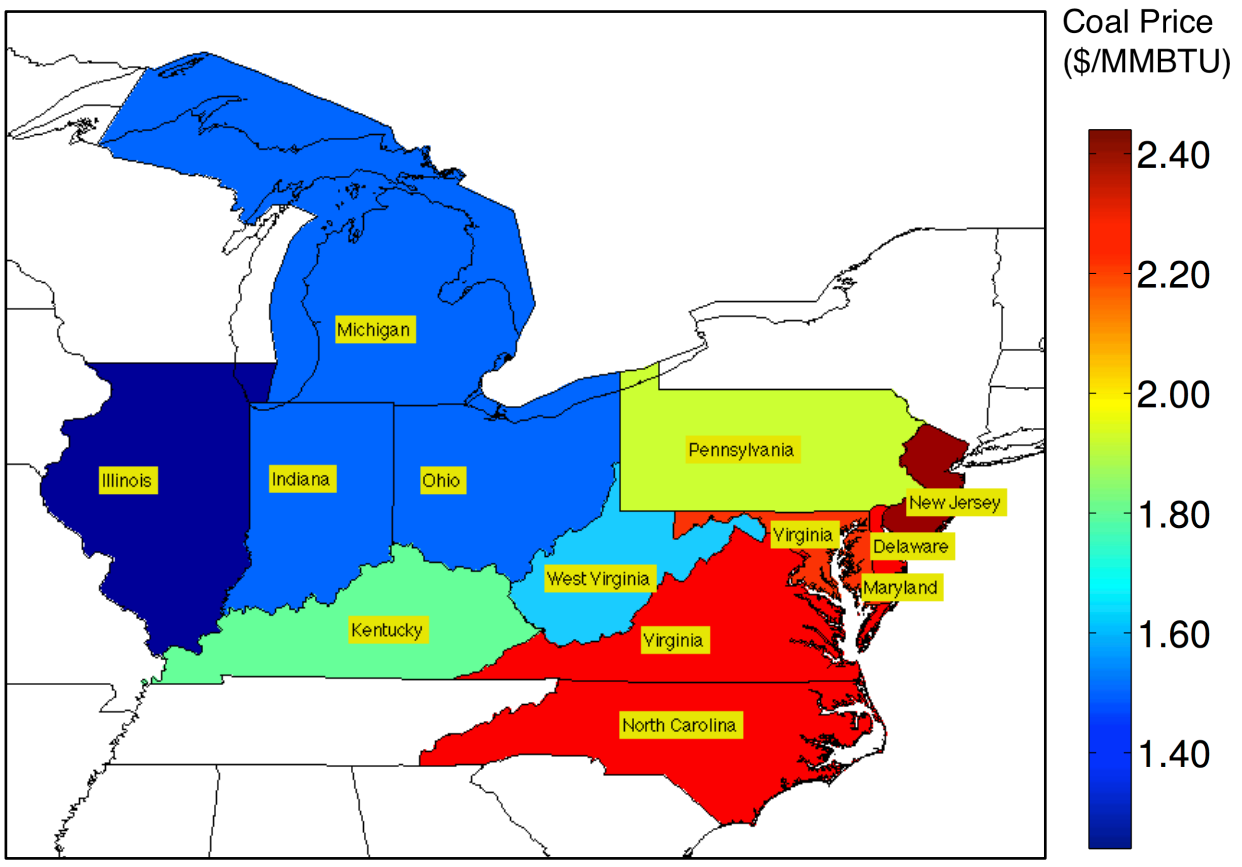

Figure B-5: Variation in utility-delivered coal prices ($/MMBTU) among the PJM member States in January 2006 [19]. Values range from $1.24/MMBTU in Illinois through $2.44/MMBTU in New Jersey, almost a 100% difference. Month by month variation exists, but is much smaller than spatial variation (maximum COV for temporal variation is 10%, compared to 25% for spatial variation).

B.5 Availability

Accounting for availability is an important component of a unit commitment and economic dispatch model, due to the non-trivial forced outage rates displayed by units in the system. In order to capture this effect, equivalent forced outage rate data were obtained from PJM, broken out by unit type and by month. A model was then constructed to generate time series outage data, based on these aggregate numbers. The simulated outage time series were held constant across all scenarios considered in the paper.

In order to simulate outage time series, the number of annual outage events was considered to be a Poisson process, as was the duration of each outage event. Equation (3.5) shows the calculation

of the expected number of outages $N_{i,t}$ for unit type i in month t given the equivalent forced outage rate $EFORd_{i,t}$ for that type and period, the length of the period T_t, and the expected outage duration L. Since no data were available for the parameter L, it was assumed to be four days.

$$N_{i,t} = \frac{EFORd_{i,t} \times T_t}{L} \tag{3.5}$$

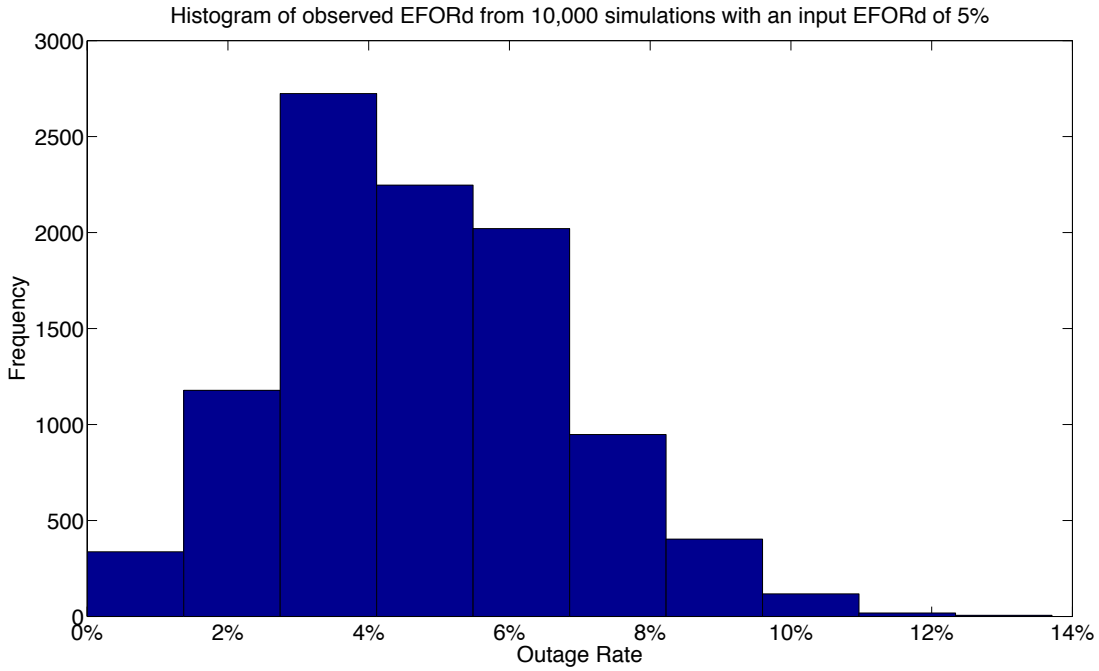

Figure B-6: Histogram of outage rates for 10,000 simulations of 10,000 hours.

B.6 Cycling, Ramping, and Hourly Time Step

Katzenstein and Apt [4] determined the impact of ramping (and power output) on CO_2 and NO_X emissions rates of a GE LM6000 simple-cycle gas turbine and a Siemens 501FD combined cycle gas turbine. Using one-minute data, their analysis found that ramp rate was not a statistically significant explanatory variable of CO_2 or NO_X emissions rates for the 501FD, but that it was a significant explanatory variable for emissions rates of the LM6000 in certain parts of the unit's operating space.

In a model with an hourly time step, it is not possible to reach very high ramp rates. For instance, a 60 MW unit can only sustain ramp rates between -1MW/min and 1MW/min for an hour without exceeding its operating limits. In Figure B-7, we used the emissions models reported by [4] to plot NO_X and CO_2 emissions across this constrained operating space. As is evident from the plots, the effect of ramp rate on emissions in the constrained operating space is very small. We present this result as evidence that when hourly data are all that is available, power output is a sufficient input to an emissions model.

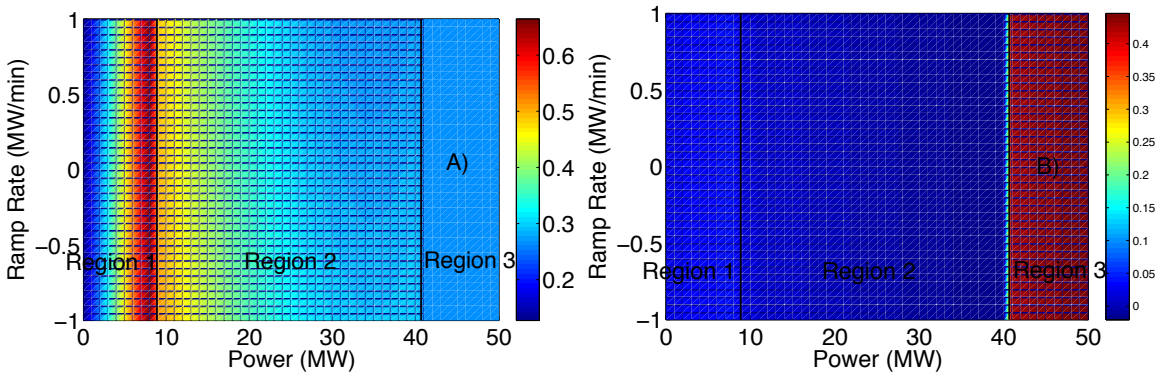

Figure B-7: A) LM6000 NO_X emissions rates (kg/min) and B) LM6000 CO_2 emissions rates (ton/min) based on the Katzenstein model over the operating space reachable at hourly time steps. Katzenstin divided the operating space of the LM6000 into four regions that were modeled with separate emissions models. Three of these regions intersect with the constrained operating space available in an hourly model and are shown here. Gradients in the ramp-rate direction are very small in both cases.

The limitation of our emissions modeling is not that it does not include ramp rate as an input variable, but that the UCED operates at an hourly time step. Changes in sub-hourly ramping that occur with wind are not reflected in this work. Due to the character of the variability of wind power, namely the decrease in power spectral density with frequency [28], we expect the variability introduced at sub-hourly time scales to be smaller than that introduced at inter-hour time scales.

B.7 Emissions Model Comparison

In order to validate our emissions modeling, we used results from [4] to determine the expected NOX emissions during a startup cycle. Power/Ramp Rate observations were fit using a non-

parametric fitting function to determine a trajectory through the power/ramp rate operating space that the LM6000 unit traverses during startup. This trajectory, is shown in Figure B-8 A), along with modeled NOX emissions rates. This trajectory defines a differential equation that we solved to determine power as a function of time for the LM6000 during startup. This startup as a function of time curve is shown in Figure B-8 B), along with the cumulative emissions curve determined by performing a path integral along the trajectory defined by the constraint curve in A). This analysis indicated that the LM6000 GT emits approximately 1.5 kg of NO_X during the course of its 4-minute startup sequence.

Figure B-8 C) compares the LM6000 startup emissions to the range of startup emissions for gas turbine units determined using the methods of this work. As is clear from the figure, the LM6000 startup emissions determined using high resolution data are similar to those determined using the methods of this model, though generally smaller.

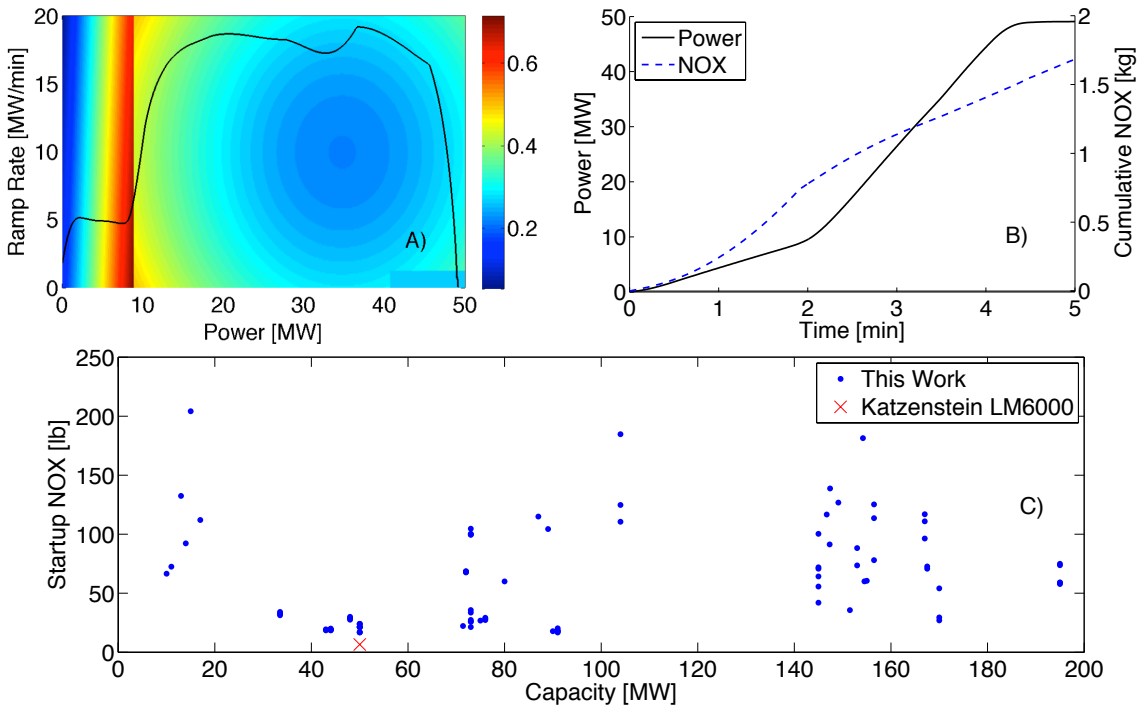

Figure B-8: LM6000 NO_X emissions model from [4] (kg/min) and startup constraint curve (black line) showing startup trajectory. B) Power output and Cumulative NOX emissions based on the startup trajectory and emissions model in A). The LM6000 emits approximately 1.5 kg of NO_X during startup. C) PJM West Gas Turbine startup NO_X emissions calculated using the method of this work, and the equivalent calculated using B). Note that emissions have been converted

from kg to lb and multiplied by two to reflect the fact that "startup" emissions figures in this model are doubled to account for startup and shutdown emissions.

B.8 Comparison of Heat Rate Penalty Curves

Here we compare our results to those that would have been obtained had we used the emissions curves attributed to [3]. Figure B-9 shows heat rate penalty curves for coal, gas combined cycle, gas turbine, and oil turbine units as used in this work. It also shows the estimates of heat rate penalty at 25%, 50%, 75%, and 100% as reported in the work of [3]. While both show inversely correlated heat rate penalties and outputs are similar, the magnitudes of the effect are noticeably different for reasons we do not fully understand.

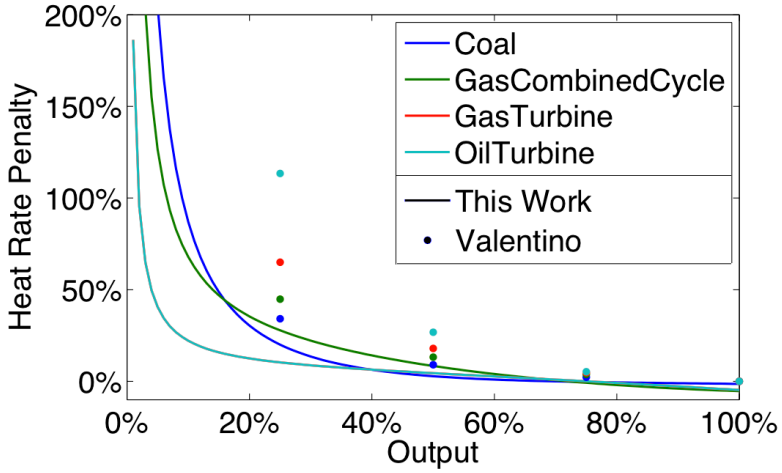

Figure B-9: Comparison of heat-rate penalty curves used in this work and those used by Valentino [3] showing similarity in trend but disagreement in magnitude.

In Table B-2, we compare startup emissions determined using the emissions penalties curves from this work to those determined by fitting a smooth curve to the point estimates provided by [3]. Despite the visible difference in heat rate curves, the maximum difference in startup emissions across pollutants and scenarios is about 10%. Note that in this work, heat rate penalty curves are not used in calculation of normal operations emissions.

Table B-2: Startup emissions calculated using the heat rate penalty curves from this work, and those of [3]. All difference in startup emissions results were below 10%.

		0% Wind, Low Coal Start Cost	0% Wind, Elevated Coal Start Cost	20% Wind, Low Coal Start Cost	20% Wind, Elevated Coal Start Cost
This Work Startups	CO_2 [M ton]	1.0	0.63	2.0	0.99
	NO_X [M lb]	44	21	95	35
	SO_2 [M lb]	180	91	420	150
Valentino Startups	CO_2 [M ton]	1.1	0.68	2.2	1.1
	NO_X [M lb]	47	23	100	38
	SO_2 [M lb]	200	100	450	170

B.9 APTECH Start Cost Figures

Collaboration between NREL and APTECH has produced new startup cost figures [29] than those used in this analysis. The figures represent APTECH's estimated *lower bound* start costs and are provided for a range of different unit types. We performed a three-month model run (January-March) to examine the effects of using these new costs rather than the costs used in the paper. Using these new startup figures does not appear to alter the conclusions of the paper.

The elevated start costs used in our analysis were mid-point estimates. In [29], APTECH was reporting lower bound costs. We therefore decided to use the 75th percentile of the cost values in the latter study, in order to obtain costs on a comparable level to what we employed in the paper. The elevated costs used are reported in Table B-3. Note that nuclear costs were not reported and remain unchanged from the base case used in the paper.

Table B-3: Average elevated start costs adapted from [29].

	Elevated Cold Start Cost [$1,000/start]	Elevated Warm Start Cost [$1,000/start]	Elevated Hot Start Cost [$1,000/start]
Nuclear	74	56	44
Coal	180	120	87
NG CC	100	93	56
NG CT	61	61	61
NG Steam	89	87	42
Oil CT	61	61	61
Oil Steam	120	150	47
Other	89	87	42

Figure B-10 shows changes in coal and flexible unit startups between the two scenarios. In general, the same trends were observed using the new elevated start costs as were observed under our original assumptions. Wind penetration still leads to increased startups across the board. Higher startup costs still lead to reductions in startups. The major difference under the new start costs is that flexible unit startups do not increase nearly as much in response to elevated start costs. This is to be expected, as flexible unit startup costs are now increasing as well.

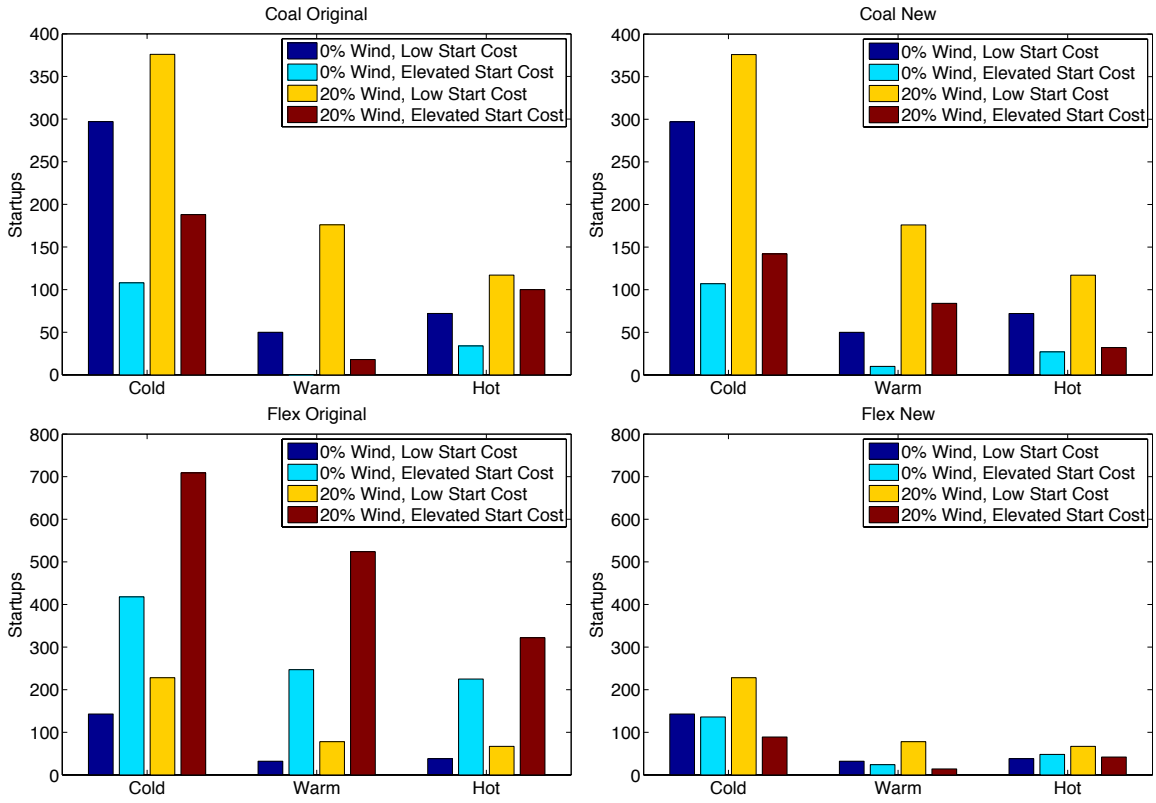

Figure B-10: Coal and flexible unit startups for January-March under the start up costs used in the paper (left column) and under the startup costs used in [29] (right column). Note that the low start cost scenarios remain unchanged.

Figure B-11 shows (capacity-weighted) capacity factors by unit type under both sets of start costs. Again, we observe the same trends. Coal unit capacity factors are reduced with wind penetration and further reduced under elevated start costs. NGCC units follow roughly the opposite

trend. With the new start costs, however, the reduction in coal capacity factor as start costs are increased is somewhat smaller.

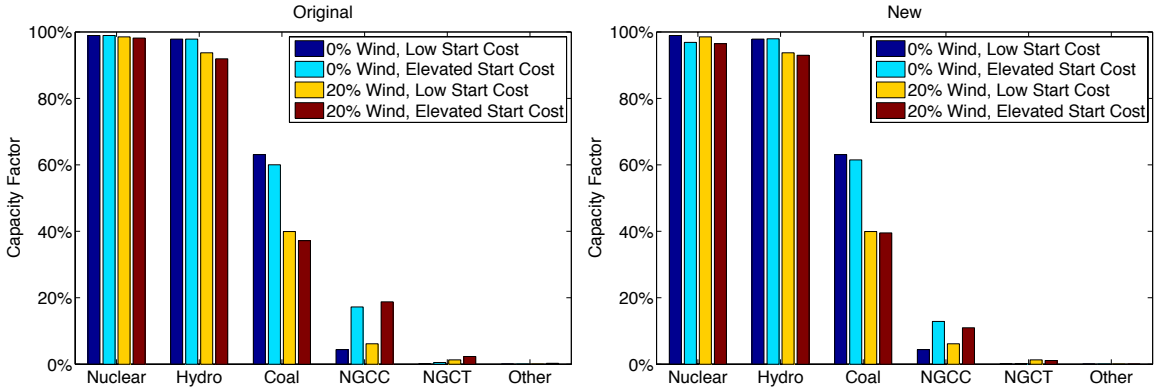

Figure B-11: Capacity factors by unit type for January-March under the start up costs used in the paper (left) and under the startup costs used in [29] (right column). Note that the low start cost scenarios remain unchanged.

Figure B-12 shows wind curtailment under the three 20% wind scenarios. Note that the new start costs lead to higher (economic) curtailment during the night time hours.

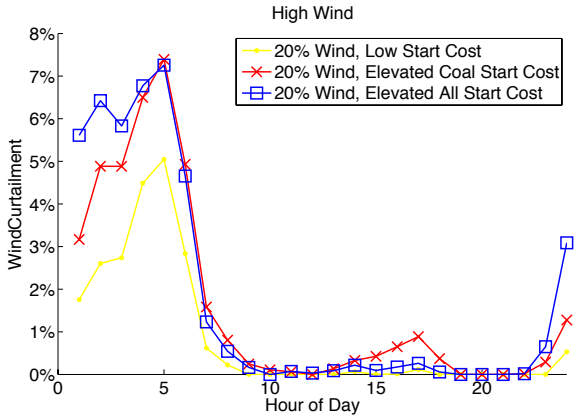

Figure B-12: Wind curtailment for January-March under the start up costs used in the paper and under the startup costs used in [29].

Table B-4 and Table B-5 show emissions under the original start costs and the new start costs, respectively. There do not appear to be any changes of note here.

Table B-4: Emissions of CO2, NOX, and SO2 for January – March under the start up costs used in the paper.

		0% Wind, Low Coal Start Cost	0% Wind, Elevated Start Cost	20% Wind, Low Coal Start Cost	20% Wind, Elevated Start Cost
Normal Operations	CO_2 [M ton]	54	52	34	33
	NO_X [M lb]	270	260	160	150
	SO_2 [M lb]	1,200	1,100	710	660
Startups	CO_2 [M ton]	0.23	0.16	0.47	0.26
	NO_X [M lb]	0.99	0.58	2.3	1.1
	SO_2 [M lb]	3.9	2.4	10	4.7

Table B-5: Emissions of CO_2, NO_X, and SO_2 for January – March under the start up costs used in [29]. Note that the low start cost scenarios remain unchanged.

		0% Wind, Low Coal Start Cost	0% Wind, Elevated Start Cost	20% Wind, Low Coal Start Cost	20% Wind, Elevated Start Cost
Normal Operations	CO_2 [M ton]	54	53	34	34
	NO_X [M lb]	270	260	160	160
	SO_2 [M lb]	1,200	1,100	710	660
Startups	CO_2 [M ton]	0.23	0.18	0.47	0.32
	NO_X [M lb]	0.99	0.72	2.3	1.6
	SO_2 [M lb]	3.9	2.7	10	6.1

Table B-6 and Table B-7 show a comparison of costs between the scenarios. Clearly, the cost figures (particularly the start-up cost figures) are directly affected by the new start costs. More interesting, however, is the change in producer and consumer surpluses between the two sets of costs. Under the new start costs, producer surplus does not increase as much under the elevated start cost scenario, and consumer surplus does not decrease as much.

Table B-6: Normal operations and start costs, revenues and profits for all unit types (including coal) for January – March under the start up costs used in the paper.

	0% Wind, Low Start Cost		0% Wind, Elevated Start Cost		20% Wind, Low Start Cost		20% Wind, Elevated Start Cost	
	All	Coal	All	Coal	All	Coal	All	Coal
Normal Operations Cost ($B)	1.4	1.3	1.4	1.2	0.94	0.8	0.98	0.74
Total Start-Up Costs	0.059	0.055	0.04	0.03	0.13	0.12	0.07	0.057
PJM Start Cost ($B)	0.013	0.008	0.015	0.005	0.02	0.02	0.02	0.009
Start-up costs not included in PJM bids ($B)	0.046	0.046	0.026	0.026	0.1	0.1	0.05	0.05
Total Production Costs ($B)	1.5	1.3	1.5	1.3	1.1	0.93	1.1	0.8
Producer Revenues ($B)	2.1	1.5	2.4	1.5	1.4	0.85	1.6	0.9
Producer Surplus ($B)	0.67	0.11	0.88	0.27	0.36	-0.08	0.58	0.099
Consumer Surplus Change over 0% Wind, Low Coal Start Cost Scenario ($B)	-	-	-0.22	-0.22	0.33	0.33	0.12	0.12

Table B-7: Normal operations and start costs, revenues and profits for all unit types (including coal) for January – March under the start up costs used in [29]. Note that the low start cost scenarios remain unchanged.

	0% Wind, Low Start Cost		0% Wind, Elevated Start Cost		20% Wind, Low Start Cost		20% Wind, Elevated Start Cost	
	All	Coal	All	Coal	All	Coal	All	Coal
Normal Operations Cost ($B)	1.4	1.3	1.4	1.3	0.94	0.8	0.96	0.8
Total Start-Up Costs	0.059	0.055	0.041	0.022	0.13	0.12	0.05	0.038
PJM Start Cost ($B)	0.013	0.008	0.011	0.006	0.02	0.02	0.02	0.013
Start-up costs not included in PJM bids ($B)	0.046	0.046	0.03	0.016	0.1	0.1	0.03	0.024
Total Production Costs ($B)	1.5	1.3	1.5	1.3	1.1	0.93	1	0.84
Producer Revenues ($B)	2.1	1.5	2.2	1.5	1.4	0.85	1.5	0.87
Producer Surplus ($B)	0.67	0.11	0.78	0.21	0.36	-0.08	0.46	0.039
Consumer Surplus Change over 0% Wind, Low Coal Start Cost Scenario ($B)	-	-	-0.12	-0.12	0.33	0.33	0.3	0.3

B.10 Model Formulation

Sets

i	Generators, $i \in I$
k	Hourly time index counting backwards from first period, $k \in K$
t	Hourly time index, $t \in T$
$out(i,t)$	Two-dimensional set indicating outage of unit i in period t, $out(i,t) \in (I,T)$
z	Two-dimensional set indicating unit i is not experiencing outage in period t $notout(i,t) \in (I,T)$

Parameters

D_t	System demand in period t [MWh]
HR_i	Average heat rate of unit i [MMBTU/MWh]
K_i^F	Fuel cost of unit i [$/MMBTU]
K_i^{VOM}	Variable operation and maintenance cost of unit i [$/MWh]
K_i^{SUHOT}	Cost of a hot start for unit i [$/start]
K_i^{SUWARM}	Cost of a warm start for unit i [$/start]
K_i^{SUCOLD}	Cost of a cold start for unit i [$/start]
LOL_i	Lower operating limit of unit i [MW]
UOL_i	Upper operating limit of unit i [MW]
$MINDOWN_i$	Minimum down time for unit i
$MINUP_i$	Minimum up time for unit i
P_i	Output of unit i in the period before the start of optimization horizon [MW]
RD_i	Ramp-down limit of unit i [MW/h]
RU_i	Ramp-up limit of unit i [MW/h]
$SDMAX_i$	Maximum power allowed in period before shutdown $= \max\{LOL_i, RD_i\}$ [MW]
$SUMAX_i$	Maximum power reachable in period after startup $= \max\{LOL_i, RU_i\}$ [MW]
$SUCT$	Number of periods defining a cold start
$SUWT$	Number of periods defining a warm start
$V_{i,k}$	Binary parameter indicating that unit i was online k periods before current optimization horizon {0,1}
W_t	Available wind energy in period t [MWh]

Variables

$x_{i,t}^E$	Energy produced by unit i in period t [MWh]
$x_{i,t}^{SPIN}$	Spinning reserve provided by unit i in period t [MW]
x_t^{WC}	Wind curtailed in period t [MWh]
$y_{i,t}$	Binary variable indicating that unit i is online in period t {0,1}
$y_{i,t}^{SU}$	Binary variable indicating that unit i started up in period t {0,1}

$y_{i,t}^{SD}$	Binary variable indicating that unit i shut down in period t {0,1}
$y_{i,t}^{SUWARM}$	Binary variable indicating that unit i performed a hot or warm start in period t {0,1}
$y_{i,t}^{SUCOLD}$	Binary variable indicating that unit i performed a hot, warm or cold start in period t {0,1}

Objective

The optimization attempts to minimize the total production costs over a 48-hour period. Production costs include fuel costs, variable O&M, as well as startup costs. Startup costs are different depending on whether they are hot, warm, or cold starts.

$$\min_{x,y} \sum_{i,t} (K_i^F HR_i + K_i^{VOM}) x_{i,t}^E + y_{i,t}^{SU} K_i^{SUHOT} + y_{i,t}^{SUWARM} (K_i^{SUWARM} - K_i^{SUHOT}) + y_{i,t}^{SUCOLD} (K_i^{SUCOLD} - K_i^{SUWARM}) \quad [43]$$

System Supply-Demand Balance

The supply-demand balance ensures that the total energy produced by dispatchable generators is equal to the net load (demand minus wind).

$$D_t - W_t + x_t^{WC} = \sum_i x_{i,t}^E; \forall t \quad [44]$$

System Reserve Requirements

The spinning reserve requirement of the system is set at 3% of the maximum load in each 24-hour period, plus 5% of forecast wind in each hour. Non-spinning reserve requirement is set at 3% of the maximum load in each 24-hour period. Equations 45-48 apply these reserve requirements. Equations 49 and 50 ensure that the spinning and non-spinning reserves provided by each unit are, on aggregate, sufficient to cover the requirements.

$$R_t^S = 0.03 \max_{t' \in [1,24]} \{D_{t'}\} + 0.05 W_{t'}; \forall t \in [1,24] \quad [45]$$

$$R_t^S = 0.03 \max_{t' \in [25,48]} \{D_{t'}\} + 0.05 W_{t'}; \forall t \in [25,48] \quad [46]$$

$$R_t^{NS} = 0.03 \max_{t' \in [1,24]} \{D_{t'}\}; \forall t \in [1,24] \quad [47]$$

$$R_t^{NS} = 0.03 \max_{t' \in [25,48]} \{D_{t'}\}; \forall t \in [25,48] \quad [48]$$

$$R_t^S \leq \sum_i x_{i,t}^{SPIN}; \forall t \quad [49]$$

$$R_t^{NS} \leq \sum_i (1 - y_{i,t}); \forall t \quad [50]$$

Wind Curtailment

Equation 51 ensures that the wind energy curtailed in each period is less than the available wind energy.

$$x_t^{WC} \leq W_t; \forall t \quad [51]$$

Unit L.O.L. and U.O.L.

Equations 52 and 53 ensure that the Lower Operating Limit and Upper Operating Limit of each unit is enforced. Both constraints involve the unit on/off binary variable to ensure that the unit is able to shut down.

$$x_{i,t}^E \geq y_{i,t} LOL_i; \forall i,t \quad [52]$$

$$x_i^E + x_{i,t}^{SPIN} \leq y_{i,t} UOL_i; \forall i,t \quad [53]$$

Unit Ramp Rate

Equations 54 - 57 impose up and down ramp rate limitations on each unit. Since the equations depend on the on/off state of the unit in the previous period, they have a different form in the first period of the optimization, in which the on/off state in the period before the start of the optimization (a parameter) is referenced. Down ramp-rate constraints are not enforced if the unit is subject to a forced outage.

$$x_{i,t}^E \leq x_{i,t-1}^E + RU_i y_{i,t-1} + SUMAX_i y_{i,t}^{SU}; \forall t > 1, i \quad [54]$$

$$x_{i,t}^{E} \le P_i + RU_i V_{i,k} + SUMAX_i y_{i,t}^{SU}; \forall t = 1, k = |K|, i \quad [55]$$

$$x_{i,t}^{E} \ge x_{i,t-1}^{E} - RD_i y_{i,t} - SDMAX_i y_{i,t}^{SD}; \forall notout(i, t > 1) \quad [56]$$

$$x_{i,t}^{E} \ge P_i - RD_i y_{i,t} - SDMAX_i y_{i,t}^{SD}; \forall notout(i, t = 1) \quad [57]$$

Unit Startup and Shutdown Binary Variable Definitions

Equations 58 - 61 define the startup and shutdown binary variables for each unit. The definitions have a slightly different form in the first period of the optimization because of the lagged variable.

$$y_{i,t}^{SU} \ge y_{i,t} - y_{i,t-1}; \forall i, t > 1 \quad [58]$$

$$y_{i,t}^{SU} \ge y_{i,t} - V_{i,k}; \forall i, t = 1, k = |K| \quad [59]$$

$$y_{i,t}^{SD} \ge y_{i,t-1} - y_{i,t}; \forall i, t > 1 \quad [60]$$

$$y_{i,t}^{SD} \ge V_{i,k} - y_{i,t}; \forall i, t = 1, k = |K| \quad [61]$$

Unit Warm and Cold Start Binary Variable Definitions

Equations 62 - 65 define the warm and cold start variables, indicating that a warm or a hot start has occurred for unit i in period t. Note that $y_{i,t}^{SUCOLD} \Rightarrow y_{i,t}^{SUWARM}$ and $y_{i,t}^{SUWARM} \Rightarrow y_{i,t}^{SU}$, i.e. the warm start variable counts starts that are actually cold starts, and the startup variable counts starts that are actually warm and cold starts. This fact is accounted for in the objective function.

$$y_{i,t}^{SUWARM} \ge y_{i,t}^{SU} - \sum_{t'=t-SUWT}^{t'=t-1} y_{i,t'}; \forall i, t > SUWT \quad [62]$$

$$y_{i,t}^{SUWARM} \ge y_{i,t}^{SU} - \sum_{t'=1}^{t'=t-1} y_{i,t'} - \sum_{k=|K|+t-SUWT}^{k=|K|} V_{i,k}; \forall i, t > SUWT \quad [63]$$

$$y_{i,t}^{SUCOLD} \ge y_{i,t}^{SU} - \sum_{t'=t-SUCT}^{t'=t-1} y_{i,t'}; \forall i, t > SUCT \quad [64]$$

$$y_{i,t}^{SUCOLD} \ge y_{i,t}^{SU} - \sum_{t'=1}^{t'=t-1} y_{i,t'} - \sum_{k=|K|+t-SUCT}^{k=|K|} V_{i,k}; \forall i, t > SUCT \quad [65]$$

Unit Minimum Down and Up Time

Equations 66 - 69 impose the minimum down and up time constraints of each unit. The minimum down time constraints require each unit to wait until it has been offline for MINDOWN periods until it starts up. The minimum up time constraints require each unit to wait until it has been online for MINUP periods until it shuts down.

$$(1 - y_{i,t}^{SU}) \geq \frac{\sum_{t'=t-MINDOWN_i}^{t'=t-1} y_{i,t'}}{MINDOWN_i}; \forall t > MINDOWN_i, i \quad [66]$$

$$(1 - y_{i,t}^{SU}) \geq \frac{\sum_{t'=1}^{t'=t-1} y_{i,t'}}{MINDOWN_i} + \frac{\sum_{k=|K|+t-MINDOWN_i}^{k=|K|} V_{i,k}}{MINDOWN_i}; \forall t \leq MINDOWN_i, i \quad [67]$$

$$(1 - y_{i,t}^{SD}) \geq \frac{\sum_{t'=t-MINUP_i}^{t'=t-1} (1 - y_{i,t'})}{MINUP_i}; \forall t > MINUP_i, i \quad [68]$$

$$(1 - y_{i,t}^{SD}) \geq \frac{\sum_{t'=1}^{t'=t-1} (1 - y_{i,t'})}{MINUP_i} + \frac{\sum_{k=|K|+t-MINUP_i}^{k=|K|} (1 - V_{i,k})}{MINUP_i}; \forall t \leq MINUP_i, i \quad [69]$$

Unit Outage

Units are forced to be offline during pre-determined periods to simulate the effect of forced-outages.

$$y_{out(i,t)} = 0; \forall out(i,t) \quad [70]$$

Unit Available Spinning Reserve

The amount of spinning reserve a unit is allowed to provide is limited by the additional power it can produce within 10 minutes.

$$x_{i,t}^{SPIN} \leq RU_i / 6; \forall i,t \qquad [71]$$

Chapter 4: ECONOMIC AND ENVIRONMENTAL EFFECTS OF THE EPA'S PROPOSED CLEAN POWER PLAN

Abstract

We performed an analysis to determine the effects of compliance with the Environmental Protection Agency's (EPA's) proposed existing power plant CO_2 emissions standard (the 111(d) rule) on the operation of power systems in PJM West, the Electric Reliability Council of Texas (ERCOT), and ISO New England (ISO NE). We used linear dispatch models of these regions to determine threshold CO_2 prices to achieve compliance. We then used a three-stage Unit Commitment and Economic Dispatch (UCED) model to assess power system operations in more detail. We found that compliance required CO_2 prices of approximately 25 $/ton in PJM West and ERCOT but that no CO_2 price was required to achieve compliance under baseline conditions in ISO NE. Across regions, we found that complying with the 111(d) rule reduced total emissions of CO_2, NO_x, and SO_2 despite small increases in idling and startup emissions. Compliance also reduced production costs (production costs *do not* include the cost of building new capacity) due to the large amount of energy efficiency and wind energy in the compliance scenario. However, if the energy efficiency anticipated by the EPA does not materialize, our results show that production costs increase dramatically even while emissions stay at approximately the same level compared to compliance with the EPA's forecasted energy efficiency. It therefore appears that while air emissions achieved by the 111(d) rule are fairly stable, compliance costs may be sensitive to the amount of energy efficiency that can be procured. Our results also indicate that natural gas generation will increase substantially in PJM West and ERCOT under compliance without the EPA's anticipated energy efficiency. This result may be important for gas infrastructure development.

This paper is in preparation for submission to Energy Policy.

4.1 Introduction

In June of 2014, the EPA proposed the Carbon Pollution Emission Guidelines for Existing Stationary Sources [1] (hereafter "the 111(d) rule"). The 111(d) rule uses the EPA's authority under section 111(d) of the Clean Air Act (CAA) to regulate CO_2 emissions from most of the fossil fueled Electricity Generating Units (EGUs) in the United States. The 111(d) rule follows the EPA's proposal of a rule for CO_2 emissions from new sources, using the agency's authority under section 111(b) of the CAA.

The 111(d) rule imposes CO_2 emissions standards that states must meet. The agency set the standards by first defining the "Best System of Emissions Reduction" (BSER) and then determining the scale of emissions reductions possible in each state using the BSER. The EPA defined BSER to include four building blocks: heat rate improvements at coal and oil-fired EGUs, fuel switching from coal and oil to natural gas combined cycle, increased use of zero carbon sources in the form of non-hydro renewables and "new and at-risk" nuclear, and demand side energy efficiency. The agency determined the extent of changes for each building block that constituted BSER. Table 4.1 shows a brief summary of these determinations.

Table 4.1: Extent of the measures for each of the four building blocks determined by EPA to constitute the Best System of Emissions Reduction (BSER). NGCC refers to Natural Gas Combined Cycle EGUs. RPS refers to Renewable Portfolio Standard. EIA refers to the Energy Information Administration.

Building Block	Target
1. Heat Rate Improvement at Coal/Oil EGUs	6% improvement in coal heat rates
2. Fuel Switching from Coal/Oil to NGCC	NGCC units achieve 70% capacity factor
3. Non-Hydro Renewables and "New and At-Risk" Nuclear	Average of RPS target of states that *have* an RPS within their region. States continue to use at-risk nuclear as defined by EIA
4. Demand Side Energy Efficiency (EE)	Incremental EE growth of 0.2% per year from 2012 baseline to "best practice" level of 1.5% per year, then sustained through 2030

While the EPA used the BSER concept to set standards, the agency does not require that states comply using the BSER measures. Instead, states are free to choose whatever means they see fit to comply with the 111(d) standard. In order to determine a state's compliance, the agency will then compare a quantity we refer to as the "111(d) rate" to the 111(d) standard. The 111(d) rate, which we will discuss in more detail in section 4.2.4, is similar to the average output emissions rate of fossil fuel units in a state. However, it differs in that generation from non-hydro renewables, generation from new and "at-risk" nuclear EGUs, and avoided generation from energy efficiency can be used to comply.

While the EPA's base compliance scenario (called Option 1 - State) envisions states complying on their own, the agency will also allow states to comply cooperatively. Cooperating states would ensure that the average of their 111(d) rates was less than the average of their standards. The agency will also allow states to comply with a "mass-based standard" (as opposed to the "rate-based standard"). This would involve converting a state's 111(d) standard into a CO_2 emissions limit (in ton/y) and requiring that annual emissions from the state are lower than this quantity.

The EPA uses a tool called the Integrated Planning Model (IPM) to study the effects of major new policies affecting the electricity system [2]. The IPM is primarily an electricity system model, though it includes some representation of fuel markets. The model builds and retires EGUs in order to meet forecast future demand for electricity at least cost, subject to a number of policy and operating constraints. The model includes transmission constraints between 64 transmission regions in the continental U.S. The model also represents Canadian provinces endogenously and models interties with Mexico.

While the IPM is able to represent electricity and fuel markets at large geographical scales (the model represents U.S. and Canadian power systems) and temporal scales (the model has a 45 year planning horizon), it does so at the cost of some detail in its representation of the technical

constraints of real-world power systems. In particular, the model does not have an hourly representation of power system operation, instead breaking the year's load into a number of representative segments. Furthermore, the IPM does not represent start ups or shut downs of fossil fueled plants, minimum run times, minimum down times, ramp rate constraints, or forecast errors.

In this work, we modeled compliance with the 111(d) rule in three regions of the continental U.S. (ERCOT, ISO NE, and PJM West) using a more detailed power system model than the IPM. Rather than modeling compliance within individual states, we modeled compliance on average within these regions. Our goal was to examine a number of effects not considered in the EPA's Regulatory Impact Analysis [3]. We also evaluated compliance under a number of scenarios that the EPA did not consider. These alternative compliance scenarios included compliance in the absence of energy efficiency and compliance with the current (2016) fleet of EGUs. Since our model included wind forecast error in the base case, we also considered a scenario *without* forecast error to determine the impact of this error on results. We studied the effects of compliance in 2030 using the EPA's compliance fleet from the IPM, but we did not evaluate the costs of capacity changes up to that point. For each scenario, we report and discuss threshold short-run CO_2 prices required to achieve compliance, total emissions of CO_2, SO_2, and NO_X as well as the portion of emissions from idling and startups, production costs, and the breakdown of electricity generation by fuel type.

This work evaluates several possible compliance scenarios, but does not attempt to study all possible compliance scenarios or to find an optimal compliance scenario. States have wide latitude in terms of how they comply with the 111(d) rule. Fundamentally, however, states have three categories of mechanisms to achieve compliance: 1) altering the generation fleet by building low-emitting capacity, retiring high-emitting capacity, or retrofitting existing capacity to reduce emissions; 2) reducing load via energy efficiency; and 3) re-dispatching the existing fleet in favor of lower-emitting EGUs. This work models only re-dispatch, with fixed generation fleet alterations and load

reduction in each scenario. We achieve this re-dispatch using a CO_2 price adder that imposes an additional generation cost proportional to the emissions rate of the EGU in question. Other methods, such as a cap and trade mechanism, an emissions rate credit system, or limitations on the capacity factors of certain units, might also be viable means of achieving re-dispatch. We consider it unlikely that these methods would lead to a lower-cost re-dispatch than the CO_2 price adder method, but emphasize that other methods are clearly available and some states may choose them.

4.2 Methods

Our power system model is a multi-stage unit commitment and economic dispatch (UCED) model incorporating EGU outages, wind forecast error, and deployable reserves. We modeled compliance and non-compliance scenarios for three power systems - ERCOT, ISO NE, and PJM West - in the year 2030. This is the first year that full compliance is required under the proposed 111(d) rule [1]. We modeled compliance by using a simple dispatch model (as opposed to the full unit commitment model) to determine the threshold compliance CO_2 price and then applying that CO_2 price to the full UCED model. As will be discussed in section 4.2.6, the model uses input data from a variety of sources, but primarily from the EPA's Integrated Planning Model (IPM) data. These data include the EGU fleet in 2030 as forecast by the EPA in their Regulatory Impact Analysis [3].

4.2.1 Multi-Stage Unit Commitment and Economic Dispatch

The UCED in this work expands both on a model presented by Morales-Espana, Latorre, and Ramos [4] and on our previous work [5]. The UCED meets demand for electricity at least production cost, subject to a number of technical constraints. The model is a mixed integer linear program, using integer variables to represent the on/off commitment status of EGUs and continuous variables to represent the output of these EGUs. Production costs include fuel costs

(which are a linear function of electricity output, with a positive intercept), non-fuel variable operations and maintenance (O&M), startup and shutdown costs, and the cost of importing electricity via tie lines. Technical constraints include contingency and wind spinning reserve requirements, minimum and maximum generation levels for EGUs, ramp rate limits, minimum run times, and minimum down times. The full formulation of the model is available in the Appendix.

We selected a high import cost of $300 for all regions. This value mimics that of an ISO NE study [6] under a scenario intended to minimize reliance on imports. We aimed to minimize reliance on imports in order to minimize our model's limitation that it does not represent external regions. Under compliance with the 111(d) rule, the price of imports from external regions would likely increase, as the exporting region would also have to take measures to reduce its CO_2 emissions (though in the case of imports to ISO NE from Quebec, this is not the case). We note that this high import cost has a significant impact on threshold CO_2 prices and likely production costs, particularly in ERCOT and PJM West under the no efficiency scenario. In section C.6 of the Appendix, we compare threshold CO_2 prices under import prices of $300/MWh and $50/MWh.

In order to account for the effects of wind forecast error, we implemented a multi-stage unit commitment and economic dispatch process. In stage 1, day-ahead wind forecasts are used to commit all generating units for a 24-hour period. In stage 2, 6 hour-ahead wind forecasts are used to commit units with minimum downtime of 6 hours or less (in practice this is mostly simple and combined-cycle gas turbines) and dispatch remaining units for a 6-hour period. The commitment of units with minimum downtime longer than 6 hours is fixed at the levels established in stage 1. The stage 2 model is run four times for every run of the stage 1 model, incorporating updated forecasts for each run. In stage 3, hour-ahead wind forecasts are used to commit units with minimum downtime of 1 hour or less (in practice this is mostly simple-cycle gas turbines) and dispatch remaining units for a 1-hour period. The commitment of units with minimum downtime longer than

1 hour is fixed at the levels from stage 2. The stage 3 model is run 6 times for every run of the stage 2 model, incorporating updated forecasts for each run. Note that while the stage 2 and stage 3 models only allow commitment of a subset of units, they also continue to enforce minimum up and downtimes for all units. Figure 4.1 shows the flow of information between the stages in the model.

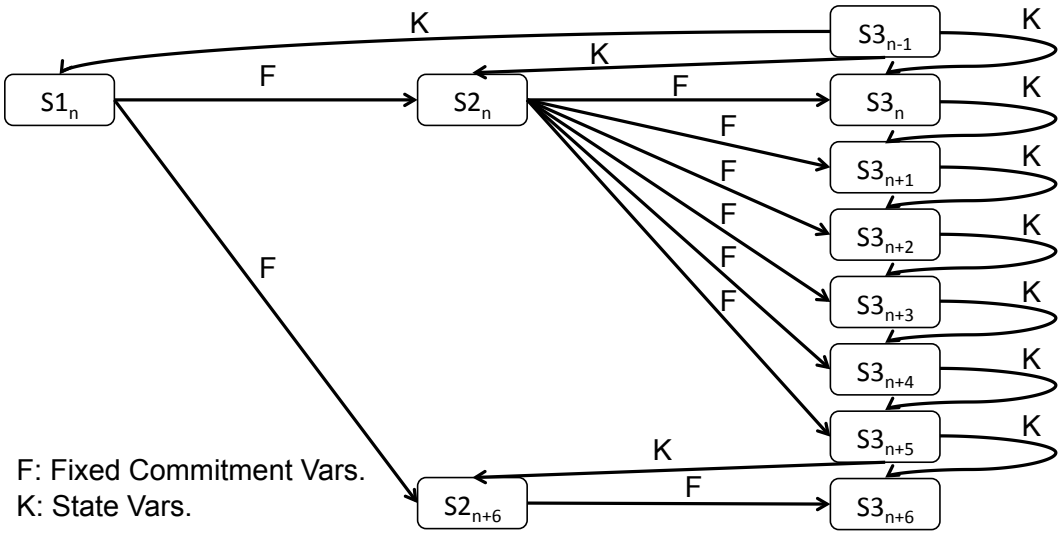

Figure 4.1: Flow of information between S1 (24 hour-ahead), S2 (6 hour-ahead), and S3 (real time) models. The subscripts refer to hours in the model, with n being an arbitrary hour at the beginning of a day. The vertical dimension in the figure represents time (increasing downward) in the model. The model stages are laid out from left to right in the figure, though the horizontal dimension doesn't have any specific interpretation.

In order to avoid infeasibilities, stages 2 and 3 of the model are allowed to deploy reserves. There are two types of reserves in the model – contingency reserves and wind reserves. The latter are deployed first. The model deploys reserves by first executing a model run with contingency and wind reserve requirements imposed as hard constraints. If this model proves infeasible, a second model run is executed where the contingency and wind reserve requirements are imposed as soft constraints. The penalties on wind and contingency reserve violations are set such that wind reserves are deployed first. We do not include the cost of these violations in the production costs reported in the results of this paper.

4.2.2 Model Regions

We evaluate results in three power systems in this work: ERCOT, ISO NE, and PJM West. These regions correspond to all (ERCOT and ISO NE) or part (PJM West) of a de-regulated electricity market. The regions are located in different parts of the country with different seasonal load characteristics. Figure 4.2 shows the approximate locations of these regions. More precisely, the model regions correspond to groups of model regions from version 5.13 of the EPA's IPM model [2]. ERCOT corresponds to the ERC_FRNT, ERC_GWAY, ERC_REST, and ERC_WEST IPM model regions. ISO NE corresponds to the NENG_CT, NENG_ME, and NENGREST IPM model regions. PJM West corresponds to the PJM_West, PJM_Dom, PJM_AP IPM model regions. We included PJM_Dom and PJM_AP to allow results to be more directly compared with those of our previous work [5].

Figure 4.2: Approximate locations of the regions studied in this work.

In addition to their different geographical locations, the regions also have significantly different fuel mixes. Table 4.2 shows the fuel mix of each region broken for the 2030 model year in the base case (without the 111(d) standard). PJM West, with 45% coal capacity, has significantly more coal generation than the other two systems. ERCOT has significant quantities of simple and combined

cycle gas turbines and gas steam EGUs: between them, they account for nearly 70% of ERCOT's capacity. ISO NE is also a very gas-heavy system (67%) that also has a higher portion of nuclear capacity than the other systems (16%).

Table 4.2: Installed conventional EGU capacity (excluding hydro and non-hydro renewables) in 2030 base case in each the power systems under study. Data from [2]. NGCC refers to Natural Gas Combined Cycle, NGCT refers to Natural Gas Combustion Turbine, NG refers to Natural Gas, and CT refers to Combustion Turbine.

Capacity (MW)	ERCOT	ISO NE	PJM West
Biomass	210	610	810
Coal	19,000	140	31,000
NGCC	37,000	12,000	17,000
NGCT	5,600	1,500	9,100
NG Steam	15,000	3,300	340
Nuclear	5,000	4,000	7,500
Oil CT	28	1,700	2,100
Oil Steam	1,100	840	1,600
Other	360	660	520
Total	83,000	25,000	69,000

4.2.3 Actual and Forecast Wind Data

The EPA envisions that states will install substantial new wind capacity in order to comply with the 111(d) standard [3]. In order to study the effect of wind penetrations larger than those currently in place, we used simulated wind and forecast data from the National Renewable Energy Laboratory's Eastern Wind Interconnection and Transmission Study's (EWITS) Eastern Wind Dataset [7]**.** The study used a numerical weather prediction model to generate simulated wind and forecast data at a number of sites in the Eastern Interconnection. We used the EWITS data to ensure that the wind power time series used in this work was appropriately correlated with electricity load.

We assumed that the EPA's proposed goals for state renewable energy [1] would be met using wind energy. We then converted EPA's state-level renewables targets into targets at the level of the regions in our modeling framework. We did this by performing a 2012 generation-weighted average of the renewables targets (expressed as a fraction of total generation) for each state in our region and

then multiplying by the generation in the model region. The resulting wind energy targets are shown in Table 4.3.

Table 4.3: Wind penetration in each region in the absence of the policy and under compliance scenarios.

Region	No-Policy [TWh/y]	Compliance [TWh/y]
ERCOT	27	66
ISO NE	9	22
PJM West	8	39

To generate a single wind output time series, we selected EWITS wind sites in the footprint of our model regions, in order of descending capacity factor. We aggregated the hourly wind output and forecasts for these sites up to the target wind penetration (from Table 4.3). Figure 4.3 shows the simulated 24 h-ahead, 6 h-ahead forecasts as well as real time wind. The figure gives an indication of the size of forecast error present in the EWITS data.

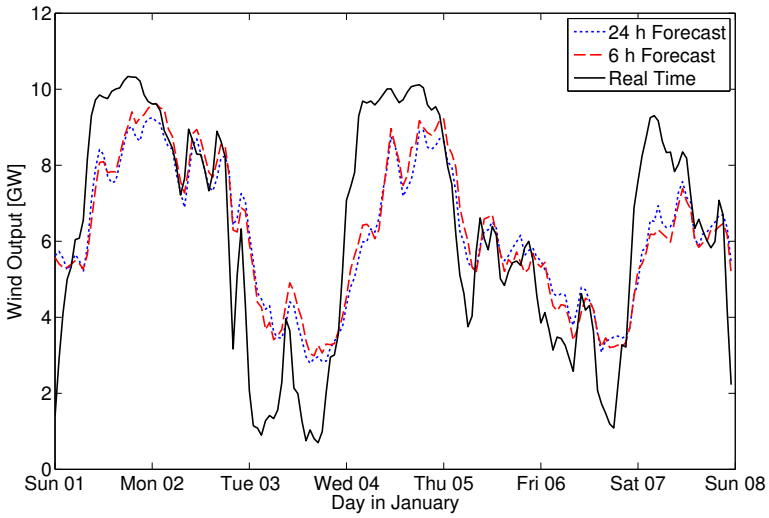

Figure 4.3: Illustration of 24 h-ahead, 6 h-ahead, and realized wind over a 48-hour period in January in ERCOT.

Table 4.4 shows several wind forecast error statistics for each region. For all regions and all statistics, forecast errors decline between the 24 hour ahead and 6 hour ahead forecasts. However, substantial error remains even at 6 hours ahead. Furthermore, mean errors are positive in all regions for both forecast time horizons, indicating that forecast wind is systematically larger than actual wind.

Table 4.4: Wind forecast statistics, including Mean Absolute Error (MAE), Root Mean Squared Error (RMSE), and Mean Error (ME) for each forecast at each time increment. Table also shows Mean (Actual) Wind for scale.

	MAE (MW)		RMSE (MW)		ME (MW)		Mean Wind
	24h Ahead	6h Ahead	24h Ahead	6h Ahead	24h Ahead	6h Ahead	(MW)
ERCOT	1727	1693	2117	2081	79	74	7524
ISO NE	524	513	649	638	33	32	2530
PJM West	1281	1236	1575	1523	51	52	4451

4.2.4 The 111(d) Rule

The 111(d) rule limits CO_2 emissions by requiring states to submit plans that would lower emissions from affected fossil EGUs in their jurisdictions down to a level consistent with the 111(d) standard. The EPA was adamant that the rule does not mandate the particular means states should use to comply with the standard, it only requires that they comply. In the context of this work, we consider the standard as given (at the values shown in Table C-1) and ensure that our UCED model generate a solution that satisfies the standard. We discuss the mechanism for generating a compliance scenario with our UCED in section 4.2.5. Here we discuss the form of the 111(d) rule itself.

The 111(d) standard is expressed in units of lb/MWh. These are the units of an average emissions rate. However, while the form of the 111(d) rule is in many ways similar to a limit on the average emissions rate of affected units, it isn't exactly this. Equation (4.1) shows the 111(d) rule expressed as a constraint. Table 4.5 defines all symbols used in the equation. The left hand side of the equation, which we will refer to as the "111(d) rate," is a function of the output of EGUs in the compliance region. The right hand side, which we will refer to as the "111(d) standard" is, at least in the context of this work, a fixed quantity provided by the EPA [1]. The 111(d) rule therefore states that the quantity defined by the 111(d) rate must be less than or equal to the 111(d) standard.

Table 4.5: Symbols used in equation (4.3).

Variable	Description
$x_{j,t}^{P}$	Energy produced by affected unit j in period t [MWh]
$e_j\left(x_{j,t}^{P}\right)$	CO_2 emissions of unit j as a function of energy produced in period t [lb]
S_R	Rate-based 111(d) standard [lb/MWh]
R_t	Renewables generation in period t [MWh]
N	Energy from new and at risk nuclear per period (constant) [MWh]
η	Avoided energy from energy efficiency per period (constant) [MWh]

The 111(d) rate is given by the emissions from affected EGUs, divided by the sum of the output from affected EGUs, output from non-hydro renewables, output from new and at risk nuclear EGUs, and energy avoided due to energy efficiency programs. The fact that the emissions are divided by a quantity larger than the generation from affected EGUs means that the 111(d) rate will be lower than the average emissions rate of affected units. In general, in order to keep the 111(d) rate less than or equal to the 111(d) standard, EGUs with lower emissions rates will have to be dispatched more frequently than they would be absent the standard.

$$\frac{\sum_t \sum_j e_j\left(x_{j,t}^{P}\right)}{\sum_t \left(\sum_j \left(x_{j,t}^{P}\right) + R_t + N + \eta\right)} \leq S_R \tag{4.1}$$

4.2.5 Threshold CO_2 Price Method

The 111(d) rule essentially takes the form of a cap on emissions rates. It might seem that the most obvious way to implement such a cap would be to apply it directly as a constraint in our UCED rather than to construct a separate dispatch model to evaluate a threshold CO_2 price. Such a constraint would ensure that the 111(d) rate evaluated over the model's time horizon remained under the 111(d) standard.

However, our UCED model was constructed to operate 24 hours at a time. In a model with a 24-hour time horizon, it is only possible to impose an emissions rate constraint on a daily basis. The intention of the 111(d) rule is not to create a limit that is binding on a daily level, but rather to create a rate cap that is binding on an annual level [1]. Due to large seasonal changes in load and generator

availability, and the non-linear shape of the emissions curve of the power systems under study, satisfying the emissions rate standard on a daily basis will produce a very different solution than satisfying it on average over the course of the year. Thus, directly implementing the standard in our model would create highly misleading results.

In principle, we could modify our model to use a longer look-ahead. However, we chose a 24-hour look-ahead because this approximates the values used by current system operators such as the PJM Interconnection [8]. We consider it highly unlikely that such operators would modify their algorithms to run for a full year in order to implement the 111(d) rule. This mechanism would be similar to the existing cap and trade mechanisms for SO_2 and NO_X. Furthermore, even if it were desirable, implementing an annual look-ahead in our model would be computationally intractable.

Instead of using an annual constraint, we therefore used a two-part method to model the effect of the 111(d) rule on power systems in the U.S. First, we constructed simple dispatch models of each region (from section 4.2.2) (more details in C.2). Using these simplified dispatch models, we imposed a range of CO_2 emissions prices, evaluated the 111(d) rate (left side of equation (4.1)) for each CO_2 price, and solved for the "threshold" CO_2 price such that the 111(d) rate was equal to the 111(d) standard (right side of equation (4.1)). Having identified threshold CO_2 prices, we used these prices as inputs to our UCED model by requiring that each fossil EGU pay this CO_2 price.

Here we articulate the rationale for this method in more detail. An increasing CO_2 emissions price leads to increased marginal costs for all EGUs that emit CO_2. This results in an upward shift in the supply curve (this can be seen in Figure 4.8). Since different EGUs have different CO_2 emissions rates, the increase in price affects high-emitting EGUs more than low-emitting EGUs. An increasing CO_2 price therefore progressively re-shuffles the dispatch order such that lower-emitting units are dispatched before higher-emitting units. The 111(d) compliance rate therefore decreases as the CO_2 price increases. Figure 4.4 shows the relationship between the 111(d) rate as calculated from the

simple dispatch model and the effective CO_2 price for ERCOT, ISO NE, and PJM West. The figure also shows the 111(d) standard and the threshold CO_2 price for each region.

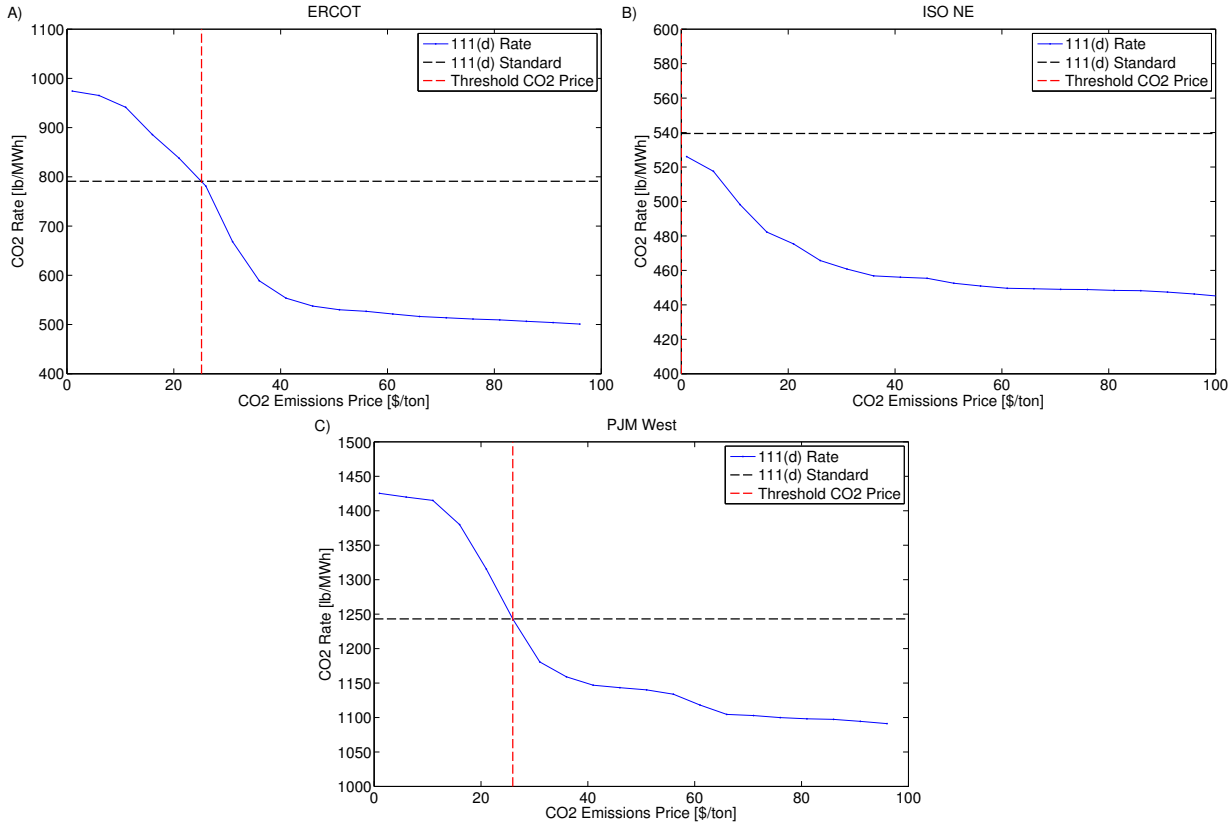

Figure 4.4: 111(d) Compliance Rate vs. effective CO_2 price in A) ERCOT, B) ISO NE, and C) PJM West under OPTION1 compliance. Also shows the 111(d) Standard for each region and the Threshold CO_2 price required to achieve the standard. Note that the threshold CO_2 price in ISO NE is 0 $/ton.

4.2.6 Outages

EGU outages are an important consideration when modeling power systems with a UCED. Outages reduce availability of EGUs by an average 10% [2], a rather significant effect. In this work, we modeled outages using a two-state, length-one Markov chain model, following [9]. In the model, EGUs can either be available or on outage. The probability of an EGU outage in the next period depends only on whether the EGU is on outage this period. The two parameters for this model are the average outage probability, which we obtained from [2], and the duration of an average outage,

which we obtained from [10]. These parameters varied between winter and summer and between EGU types.

4.2.7 Emissions Model

We evaluated three different types of emissions resulting from the operation of the fleet of fossil EGUs:

- *Normal Operations Emissions*: emissions resulting from operating fossil EGUs above their lower operating limit and assuming that their efficiency is constant at its highest level on the unit's operating range
- *Idling Emissions*: incremental emissions in addition to Normal Operations Emissions produced due to reduced efficiency while operating an EGU at less than maximum capacity
- *Startup Emissions*: emissions produced while starting up an EGU

We modeled emissions from fossil EGUs as linear functions of the unit's output, with a positive intercept. Equation (4.2) shows the form of this linear function, using CO_2 emissions as an example. Table 4.6 defines the symbols used in equation (4.2).

Table 4.6: Definition of symbols for equation (4.2).

Variable	Description
$E_{j,t}$	CO_2 emissions from unit j in period t [lb/h]
$x^P_{j,t}$	Electricity produced by unit j in period t [MWh]
$y^u_{j,t}$	On/Off commitment status of unit j in period t [dimensionless]
e_j	Input CO_2 emissions rate of unit j [lb/MMBTU]
h^r_j	Incremental heat rate of unit j [MMBTU/MWh]
h^{nl}_j	No-load heat input of unit j [MMBTU/h]

$$E_{j,t} = e_j(x^p_{j,t}h^r_j + y^u_{j,t}h^{nl}_j) \tag{4.2}$$

Figure 4.5 shows a plot of CO_2 emissions vs. power output for a coal EGU in PJM West. In the notation of equation (4.2), the slope of the solid black line is $e_j h^r_j$ and the intercept is h^{nl}_j. The figure shows the breakdown between Normal Operations Emissions and Idling Emissions for this unit. According to the linear CO_2 emissions model, the unit's output emissions rate (in ton/MWh) is

given by the slope of a line starting at the origin and intersecting the Normal + Idling Emissions line at the output level of the unit. The emissions rate of the unit is therefore lowest when the unit is operated at full output and increases as the output of the unit is reduced. The solid grey line in Figure 4.5 represents what emissions from the EGU would have been if the unit had a constant emissions rate, equal to its emissions rate at maximum output, across its operating range. This is the quantity we refer to as Normal Operations Emissions. The difference between total emissions, shown by the solid black line in Figure 4.5, and Normal Operations Emissions, we refer to as Idling Emissions.

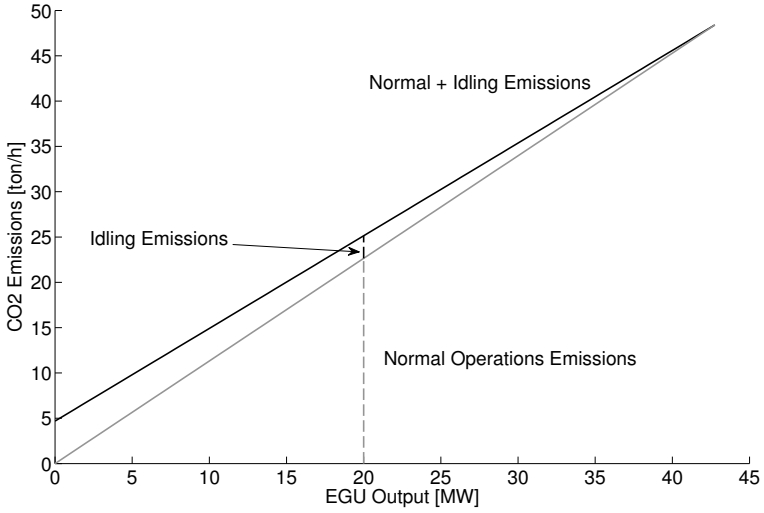

Figure 4.5: CO_2 emissions from a coal EGU in PJM West, showing Normal Operations Emissions and Idling Emissions. The plot shows the breakdown between Normal Operations Emissions

To determine startup emissions, we assumed that a unit would start up by ramping up to its lower operating limit at its ramp-up rate limit and shut down by ramping down from its lower operating limit at its ramp down rate limit. We then integrated the total emissions function (as in Figure 4.5) for CO_2, SO_2, and NO_X over a startup-shutdown cycle and allocated these emissions to each startup.

4.2.8 Scenarios

In order to assess the impact of the 111(d) rule, we modeled four compliance scenarios and one reference scenario. Table 4.7 shows details for each of the five scenarios. The Business As Usual (BAU) scenario is the reference scenario, modeling the 2030 compliance year in the absence of the 111(d) rule. The Option 1 (OPTION1) compliance scenario corresponds to the EPA's Option 1 compliance scenario, with no cooperation between states. The No Efficiency (NOEFF) compliance scenario is the same as OPTION1, except that the energy efficiency that forms a part of compliance under OPTION1 does not materialize. Compliance with the Current Fleet (NOW) is a scenario that attempts to meet the 111(d) rule using the current (2016) fleet, without the energy efficiency, renewable energy, or load growth anticipated before 2030. The No Forecast Error (NFE) scenario is identical to the OPTION1 scenario, with the exception that the UCED is run with no forecast error. Due to the fact that load profiles and fleet data came from different sources, we had to adjust the load profiles somewhat to ensure feasibility. This was done without affecting total annual load using a procedure described in Appendix C.5.

Table 4.7: Note that Unit Technical Constraints and Costs were based on 2025 data from the IPM because these data were not available for 2030. Load profiles were scaled by multiplying hourly loads by a constant scaling factor such that total annual load matched the target.

Name	Business as Usual	Option 1	No Efficiency	Current Fleet	No Forecast Error
Short Name	BAU	OPTION1	NOEFF	NOW	NFE
Unit Constraints and Costs	IPM v.5.13 Base 2025	IPM v.5.13 Option 1 2025	IPM v.5.13 Option 1 2025	IPM v.5.13 Base 2016	IPM v.5.13 Option 1 2025
Load	2006 Load Profiles from [11], [12], [13] Scaled by 2030 Total Load from [14]	2006 Load Profiles from [11], [12], [13] Scaled by 2030 Total Load from [15]	2006 Load Profiles from [11], [12], [13] Scaled by 2030 Total Load from [14]	2006 Load Profiles from [11], [12], [13] Scaled by 2016 Total Load from [14]	2006 Load Profiles from [11], [12], [13] Scaled by 2030 Total Load from [15]
Wind	EWITS 2006 Wind Sites With Total Capacity in IPM v.5.13 Base 2016	EWITS 2006 Wind Sites With Total Capacity in IPM v.5.13 Option 1 2030	EWITS 2006 Wind Sites With Total Capacity in IPM v.5.13 Option 1 2030	EWITS 2006 Wind Sites With Total Capacity in IPM v.5.13 Base 2016	EWITS 2006 Wind Sites With Total Capacity in IPM v.5.13 Option 1 2030
Hydro	IPM v.5.13 Base Case 2030	IPM v.5.13 Option 1 2030	IPM v.5.13 Option 1 2030	IPM v.5.13 Base Case 2016	IPM v.5.13 Option 1 2030
CO_2 Price	None	As in Table 4.8	As in Table 4.8	As in Table 4.8	As in Table 4.8

4.2.9 Sensitivity Analysis

The UCED model used for this work takes many days to solve and is therefore too slow to perform the multiple iterations required for a sensitivity analysis. However, the simplified model we used to determine threshold CO_2 prices solved fast enough to enable this sort of analysis. We used this simplified model to determine the sensitivity of some of our results (those that did not directly depend on the integer variables in the UCED) to natural gas prices, coal prices, and load.

To assess sensitivity to natural gas and coal prices, we performed model runs with varying average (across units) natural gas prices. We then report model outputs as a function of these prices. Note that natural gas and fuel prices in our model differ across EGUs and across scenarios. In scaling the average natural gas and coal prices, we maintained the ratios of natural gas and coal prices across scenarios and across units. Therefore, the ratio of natural gas and coal prices between scenarios is the same after scaling as it was in the original data.

Assessing sensitivity to load was a somewhat more complicated problem. While mean load is an important determinant of model outputs, the standard deviation of load is also important. In fact, all moments of the distribution of load can potentially affect results. This fact suggested the use of a non-parametric method to perform the sensitivity. We elected to use a Dirichlet Process (DP) to model variability in the distribution of load [16]. In contrast to more familiar distribution over real numbers, the DP is a distribution over probability distributions. A draw from a DP is itself a distribution over real numbers. The DP has two parameters: F0, and α. F0 specifies the central distribution around which draws from the DP will fall. The "concentration parameter", α (which is a non-negative real number), specifies how tightly clustered around F0 draws from the DP will be: high values correspond to draws tightly clustered around F0 and low values correspond to draws

that are more spread out. In this work, we let F0 be the empirical distribution of net load in each region in the compliance year. Figure 4.6 shows the central distribution and 100 draws from the DP.

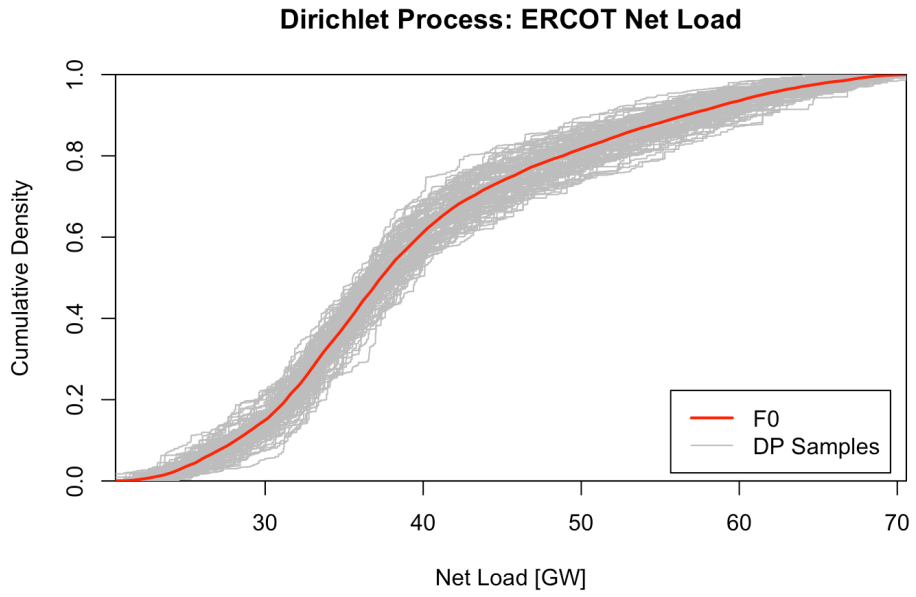

Figure 4.6: 100 draws from the Dirichlet Process centered around the empirical distribution of net load in ERCOT in the compliance year, with α=100. Also shows F0, the empirical distribution of net load.

To choose α, we calculated the distribution over total load induced by the DP. Figure 4.7 shows this distribution, along with the maximum range of year over year variability in ERCOT load from 2003-2013 [17]. The figure shows that the value of α=100 provides a range of mean loads that is somewhat wider than historic variability in ERCOT. We used the same value of α for ISO NE and PJM West, though we adjusted F0 to match the empirical distribution of net load in these regions.

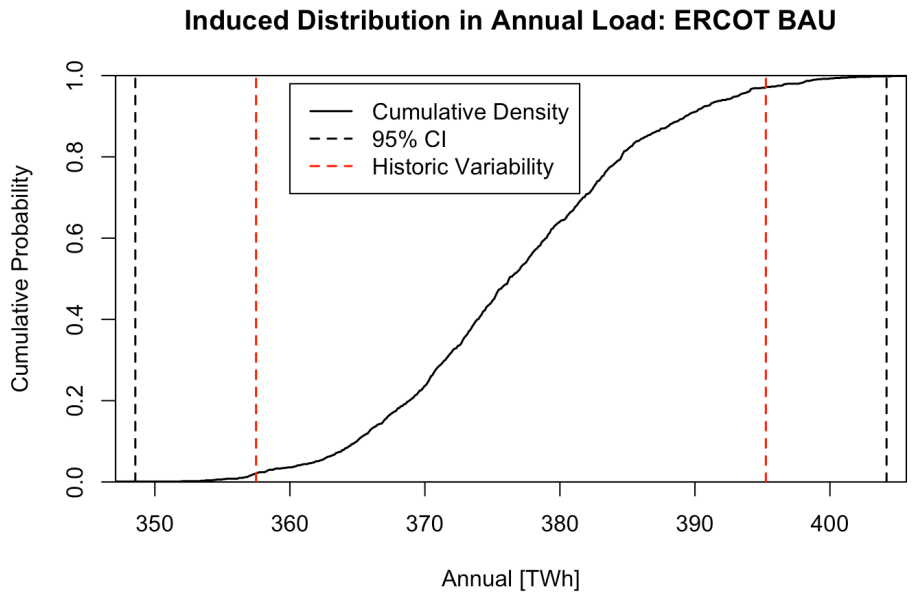

Figure 4.7: Distribution of mean load, induced by the Dirichlet process in Figure 4.6, showing the 95% confidence interval for mean load and the maximum year-over-year variability in ERCOT's load from 2003-2013 from [17].

For the most part, varying natural gas prices, coal prices, and load did not affect our qualitative results. We therefore report the majority of the results of the sensitivity analysis in Appendix C.7. In those cases where the sensitivity analysis yielded new information, we discuss in the results section.

4.3 Results and Discussion

We present results in six sections. In section 4.3.1 we discuss threshold CO_2 prices for each compliance scenario. We found that achieving compliance in PJM West and ERCOT required threshold CO_2 prices of around 25 $/ton, but achieving compliance did not require a CO_2 price at all in ISO NE. We found that the threshold CO_2 price in ISO NE had a chance of becoming positive under high natural gas prices. We also found that threshold CO_2 prices increased significantly when complying without energy efficiency and that complying with the current fleet was not possible in ERCOT or ISO NE.

In section 4.3.2, we discuss the breakdown of electricity generated by different sources. Not surprisingly, we found that coal generation decreased compared to BAU in all compliance scenarios.

Natural gas generation also decreased compared to BAU under OPTION1 compliance, but significantly increased compared to BAU under the NOEFF scenario in PJM West and ERCOT. This increase in NG generation held for high natural gas and low coal prices, but could be reversed with high coal prices and low natural gas prices.

In section 4.3.3 and 4.3.4, we discuss emissions results. We found that total emissions of CO_2, SO_2, and NO_X decreased significantly under all compliance scenarios, including the NOEFF scenario. We also found that emissions due to startups and idling increased significantly under the compliance scenarios, but remained a small fraction (never more than 6%) of the total.

Section 4.3.5 discusses the production cost impacts of the 111(d) rule. Production costs were found to decline under OPTION1 compliance compared to BAU, largely due to the fact that total load was significantly reduced in this scenario as a result of energy efficiency interventions. However, production costs increased under the NOEFF and NOW scenarios.

Section 4.3.6 discusses some of the results of our sensitivity analysis. In particular, we discuss our finding that threshold CO_2 prices are zero under OPTION1 in ISO NE and that natural gas consumption increased from OPTION to NOEFF in PJM West and ERCOT. The sensitivity analysis did not alter the remainder of our qualitative results. Note that, since we did not evaluate probabilities for future natural gas and coal prices, electing instead to treat them simply as varying parameters, we are not able to report error bars in the figures in this section. Please refer to section C.7 of the Appendix for more results from the sensitivity analysis.

4.3.1 Threshold CO_2 Prices

Table 4.8 shows the threshold CO_2 prices required to achieve compliance with the proposed 111(d) standard according to our simplified dispatch model. Threshold CO_2 prices for OPTION1 compliance were around 25 $/ton in ERCOT and PJM West. However, the threshold price was zero in ISO NE. In other words, we found that the 111(d) rule was not binding in ISO NE during

the compliance year. However, we found that a positive CO_2 price was possible in ISO NE under certain load distributions (see Figure 4.13). We emphasize, however, that the fleet under OPTION1 incorporates changes that the EPA anticipates will be needed to comply with the rule. Compared to the current fleet in ISO NE, high-emitting units have been retired, low-emitting units have been built, and substantial renewable energy and energy efficiency have been added in OPTION1. The threshold CO_2 prices reported in the table are short-run marginal costs after these changes have been imposed. Note that since the simplified dispatch model does not include forecast error, threshold prices are identical for the NFE and OPTION1 scenarios.

Under the NOEFF scenario, the threshold CO_2 price increased dramatically in all regions. This increase is largely due to the fact that total load is higher under the NOEFF scenario and a larger change in the dispatch order is therefore required in order to keep emissions below the standard.

Compliance with the standard using the current fleet required a very large CO_2 price in PJM West. Compliance under the NOW scenario was not possible at all in ERCOT or ISO NE. A CO_2 price of 600 $/ton was sufficient to achieve the minimum possible emissions rate in these regions. In the remainder of section 4.2.9, we report results for the NOW scenario in ERCOT and ISO NE using 600 $/ton in place of a threshold CO_2 price.

Table 4.8: Threshold CO_2 prices [$/ton] for each compliance scenario. CO_2 prices are equal to 0 $/ton for BAU because it is not a compliance scenario. CO_2 prices are equal for the OPTION1 and NFE scenarios because forecast error is not incorporated in the simplified dispatch model used to calculate threshold prices. Values of 600$/ton were used where no CO_2 price achieved the required emissions rate.

	OPTION1	NOEFF	NFE	NOW
ERCOT	25	35	25	*600*
ISO NE	0	580	0	*600*
PJM West	26	161	26	262

Figure 4.8 shows supply curves for each of the three regions under the Business As Usual, Option 1, and No Efficiency scenarios. The presence of CO_2 prices both translates the supply curves upward and re-orders the EGUs making up the curves. The magnitude of these effects

depends on the prevailing CO_2 price and the relative emissions rates of the EGUs in each system. EGUs with lower emissions rates tend to move to positions earlier in the dispatch order, while units with higher emissions rates tend to move to positions later in the order.

ERCOT and PJM West have threshold CO_2 prices for OPTION1 compliance of around 25 $/ton. Such prices have a noticeable effect on the position of the OPTION1 supply curve relative to the BAU supply curve and on the order of coal and NGCC units in the dispatch order. The threshold CO_2 price for OPTION1 in ISO NE is 0 $/ton, so of course, there is no change to the dispatch order under this scenario.

In ISO NE and PJM West, the threshold CO_2 prices are substantially higher for NOEFF compliance compared to OPTION1. Consequently, the supply curves for NOEFF compliance in these regions are visibly different than those for OPTION1 compliance. In ERCOT, the threshold CO_2 price is similar under OPTION1 and NOEFF compliance.

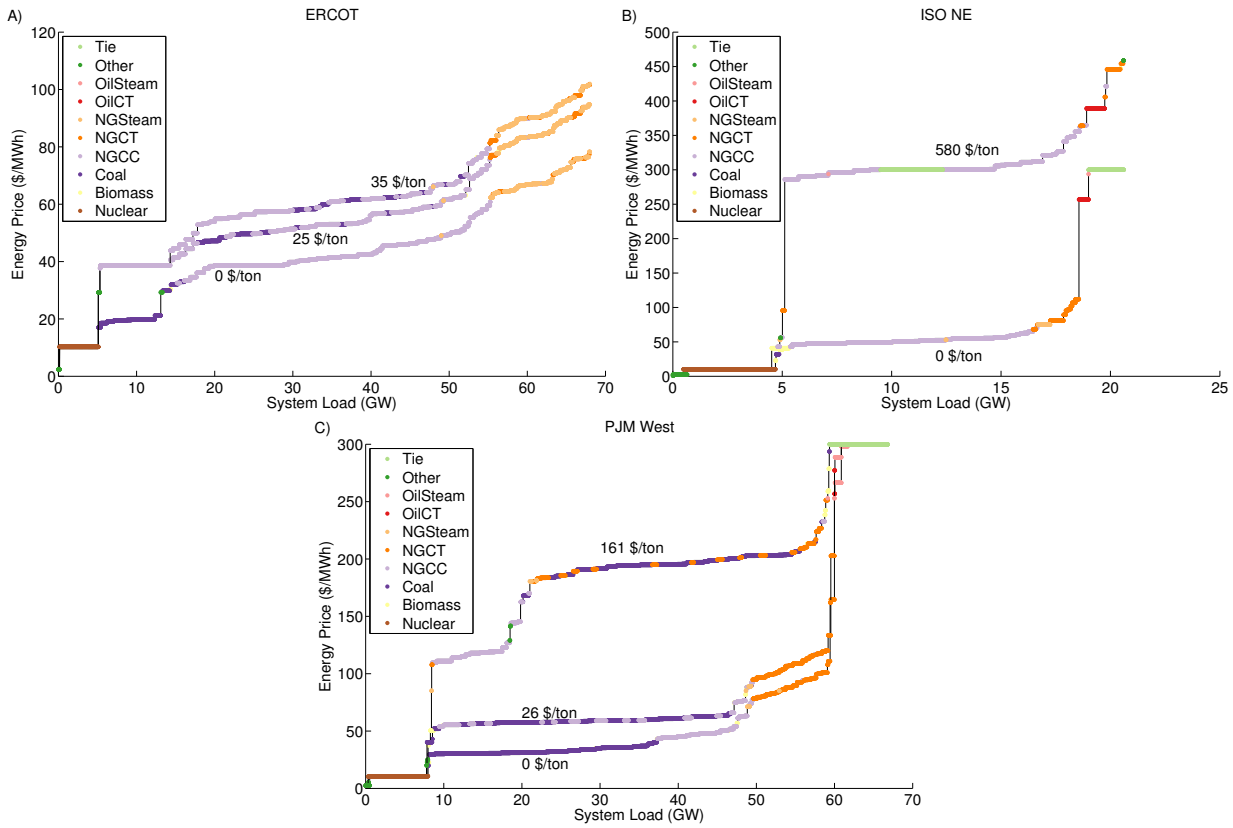

Figure 4.8: Supply curves for A) ERCOT, B) ISO NE, and C) PJM West showing the effects of the threshold CO_2 prices for the OPTION1 and NOEFF compliance scenarios.

4.3.2 Resource Use

Figure 4.9 shows the breakdown of electricity generated by unit type for each scenario in each region. The total height of each bar indicates the total annual load for each scenario. The BAU and NOEFF scenarios both feature larger total load than the OPTION1, NFE, and NOW scenarios because they do not include energy efficiency measures instituted to comply with the standard. Available wind is larger in the OPTION1, NOEFF, and NFE compliance scenarios compared to the BAU and NOW cases.

Compliance resulted in reduced coal generation compared to the BAU case in all regions. Coal generation decreased by 63% in ERCOT, 21% in ISO NE (though from a small baseline hardly visible in Figure 4.9), and 21% in PJM West in OPTION1 compared to BAU. In PJM West,

compliance under the NOEFF scenario resulted in a further reduction in coal generation, to 33% below BAU.

Under OPTION1 compliance, natural gas generation remained approximately constant in ERCOT, and declined substantially in ISONE (41%) and PJM West (29%) compared to BAU. However, under NOEFF compliance, natural gas generation increased significantly over the BAU case in ERCOT (31%) and PJM West (33%). In our sensitivity analysis, we showed that the increase in natural gas generation under NOEFF held provided natural gas prices did not become very low relative to coal prices (see Figure 4.14 and Figure 4.15).

In Figure 4.9, tie line imports met a significant portion of demand in PJM West under the NOW scenario and in ISO NE under the NOEFF and NOW scenarios. In our modeling framework, we chose not to account for CO_2 emitted while producing imported electricity in the emissions budget of the importer. This is consistent with the EPA's proposal, which would account for all emissions in the states where they are produced. However, we emphasize that we also used a fixed cost to model imports. Under a scenario where the whole country was required to comply with the 111(d) rule, the price of imports might in fact increase significantly as the exporting region would also have to comply with the rule. We try to account for this by using a high import price in our model (300 $/MWh), but our results in regions and scenarios that use significant imports to achieve compliance may underestimate the cost of compliance.

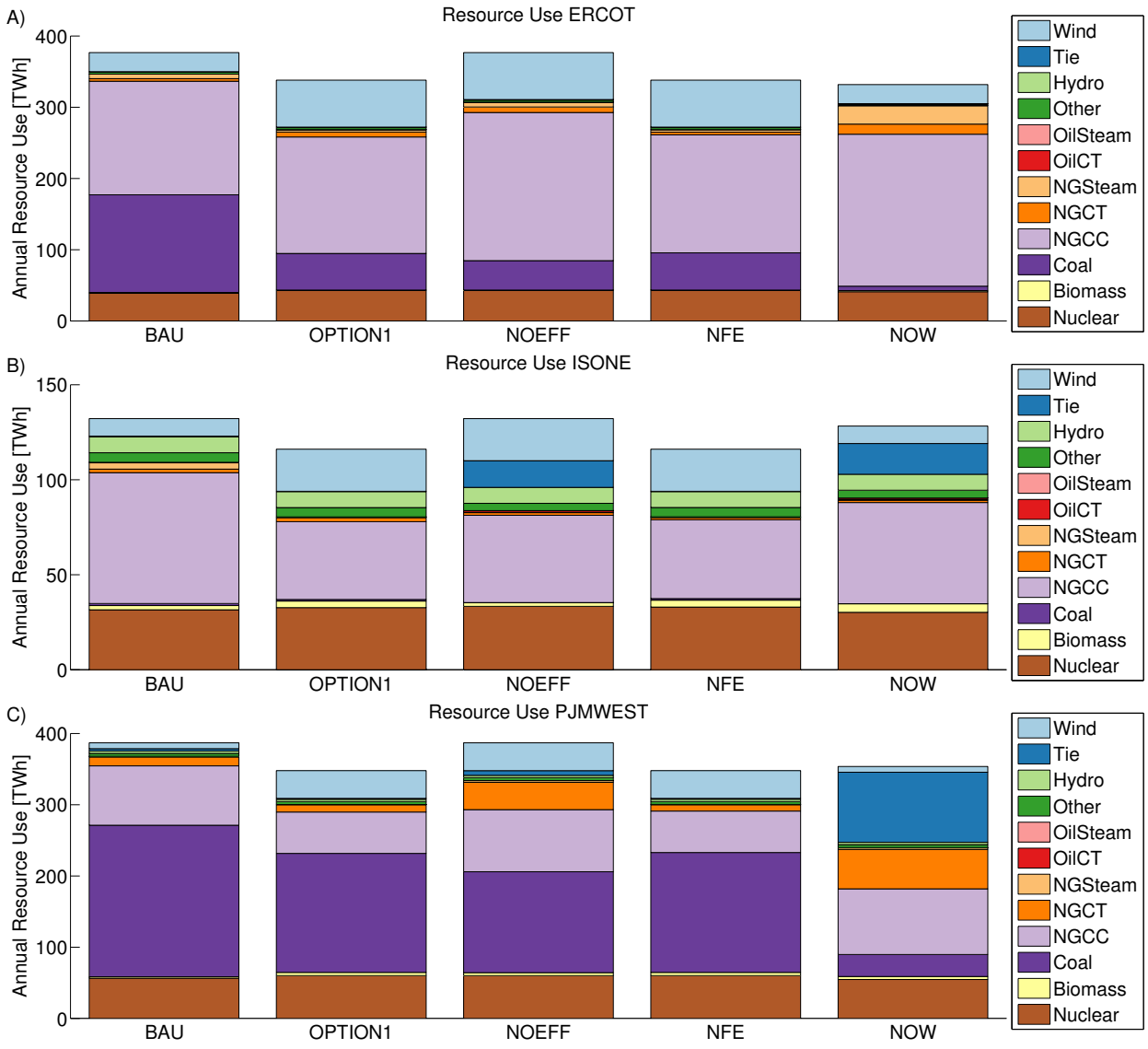

Figure 4.9: Resource use in A) ERCOT, B) ISO NE and C) PJM West showing energy contributed by source type across cases.

4.3.3 Emissions

Compliance with the 111(d) standard resulted in significant reductions in emissions of CO_2, SO_2, and NO_X in each of the systems under study. Average emissions under OPTION1 compliance were 29% below BAU for CO_2, 40% for SO_2, and 28% for NO_X. These figures can be compared to the nationwide figures forecasted by the EPA of 25% reduction for CO_2, 23% for SO_2, and 24% for NO_X [3]. Due to the fact that the EPA emissions figures are at the national level, they cannot be directly compared to our regional figures.

Figure 4.10 shows total emissions of CO_2, SO_2, and NO_X for all regions and all scenarios. The figure shows that percentage reductions in CO_2 under OPTION1 compliance differ by a factor of two across regions, with ERCOT showing the greatest (40%) reduction and PJM West showing the smallest (20%) reduction. ERCOT also achieves the largest percentage reductions in SO_2 and NO_X emissions (61% and 41%, respectively), followed by PJM West (28% and 21%, respectively) and ISO NE (6% and 17%, respectively).

Emissions reductions achieved under the NOEFF scenarios are very similar to those achieved under OPTION1. This result may at first appear counter-intuitive. Indeed, total load under the no efficiency scenarios is substantially larger than under OPTION1. However, as Table 4.8 shows, so too are the threshold CO_2 prices. The higher CO_2 prices in the NOEFF scenarios ensured that total emissions were held roughly constant even as the electricity generation increased. The results in the No Forecast Error scenarios were very similar to those under OPTION1, suggesting the impact of forecast error was minimal.

Emissions reductions under the NOW scenario in PJM West were significantly larger than under OPTION1. Due to the fact that the NOW scenario has no energy efficiency and significantly less renewables than the OPTION1 scenario, this larger reduction in CO_2 emissions was necessary to bring the 111(d) rate below the 111(d) standard (see equation (4.1)). In ERCOT and ISO NE, reductions under the NOW scenario were comparable to those achieved under OPTION1. However, as pointed out in section 4.3.1, CO_2 emissions reductions were too small to comply with the 111(d) rule in this scenario. The fact that CO_2 emissions were essentially the same under the OPTION1 and NOW scenarios, but that compliance was not possible under the NOW scenario, illustrates one potentially unexpected consequence of the form of the 111(d) rule.

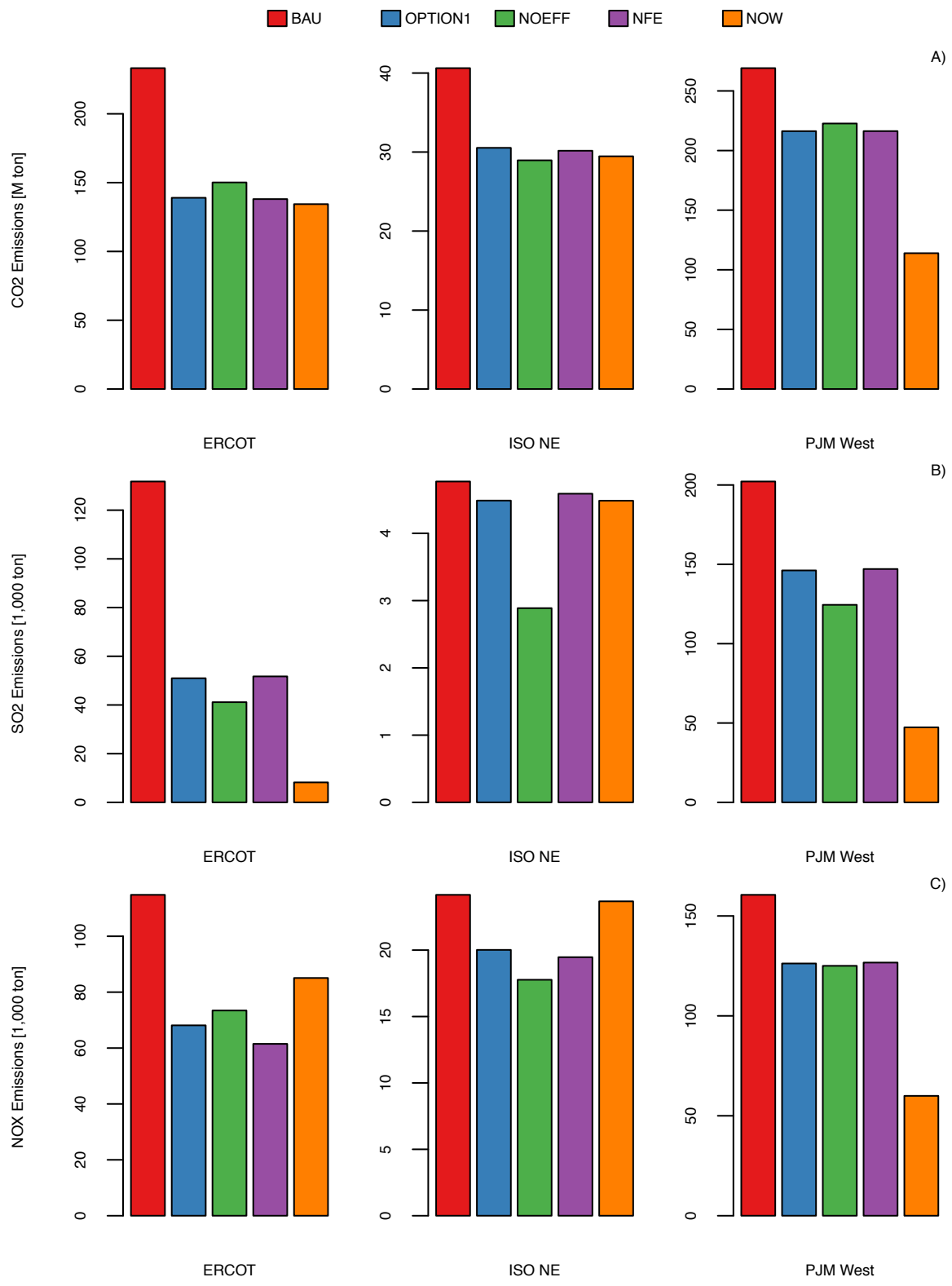

Figure 4.10: Total annual emissions of A) CO_2, B) SO_2, and C) NO_X in the compliance year.

4.3.4 Startup and Idling Emissions

In addition to calculating total emissions, we also determined the contribution to total emissions arising from startups, idling, and normal operations. The components due to startups and idling are shown in Figure 4.11. Comparing the scales of Figure 4.10 and Figure 4.11, it is clear that idling and startup emissions are a small fraction of total emissions. The contribution of idling and startup to total emissions, averaged across the three regions in the BAU case, is 2.4% for CO_2, 0.77% for SO_2, and 2.2% for NO_X. As will be discussed below, these emissions increase on average in the compliance scenarios. However, even at their maximum level under the NOEFF compliance scenario, idling and startup emissions account for only a small fraction of the total: 4% for CO_2, 3% for SO_2, and 7% for NO_X.

We saw in Figure 4.10 that total emissions decrease from BAU to the OPTION1 compliance scenario. However, the trend for startup and idling emissions is less clear. Without examining the result, it is difficult to say whether startup and idling emissions will increase or decrease under compliance scenarios. On the one hand, compliance reduces the number of hours that high-emitting EGUs spend online. This could reduce the number of startups. It could also reduce idling emissions simply by reducing the total number of hours a unit spends online. On the other hand, since most of the compliance scenarios have larger amounts of non-dispatchable wind power than BAU, we might expect startups to increase. Similarly, we might expect units to spend a greater number of their online hours operating at part load and idling emissions to increase.

Figure 4.11 shows that idling and startup emissions increased from BAU to OPTION1 compliance in almost every case, the only exceptions being SO_2 and NO_X emissions in ISO NE. In ERCOT and PJM West, startup and idling emissions were larger, or roughly equal, under NOEFF compared to under OPTION1. The opposite was true in ISO NE, likely due to the NOEFF scenario's reliance on imports in ISO NE. The figure also shows that in every case, startup and

idling emissions were lower in the absence of forecast error than under OPTION1. This result is not surprising, as additional startups and idling can be required to correct for forecast errors.

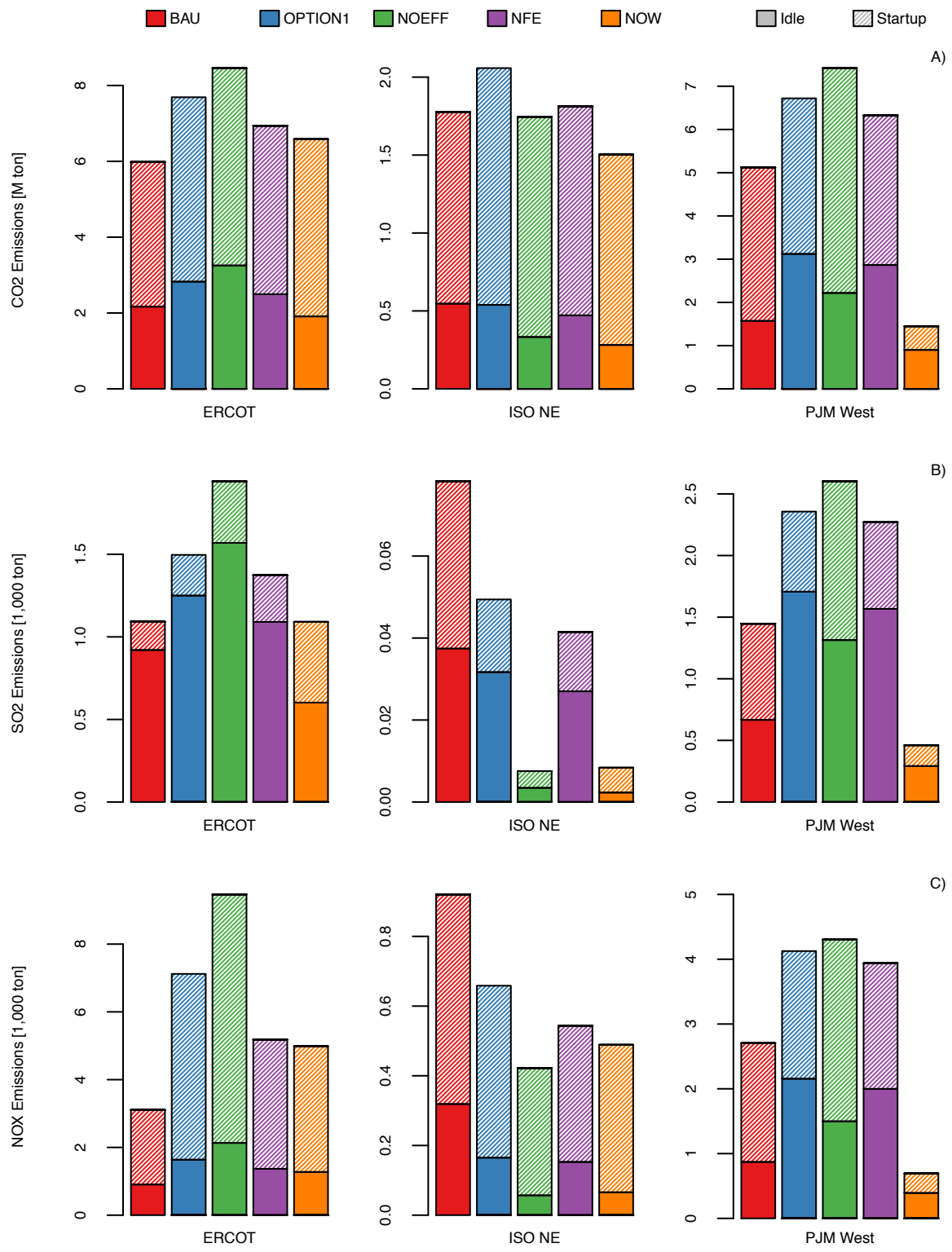

Figure 4.11: Idling and startup emissions by scenario for A) CO_2, B) SO_2, and C) NO_X.

4.3.5 Production Costs

Our results indicated that production costs declined in the OPTION1 compliance scenario compared to BAU. This decline was due primarily to three factors. First, the large amount of energy efficiency in the OPTION1 scenario served to reduce total load, thereby requiring less generation to meet load and therefore lower expenditures. Second, OPTION1 incorporates significantly larger amounts of zero marginal cost wind energy than BAU. Third, the fleet of EGUs under OPTION1 incorporated the effect of the heat rate improvements envisioned by the EPA as one of the compliance building blocks. The fleet of EGUs is therefore more efficient under OPTION1 than under BAU. We emphasize that we are reporting changes in *production costs* here, rather than total costs. Production costs include the cost of fuel, variable O&M for EGUs, startup costs, and the cost of importing electricity into the region. They do not include the cost of building new renewable or other generating capacity or installing technology to increase energy efficiency.

Under the NOEFF compliance scenario, production costs increased significantly over OPTION1. In ERCOT and PJM West, production costs returned approximately to their levels under BAU, and in ISO NE, production costs increased to a level substantially greater than BAU. The large increase under NOEFF in ISO NE was due to the need to import substantial electricity. Note that costs are high in the NOEFF scenario despite the fact that the scenario incorporates nearly triple (190% more) the amount of zero marginal cost wind compared to BAU.

The NOW scenario featured higher production costs than the NOEFF scenario in all regions. As shown in Table 4.8, neither ERCOT or ISO NE was able to reach the 111(d) standard under the NOW scenario. PJM West was able to reach the standard, but only by increasing production costs by 166% compared to BAU. Even this may be an underestimate, as the compliance using the current fleet in PJM West relied on significant imports whose cost might well increase under a nation-wide compliance scenario.

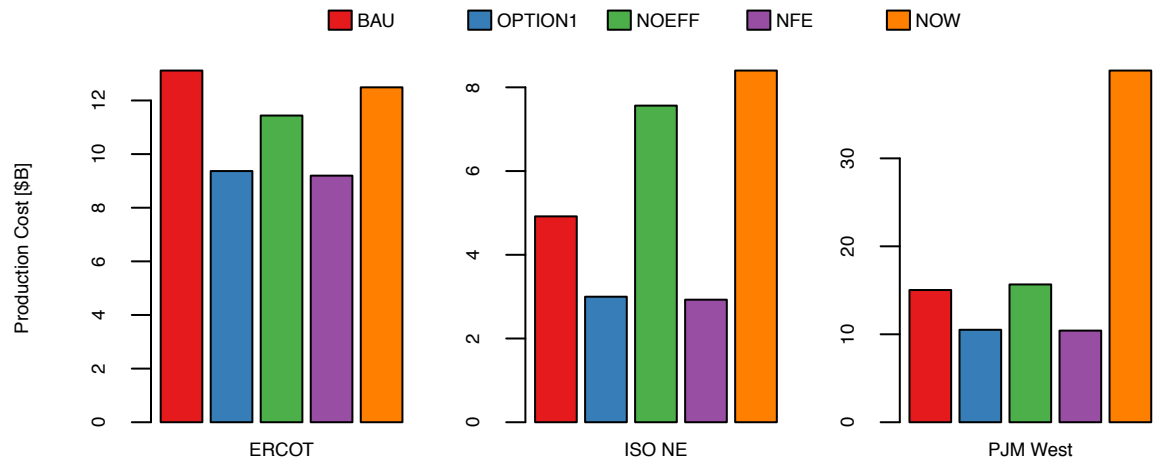

Figure 4.12: Production costs for all scenarios in all regions.

4.3.6 Sensitivity Analysis Results

Figure 4.13 shows the 95th percentile of the distribution of CO_2 prices in ISO NE. The figure shows that for high NG prices, there is some probability of a positive CO_2 price. Under the central load distribution, we do not observe this result. Therefore, we conclude that the threshold CO_2 price in ISO NE is sensitive to the distribution of load at high NG prices.

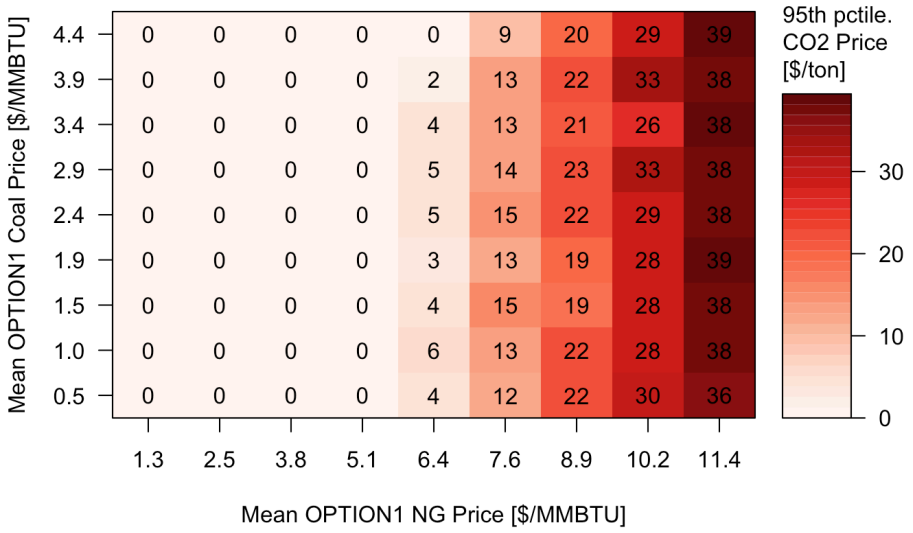

Figure 4.13: 95th percentile of the distribution of threshold CO_2 prices in ISONE.

Figure 4.14 shows the percent increase in natural gas generation from BAU to the NOEFF scenario in PJM West using the central load distribution, i.e. ignoring variability in load (in Appendix C.7, we show that the result discussed here also holds when load is allowed to vary). Figure 4.15 shows the same results for ERCOT. The figures show that under the fuel prices used in the UCED, natural gas generation increases from BAU to NOEFF. However, for low natural gas prices and high coal prices, natural gas generation *decreases* under NOEFF compared to BAU. This may seem counter-intuitive, as one might think that lower natural gas prices would lead to more natural gas consumption rather than less. However, under very low natural gas prices relative to coal, gas is dispatched before coal even under BAU (i.e. without a carbon price). The NOEFF scenario has significantly more wind penetration than BAU, and under these price conditions, wind displaces natural gas generation, leading to the reductions we see in the figures.

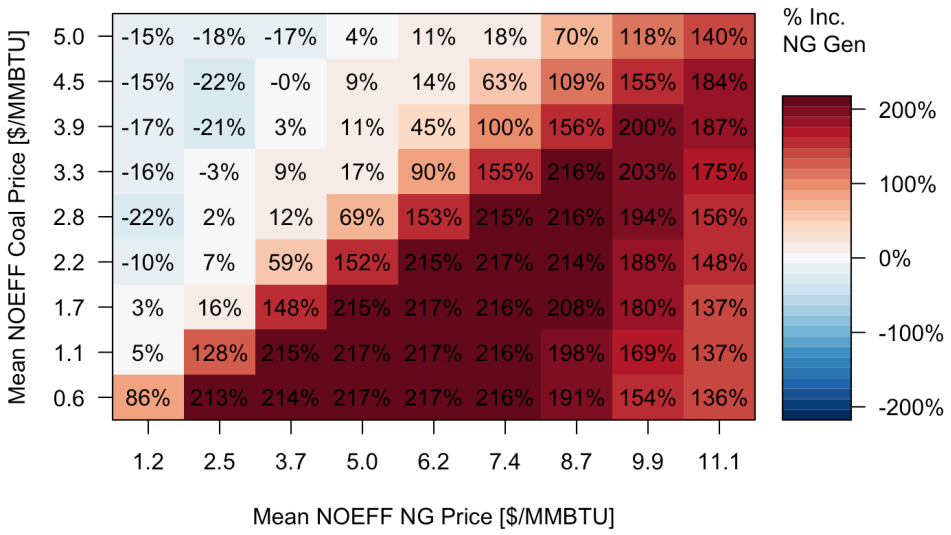

Figure 4.14: Percent increase in NG generation under the NOEFF scenario compared to OPTION1 scenario in PJM West, using the central load distribution.

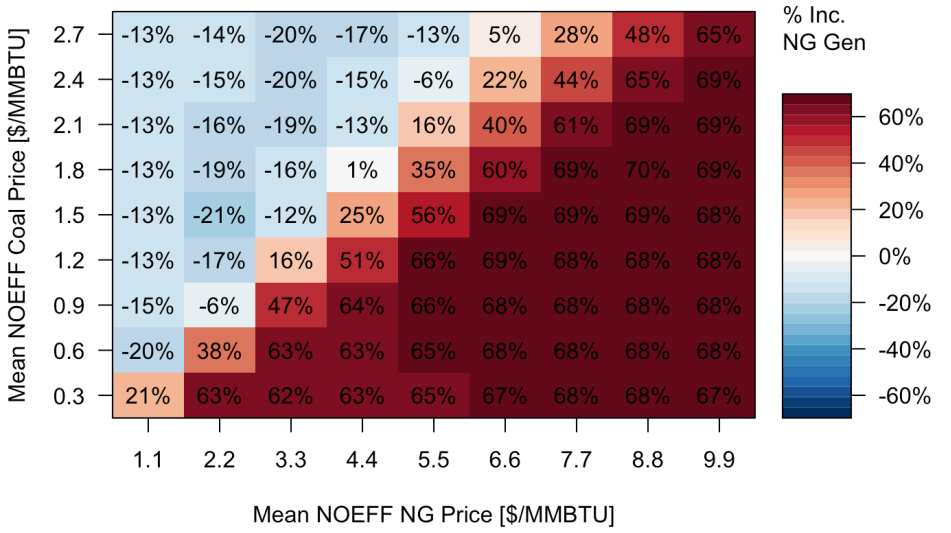

Figure 4.15: Percent increase in NG generation under the NOEFF scenario compared to OPTION1 scenario ERCOT, using the central load distribution.

Note that the simplified model shows substantially lower natural gas generation under BAU than does the UCED. This is why the percent increases in Figure 4.14 and Figure 4.15 are larger than those shown in Figure 4.9.

4.4 Conclusions

Results from our simple dispatch model indicated threshold short-run CO_2 prices of around 25 $/ton were required to achieve compliance under OPTION1 in ERCOT and PJM West. However, we found that no CO_2 price was required to achieve compliance under OPTION1 in ISO NE with our baseline natural gas prices, coal prices, and load. We found a possibility of a positive CO_2 price in ISO NE for high natural gas prices. The result that different regions have different CO_2 prices is not new (the EPA reports shadow prices of CO_2 in the RIA, showing the cross-state variation [18]). However, our results confirm that as long as regions are not cooperatively complying, we should not expect the marginal price of CO_2 to converge as we would with a national cap and trade scheme. Our results further show that CO_2 prices can be sensitive to load, even under a rate-based standard.

Our simple dispatch model also indicated that threshold CO_2 prices increased dramatically for compliance in the absence of energy efficiency. Using our full UCED model, we also found that production costs increased when complying without energy efficiency. These finding suggests that compliance costs could be significantly higher than anticipated if the energy efficiency anticipated by the EPA does not materialize.

We determined the contribution of idling and startups to total emissions of CO_2, SO_2, and NO_X. While startup and idling emissions increased under compliance scenarios, they remained a small portion (less than 6%) of total emissions. The increase in startup and idling emissions was too small to have a noticeable effect on the reduction in total emissions, which declined 30%-40% in compliance scenarios. We also examined the effect of wind forecast errors, finding that such forecast errors increased production costs and total emissions by about 1-3%. These results suggest that the EPA's neglect of startup and idling emissions and forecast error in the IPM will not significantly affect the results of their Regulatory Impact Assessment.

Under OPTION1 compliance, we found that coal generation decreased by up to 60% (38% on average across regions) compared to BAU. We also found that natural gas generation decreased under OPTION1 compliance. However, when complying in the absence of energy efficiency, natural gas generation increased by about 30% above BAU in ERCOT and PJM West. This outcome may come as a surprise, as the EPA's Regulatory Impact Assessment modeled significant energy efficiency in their compliance scenarios. Increases of this scale might require additional investment in natural gas extraction and transmission infrastructure. We found that this result could be reversed for low natural gas prices relative to coal prices.

Finally, in PJM West, we found that compliance using the current fleet was possible, but only by relying heavily on imports and by increasing production costs by more than 2.5 times over BAU. In ERCOT and ISO NE, compliance with the current fleet was not possible (though emissions were similar to those under OPTION1) even with a CO_2 price of 600 $/ton. We conclude that complying with the 111(d) rule without making significant changes to the fleet of EGUs is either impossible or a very bad idea.

Our work has a number of limitations that merit acknowledgment. First, the work focuses on the operational time scale and ignores capacity expansion decisions. While we consider scenarios with different fleets, we have not evaluated all possible compliance scenarios. Second, our model represents a number of regions with only limited interaction with their surroundings. We allow imports into our regions, but at a fixed import price. Our production cost and threshold CO_2 price results are potentially sensitive to this assumed import price and the price does not change to reflect the effects of the rule. Third, despite the fact that our UCED represents many operational constraints and cost terms, it has a number of limitations. It does not represent transmission constraints within each region, it does not represent ancillary service or sub-hourly markets, it assumes cost-based bidding by EGUs with linear fuel input/power output curves, and it uses a

heuristic representation of contingency and wind reserve requirements. These limitations are somewhat typical of planning models (e.g. [19]-[21] all share some of these limitations). Next, the compliance year for this work is 2030 and we are necessarily reliant on forecasts for our input parameters. These forecasts may not turn out to be accurate. Finally, the 111(d) rule is still a long way from a finished product. Numerous changes could arise during finalization and litigation that could materially affect our results.

In using the EPA's capacity expansion analysis to determine our fleet of generators, we incorporate the many assumptions underlying this analysis into our work. In particular, the agency chose not to evaluate the possibility of retrofitting existing plants with CCS in order to achieve emissions reductions. While the agency argued that the costs of CCS-retrofits are highly variable, there may be overlooked opportunities to achieve low-cost emissions reductions via such retrofits. Additionally, while the agency has proposed not to count new fossil plants (CCS equipped or otherwise) towards compliance with the 111(d) rule, allowing new CCS equipped units might result in an increased role for CCS.

4.5 References

[1] EPA, *Carbon Pollution Emission Guidelines for Existing Stationary Sources: Electric Utility Generating Units; Proposed Rule*. 79 FR 34830, 2014.

[2] EPA, *Documentation for EPA Base Case v.5.13 Using the Integrated Planning Model*. Environmental Protection Agency, 2013.

[3] EPA, *Regulatory Impact Analysis for the Proposed Carbon Pollution Guidelines for Existing Power Plants and Emission Standards for Modified and Reconstructed Power Plants*. Environmental Protection Agency, 2014.

[4] G. Morales-Espana, J. M. Latorre, and A. Ramos, "Tight and Compact MILP Formulation for the Thermal Unit Commitment Problem," *IEEE Trans. Power Syst.*, vol. 28, no. 4, pp. 4897–4908, Nov. 2013.

[5] D. L. Oates and P. Jaramillo, "Production cost and air emissions impacts of coal cycling in power systems with large-scale wind penetration," *Environ. Res. Lett.*, vol. 8, no. 2, p. 024022, 2013.

[6] ISONE, *2013 Economic Study*. ISO New England, 2014, pp. 1–96.

[7] NREL, *Eastern Wind Dataset*. National Renewable Energy Laboratory, 2013.

[8] PJM, *PJM Manual 11: Energy & Ancillary Services Market Operations*, 71st ed. 2015.

[9] R. J. R. A. J. W. Roy Billington, *Power-System Reliability Calculations*, no. 978. The MIT Press, 1973.
[10] P. Murti and A. Rudkevich, *GE Maps Input Assumptions: Eastern Interconnect*. CRA International, 2006.
[11] ERCOT, *2006 ERCOT Hourly Load Data*. Electric Reliability Council of Texas, 2013.
[12] ISONE, *2006 SMD Hourly Data*. ISO New England, 2007.
[13] PJM, *Estimated Hourly Load 2006*. PJM Interconnection, 2007.
[14] EPA, *IPM Run Files: EPA Base Case for the proposed Clean Power Plan*. Environmental Protection Agency, 2014.
[15] EPA, *IPM Run Files: Option 1 - State*. Environmental Protection Agency, 2014.
[16] T. S. Ferguson, "A Bayesian Analysis of Some Nonparametric Problems," *The Annals of Statistics*, vol. 1, no. 2, pp. pp. 209–230, 1973.
[17] ERCOT, *2014 ERCOT Planning Long-Term Hourly Peak Demand and Energy Forecast*. Electric Reliability Council of Texas, 2014.
[18] M. Celebi, K. Spees, J. M. Hagerty, S. A. Newell, D. Murphy, M. Chupka, J. Weiss, J. Chang, and I. Shavel, "EPA's Proposed Clean Power Plan: Implications for States and the Electric Industry," The Brattle Group, Jun. 2014.
[19] Denny, "Quantifying the Total Net Benefits of Grid Integrated Wind," *IEEE Trans. Power Syst.*, vol. 22, no. 2, pp. 605–615, May 2007.
[20] L. Valentino, V. Valenzuela, A. Botterud, Z. Zhou, and G. Conzelmann, "System-Wide Emissions Implications of Increased Wind Power Penetration," *Environmental Science & Technology*, vol. 46, no. 7, pp. 4200–4206, Apr. 2012.
[21] B. Nyamdash, E. Denny, and M. O'Malley, "The viability of balancing wind generation with large scale energy storage," *Energy Policy*, vol. 38, no. 11, pp. 7200–7208, Nov. 2010.
[22] NERC, *Reliability Standards for the Bulk Electric Systems of North America*. North American Electric Reliability Corporation, 2015.
[23] R. Piwko, K. Clark, L. Freeman, and G. Jordan, *Western wind and solar integration study*. National Renewable Energy Laboratory, 2010, p. 260.
[24] EPA, *Parsed File: Base Case, 2025*. Environmental Protection Agency, 2014.
[25] EPA, *Parsed File: Option 1 State, 2025*. Environmental Protection Agency, 2014.
[26] E. Krall, M. Higgins, and R. P. O'Neill, *RTO Unit Commitment Test System*. Federal Energy Regulatory Commission, 2012.

C Appendix

C.1 Comparison of the 111(d) Standards and Rates

Our method for modeling compliance with the 111(d) relied on using two separate models: a simple dispatch model to find the threshold CO_2 price and a UCED to evaluate the compliance scenarios given the threshold CO_2 price. Due to the fact that the UCED has a different structure than the simple dispatch model, there is no guarantee that the 111(d) rate will be below the 111(d) standard in our compliance scenarios. In Table C-1, we report the 111(d) standards and the 111(d) rates calculated from the UCED for each region in each compliance scenario. The table shows that while the 111(d) rates are substantially lower under the compliance scenarios than under BAU, in general the 111(d) rate is not below the standard as evaluated in the UCED. This is not particularly surprising, given that the UCED results include startup and idling emissions and the operation of the system is more tightly constrained in the UCED.

Table C-1: 111(d) standard and 111(d) rate as evaluated with the UCED (lb/MWh). Scenarios where compliance was determined not to be possible using the simple dispatch model are shown in italics.

	ERCOT		ISO NE		PJM West	
	Standard	Actual	Standard	Actual	Standard	Actual
BAU	NA	1486	NA	865	NA	1788
OPTION1	791	848	539	577	1243	1297
NOEFF	791	933	539	598	1243	1359
NFE	791	843	539	569	1243	1297
NOW	791	*918*	539	*742*	1243	1164

C.2 Simple Dispatch Model

Here we discuss the structure of the simple dispatch model used to determine threshold CO_2 prices. The 111(d) rate was evaluated using the simple dispatch model using equation (4.4). In the simplified model, there are no inter-temporal constraints (such as ramp rate constraints, minimum up times and minimum downtimes) so all periods are independent. We therefore treat load, wind, and net load as random variables (related according to equation (4.3)) and calculate the emissions

rate constraint in terms of expected values of functions of these random variables. Table C-2 defines the symbols used in equations (4.3) and (4.4).

Table C-2: Symbols used in equations (4.3) and (4.4).

Variable	Description
L	Random variable for load [MW]
W	Random variable for wind [MW]
H	Random variable for hydro [MW]
X	Random variable for load net of wind [MW]
$e(X)$	CO_2 emissions from affected units as a function of X [lb/h]
$a(X)$	Output from affected units as a function of X [MW]
$n(X)$	Output from new and at risk nuclear units as a function of X [MW]
η	Average available energy efficiency [MW]
R	111(d) emissions rate standard [lb/MWh]

The function e(X) of CO_2 emissions from affected units as a function of net load was defined for each system under study using a simple dispatch curve model. The marginal costs of each generating unit were sorted in ascending order. Cumulative emissions to each output level were then calculated from affected units. The resulting function is piecewise linear. The break points between linear segments are defined by the capacities of the generating units. The segments corresponding to a particular generating unit have slope 0 if the unit is not an affected unit, and slope equal to the emissions rate of the unit if it is an affected unit. An example emissions curve is shown in the left portion of Figure C-1.

The function a(X) of output from affected units also relies on sorting the generating units in order of ascending marginal cost. Cumulative output from affected units was then calculated with the resulting function being piecewise linear. The break points between segments are defined by the capacities of the generating units. The segments corresponding to particular generating units have slope of 0 if the unit is not affected by the standard, and 1 if the unit is affected by the standard. The right portion of Figure C-1 shows an example of this function.

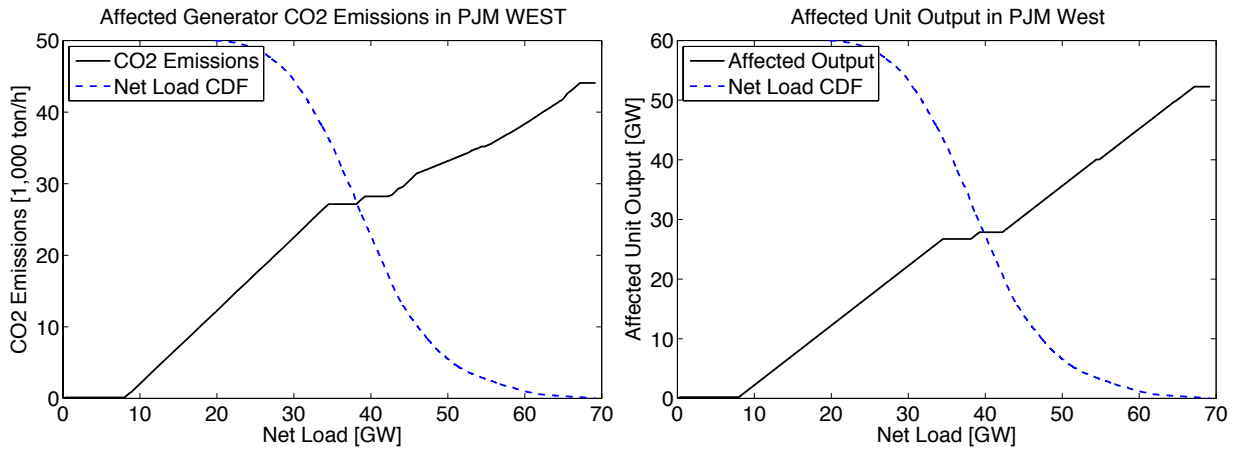

Figure C-1: CO_2 emissions from affected EGUs (Left) and generation from affected EGUs (Right) as a function of net load. Figures also show the scaled inverse CDF of net load.

$$X = L - (W + H) \tag{4.3}$$

$$R = \frac{\mathbb{E}_X[e(X)]}{\mathbb{E}_X[a(X)] + \mathbb{E}_X[n(X)] + \mathbb{E}_W[W] + \eta} \tag{4.4}$$

C.3 Electricity Prices

The effect of the 111(d) rule on electricity prices depends a great deal on how the rule is implemented. In particular, if the rule is imposed using a carbon tax or cap and trade system, it will have a very different impact on price than if it is imposed by setting up a scheme where EGUs make or receive payments based on the difference between their emissions rate and the 111(d) standard. In this work, we implemented the rule using what amounted to a carbon tax system. Due to the fact that electricity prices are sensitive to this arbitrary choice, we do not report them along with the main results. We do reproduce them in the appendix, however.

We found average energy prices decreased by 7.60 $/MWh, or 8%, below BAU in the OPTION1 compliance case, on average across the regions. This decrease was the result of reduced load due to energy efficiency. When complying without energy efficiency in the NOEFF scenario, prices increased by 110% compared to BAU, increasing by $100/MWh on average across the regions. Compliance with the current fleet in the NOW scenario drove energy prices up to 250%

above the BAU case, an increase of nearly 230 $/MWh. Note that the energy price in the NOW compliance scenario in ISO NE and PJM West is essentially set by the price of imports, 300 $/MWh.

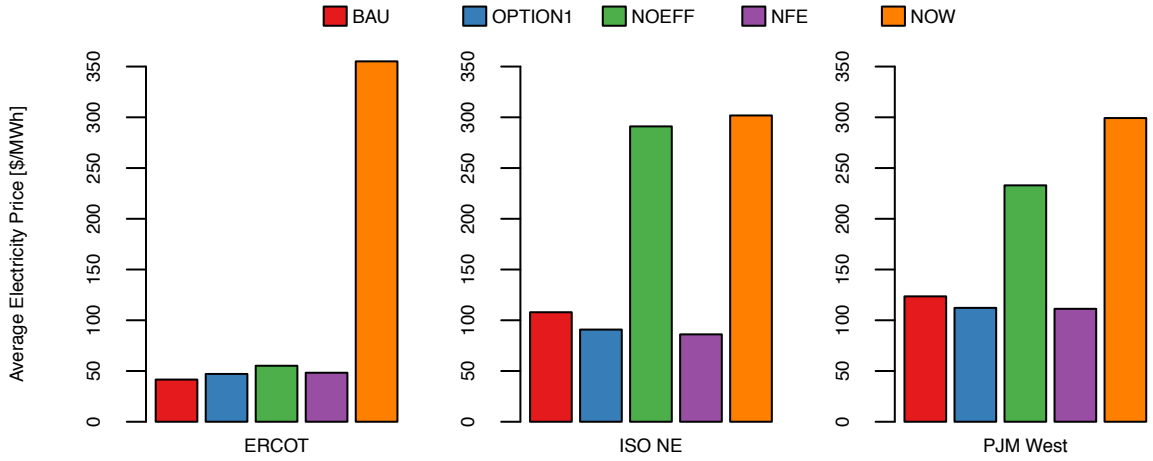

Figure C-2: Load-weighted average energy prices by scenario and region. Note that periods where reserve constraints were violated were not included in the average.

C.4 Data Sources

Table C-3 shows the input parameters for the UCED and the sources used for each one.

Table C-3: Data sources for the UCED input parameters.

Parameter	Source – No Policy	Source – With Policy
Load Profile - ERCOT	[11]	[11]
Load Profile - ISO NE	[12]	[12]
Load Profile - PJM West	[13]	[13]
Total Load	[14]	[15]
Contingency Reserve Requirement	[22]	[22]
Wind Reserve Requirement	[23]	[23]
Wind Profile	[7]	[7]
Wind Penetration	[2]	[1]
Hydro Profile and Penetration	[2]	[2]
EGU Marginal Cost	[24]	[25]
EGU No-Load Cost	[26]	[26]
EGU Startup Cost (Hot/Warm/Cold)	[26]	[26]
EGU Capacity	[14]	[14]
EGU Minimum Generation Level	[26]	[26]
EGU Ramp Rate Limit	[26]	[26]
EGU Minimum Up/Down Time	[10]	[10]
Tie Line Capacity	[14]	[14]

C.5 Load Adjustment

Due to the fact that our data on the available fleet of EGUs and load profile were not from the same source, we observed that the load profiles occasionally exceeded available capacity in our regions even after accounting for imports. We therefore used an optimization routine to slightly adjust the load profiles to ensure that a feasible solution would be obtained. The load adjustment procedure ensured that total load over the course of the year would not be altered. The procedure minimized the difference in load, and the first difference in load, across the year while requiring that the load be less than the available capacity. Figure C-3 shows an example of the effect of this adjustment in ERCOT under OPTION1 compliance.

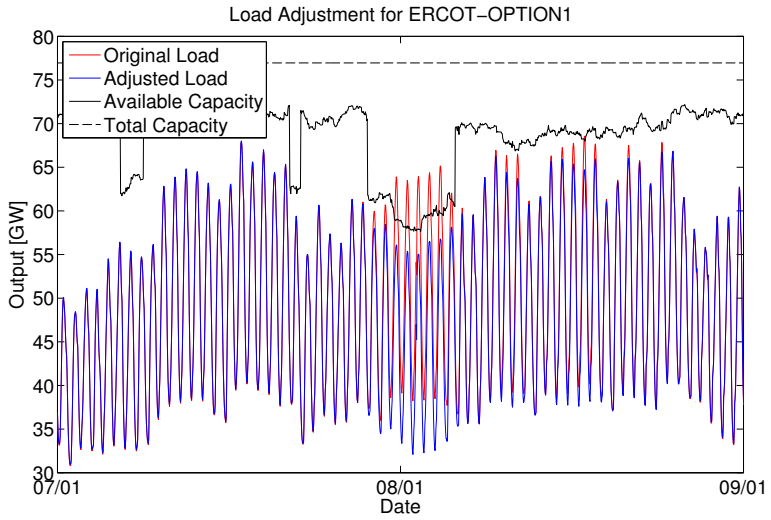

Figure C-3: Load adjustment in ERCOT under the OPTION1 compliance.

C.6 Threshold CO_2 Price Sensitivity to Import Cost

One limitation of our model is that it does not represent compliance in external regions. In order to reduce the impact of this limitation on results, we selected a high import cost of $300/MWh in order to encourage compliance with minimal reliance on imports. This choice had an impact on threshold CO_2 prices, and likely on production costs as well. In Table C-4, we report threshold CO_2 prices under a lower import cost of $50/MWh. The difference between threshold CO_2 prices under the two import costs has no effect in ERCOT, where there are no imports. The difference is greatest in ISO NE and PJM West under the NOEFF scenario, where threshold CO_2 prices are significantly lower with a $50/MWh import cost.

Table C-4: Threshold CO_2 prices ($/ton) under import costs of $300/MWh and $50/MWh.

	OPTION1		NOEFF	
	$300/MWh	$50/MWh	$300/MWh	$50/MWh
ERCOT	25	25	35	35
ISO NE	0	0	580	25
PJM West	26	17	161	19

C.7 Sensitivity Analysis Results

In this section, we provide the complete results of the sensitivity analysis. The sensitivity analysis explored seven of the qualitative results of our model. These results are listed below. We looked for result 1 in ERCOT and PJM West only and item 2 in ISO NE only, but we looked for the remainder of the results in each system.

1. NG generation increased from BAU to NOEFF in ERCOT and PJM West at high NG prices and low coal prices and decreased for low NG prices and high coal prices
2. Threshold CO_2 prices were zero under OPTION1 in ISO NE
3. Threshold CO_2 prices increased from the OPTION1 to NOEFF
4. CO_2 emissions decreased from BAU to OPTION1
5. CO_2 emissions were the same or less under NOEFF compared to OPTION1
6. Production costs under OPTION1 were less than under BAU
7. Production costs increased under NOEFF compared to OPTION1

For all results except 1 above, we report 5th or 95th percentile values for the distribution of the result variable. For instance, to test whether threshold CO_2 prices

increased from OPTION1 to NOEFF, we report the 5th percentile of the increase in CO_2 emissions. Since this value was positive (see Figures C-5, C-11, and C-17), we conclude that an increase is highly likely. Where we expect to see a decrease rather than an increase, we report 95th percentile values instead. We report these percentile values for a number of combinations of natural gas and coal prices in the figures below. To be clear, we have performed separate simulation using the Dirichlet Process for each of the combinations of natural gas and coal price shown in the Figures.

We discussed result 1 in the main text without showing the effect of variability in load (i.e. only showing the effect of varying natural gas and coal prices). In this appendix, we show that the result reported there holds when variation in load is included. To show this, we report the probability that NG generation increased (see Figures C-4, C-10, and C-16). In Figures C-4 and C-10, we observe that the probability of an NG generation increase is greater than 50% for some fuel prices and less than 50% for others.

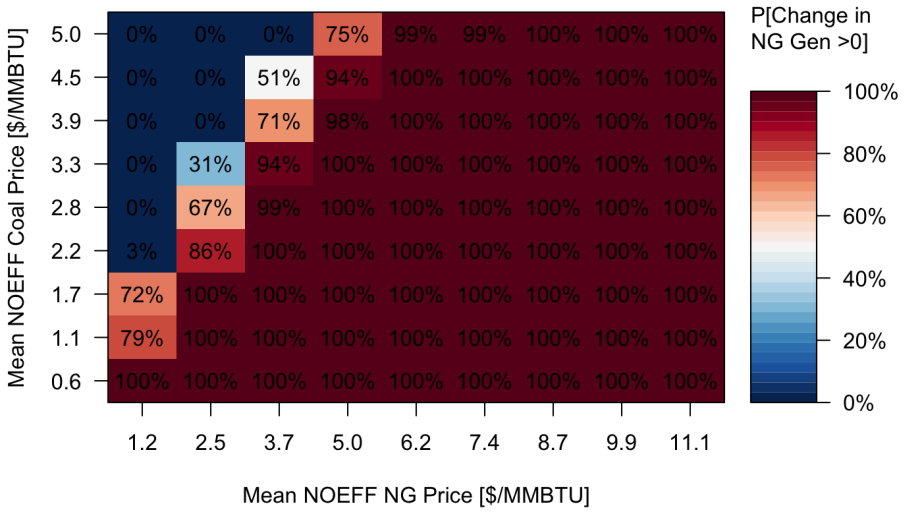

Figure C-4: Probability that NG generation increased under the NOEFF scenario compared to OPTION1 in PJM West. Note that values greater thatn 50% indicate that an increase in NG generation is more likely than a derease and values less than 50% indicate the reverse.

Figure C-5: 5th percentile of the distribution of CO_2 price increases from OPTION1 to NOEFF in PJM West.

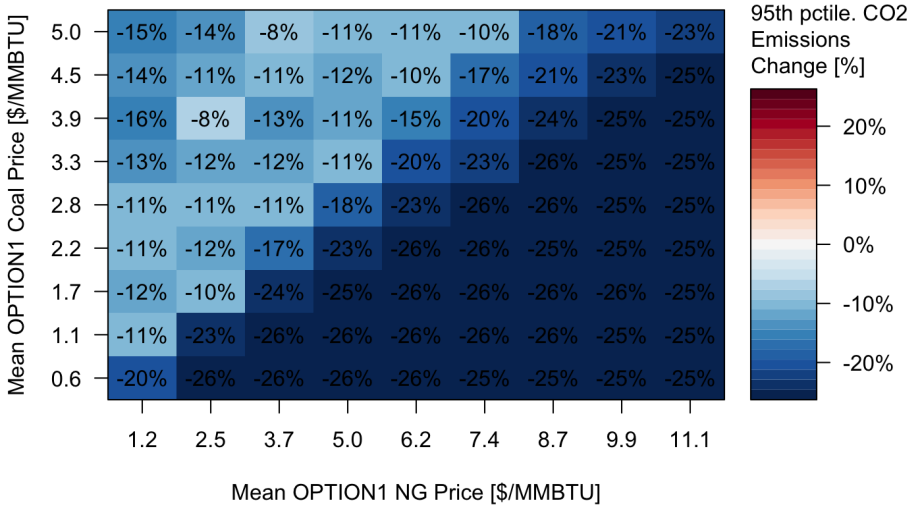

Figure C-6: 95th percentile of the distribution of CO_2 emissions increases from BAU to OPTION1 in PJM West.

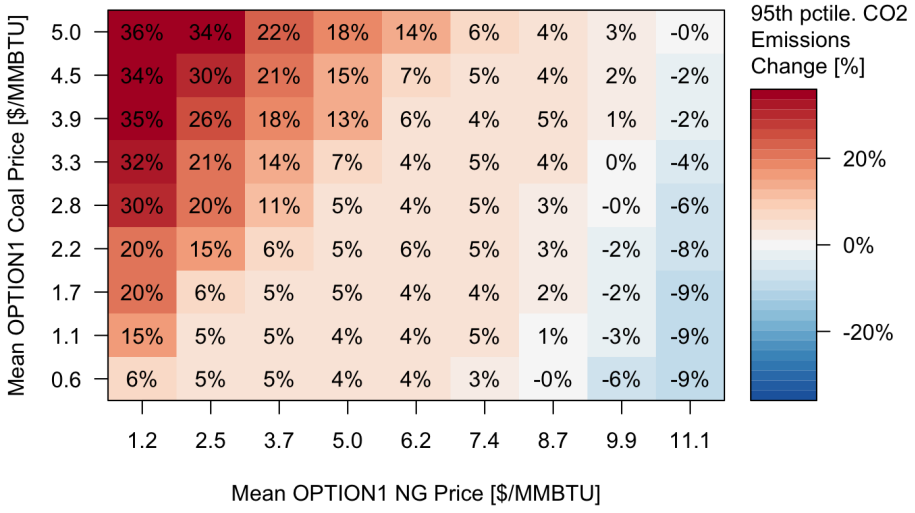

Figure C-7: 95th percentile of the distribution of CO_2 emisisons increases from OPTION1 to NOEFF in PJM West.

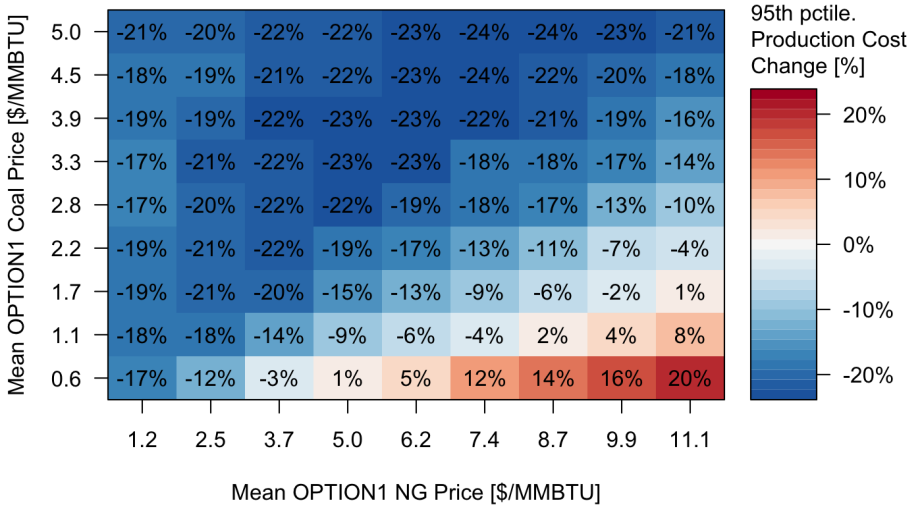

Figure C-8: 95th percentile of the distribution of production cost increases from BAU to OPTION1 in PJM West

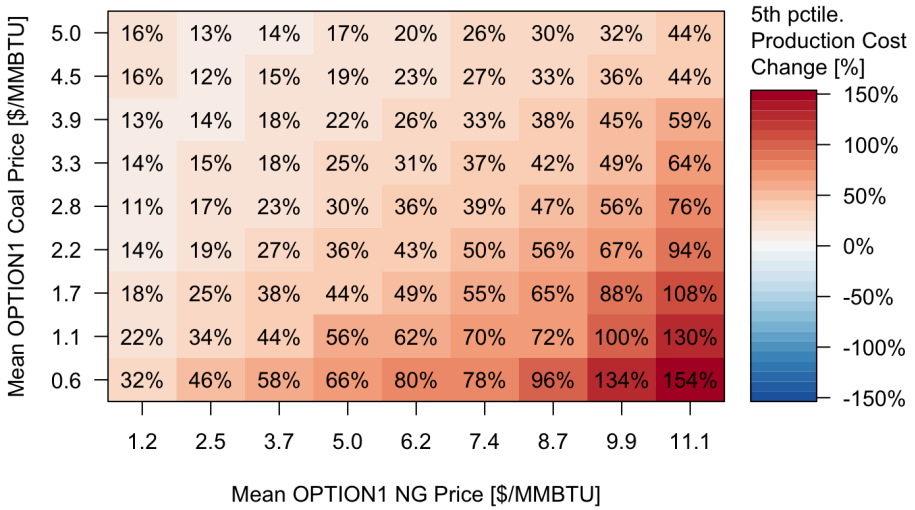

Figure C-9: 5th percentile of the distribution of production cost increases from OPTION1 to NOEFF in PJM West.

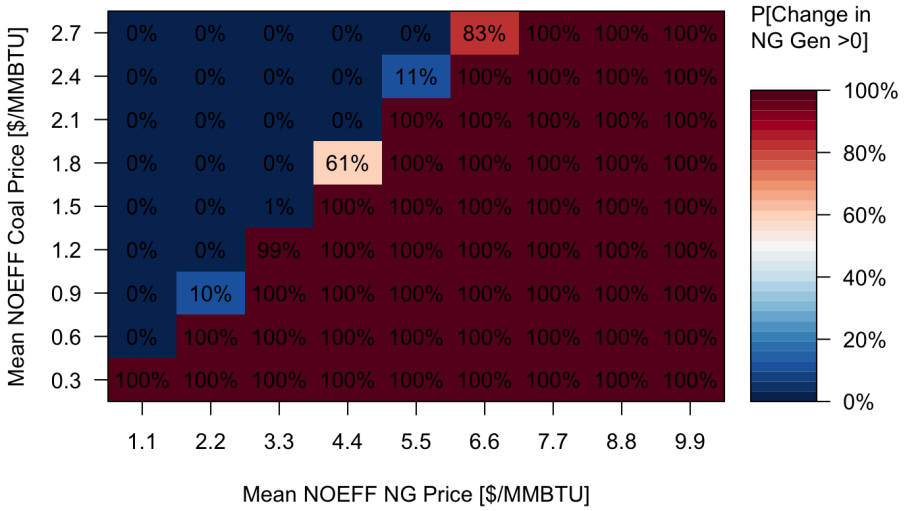

Figure C-10: Probability that NG generation increased under the NOEFF scenario compared to OPTION1 in ERCOT. Note that values greater thatn 50% indicate that an increase in NG generation is more likely than a derease and values less than 50% indicate the reverse.

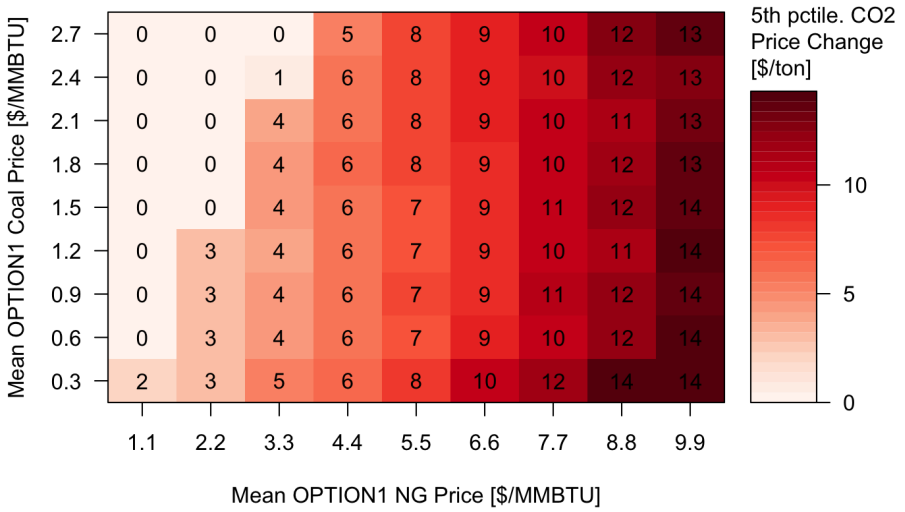

Figure C-11: 5th percentile of the distribution of CO_2 price increases from OPTION1 to NOEFF in ERCOT.

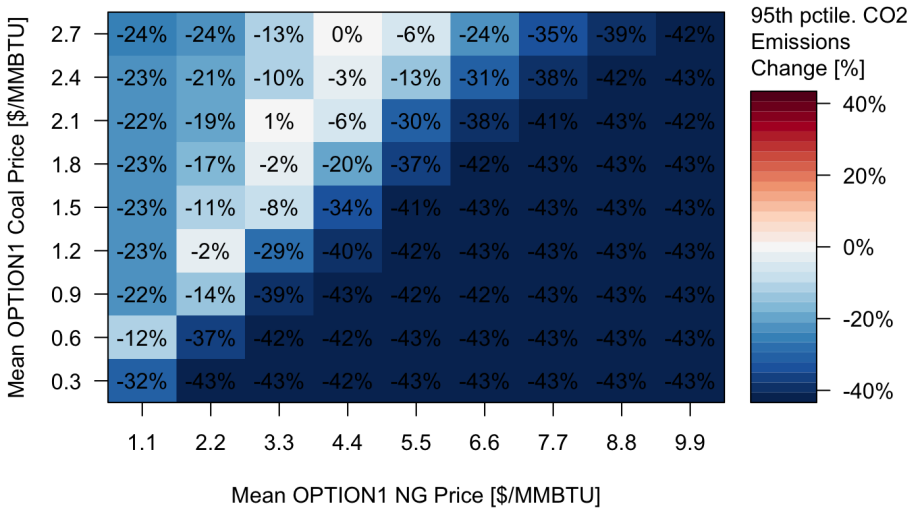

Figure C-12: 95th percentile of the distribution of CO_2 emissions increases from BAU to OPTION1 in ERCOT.

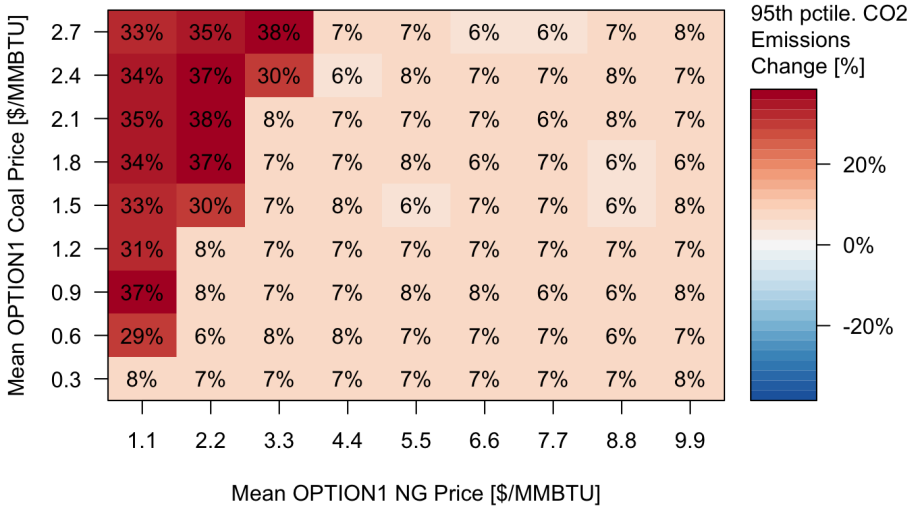

Figure C-13: 95th percentile of the distribution of CO_2 emisisons increases from OPTION1 to NOEFF in ERCOT.

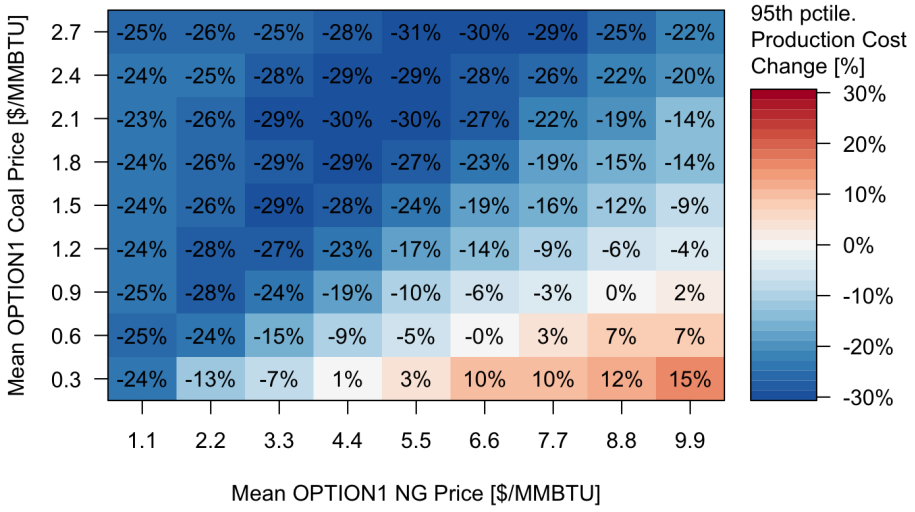

Figure C-14: 95th percentile of the distribution of production cost increases from BAU to OPTION1 in ERCOT

Figure C-15: 5th percentile of the distribution of production cost increases from OPTION1 to NOEFF in ERCOT.

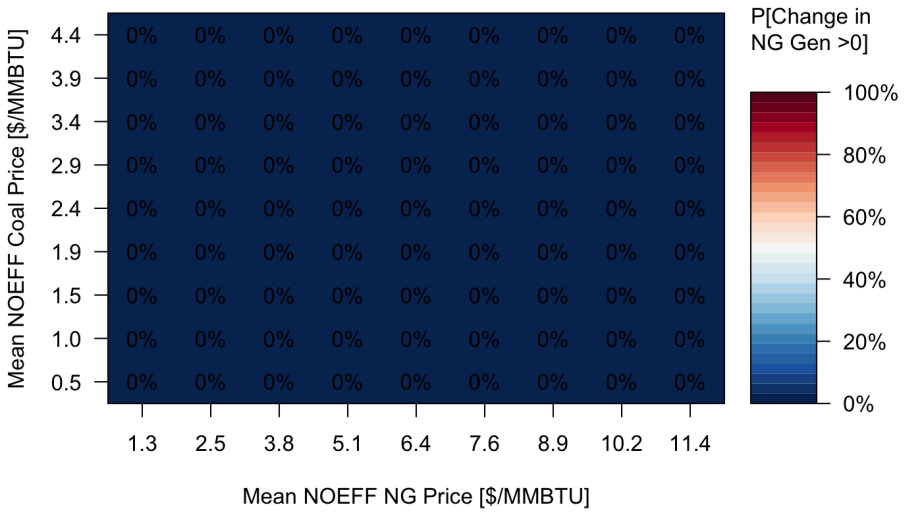

Figure C-16: Probability that NG generation increased under the NOEFF scenario compared to OPTION1 in ISONE. Note that values greater thatn 50% indicate that an increase in NG generation is more likely than a derease and values less than 50% indicate the reverse.

Figure C-17: 5th percentile of the distribution of CO_2 price increases from OPTION1 to NOEFF in ISONE.

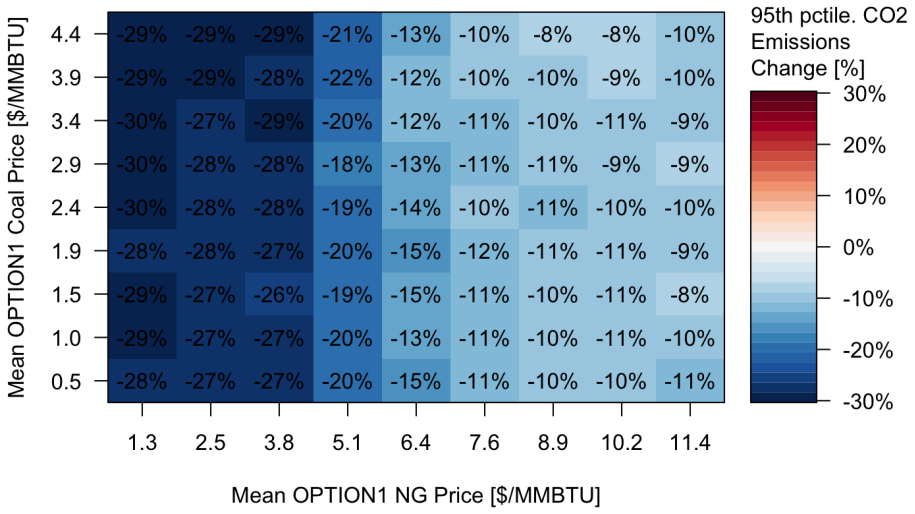

Figure C-18: 95th percentile of the distribution of CO_2 emissions increases from BAU to OPTION1 in ISONE.

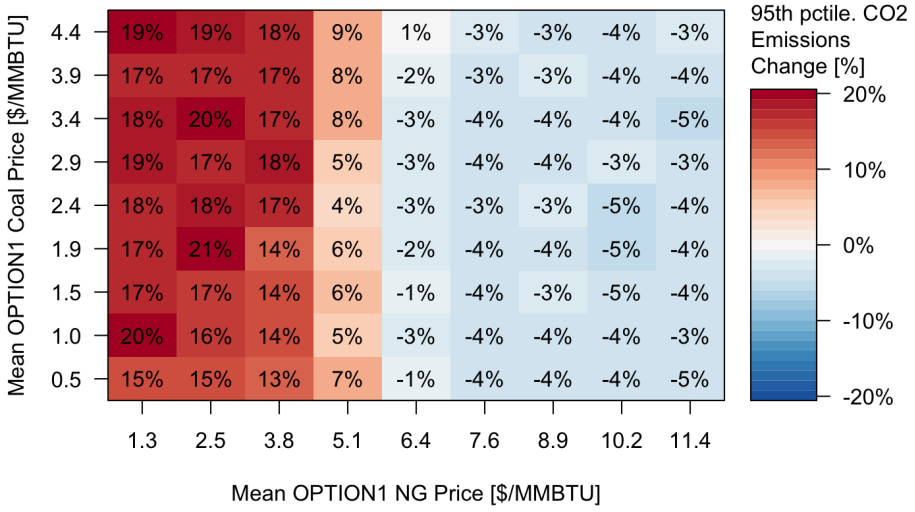

Figure C-19: 95th percentile of the distribution of CO_2 emisisons increases from OPTION1 to NOEFF in ISONE.

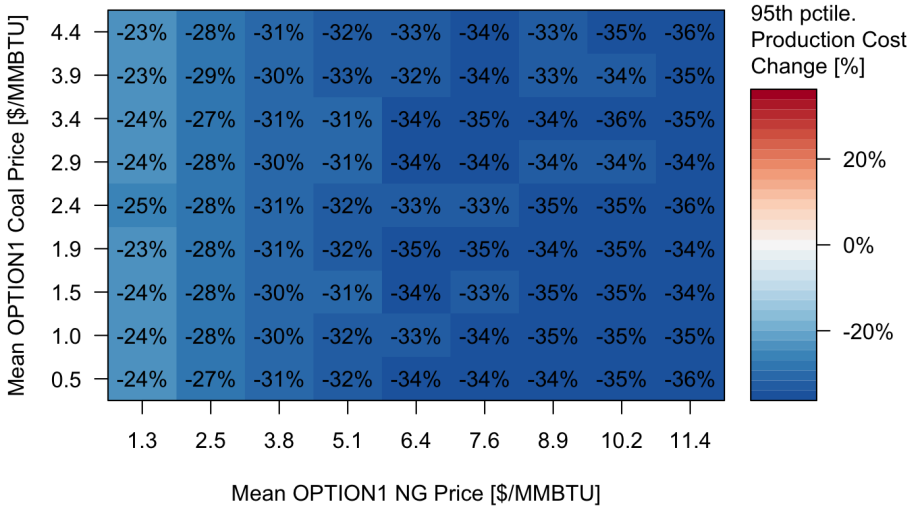

Figure C-20: 95th percentile of the distribution of production cost increases from BAU to OPTION1 in ISONE

Figure C-21: 5th percentile of the distribution of production cost increases from OPTION1 to NOEFF in ISONE.

Figure C-22: 95th percentile of the distribution of threshold CO_2 prices in ISONE.

C.8 Model Formulation

C.8.1 Introduction

The model formulation used in this work closely (but not exactly) follows the model of (Morales-Espana, Latorre, & Ramos, 2013). It is a modified version of a a model previously used by the authors in (Oates & Jaramillo, 2013). It is a mixed integer program and was formulated using GAMS and solved using IBM's CPLEX solver. In contrast to the aforementioned models, this model is a three-stage unit commitment model.

The first stage is intended to model the operation of a day-ahead unit commitment process. Its formulation very closely follows that of (Oates & Jaramillo, 2013). The first stage determines the schedule for a 24 hour period with all units available for commitment, subject to their individual minimum run times and minimum down times. It uses 24 hour-ahead forecast wind data. Spinning reserves, of both contingency and wind varieties, are modeled using hard constraints.

The second and third stages are intended to model the operation of a medium-term and a real-time unit commitment and dispatch process, respectively. The second stage operates on a six hour basis. Units with minimum down times of six hours or less (simple- and combined-cycle turbines in our data set) are able to be committed, subject to their

individual minimum run times and minimum down times. The third stage operates on an hourly basis. Units with minimum down times of one hour or less (simple-cycle turbines in our data set) are able to be committed, subject to their individual minimum run times and minimum down times. All other units have their commitment state fixed at the levels set in the previous stage and can only be dispatched. Stage 2 uses 6 hour-ahead wind forecast data and stage 3 uses real-time wind data. Spinning reserves are modeled using hard constraints, with violation penalties greater for contingency reserves than for wind reserves.

Since some commitment variables are fixed with forecast data, there may be infeasibilities at the second or third stages. Both the second and third stages therefore have soft-constraint versions. These versions emply soft constraints for contingency and wind spinning reserves and are solved if the second or third stage with hard reserve constraints returns an infeasibility.

The formulation is presented in three sections: Stage 1, Stage N, and Stage N Soft. Stage N, with different inputs, serves as the formulation for both Stage 2 and Stage 3. Stage N Soft serves as the formulation for the version of Stage 2 and Stage 3 with soft reserve constraints.

C.8.2 Phase 1

C.8.2.1 Symbols

Sets

$j \in J$	Index over all units
$j \in G \subseteq J$	Subset of units with minimum up time of 1
$j \in G^c \subseteq J$	Subset of units with minimum up time greater than 1
$l \in \{1,2,3\}$	Startup types from 1 (hottest) 3 (coldest)
$t \in T$	All time periods
$(j,t) \in O \subseteq J \otimes T$	Period t during which generator j is on outage
$(j,t) \in O^c \subseteq J \otimes T$	Period t during which generator j is not on outage

Continuous Parameters

d_t Demand in period t [MWh]

s_t^c Spinning reserve requirement (contingency) in period t [MW]

s_t^w Spinning reserve requirement (wind) in period t [MW]

w_t Available wind energy in period t [MWh]

h_t Available hydro energy in period t [MWh]

c_j^m Marginal cost of unit j [$/h]

c_j^{nl} No-load cost of unit j [$]

c_j^{sd} Shut down cost of unit j [$]

c_j^{su} Start up cost of unit j [$]

$\bar{p}_j$ Maximum power output of unit j [MW]

$\underline{p}_j$ Minimum power output of unit j without shutting down [MW]

r_j^d Ramp down limit of unit j [MW/h]

r_j^u Ramp up limit of unit j [MW/h]

r_j^{sd} Shut down ramp limit (during last period of operation) of unit j [MW/h]

r_j^{su} Start up ramp limit (during first period of operation) of unit j [MW/h]

t_j^d Minimum down time of unit j [h]

t_j^u Minimum up time of unit j [h]

$t_{j,l}^{su}$ Time required for unit j to perform startup of type l [h]

k_j^p Power output of unit j in period preceding time frame [MW/h]

k_j^s Reserve contribution of unit j in period preceding time frame [MW]

c^{tie} Cost/revenue of/from energy imported/exported from/to tie line [$/MWh]

$\bar{f}$ Maximum importable energy per period from tie line [MWh]

$\underline{f}$ Maximum exportable energy per period to tie line [MWh]

Integer Parameters

k_j^u On/off status of unit j in period preceding time frame

k_j^v Startup binary status of unit j in period preceding time frame

k_j^w Shutdown binary status of unit j in period preceding time frame

k_j^{tu} Number of periods unit j has been up before start of time frame

k_j^{td} Number of periods unit j has been down before start of time frame

k_j^{ru} Number of periods until unit j can shut down at start of time frame

k_j^{rd} Number of periods until unit j can start up at start of time frame

Unbounded Variables

These variables are continuous, but not inherently bounded (by e.g. 0).

x_t^{tie} Tie line net inflow in period t [MWh]

Positive Variables

These variables must take on values greater than or equal to 0.

$x_{j,t}^p$ Energy produced above minimum output by unit j in period t [MWh]

$x_{j,t}^s$ Spinning reserve contribution of unit j in period t [MW]

x_t^w Wind energy used in period t [MWh]

x_t^h Hydro energy used in period t [MWh]

Binary Variables

These variables can only take values $\in \{0, 1\}$.

$y^{u}_{j,t}$ On/off status of unit j in period t

$y^{v}_{j,t}$ Startup binary status of unit j in period t

$y^{w}_{j,t}$ Shutdown binary status of unit j in period t

$y^{d}_{j,t,l}$ Indicator that unit j performed a startup of type l in period t

C.8.2.2 Initialization

The equations in this section fix or bound the values of some variables based on input parameters. Equation 1 sets the value of the on/off binary in the early periods of the model to its value in the previous model run. Equation 2 sets the on/off binary to 0 when the unit is undergoing an outage. Equation 3 ensures startup types are adhered to in the early period the model. Equation 4 ensures that the wind energy used in each period is less than or equal to the available wind and equation 5 does the same for hydro. Equation 6 limits the amount of tie line imports and exports.

$$y^{u}_{j,t} = k^{u}_{j} \qquad \forall j,t \leq (k^{ru}_{j} + k^{rd}_{j}) \tag{1}$$

$$y^{u}_{j,t} = 0 \qquad \forall (j,t) \in O \tag{2}$$

$$y^{d}_{j,t,l} = 0 \qquad \forall j, l < 3, t^{su}_{j,l+1} - k^{td}_{j} < t < t^{su}_{j,l+1} \tag{3}$$

$$x^{w}_{t} \leq w_{t} \qquad \forall t \tag{4}$$

$$x^{h}_{t} \leq h_{t} \qquad \forall t \tag{5}$$

$$-\underline{f} \leq x^{tie}_{t} \leq \bar{f} \qquad \forall t \tag{6}$$

C.8.2.3 Objective

Equation 7 defines the objective function to be minimized. The first line shows the fuel-related costs. The no-load cost is multiplied by the on/off binary and added to the product of the marginal cost and the total power output. On the second line, the start up and shut down costs are applied. On the third line, tie line costs are applied.

$$\sum_{j,t}\left(c_j^{nl}y_{j,t}^{u}+c_j^{m}(\underline{p}_j y_{j,t}^{u}+x_{j,t}^{p})\right) + \sum_{j,t,l}\left(c_{j,l}^{su}y_{j,t,l}^{d}\right)+\sum_{j,t}\left(c_j^{sd}y_{j,t}^{w}\right) + \sum_{t} c^{tie}x_t^{tie} \quad (7)$$

C.8.2.4 Supply Equation

Equation 8 ensures a balance, in each period, between energy generated by conventional units, wind, hydro, and net tie line inflows, and load.

$$\sum_{j}\left(\underline{p}_j y_{j,t}^{u}+x_{j,t}^{p}\right)+x_t^{w}+x_t^{h}+x_t^{tie}=d_t \qquad \forall t \qquad (8)$$

C.8.2.5 Logic Equations

Equations 9-11 ensure that the on/off, startup, and shutdown binary variables relate to each other in the expected way.

$$y^{u}_{j,t} - y^{u}_{j,t-1} = y^{v}_{j,t} - y^{w}_{j,t} \qquad \forall j, t > 1 \tag{9}$$

$$y^{u}_{j,t} - k^{u}_{j} = y^{v}_{j,t} - y^{w}_{j,t} \qquad \forall j, t = 1 \tag{10}$$

$$y^{v}_{j,t} + y^{w}_{j,t} \leq 1 \qquad \forall j, t \tag{11}$$

C.8.2.6 Startup

Equation 12 ensures that cold, warm, and hot starts occur only when the unit has been offline for the appropriate amount of time. Equation 13 ensures that $y^{d}_{j,t,l}$ and $y^{w}_{j,t}$ agree and ensures that only one type of startup occurs at a time.

Note that equation 12 only requires that a warm start be recorded when the unit has been offline longer than the warm start time and that a cold start be recorded when the unit has been offline longer than the cold start time. They do not force a hot start when the warm start time *has not* been exceeded, or a warm start when the cold start time *has not* been exceeded. These effects rely on increasing start costs from hot through cold.

$$y^{d}_{j,t,l} \leq \sum_{t'=t-t^{su}_{j,l+1}+1}^{t-t^{su}_{j,l}} y^{w}_{j,t'} \qquad \forall j, t \geq t^{su}_{j,l+1}, l < 3 \tag{12}$$

$$\sum_{l} y^{d}_{j,t,l} \leq y^{v}_{j,t} \qquad \forall j, t \tag{13}$$

C.8.2.7 Spinning Reserve Equation

Equation 14 ensures that the amount of procured spinning reserve is greater than or equal to the reserve requirement in each period.

$$\sum_{j} x^{s}_{j,t} \geq s^{c}_{t} + s^{w}_{t} \qquad \forall t \qquad (14)$$

C.8.2.8 Minimum Up and Down Times

Equations 15 and 16 impose the minimum up time constraints. Note that these equations are relaxed if the unit is not on outage (i.e. they are only applied for $(j,t) \in O^{c}$). Equations 17 and 18 impose the minimum down time constraints. Equations 16 and 18 are modifications that apply to early periods in the time frame.

$$\sum_{t'=t-t^{u}_{j}+1}^{t} y^{v}_{j,t'} \leq y^{u}_{j,t} \qquad \forall (j,t) \in O^{c}, t \geq t^{u}_{j} \qquad (15)$$

$$\sum_{t'=1}^{t} y^{v}_{j,t'} \leq y^{u}_{j,t} \qquad \forall (j,t) \in O^{c}, t < t^{u}_{j} \qquad (16)$$

$$\sum_{t'=t-t^{d}_{j}+1}^{t} y^{w}_{j,t'} \leq 1 - y^{u}_{j,t} \qquad \forall j, t \geq t^{d}_{j} \qquad (17)$$

$$\sum_{t'=1}^{t} y^{w}_{j,t'} \leq 1 - y^{u}_{j,t} \qquad \forall j, t < t^{d}_{j} \qquad (18)$$

C.8.2.9 Capacity Equations

Equations 19 - 23 ensure that the output and reserve contributions of conventional units are properly bounded during normal operation, but also allow the unit to start up and shut down. To avoid infeasibility, different constraints are applied to units with a mini-

mum up time of 1 (i.e. for $j \in G$) and units with minimum up time greater than 1 (i.e. for $j \in G^c$).

$$x^p_{j,t-1} + x^s_{j,t-1} \leq (\bar{p}_j - \underline{p}_j) y^u_{j,t-1} - (\bar{p}_j - r^{su}_j) y^v_{j,t-1} - (\bar{p}_j - r^{sd}_j) y^w_{j,t} \quad \forall j \in G^c, t > 1 \quad (19)$$

$$k^p_j + k^s_j \leq (\bar{p}_j - \underline{p}_j) k^u_j - (\bar{p}_j - r^{su}_j) k^v_j - (\bar{p}_j - r^{sd}_j) y^w_{j,t} \quad \forall j \in G^c, t = 1 \quad (20)$$

$$x^p_{j,t} + x^s_{j,t} \leq (\bar{p}_j - \underline{p}_j) y^u_{j,t} - (\bar{p}_j - r^{su}_j) y^v_{j,t} \quad \forall j \in G, t \quad (21)$$

$$x^p_{j,t-1} + x^s_{j,t-1} \leq (\bar{p}_j - \underline{p}_j) y^u_{j,t-1} - (\bar{p}_j - r^{sd}_j) y^w_{j,t} \quad \forall j \in G, t > 1 \quad (22)$$

$$k^p_j + k^s_j \leq (\bar{p}_j - \underline{p}_j) k^u_j - (\bar{p}_j - r^{sd}_j) y^w_{j,t} \quad \forall j \in G, t = 1 \quad (23)$$

C.8.2.10 Ramp Up and Ramp Down

Equations 24 and 25 apply the up ramp rate limits and equations 26 and 27 apply the down ramp rate limits for all units.

$$(x^p_{j,t} + x^s_{j,t}) - x^p_{j,t-1} \leq r^u_j \quad \forall j, t > 1 \quad (24)$$

$$(x^p_{j,t} + x^s_{j,t}) - k^p_j \leq r^u_j \quad \forall j, t = 1 \quad (25)$$

$$-x^p_{j,t} + x^p_{j,t-1} \leq r^d_j \quad \forall j, t > 1 \quad (26)$$

$$-x^p_{j,t} + k^p_j \leq r^d_j \quad \forall j, t = 1 \quad (27)$$

C.8.3 Phase N

C.8.3.1 Symbols

Sets

$j \in J$	Index over all units
$j \in G \subseteq J$	Subset of units with minimum up time of 1
$j \in G^c \subseteq J$	Subset of units with minimum up time greater than 1
$j \in C \subseteq J$	Subset of units that can be committed in stage N
$j \in C^c \subseteq J$	Subset of units that cannot be committed in stage N
$l \in \{1,2,3\}$	Startup types from 1 (hottest) 3 (coldest)
$t \in T$	All time periods
$(j,t) \in O \subseteq J \otimes T$	Period t during which generator j is on outage
$(j,t) \in O^c \subseteq J \otimes T$	Period t during which generator j is not on outage

Continuous Parameters

d_t Demand in period t [MWh]

s_t^c Spinning reserve requirement (contingency) in period t [MW]

s_t^w Spinning reserve requirement (wind) in period t [MW]

w_t Available wind energy in period t [MWh]

h_t Available hydro energy in period t [MWh]

c_j^m Marginal cost of unit j [$/h]

c_j^{nl} No-load cost of unit j [$]

c_j^{sd} Shut down cost of unit j [$]

c_j^{su} Start up cost of unit j [$]

$\bar{p}_j$ Maximum power output of unit j [MW]

$\underline{p}_j$ Minimum power output of unit j without shutting down [MW]

r_j^d Ramp down limit of unit j [MW/h]

r_j^u Ramp up limit of unit j [MW/h]

r_j^{sd} Shut down ramp limit (during last period of operation) of unit j [MW/h]

r_j^{su} Start up ramp limit (during first period of operation) of unit j [MW/h]

t_j^d Minimum down time of unit j [h]

t_j^u Minimum up time of unit j [h]

$t_{j,l}^{su}$ Time required for unit j to perform startup of type l [h]

k_j^p Power output of unit j in period preceding time frame [MW/h]

k_j^s Reserve contribution of unit j in period preceding time frame [MW]

c^{tie} Cost/revenue of/from energy imported/exported from/to tie line [$/MWh]

$\bar{f}$ Maximum importable energy per period from tie line [MWh]

$\underline{f}$ Maximum exportable energy per period to tie line [MWh]

Integer Parameters

k_j^u On/off status of unit j in period preceding time frame

k_j^v Startup binary status of unit j in period preceding time frame

k_j^w Shutdown binary status of unit j in period preceding time frame

k_j^{tu} Number of periods unit j has been up before start of time frame

k_j^{td} Number of periods unit j has been down before start of time frame

k_j^{ru} Number of periods until unit j can shut down at start of time frame

k_j^{rd} Number of periods until unit j can start up at start of time frame

$f_{j,t}^u$ Commitment status set in previous stage for unit j in period t

$f_{j,t}^v$ Startup status set in previously stage for unit j in period t

$f_{j,t}^w$ Shutdown status set in previous stage for unit j in period t

$f_{j,l,t}^d$ Startup type l set in previous stage for unit j in period t

Unbounded Variables

These variables are continuous, but not inherently bounded (by e.g. 0).

x_t^{tie} Tie line net inflow in period t [MWh]

Positive Variables

These variables must take on values greater than or equal to 0.

$x_{j,t}^p$ Energy produced above minimum output by unit j in period t [MWh]

$x_{j,t}^s$ Spinning reserve contribution of unit j in period t [MW]

x_t^w Wind energy used in period t [MWh]

x_t^h Hydro energy used in period t [MWh]

Binary Variables

These variables can only take values $\in \{0, 1\}$.

$y^{u}_{j,t}$ On/off status of unit j in period t

$y^{v}_{j,t}$ Startup binary status of unit j in period t

$y^{w}_{j,t}$ Shutdown binary status of unit j in period t

$y^{d}_{j,t,l}$ Indicator that unit j performed a startup of type l in period t

C.8.3.2 Initialization

The equations in this section fix or bound the values of some variables based on input parameters. Equation 28 sets the value of the on/off binary in the early periods of the model to its value in the previous model run. Equation 29 sets the on/off binary to 0 when the unit is undergoing an outage. Equation 30 ensures startup types are adhered to in the early period the model. Equation 31 ensures that the wind energy used in each period is less than or equal to the available wind and equation 32 does the same for hydro. Equation 33 limits the amount of tie line imports and exports.

Equation 34 fixes the value of the unit commitment variable $y^{u}_{j,t}$ to the values set in the previous stage for the subset of units that cannot be committed in this stage. Equations 35, 36, and 37 do the same thing for the startup, shutdown, and startup type binary variables.

$$y^{u}_{j,t} = k^{u}_{j} \qquad \forall j,t \leq (k^{ru}_{j} + k^{rd}_{j}) \tag{28}$$

$$y^{u}_{j,t} = 0 \qquad \forall (j,t) \in O \tag{29}$$

$$y^{d}_{j,t,l} = 0 \qquad \forall j, l < 3, t^{su}_{j,l+1} - k^{td}_{j} < t < t^{su}_{j,l+1} \tag{30}$$

$$x^{w}_{t} \leq w_{t} \qquad \forall t \tag{31}$$

$$x^{h}_{t} \leq h_{t} \qquad \forall t \tag{32}$$

$$-\underline{f} \leq x^{tie}_{t} \leq \bar{f} \qquad \forall t \tag{33}$$

$$y^{u}_{j,t} = f^{u}_{j,t} \qquad \forall j \in C^{c}, t \tag{34}$$

$$y^{v}_{j,t} = f^{v}_{j,t} \qquad \forall j \in C^{c}, t \tag{35}$$

$$y^{w}_{j,t} = f^{w}_{j,t} \qquad \forall j \in C^{c}, t \tag{36}$$

$$y^{d}_{j,l,t} = f^{d}_{j,l,t} \qquad \forall j \in C^{c}, l, t \tag{37}$$

C.8.3.3 Objective

Equation 38 defines the objective function to be minimized. The first line shows the fuel-related costs. The no-load cost is multiplied by the on/off binary and added to the product of the marginal cost and the total power output. On the second line, the start

up and shut down costs are applied. On the third line, tie line costs are applied.

$$\sum_{j,t}\left(c_j^{nl}y_{j,t}^{u}+c_j^{m}(\underline{p}_j y_{j,t}^{u}+x_{j,t}^{p})\right) + \sum_{j,t,l}\left(c_{j,l}^{su}y_{j,t,l}^{d}\right)+\sum_{j,t}\left(c_j^{sd}y_{j,t}^{w}\right) + \sum_{t} c^{tie}x_t^{tie} \quad (38)$$

C.8.3.4 Supply Equation

Equation 39 ensures a balance, in each period, between energy generated by conventional units, wind, hydro, and net tie line inflows, and load.

$$\sum_{j}\left(\underline{p}_j y_{j,t}^{u}+x_{j,t}^{p}\right)+x_t^{w}+x_t^{h}+x_t^{tie}=d_t \qquad \forall t \quad (39)$$

C.8.3.5 Logic Equations

Equations 40-42 ensure that the on/off, startup, and shutdown binary variables relate to each other in the expected way. Note that we only impose these constraints on the binary variables in C that can be committed during this stage.

$$y_{j,t}^{u}-y_{j,t-1}^{u}=y_{j,t}^{v}-y_{j,t}^{w} \qquad \forall j\in C, t>1 \quad (40)$$

$$y_{j,t}^{u}-k_j^{u}=y_{j,t}^{v}-y_{j,t}^{w} \qquad \forall j\in C, t=1 \quad (41)$$

$$y_{j,t}^{v}+y_{j,t}^{w}\leq 1 \qquad \forall j\in C, t \quad (42)$$

C.8.3.6 Startup

Equation 43 ensures that cold, warm, and hot starts occur only when the unit has been offline for the appropriate amount of time. Equation 44 ensures that $y^{d}_{j,t,l}$ and $y^{w}_{j,t}$ agree and ensures that only one type of startup occurs at a time.

Note that equation 43 only requires that a warm start be recorded when the unit has been offline longer than the warm start time and that a cold start be recorded when the unit has been offline longer than the cold start time. They do not force a hot start when the warm start time *has not* been exceeded, or a warm start when the cold start time *has not* been exceeded. These effects rely on increasing start costs from hot through cold.

Note also that we only impose these constraints on the binary variables in C that can be committed during this stage.

$$y^{d}_{j,t,l} \leq \sum_{t'=t-t^{su}_{j,l+1}+1}^{t-t^{su}_{j,l}} y^{w}_{j,t'} \qquad \forall j \in C, t \geq t^{su}_{j,l+1}, l < 3 \tag{43}$$

$$\sum_{l} y^{d}_{j,t,l} \leq y^{v}_{j,t} \qquad \forall j \in C, t \tag{44}$$

C.8.3.7 Spinning Reserve Equation

Equation 45 ensures that the amount of procured spinning reserve is greater than or equal to the reserve requirement in each period.

$$\sum_{j} x^{s}_{j,t} \geq s^{c}_{t} + s^{w}_{t} \qquad \forall t \tag{45}$$

C.8.3.8 Minimum Up and Down Times

Equations 46 and 47 impose the minimum up time constraints. Note that these equations are relaxed if the unit is not on outage (i.e. they are only applied for $(j,t) \in O^c$). Equations 48 and 49 impose the minimum down time constraints. Equations 47 and 49 are modifications that apply to early periods in the time frame.

$$\sum_{t'=t-t_j^u+1}^{t} y_{j,t'}^{v} \leq y_{j,t}^{u} \qquad \forall (j,t) \in O^c, j \in C, t \geq t_j^u \tag{46}$$

$$\sum_{t'=1}^{t} y_{j,t'}^{v} \leq y_{j,t}^{u} \qquad \forall (j,t) \in O^c, j \in C, t < t_j^u \tag{47}$$

$$\sum_{t'=t-t_j^d+1}^{t} y_{j,t'}^{w} \leq 1 - y_{j,t}^{u} \qquad \forall j \in C, t \geq t_j^d \tag{48}$$

$$\sum_{t'=1}^{t} y_{j,t'}^{w} \leq 1 - y_{j,t}^{u} \qquad \forall j \in C, t < t_j^d \tag{49}$$

C.8.3.9 Capacity Equations

Equations 50 - 54 ensure that the output and reserve contributions of conventional units are properly bounded during normal operation, but also allow the unit to start up and shut down. To avoid infeasibility, different constraints are applied to units with a minimum up time of 1 (i.e. for $j \in G$) and units with minimum up time greater than 1 (i.e. for $j \in G^c$).

Note that the equations below that contain only binary variables (i.e. do not contain continuous variables) are applied only for units in C that can be committed in this

stage.

$$x^{p}_{j,t-1} + x^{s}_{j,t-1} \leq (\bar{p}_j - \underline{p}_j) y^{u}_{j,t-1} - (\bar{p}_j - r^{su}_j) y^{v}_{j,t-1} - (\bar{p}_j - r^{sd}_j) y^{w}_{j,t} \qquad \forall j \in G^c, t > 1 \tag{50}$$

$$k^{p}_{j} + k^{s}_{j} \leq (\bar{p}_j - \underline{p}_j) k^{u}_{j} - (\bar{p}_j - r^{su}_j) k^{v}_{j} - (\bar{p}_j - r^{sd}_j) y^{w}_{j,t} \quad \forall j \in G^c, j \in C, t = 1 \tag{51}$$

$$x^{p}_{j,t} + x^{s}_{j,t} \leq (\bar{p}_j - \underline{p}_j) y^{u}_{j,t} - (\bar{p}_j - r^{su}_j) y^{v}_{j,t} \qquad \forall j \in G, t \tag{52}$$

$$x^{p}_{j,t-1} + x^{s}_{j,t-1} \leq (\bar{p}_j - \underline{p}_j) y^{u}_{j,t-1} - (\bar{p}_j - r^{sd}_j) y^{w}_{j,t} \qquad \forall j \in G, t > 1 \tag{53}$$

$$k^{p}_{j} + k^{s}_{j} \leq (\bar{p}_j - \underline{p}_j) k^{u}_{j} - (\bar{p}_j - r^{sd}_j) y^{w}_{j,t} \quad \forall j \in G, j \in C, t = 1 \tag{54}$$

C.8.3.10 Ramp Up and Ramp Down

Equations 55 and 56 apply the up ramp rate limits and equations 57 and 58 apply the down ramp rate limits for all units.

$$(x^{p}_{j,t} + x^{s}_{j,t}) - x^{p}_{j,t-1} \leq r^{u}_j \qquad \forall j, t > 1 \tag{55}$$

$$(x^{p}_{j,t} + x^{s}_{j,t}) - k^{p}_{j} \leq r^{u}_j \qquad \forall j, t = 1 \tag{56}$$

$$-x^{p}_{j,t} + x^{p}_{j,t-1} \leq r^{d}_j \qquad \forall j, t > 1 \tag{57}$$

$$-x^{p}_{j,t} + k^{p}_{j} \leq r^{d}_j \qquad \forall j, t = 1 \tag{58}$$

C.8.4 Phase N Soft

C.8.4.1 Symbols

Sets

$j \in J$	Index over all units
$j \in G \subseteq J$	Subset of units with minimum up time of 1
$j \in G^c \subseteq J$	Subset of units with minimum up time greater than 1
$j \in C \subseteq J$	Subset of units that can be committed in stage N
$j \in C^c \subseteq J$	Subset of units that cannot be committed in stage N
$l \in \{1,2,3\}$	Startup types from 1 (hottest) 3 (coldest)
$t \in T$	All time periods
$(j,t) \in O \subseteq J \otimes T$	Period t during which generator j is on outage
$(j,t) \in O^c \subseteq J \otimes T$	Period t during which generator j is not on outage

Continuous Parameters

d_t Demand in period t [MWh]

s_t^c Spinning reserve requirement (contingency) in period t [MW]

s_t^w Spinning reserve requirement (wind) in period t [MW]

w_t Available wind energy in period t [MWh]

h_t Available hydro energy in period t [MWh]

c_j^m Marginal cost of unit j [$/h]

c_j^{nl} No-load cost of unit j [$]

c_j^{sd} Shut down cost of unit j [$]

c_j^{su} Start up cost of unit j [$]

$\bar{p}_j$ Maximum power output of unit j [MW]

$\underline{p}_j$ Minimum power output of unit j without shutting down [MW]

r_j^d Ramp down limit of unit j [MW/h]

r_j^u Ramp up limit of unit j [MW/h]

r_j^{sd} Shut down ramp limit (during last period of operation) of unit j [MW/h]

r_j^{su} Start up ramp limit (during first period of operation) of unit j [MW/h]

t_j^d Minimum down time of unit j [h]

t_j^u Minimum up time of unit j [h]

$t_{j,l}^{su}$ Time required for unit j to perform startup of type l [h]

k_j^p Power output of unit j in period preceding time frame [MW/h]

k_j^s Reserve contribution of unit j in period preceding time frame [MW]

c^{tie} Cost/revenue of/from energy imported/exported from/to tie line [$/MWh]

$\bar{f}$ Maximum importable energy per period from tie line [MWh]

$\underline{f}$ Maximum exportable energy per period to tie line [MWh]

c^{rc} Cost of contingency spinning reserve violation [$/MWh]

c^{rw} Cost of wind spinning reserve violation [$/MWh]

Integer Parameters

k_j^u On/off status of unit j in period preceding time frame

k_j^v Startup binary status of unit j in period preceding time frame

k_j^w Shutdown binary status of unit j in period preceding time frame

k_j^{tu} Number of periods unit j has been up before start of time frame

k_j^{td} Number of periods unit j has been down before start of time frame

k_j^{ru} Number of periods until unit j can shut down at start of time frame

k_j^{rd} Number of periods until unit j can start up at start of time frame

$f_{j,t}^u$ Commitment status set in previous stage for unit j in period t

$f_{j,t}^v$ Startup status set in previously stage for unit j in period t

$f_{j,t}^w$ Shutdown status set in previous stage for unit j in period t

$f_{j,l,t}^d$ Startup type l set in previous stage for unit j in period t

Unbounded Variables

These variables are continuous, but not inherently bounded (by e.g. 0).

x_t^{tie} Tie line net inflow in period t [MWh]

Positive Variables

These variables must take on values greater than or equal to 0.

$x^{p}_{j,t}$ Energy produced above minimum output by unit j in period t [MWh]

$x^{s}_{j,t}$ Spinning reserve contribution of unit j in period t [MW]

x^{w}_{t} Wind energy used in period t [MWh]

x^{h}_{t} Hydro energy used in period t [MWh]

x^{rcn}_{t} Contingency spinning reserve constraint not satisfied in period t [MW]

x^{rwn}_{t} Wind spinning reserve constraint not satisfied in period t [MW]

Binary Variables

These variables can only take values $\in \{0, 1\}$.

$y^{u}_{j,t}$ On/off status of unit j in period t

$y^{v}_{j,t}$ Startup binary status of unit j in period t

$y^{w}_{j,t}$ Shutdown binary status of unit j in period t

$y^{d}_{j,t,l}$ Indicator that unit j performed a startup of type l in period t

C.8.4.2 Initialization

The equations in this section fix or bound the values of some variables based on input parameters. Equation 59 sets the value of the on/off binary in the early periods of the model to its value in the previous model run. Equation 60 sets the on/off binary to 0 when the unit is undergoing an outage. Equation 61 ensures startup types are adhered to in the early period the model. Equation 62 ensures that the wind energy used in each period is less than or equal to the available wind and equation 63 does the same for hydro. Equation 64 limits the amount of tie line imports and exports.

Equation 65 fixes the value of the unit commitment variable $y^{u}_{j,t}$ to the values set in the previous stage for the subset of units that cannot be committed in this stage. Equations 66, 67, and 68 do the same thing for the startup, shutdown, and startup type bi-

nary variables.

Equation 69 bounds the contingency spinning reserve violation at the contingency spinning reserve requirement, and equation 70 does the same for wind spinning reserve violation.

$$y^u_{j,t} = k^u_j \qquad \forall j,t \leq (k^{ru}_j + k^{rd}_j) \tag{59}$$

$$y^u_{j,t} = 0 \qquad \forall (j,t) \in O \tag{60}$$

$$y^d_{j,t,l} = 0 \qquad \forall j, l < 3, t^{su}_{j,l+1} - k^{td}_j < t < t^{su}_{j,l+1} \tag{61}$$

$$x^w_t \leq w_t \qquad \forall t \tag{62}$$

$$x^h_t \leq h_t \qquad \forall t \tag{63}$$

$$-\underline{f} \leq x^{tie}_t \leq \bar{f} \qquad \forall t \tag{64}$$

$$y^u_{j,t} = f^u_{j,t} \qquad \forall j \in C^c, t \tag{65}$$

$$y^v_{j,t} = f^v_{j,t} \qquad \forall j \in C^c, t \tag{66}$$

$$y^w_{j,t} = f^w_{j,t} \qquad \forall j \in C^c, t \tag{67}$$

$$y^d_{j,l,t} = f^d_{j,l,t} \qquad \forall j \in C^c, l, t \tag{68}$$

$$x^{rcn}_t \leq s^c_t \qquad \forall t \tag{69}$$

$$x^{rwn}_t \leq s^w_t \qquad \forall t \tag{70}$$

C.8.4.3 Objective

Equation 71 defines the objective function to be minimized. The first line shows the fuel-related costs. The no-load cost is multiplied by the on/off binary and added to the product of the marginal cost and the total power output. On the second line, the start

up and shut down costs are applied. On the third line, tie line costs are applied. On the fourth line, unserved reserve costs are applied.

$$\sum_{j,t}\left(c_j^{nl}y_{j,t}^{u}+c_j^{m}(\underline{p}_j y_{j,t}^{u}+x_{j,t}^{p})\right) + \sum_{j,t,l}\left(c_{j,l}^{su}y_{j,t,l}^{d}\right)+\sum_{j,t}\left(c_j^{sd}y_{j,t}^{w}\right) + \sum_{t}c^{tie}x_t^{tie} + \sum_{t}\left(c^{rc}x_t^{rcn}+c^{rw}x_t^{rwn}\right) \quad (71)$$

C.8.4.4 Supply Equation

Equation 72 ensures a balance, in each period, between energy generated by conventional units, wind, hydro, and net tie line inflows, and load.

$$\sum_{j}\left(\underline{p}_j y_{j,t}^{u}+x_{j,t}^{p}\right)+x_t^{w}+x_t^{h}+x_t^{tie}=d_t \qquad \forall t \quad (72)$$

C.8.4.5 Logic Equations

Equations 73-75 ensure that the on/off, startup, and shutdown binary variables relate to each other in the expected way. Note that we only impose these constraints on the binary variables in C that can be committed during this stage.

$$y_{j,t}^{u}-y_{j,t-1}^{u}=y_{j,t}^{v}-y_{j,t}^{w} \qquad \forall j\in C, t>1 \quad (73)$$

$$y_{j,t}^{u}-k_j^{u}=y_{j,t}^{v}-y_{j,t}^{w} \qquad \forall j\in C, t=1 \quad (74)$$

$$y_{j,t}^{v}+y_{j,t}^{w}\leq 1 \qquad \forall j\in C, t \quad (75)$$

C.8.4.6 Startup

Equation 76 ensures that cold, warm, and hot starts occur only when the unit has been offline for the appropriate amount of time. Equation 77 ensures that $y^{d}_{j,t,l}$ and $y^{w}_{j,t}$ agree and ensures that only one type of startup occurs at a time.

Note that equation 76 only requires that a warm start be recorded when the unit has been offline longer than the warm start time and that a cold start be recorded when the unit has been offline longer than the cold start time. They do not force a hot start when the warm start time *has not* been exceeded, or a warm start when the cold start time *has not* been exceeded. These effects rely on increasing start costs from hot through cold.

Note also that we only impose these constraints on the binary variables in C that can be committed during this stage.

$$y^{d}_{j,t,l} \leq \sum_{t'=t-t^{su}_{j,l+1}+1}^{t-t^{su}_{j,l}} y^{w}_{j,t'} \qquad \forall j \in C, t \geq t^{su}_{j,l+1}, l < 3 \tag{76}$$

$$\sum_{l} y^{d}_{j,t,l} \leq y^{v}_{j,t} \qquad \forall j \in C, t \tag{77}$$

C.8.4.7 Spinning Reserve Equation

Equation 78 ensures that the amount of procured spinning reserve is greater than or equal to the reserve requirement in each period. The equation is a soft constraint, as it can be violated if a penalty is paid.

$$\sum_{j} x^{s}_{j,t} \geq s^{c}_{t} + s^{w}_{t} - x^{rcn}_{t} - x^{rwn}_{t} \qquad \forall t \tag{78}$$

C.8.4.8 Minimum Up and Down Times

Equations 79 and 80 impose the minimum up time constraints. Note that these equations are relaxed if the unit is not on outage (i.e. they are only applied for $(j,t) \in O^c$). Equations 81 and 82 impose the minimum down time constraints. Equations 80 and 82 are modifications that apply to early periods in the time frame.

$$\sum_{t'=t-t_j^u+1}^{t} y_{j,t'}^{v} \leq y_{j,t}^{u} \qquad \forall (j,t) \in O^c, j \in C, t \geq t_j^u \tag{79}$$

$$\sum_{t'=1}^{t} y_{j,t'}^{v} \leq y_{j,t}^{u} \qquad \forall (j,t) \in O^c, j \in C, t < t_j^u \tag{80}$$

$$\sum_{t'=t-t_j^d+1}^{t} y_{j,t'}^{w} \leq 1 - y_{j,t}^{u} \qquad \forall j \in C, t \geq t_j^d \tag{81}$$

$$\sum_{t'=1}^{t} y_{j,t'}^{w} \leq 1 - y_{j,t}^{u} \qquad \forall j \in C, t < t_j^d \tag{82}$$

C.8.4.9 Capacity Equations

Equations 83 - 87 ensure that the output and reserve contributions of conventional units are properly bounded during normal operation, but also allow the unit to start up and shut down. To avoid infeasibility, different constraints are applied to units with a minimum up time of 1 (i.e. for $j \in G$) and units with minimum up time greater than 1 (i.e. for $j \in G^c$).

Note that the equations below that contain only binary variables (i.e. do not contain continuous variables) are applied only for units in C that can be committed in this

stage.

$$x^{p}_{j,t-1} + x^{s}_{j,t-1} \leq (\bar{p}_j - \underline{p}_j) y^{u}_{j,t-1} - (\bar{p}_j - r^{su}_j) y^{v}_{j,t-1} - (\bar{p}_j - r^{sd}_j) y^{w}_{j,t} \qquad \forall j \in G^c, t > 1 \tag{83}$$

$$k^{p}_{j} + k^{s}_{j} \leq (\bar{p}_j - \underline{p}_j) k^{u}_{j} - (\bar{p}_j - r^{su}_j) k^{v}_{j} - (\bar{p}_j - r^{sd}_j) y^{w}_{j,t} \quad \forall j \in G^c, j \in C, t = 1 \tag{84}$$

$$x^{p}_{j,t} + x^{s}_{j,t} \leq (\bar{p}_j - \underline{p}_j) y^{u}_{j,t} - (\bar{p}_j - r^{su}_j) y^{v}_{j,t} \qquad \forall j \in G, t \tag{85}$$

$$x^{p}_{j,t-1} + x^{s}_{j,t-1} \leq (\bar{p}_j - \underline{p}_j) y^{u}_{j,t-1} - (\bar{p}_j - r^{sd}_j) y^{w}_{j,t} \qquad \forall j \in G, t > 1 \tag{86}$$

$$k^{p}_{j} + k^{s}_{j} \leq (\bar{p}_j - \underline{p}_j) k^{u}_{j} - (\bar{p}_j - r^{sd}_j) y^{w}_{j,t} \quad \forall j \in G, j \in C, t = 1 \tag{87}$$

C.8.4.10 Ramp Up and Ramp Down

Equations 88 and 89 apply the up ramp rate limits and equations 90 and 91 apply the down ramp rate limits for all units.

$$(x^{p}_{j,t} + x^{s}_{j,t}) - x^{p}_{j,t-1} \leq r^{u}_j \qquad \forall j, t > 1 \tag{88}$$

$$(x^{p}_{j,t} + x^{s}_{j,t}) - k^{p}_{j} \leq r^{u}_j \qquad \forall j, t = 1 \tag{89}$$

$$-x^{p}_{j,t} + x^{p}_{j,t-1} \leq r^{d}_j \qquad \forall j, t > 1 \tag{90}$$

$$-x^{p}_{j,t} + k^{p}_{j} \leq r^{d}_j \qquad \forall j, t = 1 \tag{91}$$

Chapter 5: STATE COOPERATION UNDER THE EPA'S PROPOSED CLEAN POWER PLAN

Abstract

Under the Environmental Protection Agency's (EPA's) proposed CO_2 emissions rule for existing power plants (the 111(d) rule), states will have the choice of whether to comply individually or in cooperation with other states. They will also have the choice of whether to comply with a rate-based standard, a limit related to the average emissions rate of affected electricity generating units (EGUs), or a mass-based standard, a limit on the mass of CO_2 emitted by affected EGUs. In this work, we model the economic effects of these decisions. We use a linear dispatch model designed with a structure similar to that of the EPA's Integrated Planning Model (IPM). Following the IPM, our model represents that power system in the continental U.S. in 64 regions with transmission constraints between them. Our results indicate that while cooperation between states reduces total production costs of compliance, some states see a decrease in their total surplus when cooperating. This suggests a role for the agency in mediating negotiations between states. Furthermore, we find that compliance increases electricity prices, thereby increasing producer surplus (in the electric energy markets) while reducing consumer surplus. The increase in electricity prices under compliance, and the resulting increase in producer surplus and decrease in consumer surplus, is substantially larger when complying with the mass-based standard compared to the rate-based standard. Finally, though we find that producers as a whole have larger surplus under the mass-based standard, natural gas combined cycle units in states with very high (i.e. loose) standards have higher surplus under the rate-based standard.

This paper is in preparation for submission to the Electricity Journal.

5.1 Introduction

In June of 2014, the U.S. Environmental Protection Agency (EPA) proposed a rule entitled "Carbon Pollution Emission Guidelines for Existing Stationary Sources: Electric Utility Generating Units" (hereafter: "the 111(d) rule") [1]. The rule uses the agency's authority under §111(d) of the Clean Air Act (CAA) to regulate CO_2 emissions from affected Electricity Generating Units (EGUs) in the United States. In promulgating the rule, the agency acknowledged the negative impacts of climate change on the health of Americans and noted that the rule would help to mitigate these effects.

The Regulatory Impact Analysis performed by the EPA for the proposed rule [2] predicts that the rule would reduce electric power sector CO_2 emissions by 30% below 2005 levels by 2030. While likely not sufficient to reach climate stabilization targets, even if similar reductions were achieved across the economy and around the world, such reductions are large enough to require significant changes in how electricity is produced and consumed in the United States.

Section 111(d) of the Clean Air Act limits the EPA's authority with respect to how reductions in CO_2 emissions are to be achieved. The agency is able to set standards of performance for CO_2 emissions from existing EGUs, but cannot dictate how these standards are to be reached. Instead, states must decide how to achieve the standard and must submit plans to the EPA detailing the implementation of the standard. The EPA set standards of performance by first defining the Best System of Emissions Reductions (BSER) for achieving such reductions. They then determined the extent of emissions reductions achievable in each state by implementing BSER. The agency then set standards of performance achievable using BSER.

The Best System of Emissions Reduction identified by the EPA consisted of four building blocks: 1) heat rate improvements at coal and oil-fired EGUs, 2) fuel switching from coal and oil-fired EGUs to natural gas combined cycle (NGCC) EGUs, 3) increased use of non-hydro renewables and new and at-risk nuclear, and 4) increased use of demand side energy efficiency. The agency determined targets for each building block that constituted BSER and reported these in the proposed rule. Table 5.1 summarizes these targets.

Table 5.1: Four building blocks constituting BSER and their associated targets under the 111(d) rule. NGCC refers to Natural Gas Combined Cycle EGUs. RPS refers to Renewable Portfolio Standard. EIA refers to the Energy Information Administration.

Building Block	Target
1. Heat Rate Improvement at Coal/Oil EGUs	6% improvement in coal EGU heat rates
2. Fuel Switching from Coal/Oil to NGCC	NGCC units achieve 70% capacity factor
3. Non-Hydro Renewables and "New and At-Risk" Nuclear	Average of RPS target of states that *have* an RPS within their region. States continue to use at-risk nuclear as defined by EIA
4. Demand Side Energy Efficiency (EE)	Incremental EE growth of 0.2% per year from 2012 baseline to "best practice" level of 1.5% per year, then sustained through 2030

The EPA expressed the 111(d) rule performance standards as "rates" that must be met on average within each state, or within each group of states if states choose to comply cooperatively. Though expressed in units of lb/MWh, these performance standards are not true emissions rates. Because they include energy efficiency and some, but not all, renewable and nuclear generation, these rates cannot be interpreted as average CO_2 emissions rates for fossil units *or* average CO_2 emissions rates for the entire fleet of generators. We show the form of the 111(d) rule explicitly in equation (5.1).

While the agency's analysis suggests that the building blocks have been "adequately demonstrated" [1], public commenters have critiqued the proposed rule both on the basis that the measures are not achievable [3] and on the basis that they do not go far enough [4]. For the purpose

of this work, however, we take no position on the EPA's assessment of what constitutes BSER. Instead, we take the standard as given and evaluate some of the effects that would result were the standard to be implemented as proposed. This work expands on the analyses already performed by the EPA in their Regulatory Impact Analysis (RIA) [2] for the rule performed using the agency's Integrated Planning Model (IPM). We focus on the effects of two implementation decisions that states will have to make to comply with the rule: whether to comply on a mass- or rate-basis and whether to comply individually or in cooperation with other states. In particular, we examine 1) how state choices affect total costs of compliance and total CO_2 emissions, 2) how cooperation affects the distribution of surplus among the states, 3) how the rule's impacts are distributed between consumers and producers, 4) how state decisions affect shadow prices of electricity and CO_2, and 5) how state decisions affect revenues for NGCC and coal EGUs. Similar to Chapter 4, we focus here on the portion of emissions reductions achievable using re-dispatch, taking changes to the fleet and energy efficiency as given.

We note that while we have made a significant effort to interpret the 111(d) rule accurately, the rule is complex, articulated in legal language, and insufficiently specific in certain instances. It is possible that we have not interpreted the rule as the EPA would have wanted. Furthermore, the rule has not yet been finalized or interpreted by the courts. The "correct" interpretation of the rule is therefore subject to change in the future. This work is thus based on our best understanding of the 111(d) rule as proposed, rather than a definitive impact analysis.

5.2 Methods

For this analysis we constructed a production cost minimization model based on the EPA's Integrated Planning Model (IPM). The model attempts to meet hourly load in a number of transmission regions at least total cost, subject to the capacities of the EGUs in each region and

transmission constraints between the regions. In accordance with the 111(d) rule, the model also constrains the CO_2 emissions of EGUs affected by the Clean Power Plan by imposing either a rate-based or mass-based emissions constraint. The 111(d) constraint binds on each state (or group of states if regional cooperation is allowed) on average over the course of a year.

The model does not include unit commitment, and therefore does not include power plant operating constraints and objective function terms that depend on the presence of integer variables: minimum run and minimum down times, minimum generation levels, startup costs, and no-load costs. The model also does not include ramp rate constraints. We made these modeling choices to allow a computationally feasible solution for the whole country at the hourly level. In previous work [5], we found that fossil-fueled EGU startups are associated with emissions and production cost penalties, but that these are small compared to the emissions and production costs from normal operations. Therefore, though the simplified model in this chapter does not account for these effects, we don't believe these limitations will qualitatively affect our results. The full formulation of the model is available in section D.8 of the Appendix.

Our model's transmission regions in the contiguous United States align with those used in the IPM. The IPM model disaggregates the electricity transmission system in the contiguous U.S. into 64 regions with transmission constraints between them. The IPM model's regions roughly correspond to both North American Electric Reliability Corporation (NERC) Assessment Regions and to the Energy Information Administration's National Energy Modeling System (NEMS) Regions [6]. In certain cases, the IPM's regions provide further disaggregation than NERC or NEMS regions, in an effort to capture both physical transmission system constraints and administrative subdivisions. The EPA's documentation on IPM v.5.13 provides further details about these transmission regions [6].

5.2.1 EGU Aggregation

In order to reduce the solve time of the optimization problem, we implemented a procedure to reduce the number of EGUs present in the model by aggregating similar units while minimizing the effect on the results. To do this, we first subdivided EGUs in our data set by 1) transmission region, 2) state, 3) plant type, 4) fuel type, and 5) whether the unit was affected by the 111(d) rule. EGUs sharing all five attributes were then aggregated by summing minimum and maximum generation and by performing a capacity-weighted average of heat rates, current emissions factors, fuel costs, and other variable operations and maintenance (O&M) costs.

5.2.2 111(d) Constraints

For the purposes of this analysis, we took the EPA's state-by-state emissions rate standards [1] as given. In order to ensure compliance with the standards during model runs, we imposed constraints on our production cost minimization model. The rate-based compliance scenarios used equation (5.1) and the mass-based compliance scenarios used equation (5.2). In equations (5.1) and (5.2), $x^{P}_{j,t}$ is the only decision variable. All other parameters in the equations, including electricity from new and at risk nuclear and avoided energy from efficiency, are fixed at the values EPA specified in the proposed 111(d) rule [1]. Table 5.2 defines all symbols used in the equations.

Table 5.2: Symbols used in rate-based and mass-based emissions constraints.

Variable	Description
e_j	CO_2 emissions rate of unit j [lb/MWh]
$x^P_{j,t}$	Electricity produced by unit j in period t [MWh]
S_R	Rate-based standard [lb/MWh]
S_M	Mass-based standard [lb]
R_t	Renewables generation in period t [MWh]
N	Electricity from new and at risk nuclear in period t [MWh]
η	Avoided energy from energy efficiency per period (constant) [MWh]

Equation (5.1) constrains the CO_2 emissions from affected units (left-hand side) to be less than or equal to the standard times the quantity of generation from affected units, plus non-hydro renewables generation, plus new and at-risk nuclear generation, plus energy efficiency (right-hand

side). Note that equation (5.1) does not constrain mass emissions of CO_2 directly. If more or less electricity is generated in a particular region, the effective mass limit of CO_2 increases or decreases, respectively.

Equation (5.1) presents a slightly simplified version of the rate-based constraint used in the full model. The rate-based standard S_R actually applies only to EGUs within the state (or group of states if cooperation is allowed) to which an EGU belongs. Therefore, there are actually multiple constraints similar to equation (5.1) in each model run – one for each compliance region. Each constraint only constrains a subset of all affected EGUs. The full constraint is shown in section D.8 of the Appendix.

$$\sum_j \sum_t e_j x_{j,t}^P \leq S_R \sum_t \left(\sum_j x_{j,t}^P + R_t + N + \eta \right) \tag{5.1}$$

Equation (5.2) constrains the CO_2 emissions from affected units (left-hand side) to be less than or equal to a constant: the mass-based standard. In the original proposal, the EPA specifically allowed for states to comply on a mass-basis [1], but did not specify alternate mass-based standards for each state. For the purposes of this work, we assumed that the EPA would allow sates to set mass-based standards at the level of emissions that would occur if the states were to comply with a rate-based standard. We therefore elected to use the mass emissions resulting from compliance with a rate-based standard as the mass-based standard in this work. To do this, we used the results from our model under compliance with the rate-based standard, calculated the quantity on the right hand side of equation (5.1), and used this quantity as the mass based standard S_M in equation (5.2) for our mass-based compliance scenarios.

$$\sum_j \sum_t e_j x_{j,t}^P \leq S_M \tag{5.2}$$

However, in a recent notice [7], the EPA provided more information about how mass-based standards might be calculated and example calculations for each state. The method used by the agency to calculate mass-based standards yielded results very similar to our own. Nationwide, the agency's mass-based standard is 1% less than the mass-based standard used in this work. This difference is largely due to the fact that the agency did not incorporate load-growth in their conversion from a rate-based to a mass-based standard, whereas the method used in this work implicitly does incorporate such growth (by using compliance year load when solving our rate-based model). We also note that the agency's method results in some differences in state-by-state mass-based caps compared to the method used in this work. See section D.6 of the Appendix for more details.

5.2.3 Surplus Calculation and Allocation

In section 5.3, we report differences between producer, consumer, and government surpluses across scenarios. We calculated surplus values in post-processing, using the primal and dual values of the scheduling optimization model at optimality. First, we assumed an inelastic demand curve for electricity, with a cutoff value, L [$/MWh], representing the price above which the quantity of electricity demanded drops to zero. In this work, we report only *differences* in surplus across scenarios, such that L drops out of the calculations.

Second, we used the shadow prices of electricity in each transmission region in each period to divide total surplus between producers and consumers. Third, in the mass-based compliance scenarios, we assumed that the government of each state earned revenues from the sale of all CO_2 emissions allowances for that state at the prevailing shadow price of CO_2.

Fourth, we allocated congestion rents equally between producers and consumers. Congestion rents occur when transmission lines between adjacent regions are loaded to their full capacity and markets on either side of the lines have different electricity prices. Congestion rents accrue on the

transmission region level. In order to report surplus values at the state level, we allocated these transmission region-level rents to states in proportion to the dispatchable generation in each transmission region performed by generators in a particular state under the reference scenario (we discuss the scenarios in section 5.2.5). The allocation factors are therefore constant over time and between scenarios. For more detail on surplus calculations, see section D.3 of the Appendix.

5.2.4 Wind Profiles

Our compliance scenarios take the renewable energy targets specified by the EPA in the proposed 111(d) rule as given [1] (see Table D-3 in the Appendix). For modeling purposes, we assume that the renewable energy targets will be met using wind power. We used data from the IPM to generate wind power output profiles for each hourly period in our optimization model. Using data from the National Renewable Energy Laboratory (NREL) [6], the IPM provides winter- and summer-day wind profiles by wind and cost class in each transmission region and state. The IPM also provides the total potential wind capacity in each region. In order to generate the wind profiles used in this work, we selected profiles in order of increasing cost class and decreasing wind class within each state. We then aggregated these profiles such that the annual wind energy in each state was equal to the target. Note that we could have used data from NREL's Eastern Wind Interconnection and Transmission Study (EWITS) [8] to generate our wind profiles. However, in order to keep our results in alignment with those in the IPM, we chose to use the EPA's data instead.

5.2.5 Scenarios Studied

We examined seven scenarios in this work: one reference scenario and six compliance scenarios. The reference scenario does not have any compliance constraints. The compliance scenarios consist of combinations of three types of cooperation for compliance (state, regional, and national) and two

types of standard (rate-based and mass-based). Each compliance scenario has a compliance constraint as defined by equation (5.1) or (5.2). In the regional compliance scenarios, we used the regional cooperation groups EPA suggested in the 111(d) rule regulatory impact analysis [2]. Our national compliance scenarios allowed cooperation among all of the states in the contiguous U.S.

The reference scenario deserves further discussion. The fact that the reference scenario lacks compliance constraints is the *only* difference between it and the compliance scenarios. Load profiles, fuel costs, wind and hydro profiles, CO_2 emissions rates, tie line capacities, and the fleet of generators in service are the same under the reference scenario as they are under the compliance scenarios. This means, in particular, that changes in the fleet occurring in response to the 111(d) rule are reflected in the reference scenario. Conceptually, the reference scenario can be interpreted as the result that would occur if capacity expansion decisions were to be made in the expectation that the 111(d) rule was going to come into full effect into 2030, but the rule were then not to actually come into effect. The comparisons between the reference scenario and the compliance scenarios therefore only reflect the dispatch stage effects of the 111(d) rule, ignoring the capacity expansion implications.

5.3 Results and Discussion

Our results indicate that, of the compliance scenarios, total production costs were lowest under mass-based compliance with maximum cooperation, with short-term compliance costs (short term in that they only include dispatch costs in the compliance year) ranging from 17 $/ton – 24 $/ton depending on the scenario. Total production costs declined with cooperation under both rate-based and mass-based compliance. However, despite the decline in costs country-wide, some states fared worse under regional or national cooperation schemes compared to no-compliance scenarios.

Compliance with the 111(d) rule tended to increase producer surplus and decrease consumer surplus compared to the reference scenario, likely due to increases in electricity prices under compliance scenarios. These surplus and electricity price effects were most pronounced under mass-based compliance. The shadow price of CO_2 was quite stable under all compliance scenarios, with the exception of certain states having very high prices and others having prices of zero under rate-based compliance without cooperation. The Northeast states also had a shadow price of CO_2 of zero under rate-based compliance with regional cooperation

Not surprisingly, we also found that compliance increases net revenues for NGCC units and decreases net revenues for coal units. Nationally, both types of units had higher surplus under mass-based compliance than under rate-based compliance. However, in a few states with very high (i.e. loose) rate-based standards, NGCC units had higher surplus under rate-based compliance than under mass-based compliance.

5.3.1 Production Costs and Emissions

Figure 5.1 shows tradeoffs between total production costs and CO_2 emissions on an annual basis between the scenarios. The figure also shows dashed lines connecting the reference scenario to the highest and lowest cost compliance scenarios. The slope of these lines can be interpreted as a cost of mitigation, though we emphasize that the values reported here include only the incremental *production costs*. Notably, costs for implementing energy efficiency programs, installing additional renewable and NGCC capacity, and preventing retirement of at-risk nuclear EGUs are *not* included in these cost estimates.

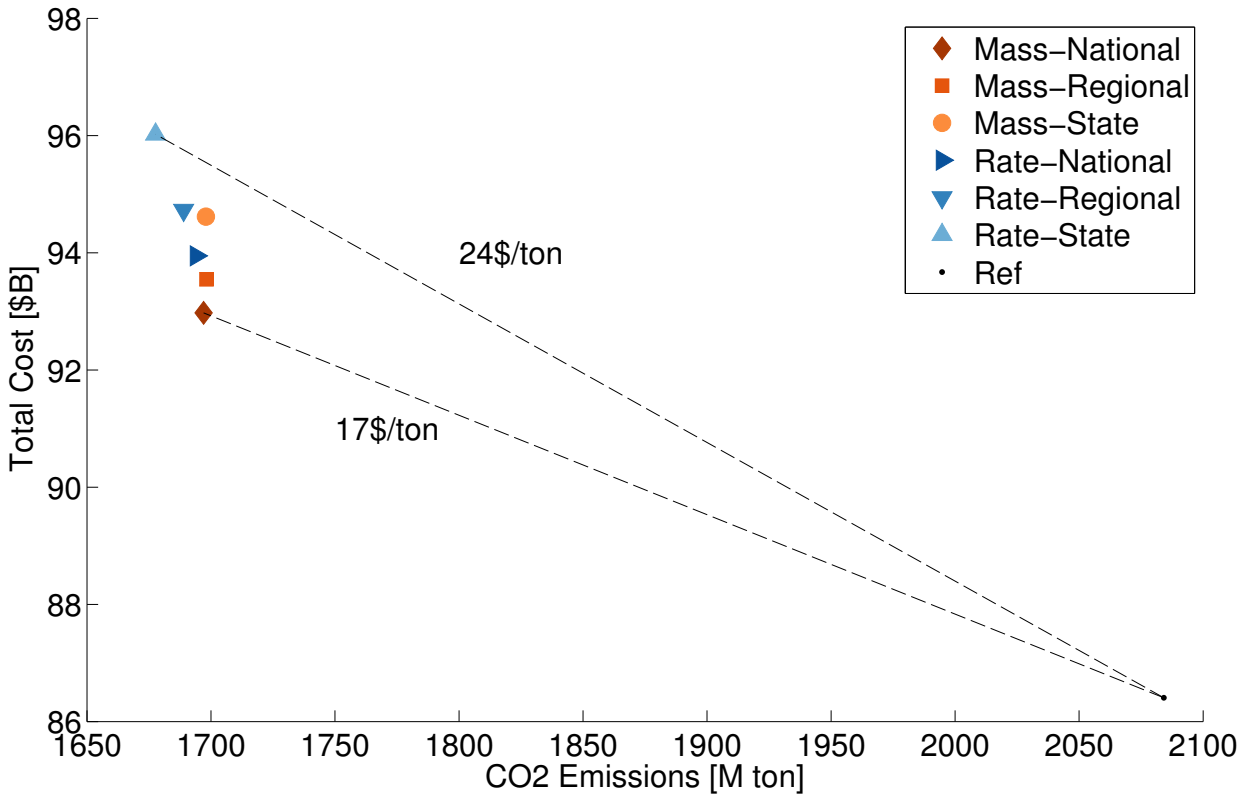

Figure 5.1: Production cost - CO_2 emissions tradeoff. Note that both axes have been truncated.

Figure 5.1 indicates that the cost of compliance ranges from 17 $/ton to 24 $/ton, depending on the compliance scenario. The figure also indicates that, for either the rate-based or the mass-based standard, production costs decrease as the level of cooperation increases. Furthermore, the figure shows that, for a given level of cooperation, compliance costs under the mass-based standard are consistently lower than under the rate-based standard. Finally, the figure shows that total emissions *increase* with cooperation under the rate-based standard, but the rate standard consistently has slightly lower emissions than the mass-based standard.

Production costs are lower and emissions are higher under the mass based constraint compared to the rate-based constraint (for a given level of cooperation) due primarily to the fact that the form of the mass-based constraint allows more leakage to non-affected units. Under the rate-based constraint, shifting production from affected units to non-affected units is not a very good strategy to achieve compliance since reducing the generation of affected units also reduces the effective

emissions cap according to equation (5.1). However, under the mass-based standard, shifting production from affected units to non-affected units (or to Canada – section D.3 of the Appendix shows net exports to Canada under rate-based compliance and net imports under mass-based compliance) simply reduces the emissions on the left hand side of equation (5.2). Higher emitting, but lower cost, affected units can then be used to fill the additional emissions budget.

Total emissions increase with cooperation under the rate-based standard primarily due to the fact that, under state compliance, some of the rate-based emissions constraints are not binding. Similarly, under regional cooperation with a rate-based standard, the Northeast region's constraint is not binding. Figure 5.4 shows these results clearly. This means that, by increasing levels of cooperation under rate-based compliance, the slack in the regions where constraints are non-binding can be shifted to regions where constraints are binding, leading to higher emissions.

5.3.2 Surplus Change with Compliance

Figure 5.2 shows the change in consumer, producer, and government surplus from the reference scenario to compliance scenarios with no cooperation. In general, the figure indicates that compliance leads to increases in producer surplus and losses in consumer surplus. The magnitude of these impacts varies from state to state. Additionally, the magnitude of the impact is much larger under mass-based compliance than under rate-based compliance.

Under the mass-based scheme, government proceeds from allowance auctions (indicated by government surplus in Figure 5.2) are significant. Due to the significantly larger negative impact on consumers of a mass-based standard, state governments choosing to comply on a mass basis should consider using auction proceeds to compensate consumers. Variation in auction proceeds between the states mean that this will be easier for some states than others. Nation-wide, allocating auction proceed to consumers could offset 94% of the additional loss in consumer surplus resulting from mass-based compliance compared to rate-based compliance.

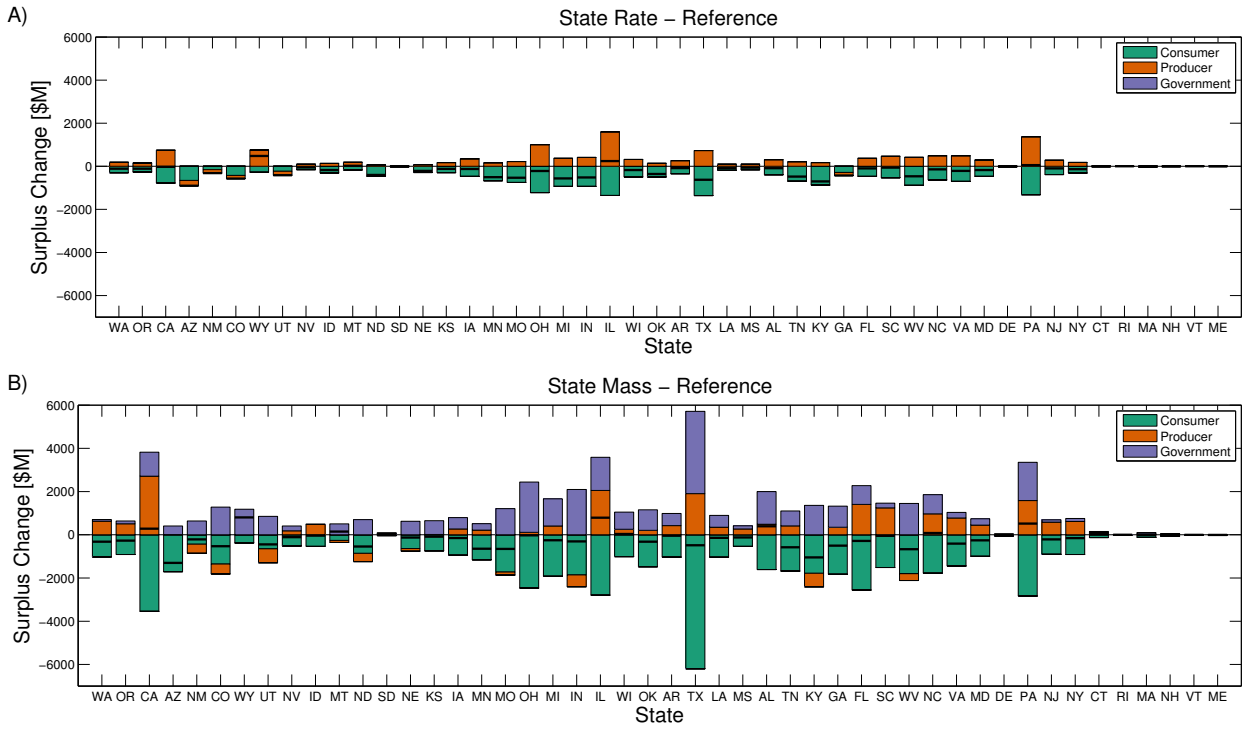

Figure 5.2: Changes in consumer, producer, and government surplus from non-compliance to no-cooperation compliance for A) a rate-based standard and B) a mass-based standard. Black lines indicate net surplus change.

5.3.3 Total Surplus Change with Cooperation

Figure 5.3 shows the change in total surplus (producer surplus + consumer surplus + government surplus) between a regional cooperation scenario and a no-cooperation scenario. Summed across the country, the total surplus change is positive, reflecting the fact that total costs are lower under regional cooperation (as shown in Figure 5.1). However, under both rate-based and mass-based standards, some states have lower total surplus under regional cooperation than under no-cooperation.

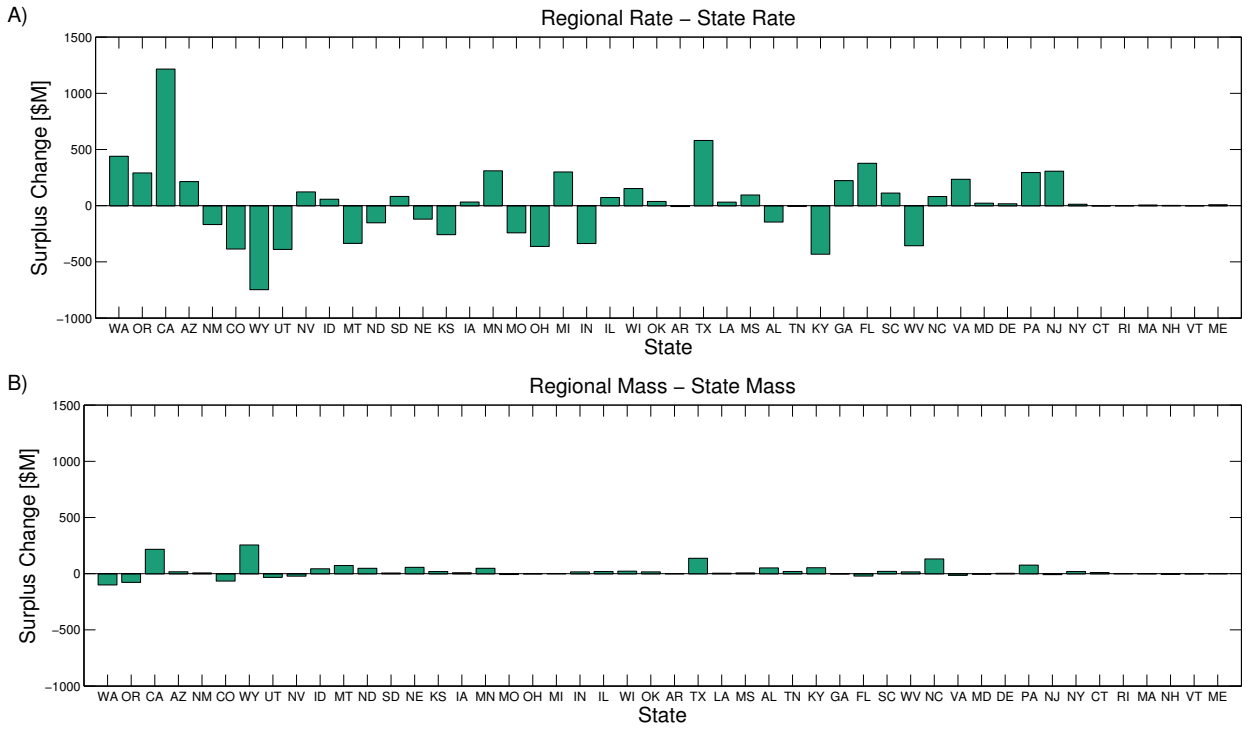

Figure 5.3: Changes in total surplus from no-cooperation compliance to regional-cooperation compliance for A) a rate-based standard and B) a mass-based standard.

Figure 5.3 shows that, despite the fact that cooperation will lead to lower costs overall, it is not clear that all states will want to cooperate. There may therefore be a role for a federal body, such as the EPA, to facilitate negotiations between states to enable the achievement of a lower-cost cooperative outcome. Such negotiations would be complicated both by the fact that the surplus losses shown in Figure 5.3 are born by three groups of entities (consumers, producers, and state governments) and by the overlapping jurisdictions of states and transmission organizations such as RTOs. See Figure D-2 for the distribution of surplus changes between consumers, producers, and the government.

5.3.4 Shadow Prices of Electricity and CO_2

The shadow prices of electricity and CO_2 that emerge from the optimization lend insight into the distribution of economic impacts of the policy between consumers and producers. Figure 5.4 shows both sets of shadow prices. The electricity price portion of the figure shows a number of

qualitative results. First, compliance leads to increased electricity prices compared to the reference case. We note that this result is at odds with some of the results reported by the EPA. This is likely due to the fact that our reference case already includes the effects of energy efficiency, whereas the EPA's does not. Second, it is clear from the figure that electricity prices increase much more significantly under mass-based compliance than under rate-based compliance. This result will be explained in more detail below.

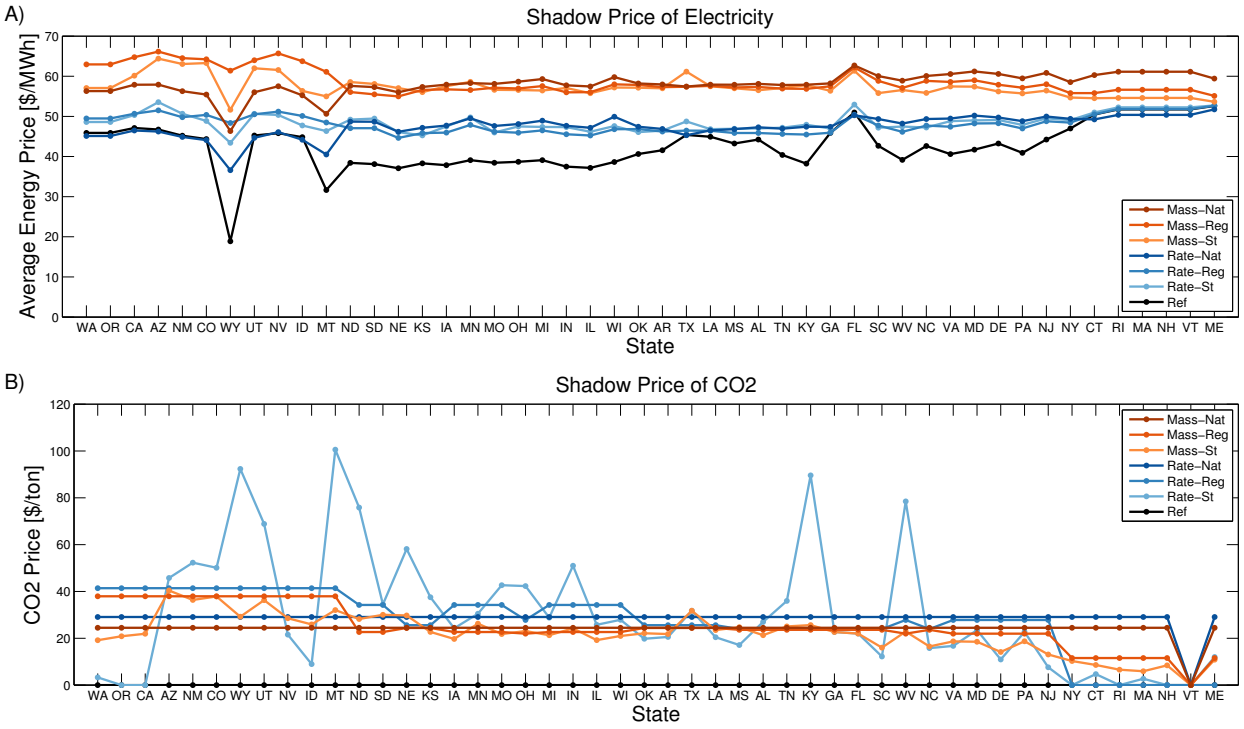

Figure 5.4: Shadow prices of A) electricity and B) CO_2 under all scenarios.

Figure 5.4 B) also provides a number of qualitative insights. First, shadow prices of CO_2 are significantly higher than average for a number of states under rate-based compliance with no cooperation. Shadow prices of CO_2 for Wyoming, Montana, Kentucky, and West Virginia all exceed the 90th percentile of state prices under rate-based compliance with no cooperation. All of these states lack affected NGCC capacity. This means that in these states, it can be much more costly to achieve emissions reductions at the margin. Note that the shadow CO_2 prices in Figure 5.4 can be

understood as the *marginal* costs of reducing CO_2 emissions by 1 ton. This in contrast to the values in Figure 5.1, which are the *average* costs of reducing CO_2 emissions by hundreds of millions of tons.

Second, shadow prices of CO_2 are zero for a number of states under state-based compliance without cooperation. Similarly, the Northeast region has a shadow price of CO_2 of zero under regional cooperation. Shadow prices are never zero (except in Vermont, where there is no standard) under mass-based compliance or under rate-based compliance with national cooperation.

Equations (5.3) and (5.4) explain the reason for the significantly higher shadow price of electricity under a mass based standard compared to a rate-based standard (Table 5.3 defines the symbols used in the equations). Equations (5.3) and (5.4) show one of the Karush–Kuhn–Tucker (KKT) conditions that must be satisfied *for the marginal unit only* at optimality for mass-based compliance and rate-based compliance, respectively. Other dual variables that have a value of zero for the marginal unit have been left out of the equations.

Table 5.3: Symbols used in electricity price comparison.

Variable	Description
$\lambda^M_{k,t}$	Shadow price of electricity under mass standard in transmission region k during time t [$/MWh]
$\lambda^R_{k,t}$	Shadow price of electricity under rate standard in transmission region k during time t [$/MWh]
c_j	Marginal cost of marginal unit j (in transmisison region k and compliance region l) [$/MWh]
μ^M_l	Shadow price of CO_2 under mass standard in compliance region l [$/lb]
μ^R_l	Shadow price of CO_2 under rate standard in compliance region l [$/lb]
e_j	CO_2 emissions rate of marginal unit j [lb/MWh]
s^R_l	Rate standard in compliance region l [lb/MWh]

One interpretation of equation (5.3) is that the shadow price of electricity, under a mass-based standard, must be high enough to compensate the marginal unit for its marginal costs plus its CO_2 emissions costs. These CO_2 emissions costs, under a mass-based standard, are given by the product of the shadow price of CO_2 and the emissions rate of the marginal unit. As the shadow price of CO_2 and the emissions rate are both positive quantities, the CO_2 emissions costs for the marginal unit are always positive.

$$\lambda_{k,t}^{M} = c_j + \mu_l^{M} e_j \tag{5.3}$$

One interpretation of equation (5.4) is that the shadow price of electricity, under a rate-based standard, must again be high enough to compensate the marginal unit for its marginal costs plus its CO_2 emissions costs. While the marginal costs will be the same under a rate-based standard, the CO_2 emissions costs have a different form. Under the rate-based standard, CO_2 emissions costs are given by the product of the shadow price of CO_2 and the difference between the marginal unit's emissions rate and the rate-based standard. Due to the fact that some units have emissions rates lower than the rate-based standards, this quantity can be negative. For such a marginal unit, "CO_2 emissions costs" are actually a CO_2 emissions revenue.

$$\lambda_{k,t}^{R} = c_j + \mu_l^{R} \left(e_j - s_l^{R} \right) \tag{5.4}$$

Figure 5.4 shows that, for the same level of cooperation, shadow prices of CO_2 are quite similar under rate-based and mass-based compliance. It therefore follows that CO_2 costs are, for the most part, lower under a rate-based standard than under a mass-based standard. It follows from equations (5.3) and (5.4) that the shadow price of electricity is lower as well.

5.3.5 Effect of Compliance on Coal and NGCC Unit Revenues

Figure 5.5 shows national-average revenues for NGCC and coal EGUs under each scenario, including the breakdown between revenues from electricity sales, costs for fuel and variable O&M, and CO_2 emissions costs or revenues. Note that the figure does not include the portion of congestion rents allocated to producers. The figure shows that net revenues increase for NGCC units and decrease for coal units under compliance scenarios. In fact, NGCC net revenues more than double, while coal net revenues decrease by more than 85% under a rate-based standard with no cooperation compared to the reference case. For both NGCC and coal units, net revenues are

higher under mass-based compliance than under rate-based compliance. In both cases, this is largely due to the higher electricity price under mass-based compliance.

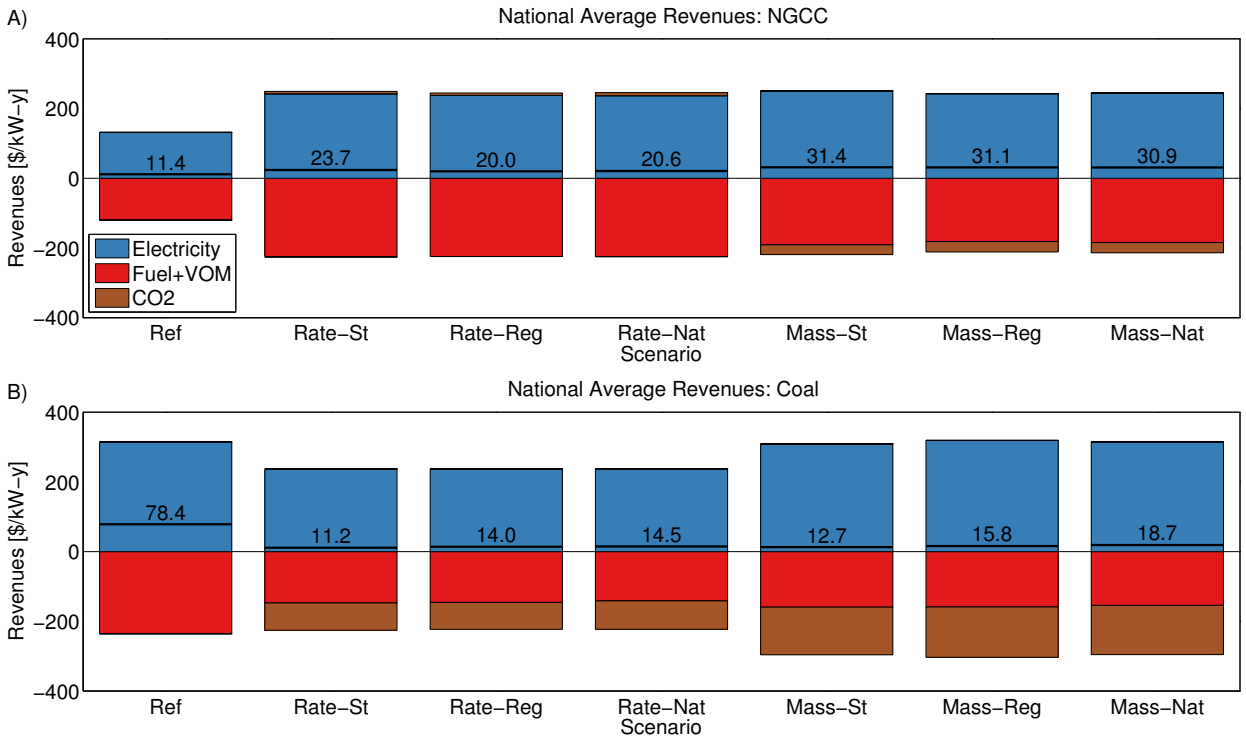

Figure 5.5: National average net revenues, showing contributions of electricity market revenues, fuel + variable O&M (VOM) costs, and CO_2 costs or revenues, for A) NGCC units, and B) Coal units. Black lines indicate net revenues, which are also labeled.

Figure 5.5 also shows that for NGCC units under a mass-based standard and coal units under both rate-based and mass-based standards, participation in CO_2 markets entails a cost. However, for NGCC units under a rate-based standard, participating in CO_2 markets generates revenue. Due to the fact that NGCC units have, on average, emissions rates lower than the rate-based standards, these units receive a payment under rate-based compliance scenarios. The reasons for this were discussed in section 5.3.4. Also note that while coal units always incur costs in CO_2 markets, they pay substantially less under a rate-based standard than under a mass-based standard.

The national average net revenues reported in Figure 5.5 disguise significant regional variation. Figure 5.6 A) shows the variation in NGCC net revenues across all states for all scenarios. Despite the fact that national average net revenues for NGCC units are higher under a mass-based standard,

several states show the opposite trend. Figure 5.6 B) shows the same information as Figure 5.6 A), but for a subset of states. These states have at least one NGCC unit affected by the 111(d) rule and rate-based standards of 1,200 lb/MWh or greater.

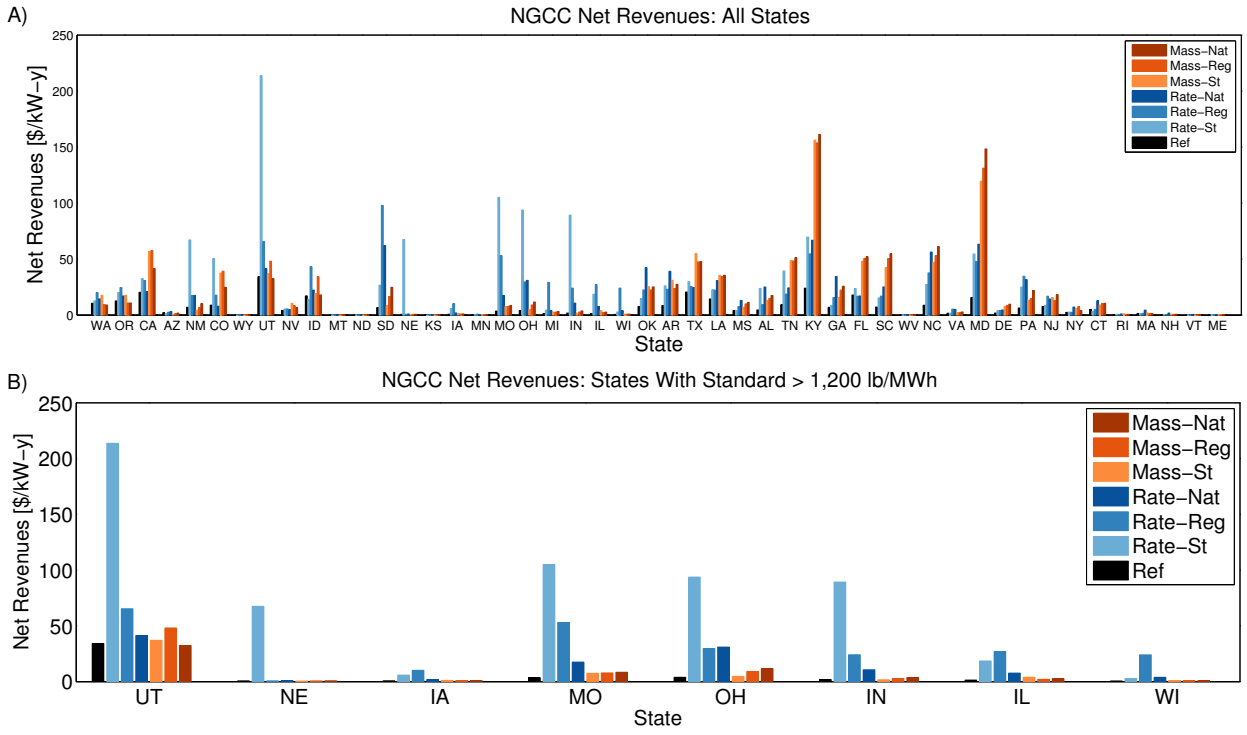

Figure 5.6: Net revenues for NGCC units across all scenarios for A) all states, and B) states having more than 100 MW of affected NGCC capacity and an emissions rate standard greater than 1,200 lb/MWh.

In the states shown in Figure 5.6 B), NGCC units have higher net revenues under the rate-based standard than under the mass-based standard for a given level of cooperation. This is despite the fact that electricity prices are higher, even in these states, under the mass-based standard. The fact that net revenues for NGCC units are higher in states with very high rate-based standards follows from equation (5.4): CO_2 revenues (which only exist under the rate-based standard) are proportional to the standard. Indeed, NGCC units in the states shown in Figure 5.6 B) obtained 19% of their revenues from CO_2 under rate-based compliance with no cooperation, compared to 7% nationwide.

5.4 Conclusions

Our analysis indicated that production costs of compliance decreased with increasing cooperation and with mass-based compliance compared to rate-based compliance. Of the six compliance scenarios considered, production costs were lowest under mass-based compliance with national cooperation and highest under rate-based compliance with no cooperation. Given the savings in production costs, states should be interested in collaborating with each other and the EPA should encourage them to do so.

However, our analysis also indicated that some states had lower total surplus when cooperating at a regional or national level compared to complying with no-cooperation. These states may be inclined to hold out rather than cooperate with other states. States interested in cooperative compliance should consider compensation schemes for hold out states when establishing the terms of cooperation. The EPA should consider the possibility of brokering such compensation schemes.

Our analysis also found that compliance, compared to a reference scenario including energy efficiency, tended to increase electricity prices. This increase in prices increased short-term producer surplus at the expense of consumer surplus. These effects were most dramatic under mass-based compliance, even though total production costs were lower for mass-based compliance. Costs were lower under the mass-based standard compared to the rate-based standard due to the fact that the mass-based standard allows more leakage to non-affected units and to Canada. Electricity prices were higher under the mass-based standard due to the fact that the marginal unit's marginal costs include a higher cost of CO_2 emissions than they do under the rate-based standard. States should be aware of this distinction when deciding between rate-based and mass-based compliance. If states decide to use mass-based compliance, they should consider using proceeds from allowance auctions to offset the costs to consumers.

Finally, we observed that compliance tended to significantly increase net revenues for NGCC units and reduce net revenues for coal units. At the national level, mass-based compliance led to higher net revenues compared to rate-based compliance (for a given level of cooperation) for both NGCC and coal units. However for a select group of states with very high rate-based standards, NGCC units fared better under rate-based standards than mass-based standards.

The 111(d) rule is the latest piece of climate related regulation promulgated using the EPA's authority to regulate greenhouse gases under the Clean Air Act. The rule's focus on existing EGUs, its national scope, and its meaningful performance standards mean it is potentially the most significant in terms of its potential to reduce emissions of greenhouse gases over the next decade and a half. However, the rule's complexity and the significant flexibility allowed to states in deciding how to comply mean that the rule may have some potentially counter-intuitive effects. We hope that our analysis of some of these effects may help state governments and other affected entities to make more informed decisions when complying with the rule.

Our analysis has a number of limitations that are worth discussing. First, similar to the work of chapter 4, the work in this chapter focuses on operational decisions and does not represent capacity expansion decisions. Additionally, here we do not consider scenarios with different fleets: all scenarios considered in this chapter use the EPA's compliance fleet. Second, our model does not incorporate any forecast error: all generation and transmission scheduling decisions are performed with perfect information about future net load. Third, though our dispatch model represents the whole continental U.S., it does so in a highly simplified way. No distinction is made between regions with regulated and de-regulated electricity systems, reserve margins are not enforced, and inter-temporal constraints (such as ramp rates and minimum up and down times) are not modeled, and sub-hourly markets are ignored. Next, the model is run for the compliance year of 2030 and therefore relies on potentially erroneous forecasts for parameters including load, fuel prices, the

configuration of the transmission system, and the generation fleet. Finally, the 111(d) rule is not yet finalized and any changes that happen between now and implementation could affect results.

5.5 References

[1] EPA, "Carbon Pollution Emission Guidelines for Existing Stationary Sources: Electric Utility Generating Units; Proposed Rule," no. 79, Jun. 2014.

[2] EPA, "Regulatory Impact Analysis for the Proposed Carbon Pollution Guidelines for Existing Power Plants and Emission Standards for Modified and Reconstructed Power Plants," Online, Jun. 2014.

[3] EPRI, "Comments of the Electric Power Research Institute on Environmental Protection Agency 40 CFR Part 60 [EPA-HQ-OAR-2013-0602; FRL-9911-86-OAR]," Oct. 2014.

[4] SierraClub, "Comments of Sierra Club and Earthjustice - Carbon Pollution Emission Guidelines for Existing Stationary Sources: Electric Utility Generating Units," Dec. 2014.

[5] D. L. Oates and P. Jaramillo, "Production cost and air emissions impacts of coal cycling in power systems with large-scale wind penetration," *Environ. Res. Lett.*, vol. 8, no. 2, p. 024022, May 2013.

[6] EPA, "Documentation for EPA Base Case v.5.13 Using the Integrated Planning Model," Nov. 2013.

[7] EPA, "Translation of the Clean Power Plan Emission Rate-Based CO2 Goals to Mass-Based Equivalents," Nov. 2014.

[8] NREL, "Eastern Wind Dataset," Mar. 2013.

[9] EPA, "Standards of Performance for Greenhouse Gas Emissions from New Stationary Sources: Electric Utility Generating Units," no. 79, Jan. 2014.

D Appendix

D.1 111(d) Standards By State

In Figure D-1, we report the 111(d) rule performance standards for each state. As is evident from the figure, there is very large variation between states. In the figure, we also report the new source standards that were previously proposed by the agency using its authority under §111(b) of the CAA [9] for comparison. Some states have standards under the 111(d) rule that are more stringent than the new source standards, while others have existing plant standards that are less stringent. There are two reasons for this variation. First, the current emissions rates vary substantially across states, due to differences in the generation fleet across the country. Second, the degree to which the building blocks specified in Table 5.1 reduce CO_2 emissions depends on the characteristics of each state's power system in the base year.

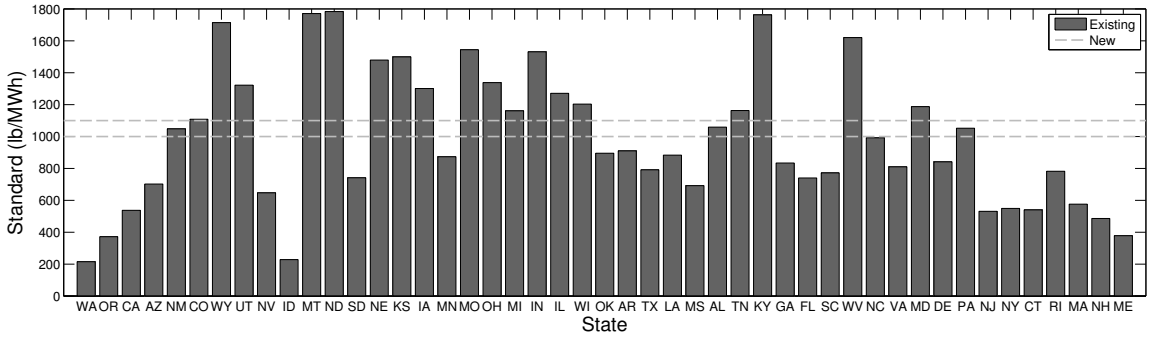

Figure D-1: Existing plant standards by State for Option 1 compliance under the 111(d) rule and national New Source standards for reference.

D.2 Data

In addition to using the IPM as a source for our model's structure, we also used it as a source for our input data. Most of the input data were based on the IPM v.5.13 files associated with the EPA's Regulatory Impact Analysis of the 111(d) rule [2]. Other inputs were based on the 111(d) rule itself [1]. Table D-1 shows the sources of all parameters used in the model.

Table D-1: Major input parameters for the model used in this work, showing index, summary value, and summary value description. Marginal Cost includes fuel cost and other VOM, but not CO_2 costs.

Parameter	Source(s)
Demand	[2]
Available Wind	Profiles [2], Target Penetration [1]
Available Hydro	[2]
Marginal Cost (Fuel +other VOM)	[2]
Maximum Generation Level	[2]
CO_2 Emissions Rates	[2]
Tie Line Capacity	[2]
External Tie Line Capacity	[2]
Clean Power Plan CO_2 emissions rate standard	[1]
New and At Risk Nuclear	[1]
Energy Efficiency	[1]
External Region Price	[2]
Transmission Loss	[2]

Since fuel prices are extremely important inputs, we report them by fuel type in Table D-2. The table shows the capacity-weighted average (the average of fuel prices across units weighted by these units' capacities) and standard deviation of fuel prices used in the model. These prices are based on the EPA's forecasts for the 2030 compliance year for the 111(d) standard.

Table D-2: Capacity-weighted average and standard deviation of fuel prices used in the model, based on IPM v.5.13. The fuel prices here are based on the IPM's EGU-level data, where available. Where EGU-level fuel prices were not available, we used the average price from available data.

Fuel	Average Price [$/MMBTU]	Standard Deviation of Price [$/MMBTU]
Biomass	2.73	0.5
Coal	2.40	0.6
Fossil Waste	0.00	0.0
Geothermal	0.00	0.0
LF Gas	0.00	0.0
MSW	0.00	0.0
Natural Gas	6.06	0.6
Non-Fossil Waste	0.00	0.0
Nuclear	0.96	0.0
Oil	25.0	0.03
Pet. Coke	3.05	0.07
Waste Coal	2.20	0.0

Table D-3 shows state-level data on rate and mass-based standards, available energy efficiency, new and at risk nuclear, and renewables. All columns except the mass-based standard column were taken from the proposed 111(d) rule [1]. The mass-based standard column was calculated using our model as described in section 5.2.2.

Table D-3: State-level input data, based on IPM v.5.13. We calculated the mass-based standard as the CO_2 emissions from affected units in each state under the state-rate compliance scenario. Note that there are no affected units in VT and there is therefore no standard for that state.

State	Rate-Based Standard [lb/MWh]	Mass-Based Standard [M Ton/y]	Efficiency [TWh]	New and At Risk Nuclear [TWh]	Renewables Target [TWh]
AL	1059	71	8.79	2.33	13.8
AR	910	25.8	4.89	0.842	4.55
AZ	702	9.91	9.22	1.82	4.44
CA	537	50.7	22.9	1.04	41.9
CO	1108	33.9	5.66	0	11
CT	540	5.5	3.77	0.971	3.25
DE	841	1.14	0.53	0	1.04
FL	740	39.6	21.3	1.62	22.1
GA	834	43	12.1	1.88	12.2
IA	1301	26.8	5.73	0.278	8.5
ID	228	0.74	1.32	0	3.25
IL	1271	80	18.0	5.31	17.8
IN	1531	86.6	12.6	0	8.03
KS	1499	28.3	4.12	0.543	8.88
KY	1763	53.2	9.32	0	1.8
LA	883	23.4	7.65	0.985	7.24
MA	576	9.58	5.23	0.316	8.69
MD	1187	15.7	4.65	0.788	6.05
ME	378	1.19	1.51	0	3.61
MI	1161	59	13.3	1.83	7.57
MN	873	11.5	7.10	0.84	7.83
MO	1544	55.4	8.74	0.55	2.75
MS	692	6.07	4.92	0.632	5.46
MT	1771	15.8	1.62	0	2.78
NC	992	53.8	12.2	2.3	11.7
ND	1783	24.8	1.54	0	5.42
NE	1479	21.1	3.45	0.575	3.76
NH	486	1.52	1.29	0.576	4.82
NJ	531	8.19	5.89	1.62	10.4
NM	1048	17.6	2.64	0	7.69
NV	647	7.72	3.91	0	6.33
NY	549	13.7	16.8	2.41	24.4
OH	1338	101	16.3	0.993	14.3

OK	895	43	6.36	0	15.6
OR	372	6.17	5.73	0	12.8
PA	1052	94.4	18.2	4.48	35.7
RI	782	0.573	0.94	0	0.499
SC	772	13.8	8.55	3	9.68
SD	741	2.49	1.03	0	1.81
TN	1163	27.6	7.63	1.57	4.66
TX	791	120	38.2	2.29	86
UT	1322	23.5	3.52	0	2.76
VA	810	13.9	6.27	1.65	11.3
WA	215	3.9	11.2	0.507	17.5
WI	1203	37.7	7.32	0.547	7.01
WV	1620	63.3	3.35	0	10.3
WY	1714	40.5	1.78	0	9.42

D.3 Surplus Calculation Details

We performed surplus calculations to show how the effects of the 111(d) rule are distributed between producers and consumers. Equations (5.5) and (5.6) show the calculations for producer surplus. Adding the producer surplus values in equations (5.5) and (5.6) notionally gives the total producer surplus, though the congestion rents in equation (5.6) must first be allocated to states. Equation (5.7) shows the calculation of consumer surplus, and equation (5.8) shows the calculation of government surplus. Equation (5.9) defines unit-level marginal costs under both the mass-based and rate-based standards. Table D-4 defines the symbols used in the surplus equations.

Table D-4: Symbol definitions for equations (5.5), (5.6), (5.7), (5.8), and (5.9).

Variable	Description
$PS^J_{k,t}$	EGU-generated producer surplus in transmission region k at time t [$]
$PS^T_{k,t}$	Congestion rent producer surplus in transmission region k at time t [$]
$CS_{k,t}$	Consumer surplus in transmission region k at time t [$]
GS_l	Government surplus in state l [$]
$d_{k,t}$	Demand in transmission region k in period t [MWh]
L	Inelastic demand curve cutoff price [$/MWh]
$x^P_{j,t}$	Output of generator j in period t [MWh]
$\lambda_{k,t}$	Energy price in transmission region k at time t [$/MWh]
$\Lambda^E_{k,k',t}$	Export-side transaction price for energy exported from region k to region k' [$/MWh]
$\Lambda^I_{k,k',t}$	Import-side transaction price for energy imported to region k from region k' [$/MWh]
m^S_j	Marginal cost of unit j in compliance scenario S (rate R or mass M) [$/MWh]
c_j	Fuel and variable O&M of unit j [$/MWh]
μ^M_q	Shadow price of CO_2 under mass standard in compliance region q [$/lb]
μ^R_q	Shadow price of CO_2 under rate standard in compliance region q [$/lb]
e_j	CO_2 emissions rate of marginal unit j [lb/MWh]
s^R_q	Rate standard in compliance region q [lb/MWh]
s^M_q	Mass standard in compliance region q [lb]
$x^{fin}_{k,k',t}$	Energy flow from region k' into region k in period t [MWh]
$x^{fout}_{k,k',t}$	Energy flow to region k' from region k in period t [MWh]
$x^{exfin}_{k,x,t}$	Energy flow from external region x into region k in period t [MWh]
$x^{exfout}_{k,x,t}$	Energy flow to external region x from region k in period t [MWh]
c^{ext}_x	Prevailing energy price in external region x [$/MWh]
$LOSS$	Loss factor for transmission [dimensionless]

Equation (5.5) shows the component of producer surplus generated by EGUs. This component of producer surplus for each generator in each time period is equal to the product of the output of the generator and the difference between the prevailing electricity price (which we take as equal to the shadow price of electricity from the optimization model for each period) and the marginal cost of the unit. Note that we define marginal costs slightly differently under mass-based and rate-based compliance. Equation (5.9) shows the two definitions, which we discuss at greater length below. Equation (5.5) sums the EGU-level producer surplus over all EGUs in each state. To generate the results reported in section 5.3, we also summed over time.

$$PS^J_{l,t} = \sum_{j \in l} x^P_{j,t} \left(\lambda_{k,t} - m^S_j \right) \tag{5.5}$$

Equation (5.6) shows the component of producer surplus from congestion rents. These rents are proportional to the product of the quantity of exported electricity and the difference between the export-side transaction price and the prevailing electricity price in the exporting transmission region. Note that these rents will only occur when transmission lines are congested: otherwise prices on either side of the line will differ only by a factor related to transmission losses and the export-side transaction price will be equal to the prevailing electricity price in the exporting transmission region. The first and second terms in the equation relate to congestion rents on tie lines within the U.S. and rents on tie lines to Canada, respectively. Note that these rents accrue on the transmission region level and must be allocated to states in order to report results at the state level. We discuss this allocation below. Also note that equation (5.6) only accounts for half the congestion rent – the other half is allocated to consumers in equation (5.7).

$$PS^{T}_{k,t} = \sum_{k'} x^{fout}_{k,k',t} \left(\Lambda^{E}_{k,k',t} - \lambda_{k,t}\right) + \sum_{x} x^{exfout}_{k,x,t} \left((1 - LOSS)c^{ext}_{x} - \lambda_{k,t}\right) \tag{5.6}$$

Equation (5.7) shows consumer surplus. The first term in the equation shows the portion of consumer surplus arising from the difference between the demand curve price and the clearing price in each transmission region (note that, for all results presented here, the demand curve price drops out of the calculation). The second and third terms show the portion of consumer surplus from congestion rents on tie lines within the U.S. and rents on tie lines from Canada, respectively. Note that these rents all accrue on the transmission region level and must be allocated to states. The allocation method is discussed below. Also note that the congestion rent terms in equation (5.7) only account for half the congestion rent – the other half is allocated to producers in equation (5.6).

$$CS_{k,t} = d_{k,t}\left(L - \lambda_{k,t}\right) + \sum_{k'} x^{fin}_{k,k',t} \left(\lambda_{k,t} - \Lambda^{I}_{k,k',t}\right) + \sum_{x} x^{exfin}_{k,x,t} \left(\lambda_{k,t} - \frac{c^{ext}_{x}}{1 - LOSS}\right) \tag{5.7}$$

Equation (5.8) shows the government surplus generated from the sale of allowances. This surplus is only generated under a mass-based standard and assumes that state governments auction

all allowances at the prevailing CO_2 price. Note that under regional and national cooperation scenarios, all states within a cooperative compliance region share the same CO_2 price.

$$GS_l = \mu_q^M s_l^M \tag{5.8}$$

Equation (5.9) shows the definition of EGU-level marginal costs under the mass-based and rate-based standards. The fuel and variable O&M costs c_j do not change with the compliance scenario. However, CO_2 payments take a different form. Under a mass-based standard, each EGU pays a cost of CO_2 equal to the product of the price of CO_2 and the unit's CO_2 emissions rate. Under a rate-based standard, EGUs pay a cost of CO_2 equal to the product of the price of CO_2 and the difference between the unit's CO_2 emissions rate and the rate-based standard. Note that for units with emissions rates below the rate-based standard, this latter quantity is negative. Under rate-based compliance, units with emissions rates higher than the standard make payments to units with emissions rates below the standard.

$$\begin{aligned} m_j^M &= c_j + \mu_q^M e_j \\ m_j^R &= c_j + \mu_q^R \left(e_j - s_q^R\right) \end{aligned} \tag{5.9}$$

Surplus calculations rely on electricity and CO_2 prices to determine the distribution of impacts between consumers in producers. In this analysis, we used shadow prices of electricity and CO_2 generated by our cost-minimization model for this purpose. Using shadow prices in this way assumes the existence of a market that achieves the same result as global cost minimization by accepting supply and demand bids from market participants. The distribution results therefore do not have much meaning in regulated electricity markets, where public utility commissions set and consumers pay rates based on average, rather than marginal, costs. Our results can be interpreted more literally in de-regulated markets, though even here, effects such as market power, imperfect information, and imperfect market design can make prices diverge from the shadow prices achieved in a global cost-minimization. We also note that in deregulated markets, the price paid by the end

user also depends on rate decisions by public utility commissions. The "consumer surplus" values calculated in this work are really surplus values for entities on the demand side in *wholesale* electricity markets.

Note that equations (5.6) and (5.7) calculate portions of producer and consumer surplus at the transmission region level. In order to report surplus values at the state level, we must allocate these components to states. In this work, we allocate surpluses at the transmission region level to states in proportion to the dispatchable generation in each transmission region performed by generators in a particular state under the reference scenario (we discuss the scenarios in section 5.2.5). The allocation factors are therefore constant over time and between scenarios.

In this work, we only report changes in surplus. We thus avoid the problem of defining the parameter L (see Table D-4) from the demand curve. Since demand is constant across all scenarios, all terms involving L drop out when evaluating surplus differences at the transmission region-level across scenarios. When evaluating surplus differences after transmission region-level surpluses have been allocated to states, the weights used to perform this allocation must remain the same across scenarios in order for all terms involving L to drop out of the result. Our choice of allocation weights satisfies this requirement.

D.4 Generation, Imports, and Transmission Losses

Table D-5 shows generation, transmission losses, and imports from Canada in each of the scenarios. Note that the sum of total dispatchable, total wind+hydro, internal transmission losses, and net imports from Canada should equal net load. Net load was held constant across scenarios.

Table D-5: Generation, transmission losses, net imports, and net load on an annual basis [TWh]. Note that under rate-based compliance, electricity is net-exported to Canada. Under mass-based compliance, electricity is net-imported from Canada.

Scenario	Ref.	State-Rate	State-Mass	Regional-Rate	Regional-Mass	National-Rate	National-Mass
Total Dispatchable	3322	3296	3208	3307	3180	3306	3185
Total Wind + Hydro	794	794	794	794	794	794	794
Internal Transmission Losses	-30	-19	-17	-18	-17	-19	-20
Net Imports from CA	-56	-40	46	-52	74	-51	71
Net Load	4030	4030	4030	4030	4030	4030	4030

D.5 Cooperation Surplus Change Breakout

Figure D-2 shows the breakdown between changes in consumer, producer, and government surplus for regional cooperation compared to no-cooperation. The net change, indicated by black lines in Figure D-2 is equivalent to the net change reported in Figure 5.3.

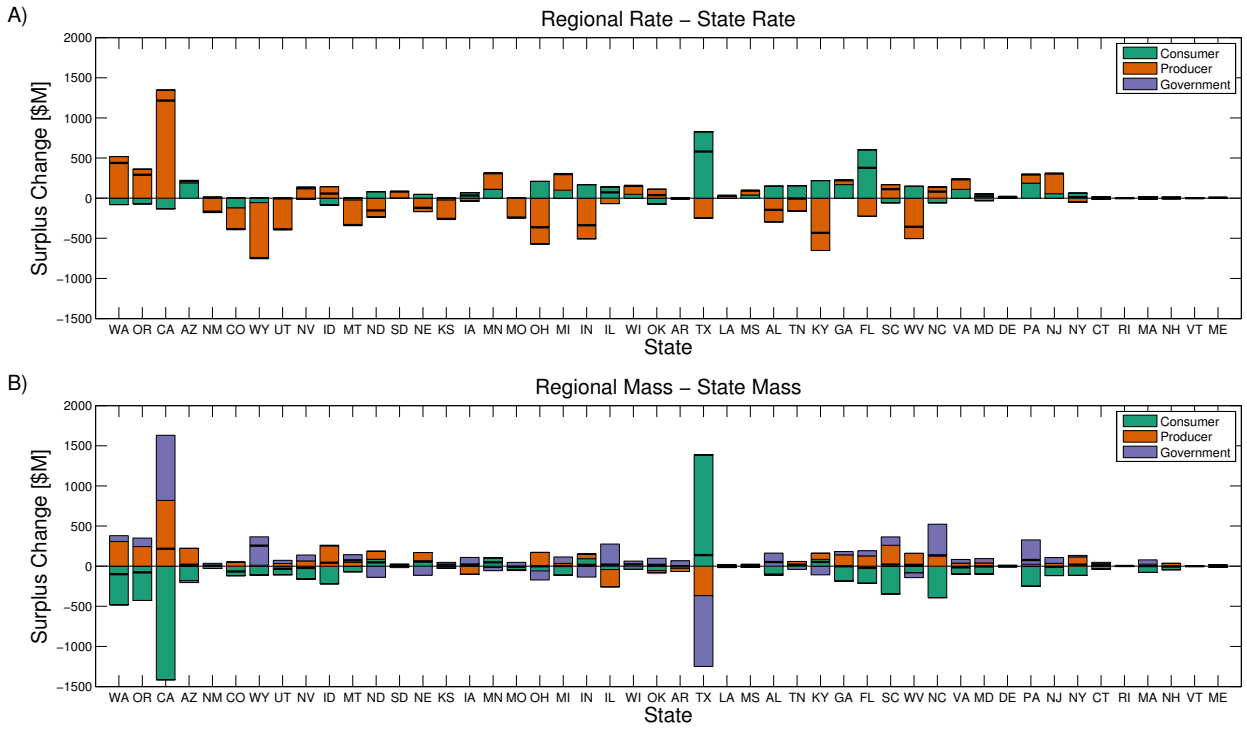

Figure D-2: Changes in all categories of surplus from no-cooperation compliance to regional-cooperation compliance for A) a rate-based standard and B) a mass-based standard. Solid black lines show net values. Net values correspond to values shown in Figure 5.3. Note that under mass-based compliance, government surplus changes with cooperation only because the value of allowances (i.e. the shadow price of CO_2) changes; the total number of allowances auctioned by each state remains the same.

D.6 Comparison of Mass-Based Caps

Figure D-3 compares the mass-based standards used in this work to those suggested by the EPA in their November 2014 notice [7]. Nation-wide, the EPA's standard is about 1% lower than the standard used in this work, due largely to the fact that the agency's method of converting rate-based standards into mass-based standards does not account for load growth, while the method used in this work does. Figure D-3 shows some state-by-state differences between the two standards. Differences in the mass-based standards reflect differences in the amount of affected generation in each state in the method used in this work compared to that in the EPA's.

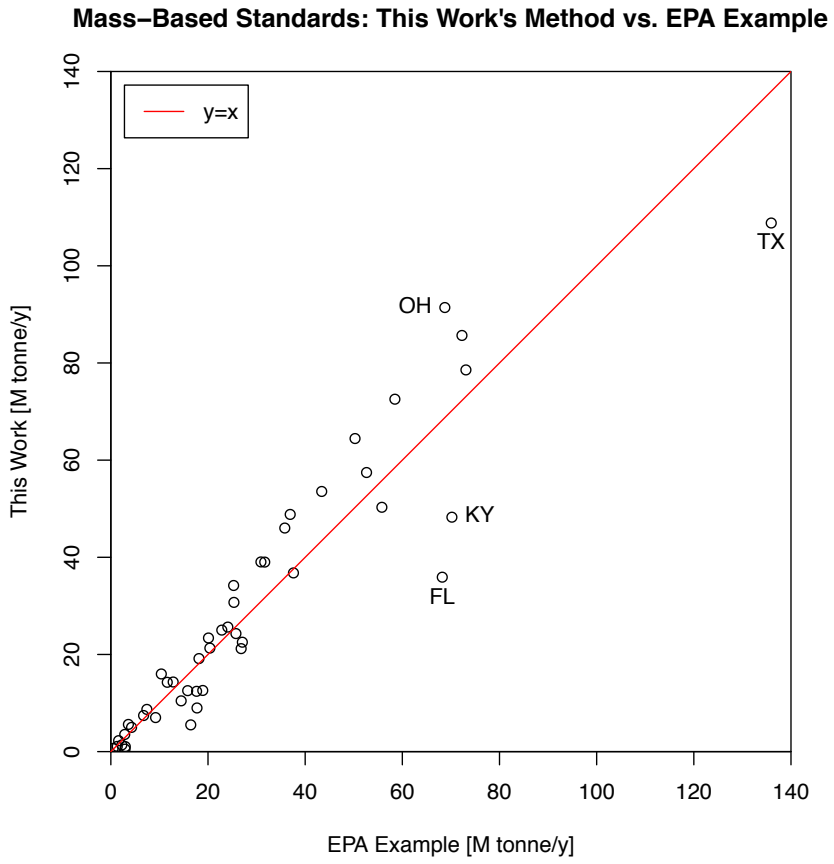

Figure D-3: Mass-based standards as used in this work compared to those suggested by the EPA in their November 2014 notice [7].

D.7 Comparison of Emissions with EPA Numbers

The Regulatory Impact Analysis for the 111(d) rule [2] provided state-level CO_2 emissions numbers for Option 1 compliance with no cooperation and a rate-based standard. Figure D-4 compares the state-by-state emissions from the RIA to the corresponding results from this work. Nation-wide, the agency reports total 2030 CO_2 emissions of 1874 M ton, compared to the 1678 M ton determined in this work.

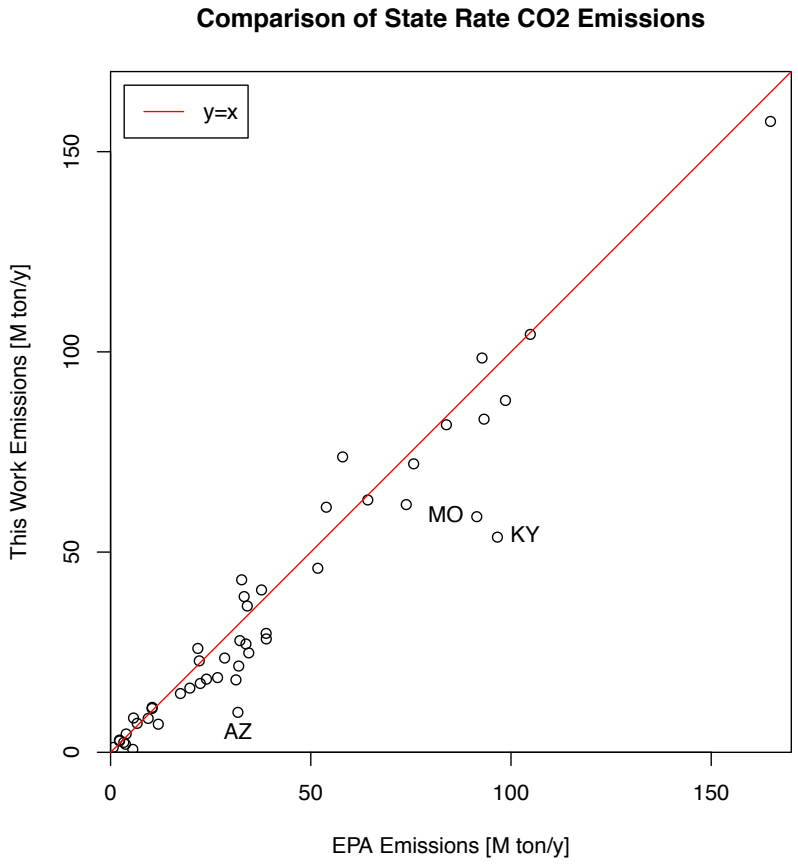

Figure D-4: CO_2 emissions for compliance with a rate-based standard with no cooperation, comparing the results of this work to those of the EPA as stated in the RIA for the 111(d) rule [2].

D.8 Model Formulation

D.8.1 Introduction

The model used in this work is a linear cost minimization model inspired by EPA's Integrated Planning Model (IPM). The transmission regions, states, and regional Clean Power Plan (CPP) compliance regions all align with those found in IPM v.5.13 and Option 1 compliance with the CPP. Electricity Generating Unit (EGU) and transmission line parameters are based on the characteristics found in the IPM's parsed files for Option 1 compliance with the proposed CPP. Wind and hydro profiles were also selected to align with input data for the IPM. As with the IPM, this model operates with perfect information about future demand in all model regions. In contrast to the IPM, this is an hourly model. Note also that, in order to reduce the size of the model, we assumed that hydro and wind were operated on a must-run basis.

This section shows the complete formulation for the model and enables a direct translation into a formulation in GAMS. The model consists of symbol definitions, an objective function, and a number of constraints. Symbols include *sets*, *parameters*, and *variables*. Parameters and variables are all *continuous*. All variables in this model are constrained to only take on positive values only.

D.8.2 Symbols

D.8.2.1 Sets

$j \in J$	Index over all units
$j \in A \subseteq J$	Subset of units affected by CPP
$j \in N \subseteq J$	Subset of nuclear units
$k \in K$	Index over transmission regions
$x \in X$	Index over external regions (Canadian provinces)
$l \in L$	Index over states
$q \in Q$	Index over CPP compliance regions
$t \in T$	Index over hourly time periods
$(j,k) \in JK \subseteq J \otimes K$	Membership of units in each transmission region
$(j,l) \in JL \subseteq J \otimes L$	Membership of units in each state
$(j,l) \in AL \subseteq A \otimes L$	Membership of *affected* units in each state
$(l,q) \in LQ \subseteq L \otimes Q$	Membership of states in each compliance region

D.8.2.2 Parameters

$d_{k,t}$	Demand in transmission region k in period t [MWh]
$w_{k,l,t}$	Available wind in transmission region k and state l in period t [MWh]
$h_{k,l,t}$	Available hydro in transmission region k and state l in period t [MWh]
c_j	Marginal cost of unit j [$/MWh]
$\bar{p}_j$	Maximum power output of unit j [MW]
e_j	CO_2 emissions rate of unit j [lb/MWh]
$tr^{int}_{k,k'}$	Transmission capacity between regions [MW]
$tr^{extout}_{k,x}$	Transmission capacity from region k to external region x [MW]
$tr^{extin}_{k,x}$	Transmission capacity to region k from external region x [MW]
s^r_q	Clean Power Plan CO_2 emissions *rate* standard [lb/MWh]
s^m_q	Clean Power Plan CO_2 emissions *mass* standard [lb]
n^{ave}_l	Average output for new and at risk nuclear in state l [MW]
η_l	Energy efficiency available in state l [MW]
c^{ext}_x	Prevailing energy price in external region x [$/MWh]
$LOSS$	Loss factor for transmission [dimensionless]

D.8.2.3 Variables

Positive Variables

These variables must take on values greater than or equal to 0.

$x^{p}_{j,t}$ Energy produced above minimum output by unit j in period t [MWh]

$x^{fin}_{k,k',t}$ Energy flow from region k' into region k in period t [MWh]

$x^{fout}_{k,k',t}$ Energy flow to region k' from region k in period t [MWh]

$x^{exfin}_{k,x,t}$ Energy flow from external region x into region k in period t [MWh]

$x^{exfout}_{k,x,t}$ Energy flow to external region x from region k in period t [MWh]

D.8.3 Initialization

The equations in this section fix or bound the values of some variables based on input parameters. Equation 1 sets the maximum output for each unit. Equation 2 sets the maximum tie line flow *out* of transmission regions and equation 3 sets the maximum tie line flow *in* to transmission regions. Equation 4 sets the maximum tie line flow from transmission regions to external regions, while equation 5 sets the maximum tie line flow to transmission regions from external regions.

$$x^{p}_{j,t} \leq \bar{p}_j \qquad \forall j \in J, t \in T \tag{1}$$

$$x^{fout}_{k,k',t} \leq t\,r^{int}_{k,k'} \qquad \forall k \in K, k' \in K, t \in T \tag{2}$$

$$x^{fin}_{k,k',t} \leq t\,r^{int}_{k,k'}(1-LOSS) \qquad \forall k \in K, k' \in K, t \in T \tag{3}$$

$$x^{exfout}_{k,x,t} \leq t\,r^{extout}_{k,x} \qquad \forall k \in K, x \in X, t \in T \tag{4}$$

$$x^{exfin}_{k,x,t} \leq t\,r^{extin}_{k,x}(1-LOSS) \qquad \forall k \in K, x \in X, t \in T \tag{5}$$

D.8.4 Objective

Equation 6 defines the objective function to be minimized. The first line shows the marginal costs of the units - fuel and other variable O&M. The marginal costs for each unit are multiplied by the output of each unit. On the second line, revenues from sales to external regions (at a price scaled down by the transmission loss) are included as a negative cost. On the third line, costs for imports from external region (at a price scaled up by the transmission loss) are included.

$$\sum_{j,t}\left(c_j x^{p}_{j,t}\right) - (1-LOSS)\sum_{k,x,t}\left(c^{ext}_{x} x^{exfout}_{k,x,t}\right) + \sum_{k,x,t}\left(c^{ext}_{x} x^{exfin}_{k,x,t}\right)/(1-LOSS) \quad (6)$$

D.8.5 Supply Equation

Equation 7 ensures, in each transmission region and each period, that load is met by energy generated by conventional units, wind, hydro, and net tie line inflows from other

transmission regions and external regions.

$$\sum_{JK}(x^{p}_{j,t}) + \sum_{l}\left(w_{k,l,t} + h_{k,l,t}\right) + \sum_{k'}\left(x^{fin}_{k,k',t} - x^{fout}_{k,k',t}\right) + \sum_{x}\left(x^{exfin}_{k,x,t} - x^{exfout}_{k,x,t}\right) = d_{k,t} \quad \forall k \in K, t \in T \quad (7)$$

D.8.6 Transmission Equation

Equation 8 ensures that tie line inflows to one transmission region are equal to outflows from another region, scaled by transmission losses.

$$x^{fin}_{k,k',t} = (1 - LOSS)x^{fout}_{k',k,t} \qquad \forall k \in K, k' \in K, t \in T \quad (8)$$

D.8.7 CPP Constraints

These equations impose the constraints required to comply with the CPP on a rate basis or a mass basis. Only one of the two equations in this section appear in each model run. Equation 9 shows the rate-based constraint as defined in the EPA's proposed rule. Equation 10 shows a mass-based constraint.

$$\sum_{LQ,AL,t}\left(e_j x_{j,t}^{p}\right) \le s_q^r \sum_{LQ}\left(\sum_{AL,t}\left(x_{j,t}^{p}\right)+\sum_{k,t}\left(w_{k,l,t}\right)+\|T\|\left(n_l^{ave}+\eta_l\right)\right) \quad \forall q \in Q \quad (9)$$

$$\sum_{LQ,AL,t}\left(e_j x_{j,t}^{p}\right) \le s_q^m \quad \forall q \in Q \quad (10)$$

Chapter 6: CONCLUSION

Any plan to mitigate climate change must focus considerable attention on the electric power sector, which is responsible for a substantial portion of CO_2 emissions in the United States. This thesis has evaluated a number of different technologies and policies intended to achieve this reduction.

Carbon Capture and Storage (CCS) has the potential to enable continued exploitation of fossil fuel resources while achieving CO_2 emissions reductions. However, partially as a result of the fact that CCS increases the cost of fossil fueled power plants, deployment has been slow. Increased flexibility, in the form of flue gas bypass and solvent storage, might allow post-combustion CCS-equipped plants to earn higher revenues in deregulated electricity markets, potentially increasing overall profitability of a plant. Previous research[8] has found that the profitability benefits of flexibility are highest at low CO_2 prices where a CCS-equipped plant may not be possible. However, this research only considered the case of a Pulverized Coal (PC) plant with a monoethanolamine-based capture fluid and used a heuristic to size the solvent storage device. In Chapter 2, we considered additional technologies and allowed optimal sizing of solvent storage, but found that the flexibility benefit declined to zero at CO_2 prices high enough for the overall plant to be profitable. We emphasize, however, that we did not consider potential revenues from ancillary service and capacity markets, which might alter our qualitative result.

Renewable Portfolio Standards (RPS) require that a target portion of electricity sold in a state be procured from renewable resources, thereby increasing renewable energy penetration. The presence of increased quantities of variable and uncertain renewable generation resources, such as wind, is

[8] Cohen, S. M., Rochelle, G. T., & Webber, M. E. (2012). Optimizing post-combustion CO2 capture in response to volatile electricity prices. *International Journal of Greenhouse Gas Control*, *8*, 180–195. doi:10.1016/j.ijggc.2012.02.011

expected to increase the requirements for cycling fossil fueled units in order to maintain balance between supply and demand in electric power systems. Cycling operations involve increased costs and air emissions and there has been concern that increased cycling might offset the cost and emissions benefits of wind penetration. However, most (but not all, see e.g. Lew et al.[9]) claims to this effect have not used a Unit Commitment and Economic Dispatch (UCED) model to evaluate the increase in cycling associated with wind. In Chapter 3, we used a UCED along with an accounting of cycling related emissions and costs to show that increases in cycling-related costs and emissions were small compared to the reductions associated with wind.

The EPA's recent proposal of its Carbon Pollution Emissions Guidelines for existing power plants (the 111(d) rule) aims to reduce CO_2 emissions from the electric power sector by up to 30% below 2005 levels by 2030. The rule has the potential to significantly affect electric power generation in the U.S. and has the potential to be very costly to implement. The EPA's Regulatory Impact Analysis, as well as other commentators (e.g. Fowlie et al.[10]) have emphasized the role of inter-state cooperation in reducing the cost of compliance. However, these commentators do not account for the potentially conflicting incentives of decision makers facing very different 111(d) standards in different states. In Chapter 5, we determined the effect of cooperation between states facing different standards, finding that while compliance costs decline nationally with cooperation, some states lose out. These states may need encouragement or compensation to be willing to cooperate.

In addition to its cost, the 111(d) rule may have unanticipated effects on natural gas generation. The agency proposed allowing states to comply with the 111(d) rule by switching from coal to natural gas generation. As the winter of 2014 effectively demonstrated, congestion in natural gas

[9] Lew, D., Brinkman, G., Ibanez, E., Hodge, B. M., & King, J. (2013). Western wind and solar integration study phase 2. *Contract*, *303*, 275–3000.

[10] Fowlie, M., Goulder, L., Kotchen, M., Borenstein, S., Bushnell, J., Davis, L., et al. (2014). An economic perspective on the EPA's Clean Power Plan. *Science*, *346*(6211), 815–816. doi:10.1126/science.1261349

transmission systems can lead to outages at electricity generating units and a large increase in natural gas generation might therefore be expected to create reliability concerns. The EPA's Regulatory Impact Analysis[11] determined that the total level of natural gas generation would be lower under the 111(d) rule than it would be otherwise, but the analysis assumed a rapid adoption of energy efficiency measures. In Chapter 4, we evaluated the impact of complying with the 111(d) rule in the absence of energy efficiency measures, finding that such compliance required a significant increase in natural gas generation in PJM West and ERCOT.

Finally, as compliance with the 111(d) rule is expected to reduce the generation of fossil-fueled plants, it might be expected to reduce their efficiency by requiring the operation of these plants below their design operating points and by increasing the amount of startup / shutdown cycling performed by the plants. NERC[12] has pointed out that reductions in efficiency might reduce the emissions benefits of the plan, but has not evaluated the magnitude of this effect. In Chapter 4, we evaluated the impacts of increased part load operations and cycling on emissions. We found that while emissions attributable to part load operations and cycling do increase under compliance with the 111(d) rule, these increases are small compared to the reductions achieved by the rule.

Chapters 4 and 5 of this thesis relied on a carbon price to achieve the re-dispatch required to achieve compliance with the 111(d) rule. It might be argued that, given the current political climate, carbon prices are unlikely. We emphasize, however, that we are not assuming that the EPA will impose a national carbon price or require that states implement a carbon price. At a fundamental level, however, the 111(d) rule allows states to comply by re-dispatching existing power plants and

[11] EPA. (2014). *Regulatory Impact Analysis for the Proposed Carbon Pollution Guidelines for Existing Power Plants and Emission Standards for Modified and Reconstructed Power Plants*. Environmental Protection Agency. Retrieved from http://www2.epa.gov/sites/production/files/2014-06/documents/20140602ria-clean-power-plan.pdf

[12] NERC. (2014). *Potential Reliability Impacts of EPA's Proposed Clean Power Plan* (pp. 1–30). Atlanta, GA: North American Electric Reliability Corporation.

such re-dispatching is likely to be significantly less expensive than building new capacity. Some states, such as California and the Regional Greenhouse Gas Initiative (RGGI) states, have already embraced a carbon price concept. While other states may employ mechanisms other than a carbon price to achieve re-dispatch, it is unlikely that such mechanisms will prove less costly than a method that prices emissions directly.

A number of recommendations for policy makers emerge from this work. Flexible CCS was found not to be privately profitable when operating in energy markets, though it may yet provide valuable grid services and be a useful compliment to variable renewables such as wind. If EPA, ISOs/RTOs, or other organizations wish to encourage flexible CCS for environmental or grid-support reasons, they will need to ensure such units can operate in ancillary service and capacity markets – energy markets will not be enough.

The EPA should not be convinced to reduce its assessment of the environmental benefits of wind due to increased emissions from cycling fossil-fueled plants. ISOs/RTOs and other reliability-concerned entities should realize that increased cycling would likely not have a significant effect on coal unit profits, and therefore retirements. However, reductions in coal capacity factors and electricity prices in a high-wind future might well lead to retirements unless measures are taken to prevent them.

As states move to prepare their 111(d) rule compliance plans, the EPA and other federal bodies should take seriously their role in encouraging cooperation between states. Though the EPA appears to believe it doesn't have the legal authority to *require* states to cooperate, it might yet be able to make an economic argument to states in favor of cooperation. Such an argument might emphasize the cost savings associated with cooperation, but should also acknowledge that some states stand to lose when cooperating, and take steps to encourage negotiation on this point. The agency might also emphasize that cooperation could reduce the wide variation in effective carbon prices and cost

structures that occurs across states in the absence of cooperation. FERC should recognize the potential for the 111(d) rule to increase electricity-natural gas interdependence, particularly if energy efficiency does not materialize, and take steps to ensure adequate supply.

In the present political climate, a straightforward national approach to reducing carbon emissions in electric power seems implausible. Efforts to decarbonize the electricity system will likely be driven by a range of policies promulgated by various parts of government. This complex policy environment will be difficult to understand, difficult to navigate, and will present a significant risk of triggering unanticipated consequences. However, if government entities take seriously their responsibility to create policies that are as flexible as possible, if the potential of many different technologies to mitigate carbon are accepted, and if diverse jurisdictions can be encouraged to cooperate, significant cost-effective reductions in carbon emissions in electric power may yet be achieved.